UCLouvain

Louvain Drug Research Institute (LDRI)

Biomedical Magnetic Resonance (REMA)

Dual EPR measurement of oxygen consumption and superoxide production: Principle and applications

Donatienne d'Hose

2021

Supervisor : Pr. Bernard Gallez

Co-supervisor : Pr. Bénédicte F. Jordan

REMERCIEMENTS

Quatre années qui semblaient interminables à surmonter au début et voilà qu'elles sont passées à la vitesse de l'éclair. Quatre années d'analyse, de mises au point, de formation, de questionnements et de doutes mais aussi quatre années pleines d'entraide, de surpassement de soi-même et de création. J'aimerai remercier toutes les personnes qui ont contribué à l'aboutissement de cette thèse mais aussi à mon épanouissement en tant que personne et chercheuse.

Mes remerciements s'adressent tout d'abord à mes promoteurs, les professeurs Bernard Gallez et Bénédicte Jordan sans qui tout ce travail n'aurait pas vu le jour. Merci de m'avoir fait confiance depuis le premier jour et de m'avoir fait autant grandir et évoluer. La RPE n'a (presque) plus de secrets pour moi et je suis plus qu'heureuse que notre toolbox ait pu donner naissance à autant d'autres projets en cours et futurs, à l'UCL et en dehors. Planter une graine et la voir se développer aussi vite est pour moi la plus belle fin de doctorat qu'on puisse avoir.

Je tiens également à remercier mon président de jury, le professeur Pierre Sonveaux ainsi que les membres de mon comité d'encadrement, les professeurs Olivier Feron et Jean-Christophe Jonas pour leur suivi et leurs conseils précieux lors de mon parcours doctoral. Merci également d'avoir été les premiers à me confier des collaborations et d'avoir contribué au développement et l'évolution de mon outil. La relève en REMA est déjà assurée et je souhaite que cette toolbox puisse connaitre un nouvel essor *in vivo* ! Je souhaite également à remercier mes deux lecteurs externes qui ont accepté de faire partie de mon jury de thèse et qui ont agrémenté ma défense privée de discussions et remarques pertinentes. Merci au professeur Micael Hardy de nous avoir fourni la MitoMetformine pour nos expériences et pour toutes ses idées de perspectives pour nos futurs projets. Et un grand merci au professeur Ange Mouithys que j'avais déjà eu l'occasion de croiser plusieurs fois en congrès et qui a toujours été de bon conseil pour mes mises au point de projets.

Je remercie également tous mes collègues REMA qui m'ont aidé à accomplir ce doctorat mais qui ont aussi fait en sorte que je pleure bien plus de rire que de tristesse. Je tenais tout d'abord à remercier Pierre qui m'a pris sous son aile et qui m'a tout appris de la RPE. Je ne suis peut-être pas aussi pro que toi mais j'ai essayé d'être à ta hauteur durant ton absence. La team badass honeybadger a su persévérer et accomplir son objectif ! Un tout grand merci également à Lionel, le « couteau Suisse » du labo qui m'a aidé sur toutes mes manips in vivo (et celles qui suivront

encore), weekends compris. Tu as été d'une aide précieuse et je t'en suis plus que reconnaissante. La malédiction de l'in vivo en REMA ne semble pas nous avoir mis trop de bâtons dans les roues, quel soulagement !

Un grand merci à mes collègues Chantale, Chloé et Jérôme avec qui je partage notre bureau. Merci à tous les trois d'avoir été si bonne ambiance, souriants, attentionnés et puis pleins d'anecdotes trop drôles, de quoi survivre à notre sous-sol sans fenêtres. Et petite pensée également pour mes anciennes collègues, les deux Célines, avec qui j'ai débuté mon doctorat et survécu aux premières années de thèse. Merci d'avoir fait passer le temps si vite et en bonne humeur !

Merci à notre brandnew doctorante Barbara qui ne m'a jamais autant fait rire en si peu de temps au labo. Bienvenue dans le monde des formations d'étudiants master ! Je crois que le baptême sera intense mais je ne doute nullement de tes capacités. Plein de courage à toi pour ton projet toolbox in vivo, rend moi fière, je croise les doigts pour toi.

Merci évidemment aux autres REMAciens, Nico, Natacha, Elise, Delphine et Caner. On n'a peut-être pas (tous) de fenêtres ni de soleil mais l'ambiance est au beau fixe ! Et rien de tel que pour mieux avancer que d'être entouré d'une équipe sympa, de bon conseil et parfois complètement farfelue à souhait. Merci d'avoir été là et d'être vous !

Un grand merci aussi à mes deux mémorantes SBIM, Heidi et Pauline, avec qui j'ai passé plus d'un an sur les projets mitotoolbox, toolbox et SDHI. Vous étiez de vraies cadeaux et élèves exemplaires. Désolé de vous avoir fait subir de très longues journées derrière la RPE. Mais grâce à vous tout a fini par payer ! Je vous souhaite de réussir dans votre vie professionnelle mais je n'ai à vrai dire aucun doute là-dessus. Ayez confiance en vous, vous êtes toutes les deux au top.

Je finirai par remercier ma famille et ma future belle famille qui ont été tous si présents pour moi. Merci à mon supporteur N1, mon père, qui me demandait chaque jour quand je publiais le prochain article et qui a lu l'entièreté de ma thèse avant ma défense pour me poser des questions. Tu m'étonneras toujours autant ! Merci aussi à ma mère d'avoir été « le bureau des pleurs » pendant ces 4 ans, et qui a su me guider dans la bonne voie quand le moral était au plus bas. Et évidemment, je remercie mon fiancé Laurent qui a su gérer toutes mes phases, bonnes ou mauvaises, lors de ce doctorat. Merci pour ton soutien inconditionnel et ton amour mais surtout ton humour incomparable et tes frasques de tous les jours qui m'ont permis de terminer cette étape sereinement et en pleine confiance.

To my sassy English granny

FOREWORD

A growing body of evidence indicates that mitochondria play a key role in many disorders as well as in cancer progression and response to treatment. Next to being the main cellular energy generator through respiration, mitochondria are also the major producer of superoxide and other downstream reactive oxygen species (ROS) in the cell. Superoxide anion may trigger cell death when produced in large excess. Potential toxic agents acting on the mitochondrial electron transport chain (ETC) such as fungicides could therefore be harmful for human health (or even eukaryotes in general). On the other hand, several drugs were shown to inhibit the oxygen consumption rate (OCR) in tumors, subsequently enhancing the efficacy of radiation therapy by increasing tumor oxygenation and potentially leading to decreased tumor volume *via* superoxide-induced cell death. However, when produced at a more moderate level, superoxide was suggested to be a key driver promoting cancer cell migration and metastasis. Therefore, these dual dose-dependent effects are important to study when considering the effect of a drug as a potential radiosensitizer in radiation therapy, but also to evaluate the potential toxicity of diverse agents before being placed on the market. So far, no technology was able to assess simultaneously the consumption of oxygen and the leakage of superoxide from the electron transport chain in a sensitive and specific manner compared to currently used tools.

The main goal of this thesis was to focus on the dual measurement of OCR and mitochondrial superoxide production as a marker of mitochondrial (dys)function.

The introduction of this thesis first presents the central role of the ETC in cellular faith, bioenergetics and signaling through oxygen consumption and ROS production modulations. Next, the current tools used to measure and modulate OCR and superoxide levels *in vitro* are described. Finally, the main subjects of the two related projects, namely succinate dehydrogenase inhibitors (SDHI) fungicides and statins, are characterized in their structure, mechanism of action and roles.

The second chapter describes the main goal and aims of the thesis.

The third chapter presents the results obtained during these four years of thesis. First, the development of a novel EPR method to simultaneously measure the oxygen consumption and superoxide production in isolated mitochondria and whole cell models to define mitochondrial (dys)function. With this new implementation in the lab, several projects in anti-cancer therapy

and toxicity assessment benefiting these measurements saw the light. Boscalid et Bixafen, two widely used SDHI fungicides, were proven to induce mitochondrial dysfunction in human cell lines. In the same way, lipid-lowering drugs Simvastatin and Fluvastatin were suggested to be potential radio sensitizing agents in prostate cancer by alleviation of tumor hypoxia. Finally, exceeding our expectations, mitochondrial ROS measurements using this tool are already exploited in diverse UCL research projects which will not be discussed in this thesis.

The last chapter consists in a discussion of the different projects results, their limitations as well as the future perspectives stemming from this work.

LIST OF ABBREVIATIONS

Aβ	Amyloid beta peptide
AA	Antimycin A
AD	Alzheimer's Disease
ADP	Adenosine diphosphate
Akt	Protein kinase B
ATP	Adenosine triphosphate
ARE	Antioxidant response element
BAK	Bcl-2 associated X protein
BAX	Bcl-2-like protein 4
BBB	Blood brain barrier
Bcl-2	B-cell lymphoma-2
BCOADH	Branched-chain 2-oxoacids dehydrogenase
BID	BH3-interacting domain death agonist
CI	Complex I
CII	Complex II
CIII	Complex III
CIV	Complex IV
CCCP	Carbonyl-cyanid-m-chlorophenyl-hydrazone
CMH	1-Hydroxy-3-methyloxycarbonyl-tetramethylpyrrolidin
COPD	Chronic obstructive pulmonary disease
CoQ_{10}	Coenzyme Q_{10}, Ubiquinone
COX	Cytochrome c-oxidase, CIV
CRP	C-reactive protein
CV	Cardiovascular
DAG	Diacylglycerol
DHODH	Dihydroorotate dehydrogenase
DIPPMPO	5-Diisopropoxyphosphoryl-5-methyl-1-pyrroline N-oxide
DNA	Deoxyribonucleic acid
DTPA	Diethylenetriaminepentaacetic acid
E^+	Ethidium
ECAR	Extracellular acidification rate

EDTA	Ethylenediamine tetraacetic acid
EGF	Epidermal growth factor
EPR	Electron paramagnetic resonance
ER	Endoplasmic reticulum
ERK	Extracellular-signal regulated Kinase
ETC	Electron transport chain
ETFQOR	Electron transferring flavoprotein:Q oxidoreductase
FCCP	Carbonyl-cyanide-p-tri-fluoro-methoxy-phenyl-hydrazone
FPP	Farnesyl pyrophosphate
GAPDH	Glyceraldehyde-3-phosphate dehydrogenase
GC	Guanylate cyclase
GDP	Guanosine diphosphate
GGPP	Geranylgeranyl pyrophosphate
GIST	Gastrointestinal stromal tumors
GLUT4	Glucose transporter 4
GMPc	Cyclic guanosine monophosphate
GRX	Glutaredoxins
GSH	Glutathione
GTP	Guanosine triphosphate
^{1}H-NMR	Proton nuclear magnetic resonance
HD	Huntington's disease
HE	Hydroethidium
HIF-1	Hypoxia inducible factor 1
HK	Hexokinase
HMG-CoA	3-Hydroxy-3-methylglutaryl-coenzyme A
HPLC	High pressure liquid chromatography
IL-6	Interleukin-6
IMS	Intermembrane space
IPP	Isopentenyl pyrophosphate Potassium chloride
LDL	Low density lipoprotein
MAPK	Mitogen Activated Protein kinase
MCL-1	Myeloid cell leukemia 1

MitoMET$_{10}$	Mito-Metformin$_{10}$
MIM	Mitochondrial inner membrane
MMP	Metalloproteinase
MOM	Mitochondrial outer membrane
Mt	Mitochondrial
mTORC	Mammalian target of rapamycin
NADH	Nicotinamide adenine dinucleotide
NOS	Nitric oxide synthase
NOX	NADPH oxidase
^{15}N-PDT	4-Oxo-2,2,6,6-tetramethylpiperidined16-^{15}N-1-oxyl
OAA	Oxaloacetate
OADH	Oxoadipate dehydrogenase
OADHC	2-Oxoacid dehydrogenase complexes
OCR	Oxygen consumption rate
OGDH	2-Oxoglutarate dehydrogenase
OXPHOS	Oxidative phosphorylation
PCC	Pheochromocytoma
PD	Parkinson's disease
PDGF	Platelet-derived growth factor
PDH	Pyruvate dehydrogenase
PDK1	Phosphate dehydrogenase kinase 1
PEG	Polyethylene glycol
PGL	Paragangliomas
PHD	Prolyl hydroxylase
P_i	Inorganic phosphate
PI3K	Phosphatidylinositol-3-Kinase
PKC	Protein kinase C
pO2	Partial pressure of oxygen
PMA	Phorbol 12-myristate 13-acetate
PRX	Peroxiredoxins
PTEN	Phosphatase and tensin homolog
PTP	Permeability transition pore

Rac-1	Ras-related C3 botulinum toxin substrate 1
RAS	Rat sarcoma virus
RET	Reverse electron transport
Rho	Rho (ϱ) factor
RNS	Reactive nitrogen species
ROS	Reactive oxygen species
SDH	Succinate dehydrogenase
SDHI	Succinate dehydrogenase inhibitor
SMP	Submitochondrial particle
SOD	Superoxide dismutase
SQR	Succinate: ubiquinone oxidoreductase
T2D	Type 2 diabetes
TCA	Tricarboxylic acid cycle
TNF	Tumor necrosis factor
TOS	Tocopheryl succinate
TPP^+	Triphenylphosphonium
TRX	Thioredoxins
TTFA	Thenoyltrifluoroacetone
UCP	Uncoupling proteins
VDAC	Voltage-dependent anion channel
VEGF	Vascular endothelial growth factor
VSMC	Vascular smooth muscle cell
XO	Xanthin oxidase

TABLE OF CONTENT

Introduction

I. Mitochondria: form & (dys)function

Over the past century, mitochondria have gained much interest as a subject of research within multiple experimental biology disciplines. Since then, considerable progress was made in unraveling its peculiar structure-function relationships as well as elucidating the intricate reaction pathways and energetics of cellular metabolism. As quoted by the American architect Louis Sullivan, "Form ever follows function", linking nature's structures to specific functions. Mitochondria are dynamic organelles performing crucial roles in diverse cellular processes including metabolism, programmed cell death, calcium homeostasis, ROS production and ATP production. In the same way, these functions are defined by the plastic mitochondrial structures adjusting according to the needs of the cell.

1. Mitochondrial structure and composition

Mitochondria are tubular organelles present in the cytoplasm of eukaryotic cells constituting a specific population called "chondriome". The number of mitochondria in a cell varies depending on the organism, tissue and cell type. In this way, hepatocytes or high energy consuming cells like spermatozoids and muscle cells can contain around 2500 units compared to 200-600 units for mammalian fibroblasts and macrophages (Robin 1988) . Variations can also be found in terms of size, shape and intracellular localization.

With the rise of high-resolution electron micrographs (Palade 1952), mitochondrial (ultra-) structure took shape, revealing its double limiting membrane and internal foldings. The outer mitochondrial membrane (MOM) shares similarities in composition to eukaryotic plasma membranes, containing pores and channels permeable to ions and small molecules. In contrast, mitochondrial inner membrane (MIM) is largely impermeable to maintain transmembrane gradient for respiratory metabolism. Because of its specific composition including cardiolipin, MIM presents ridges and invaginations called cristae, increasing surface area for chemical reactions. The different protein complexes necessary for respiratory metabolism and ATP synthesis are moreover located almost entirely on those cristae (Rich 2010). These inner and outer membranes are outlining 2 chambers; an outer chamber between the two membranes referred to as "intermembrane space", and an inner chamber surrounded by the inner membrane as "matrix". This matrix is the main site of aerobic respiration and accommodates various

enzymes for Krebs cycle, fatty acids β-oxidation and amino acids oxidation, as well as ribosomes, RNA and mitochondrial DNA (mtDNA). These findings modeling mitochondrial structure are nowadays widely accepted and still depicted as such in textbooks (**Fig.1**).

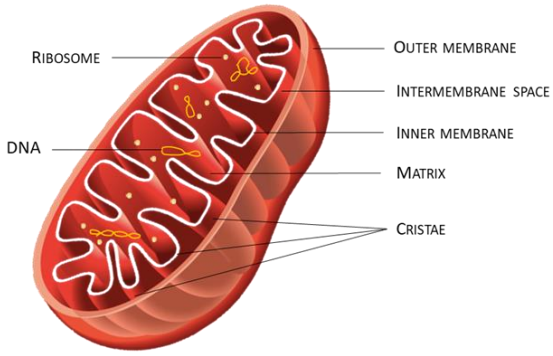

Figure 1: Schematic representation of mitochondrial structure and components.

2. Mitochondrial OXPHOS

Mitochondria are essential for cellular energy production through oxidative phosphorylation (OXPHOS). Mitochondrial cristae are therefore enriched in OXPHOS complexes producing the bulk in cellular ATP. The mitochondrial respiratory chain (**Fig.2**) is composed of approximately 90 proteins organized into 5 multi-subunits complexes (I–V) and two electron carriers; cytochrome c and ubiquinone. Each of these respiratory chain complexes is integrated into the MIM along the cristae membrane, which are assembled into supercomplexes acting as functional platform for OXPHOS (Formosa 2018). Together, respiratory complexes I, III and IV form a supercomplex named "respirasome" regulating the electron flux (Winge 2012). This OXPHOS system couples the oxidation of reducing equivalents (NADH and $FADH_2$) derived from the Krebs cycle and fatty acid oxidation to the pumping of protons across the MIM, generating an electrochemical proton gradient. At the membrane bends of the cristae tips, F_1F_0-ATP-ase, also referred to as complex V, then exploits this gradient as a source of energy in order to generate ATP from ADP and inorganic phosphate (Pi). Synthetized ATP is then moved to the cytoplasm in exchange with ADP by the ATP/ADP translocase.

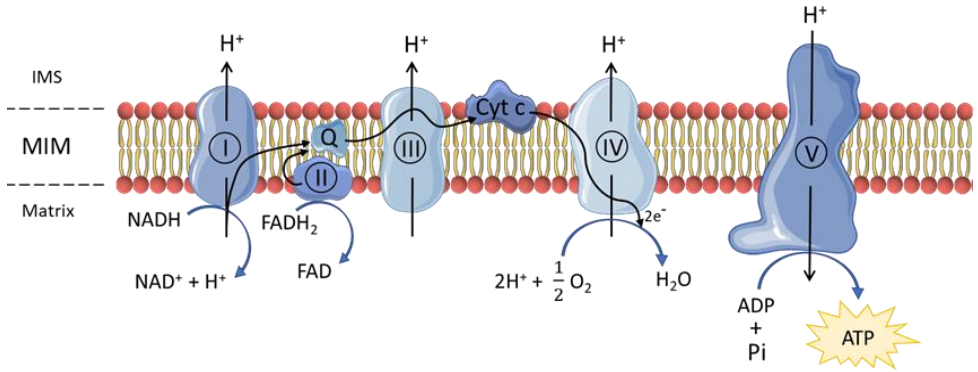

Figure 2: A schematic representation of the mitochondrial respiratory chain depicting the 5 major protein complexes designated as NADH-Coenzyme Q reductase (Complex I), succinate-Coenzyme Q reductase (Complex II), ubiquinol-cytochrome c reductase (Complex III), cytochrome c oxidase (Complex IV) and ATP synthase (Complex V) as well as 2 connecting redox-active molecules; ubiquinone (Coenzyme Q) and cytochrome c. This multi-enzyme system shuttles electrons originating from NADH and $FADH_2$ through complexes I-IV to molecular oxygen, reducing it to water. The energy derived from the electron flux is exploited to pump protons across the MIM to create a proton gradient used as energy source to synthesize ATP by the ATP synthase. Adapted from D. d'Hose 2021.

3. Mitochondrial ROS production

Aerobic respiration being one of the major functions of mitochondria in cells, the electron transport chain (ETC) is therefore precisely regulated to adapt to any change in cell demand and physiology. Disorder of its function by disruption of the electron flux leads to increased reactive oxygen species (ROS) and nitrogen species (RNS) and thus increased oxidative stress causing various neurodegenerative and inflammatory diseases. In this work, we will focus on mitochondrial ROS (mtROS) and more specifically on superoxide anion radical ($O_2^{\bullet-}$) production, which will further be referred to as "superoxide".

1.1. ROS generation & cascades

ROS are reactive molecules derived from oxygen and produced in many cellular compartments including phagosomes, peroxisomes, cellular membranes and mitochondria (Dickinson 2011). Moreover, mitochondria are considered as the main source of ROS in the cell, accounting for 90% of total cellular ROS production. In active and functional mitochondria, ROS are normal metabolic byproducts occurring as a result of electron leakage during OXPHOS and reduction of molecular oxygen (Murphy 2009). This physiological leak occurs when 0.2-2% of the electron in the ETC exit the respiratory chain prior to the reduction of oxygen to water, interacting with oxygen to produce superoxide (Turrens 2003). Superoxide anion originating from a one-electron reduction of oxygen, is considered as the primary precursor of most ROS species. $O_2^{\circ-}$ can be dismutated to hydrogen peroxide (H_2O_2) spontaneously or by superoxide dismutase (SOD), explaining its short half-life (~nsec). Unlike superoxide, H_2O_2 has a more moderate half-life (~msec-sec) and can cross cell membranes easily, acting as signaling molecule by oxidizing specific protein thiol groups. In turn, in the presence of ferrous ions, hydroxyl radicals (OH°) are generated from H_2O_2 through the Fenton reaction. Ferrous ions originate from iron-sulfur cluster located in metalloproteins such as CI and CII. It has also been reported that superoxide can inactivate mitochondrial aconitase, releasing iron and hydrogen peroxide concomitantly and in this way facilitates production of hydroxyl radical in the mitochondria (Vasquez-Vivar 2000).

Hydroxyl radical's high chemical reactivity and instability make it an extremely damaging species for all types of macromolecules (lipids, carbohydrates, proteins, nucleic acids) and it can also trigger lipid peroxidation chain reactions. In addition, hydroxyl radical cannot be eliminated by an enzymatic reaction.

The main intracellular source of $O_2^{\circ-}$ is the mitochondrial ETC, and now counting eleven distinct sites of superoxide generation in mammals (Brand 2010 and Brand 2016) (**Fig.3**). Net superoxide production at each site depends on substrates availability and antioxidant systems present in the matrix. These sites all produce superoxide into the matrix and are therefore able to damage mtDNA.

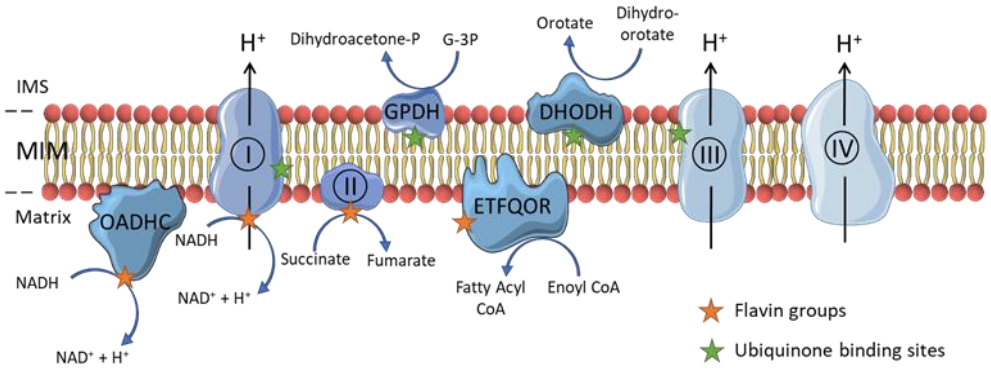

Figure 3: A schematic representation of the 11 sites of superoxide production on the mitochondrial ETC. Sites include Complex I (2 sites), complex II, complex III, the glycerol-3-phosphate dehydrogenase (GPDH), the electron transferring flavoprotein:Q oxidoreductase (ETFQOR) of fatty acid beta oxidation, the dihydroorotate dehydrogenase (DHODH) and the 2-oxoacid dehydrogenase complexes (OADHC) comprising the 2-oxoglutarate dehydrogenase (OGDH), pyruvate dehydrogenase (PDH), the branched-chain 2-oxoacids dehydrogenase (BCOADH) and 2-oxoadipate dehydrogenase (OADH). Sites of superoxide production are represented by colored stars; flavin groups (orange) and ubiquinone binding sites (green). All sites produce superoxide at the matrix side, except for CIII and GPDH which produce superoxide both at the IMS and matrix side. Inspired and adapted from Wong 2017.

Complexes I and III are the sources with the highest capacities to produce ROS; complex III releasing to both the matrix and intermembrane space and complex I releasing exclusively to the matrix (Muller 2004). Damaged or mutated complex II was also reported to produce O2°- but more likely to occur at complex I due to reverse electron flow (RET) (Murphy 2009 and Guzy 2008). However, CII is now reported to produce superoxide at high rates as well in forward reactions than RET (Quinlan 2012, Perevoshchikova 2013, Brand 2016). Other sites are glycerol 3-phosphate dehydrogenase (GPDH), the electron transferring flavoprotein:Q oxidoreductase (ETFQOR) of fatty acid beta oxidation, dihydroorotate dehydrogenase (DHODH) and the 2-oxoacid dehydrogenase complexes (OADHC). Finally, complex IV does not produce any $O_2^{\circ-}$ but its state of phosphorylation/dephosphorylation can favor $O_2^{\circ-}$ production at the other complexes (Kadenbach 2009). Other external sources of $O_2^{\circ-}$ include Xanthin Oxidase (XO), NAD(P)H oxidase (NOX), lipoxygenase, nitric oxide synthase (NOS) and cyclooxygenase.

Also, superoxide being highly membrane-impermeable, its generation stays compartmentalized meaning that there is no flux of superoxide between matrix and cytoplasm. However, intermembrane space superoxide can more easily diffuse to the cytosol using anion channels (Murphy 2009).

1.2. Antioxidant defenses

At low or moderate levels, ROS play a crucial role in many physiological processes, but at a higher concentration, they can produce adverse modifications to cell components and lead to many pathological conditions including cancer, neurological disorders (Jenner 2003, Gella 2009) and asthma (Zuo 2013). To counterbalance the harmful effects of oxidants and avoid disrupting redox balance, aerobic organisms are equipped with antioxidant defenses to maintain cellular health. These systems are divided in 2 categories; enzymatic and non-enzymatic defenses.

Major enzymatic antioxidants include SODs, catalase and glutathione peroxidase (GSH-Px) and redox proteins thioredoxins (TRX), peroxiredoxins (PRX) and glutaredoxins (GRX) (Birben 2012). SODs rapidly convert superoxide into H_2O_2 although this dismutation also occurs spontaneously. 3 forms of SOD co-exist; SOD1 (Cu,Zn-SOD) is present in the intermembrane space and cytosol, SOD2 (Mn-SOD) is present in the mitochondrial matrix and SOD3 (Cu,Zn-SOD) is extracellular (Birben 2012, Sabharwal 2014). H_2O_2 is then reduced to water by catalase which also binds NADPH as a reducing equivalent to prevent oxidative inactivation of the enzyme. H_2O_2 and lipid peroxides can also be reduced into their corresponding alcohol by GSH-Px enzymes, while it oxidizes GSH in GSSG. Glutathione (GSH) is present in a large amount (mM) in the cell and is necessary to detoxify peroxides and regenerate other antioxidants. The fluctuations in GSH/GSSG (reduced form/oxidized form) ratio is a therefore a good indicator of oxidative stress within a cell. Indeed, GSH/GSSG ratio exceeds 100:1 under normal conditions and is able to decrease to 10:1 or even 1:1 during oxidative stress (Chai 1994). Thiol containing enzymes as TRXs and PRXs (6 isoforms) are also capable of disposing H_2O_2. The TRXs are hydrogen donors, reducing oxidized cysteines on proteins with their redox active centers. The formed disulfide bond in their catalytic site is then reduced by TRX reductase and NADPH to regenerate the enzyme. It was also reported to interact with signaling molecules as thioredoxin-interacting proteins and to promote the activation of transcription factors. In the same way, PRXs are scavenging peroxides and peroxynitrites, and are regenerated by

sulfiredoxins. They can also be inactivated transiently by oxidation, allowing in this way to regulate H_20_2 intracellular signaling. Together, TRX and PRX systems form a major redox mechanism to alleviate oxidative stress as well as regulating intracellular signaling. Examples of nonenzymatic antioxidants coming predominantly from dietary source include α-tocopherol (Vit E), carotenoids, uric acid and ascorbic acid (Vit C).

When confronted with oxidative stressors, cells increase their antioxidant capacity to counteract the subsequent increased ROS production. This deviation in ROS levels is detected by a sensor molecule Kelch-like ECH-associated protein 1 (Keap1) that is physically repressing a master regulating transcription factor named nuclear factor erythroid 2-related factor 2 (Nrf2). Under normal conditions, Keap1 promotes ubiquitination of Nrf2 and its degradation by the proteasome. When intracellular ROS levels rise, multiple cysteine residues of Keap1 are oxidized, weakening its binding to Nrf2 (Zhang 2010). Nrf2 is then released and translocates into the nucleus where it induces the transcription of specific antioxidant genes like glutathione synthetizing enzymes (**Fig.4**).

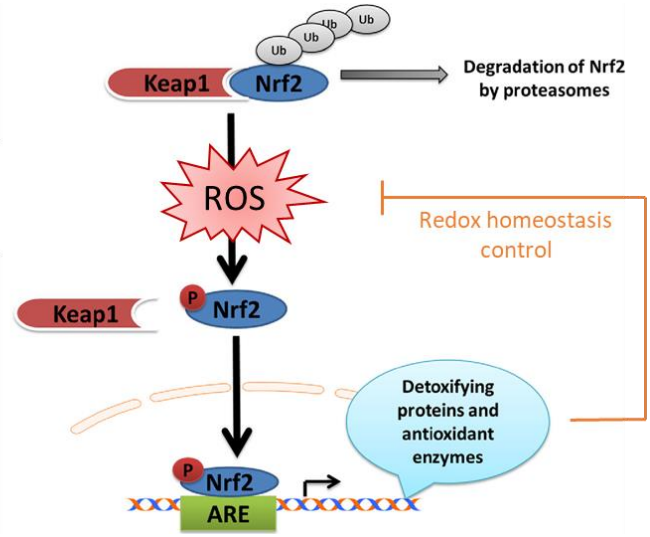

Figure 4: Schematic representation of the Nrf2-Keap1 pathway regulating redox homeostasis. Adapted from Zhang 2015.

1.3. Roles of ROS

Long thought as being exclusively toxic byproducts of aerobic metabolism causing oxidative damage, ROS are actually playing a crucial and beneficial role as regulatory mediators of physiological functions.

One of ROS main function is to participate in host defense by eradicating pathogens. By expressing high amounts of NOX2 components such as gp91phox, phagocytes (macrophages, dendritic cells, neutrophils) produce ROS and are responsible for the oxidative burst killing ingested pathogens (Sareila 2011). Next to that, other tissues and cells are reported to contain NOX2 components and to participate to immune responses, such as spleen and lymph node cells but also non-phagocytic cells like cardiomyocytes and muscle cells (Bedard 2007).

At low regulated levels, ROS act as second messengers via redox reactions in signaling cascades regulating many cellular processes, including proliferation, differentiation, apoptosis, growth and migration (Brieger 2012). H_2O_2 is capable of inducing structural changes within target proteins by oxidizing Cysteine thiolate anions (Cys-S-) to their sulfenic form (Cys-SOH). These redox-derived modifications may lead to changes in protein function, expression of cellular products and increased proteolytic degradation (Grune 1997). Hence, this first-degree oxidation of cysteine residues serves as a reversible signaling mechanism thanks to TRXs and GRXs returning the protein in its original state. Phosphatases (like PTEN and MAPK phosphatases) appear to be susceptible to these modifications as they possess cysteines in their catalytic domain (Rhee 2000). Higher levels of H_2O_2 however further oxidize thiolate anions into sulfinic (SO_2H) or sulfonic (SO_3H) species, making permanent protein damage (Schieber 2014). In this way, mtROS determine physiological outcomes; participating in autophagy by inactivating the cysteine protease Atg4, participating in aging process and boosting cell differentiation and proliferation upon receptor-dependent stimulation (Sena 2012).

It has also been demonstrated that ROS are closely related to proteins involved in mitochondrial dynamics and more specifically mitochondrial fusion and fission. ROS could modulate the expression and activity of these proteins, subsequently reorganizing mitochondrial networks (Cid-Castro 2018). In this case, oxidative stress is therefore associated to fusion/fission imbalance, triggering mitochondrial fragmentation and cell death.

Low levels of ROS are also able to induce nuclear transcriptional responses through cytoplasmic signaling pathways, resulting in long-lasting metabolic changes. This adaptive process called mitohormesis could increase cellular health and lifespan by promoting stress resistance, leaving the cell less susceptible to further perturbations. Furthermore, to reinforce the stabilization of hypoxia inducible factor 1 (HIF-1) required for metabolic adaptation under low oxygen levels (physiological hypoxia), mitochondria also release H_20_2 to activate HIF-1 concomitantly with oxygen (Chandel 1998). With the discovery of cytochrome c participating to apoptosis as well as OXPHOS, this cross-talk between mitochondrial metabolism and signaling pathways became more concrete.

1.4. ROS production in tumors

Compared to normal cells, cancer cells present an increased rate in mtROS production but also an increased superoxide production originating from NADPH oxidase (NOX) allowing them to activate signaling pathways necessary for tumor progression. This cancer specific difference in cellular redox state is due to a combination of multiple factors; oncogenic lesions leading to Phosphatidylinositol-3-Kinase (PI3K) and Mitogen Activated Protein kinase/Extracellular-signal regulated Kinase (MAP/ERK) pathway activation, combined with tumor microenvironment changes such as hypoxia leading to Hypoxia-Inducible-Factor (HIF) stabilization and activation (DeBerardinis 2016). Chronic oxidative stress is able to induce severe damage to intracellular molecules like lipids, protein and DNA. Free radicals can alter polyunsaturated fatty acids in biomembranes by triggering lipid peroxidation chain reactions, damage functional properties of proteins and enzymes as well as cause strand breaks in nucleic acids (Kehrer, 1993). More particularly, because of its close proximity to the ETC and limited repair mechanisms, mitochondrial DNA (mtDNA) is highly susceptible to ROS-damage, leading ultimately to a decline in mitochondrial function and enhanced ROS production. This suggests largely mitochondrial involvement in degenerative processes. To avoid cellular damage and activation of death-induced pathways, constant high levels of ROS in cancer cells are buffered by an increase in natural enzymatic cellular antioxidant systems via a mechanism regulated at a transcriptional level. Indeed, ROS exposure induces the production of cytoprotective enzymes (as metal-containing SODs, catalase, PRX, GSH-Px and NADPH) through the Keap1-Nrf2-ARE pathway by activating Antioxidant Response Element (ARE)-mediated genes (de Vries 2008, Zhang 2010, Zhang 2015).

As reviewed by Sosa in 2013, ROS are able to promote many biological processes and signaling pathways in order to stimulate tumor development and progression (V Sosa 2013). Indeed, ROS can act on cellular proliferation by ERK1/2 and Tyrosine kinase receptor (TKR) activation, stimulate evasion of cellular death, invasion and metastatisation as well as boost angiogenesis by releasing Vascular endothelial growth factor (VEGF) and angiopoietin. To coordinate those processes, cells call upon growth factors such as Epidermal growth factor (EGF) and Platelet-derived growth factor (PDGF) by transiently increasing NOX-dependent ROS generation to activate tyrosine kinase activity of their associated receptors. This results in the recruitment of proteins towards the receptor and consequently to the activation of transduction pathways, notably PI3K- Protein kinase B (AKT)- mammalian target of rapamycin (mTORC) and RAS-MEK-ERK-MAPK cascade. These "hijacked" machineries of normal cells are diverted by cancer cells in order to regulate cell events by controlling downstream signaling and ultimately lead to promoting sustained cell cycle progression, metastatic potential and therapy resistance. Among the 3 described classes of PI3Ks, Class I PKI3a have supported an important role in tumorigenesis because of its ubiquitous expression and its precise involvement in glucose metabolism, insulin signaling and cell growth (Liu 2018). It has also been reported to frequently acquire gain of function mutations in cancer. Subsequently, PI3K activation leads to Phosphate dehydrogenase kinase 1 (PDK1) recruitment to the membrane which, in turn, stimulates AKT by phosphorylation. By inactivating the hamartin-tuberin complex (TSC1-TSC2), AKT promotes mTORC1 stimulation and its downstream effectors (ribosomal S6 kinase and eIF4E-binding proteins), leading to protein synthesis and progression of cell cycle from phase G_0-G_1 to phase S. PI3K cascade activation also leads to the recruitment of Ras-specific GDP/GTP exchange factors promoting cell transformation. Cancer cells act on the loss of tumor suppressors like Phosphatase and tensin homolog (PTEN) to divert cellular processes into sustained activation. PTEN is an important regulator of PI3K pathway because of its phosphatase activity and its ability to inactivate PIP3, an essential mediator of cell proliferation. PTEN phosphatase activity is inactivated by H_20_2-mediated oxidation and formation of disulfide bonds between essential cysteines (Cys^{124} -Cys^{71}) in its active site (Lee 2002). Uncontrolled generation of H_20_2 could therefore inhibit signaling regulation activity of phosphatases, resulting in cell death evasion and indefinite proliferation.

4. Mitochondria & cell death

Next to mitochondria key function in cellular energy metabolism, mitochondria are also master regulators of apoptosis through release of cytochrome c and mitochondrial proapoptotic proteins. This highly regulated programmed cell death is actually mediated by two signaling pathways; the "extrinsic" pathway mediated by ligands activating death receptors (DRs) at the cell surface, and the "intrinsic" pathway initiated by mitochondria (Khan 2014). Both pathways converge together at the MOM and act on central regulatory proteins called caspases (cysteine aspartic acid specific proteases), which have to be activated in order to cleave downstream essential proteins for cell survival such as DNA repair proteins and cytoskeletal proteins (**Fig.5**). Caspases 8 and 10 make part of the initiator proteins recruited and activated following DRs stimulation (Tumor necrosis factor (TNF) Receptor superfamily) by their specific ligand. The proximity of these initiators stimulates their catalytic domain, allowing them to activate caspase effectors 3,6 and 7. On the other hand, the intrinsic pathway is activated following cellular stress signals and regulated by B-cell lymphoma 2 (BCL-2) family of proteins governing the integrity of the MOM. This family of proteins is constituted of multidomain proapoptotic proteins (BAX and BAK) mediating the permeabilization of the MOM, as well as a range of antiapoptotic proteins (BCL-2, BCL-XL, BCL-w and myeloid cell leukemia 1 (MCL-1)) preventing cytochrome c efflux. Upon intrinsic pathway activation, BH3-only proteins, a subfamily of BCL-2 proteins, are upregulated and inhibit antiapoptotic proteins activity by binding (Shamas-Din 2011). Among those BH3-only proteins, BH3-interacting death domain agonist (BID), Bcl-2 interacting mediator of the cell death (BIM) and p53 up regulated modulator of apoptosis (PUMA) are also direct activators of proapoptotic proteins BAK and BAX (Ren 2010). Ultimately, this activation of the proapoptotic phenotype is led by MOM permeabilization, release of cytochrome c and Smac into the cytosol and activation of caspase 9 and 3 to eliminate the cell.

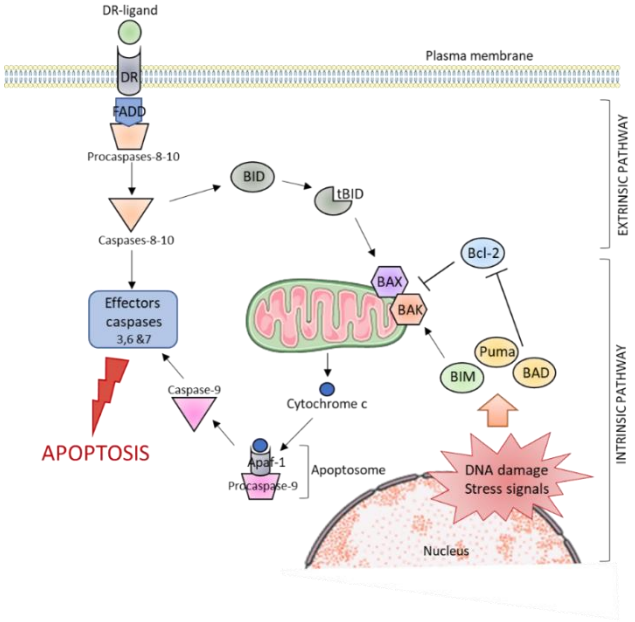

Figure 5: Schematic representation of intrinsic and extrinsic apoptotic pathways. Apoptosis can be triggered by intracellular stimuli (intrinsic pathway) as well as extracellular stimuli (extrinsic pathway). The intrinsic pathway is stimulated by cellular stress such as DNA damage while extrinsic pathway is initiated by death receptor (DR) stimulation at the cell surface.
Inspired and adapted from Schleich 2013.

In addition, it appears that metabolic and apoptotic pathways converging in the mitochondria are not independent of each other. Diverse glycolytic enzymes are indeed multifunctional and are therefore also able to regulate other processes such as transcriptional regulation, cell motility, DNA repair and autophagy (Tristan 2011). This link is also suggested by many studies reporting the implication of glucose metabolism in cell death and survival (Kim 2005, Sen 2008). As a matter of fact, several isoforms of Hexokinase (HK type 1 and type 2) are suggested to participate in the apoptotic pathway and are therefore upregulated in many poorly differentiated and highly malignant tumors (Pedersen 2002). Although the exact mechanism of HK antiapoptotic effects are not really clear, binding of type II HK to the MOM has been shown to inhibit BAX-induced cytochrome c release and apoptosis in HeLa cells (Pastorino 2002). On the other hand, the proapoptotic role of other metabolic enzymes such as glyceraldehyde-3-phosphate (GAPDH) has been demonstrated in several studies, suggesting its nuclear translocation and accumulation would trigger apoptosis (Dastoor 2001, Liiv 2012). Other studies

also suggest that GAPDH is accumulated in mitochondria during stress conditions such as starvation, oxidative stress and DNA damage and deposited on the MOM in association with voltage-dependent anion channels 1 (VDAC1) which ultimately results in mitochondrial permeability and caspase-independent cell death (Tarze 2007).

5. Mitochondrial ETC dysfunction

Defects in mitochondrial metabolism, such as respiratory complexes dysfunction due to mutations, affect the ETC and proton pumping across de MIM, leading to decreased mitochondrial membrane potential and ATP production (Distelmaier 2009, Moran 2010). Altered electron transport also induces increased rates of superoxide production that could be explained by the high reduction state of complexes upstream of the mutation. Together, structurally and functionally damaged mitochondria favor accumulation of ROS (Turrens 2003) and play an important role in the pathogenesis of multiple disorders.

Because of mtDNA higher rate of mutations and less efficient DNA repair mechanisms compared to nuclear DNA, respiratory chain complexes failure often occurs, leading to increased ROS generation. Those ROS are associated with age-related cellular damage and shortened life-span. Indeed, it has been reported that ATP production decreases by 8% in humans every decade (Short 2005) and that OXPHOS capacity decreases over time with decreasing muscle volume when aging (Conley 2000). This process is also referred to as the "free radical theory of aging"

Furthermore, mitochondrial ETC dysfunction is largely observed in neurodegenerative diseases including Alzheimer and Parkinson's disease. Alzheimer (AD) is a common form of dementia (cognitive impairment) characterized by an accumulation of neurotoxic proteins: plaques of amyloid β peptide (Aβ) and fibrillary tangles of hyperphosphorylated tau-protein. It is however still quite unclear whether those proteins are the cause or the consequence of the mitochondrial dysfunction associated with AD. Several reports demonstrated Aβ translocation from extracellular plaques into the mitochondrial matrix, exerting an effect on complex IV activity (Hashimoto 2003, Hauptmann 2006). Aβ also disrupts ETC complexes interactions into supercomplexes (Seelert 2009). On the other hand, the baseline mitochondrial functioning of each individual may initiate the accumulation of those proteins, as many mitochondrial functions are already affected in the early stages of the disease's development. Indeed, before accumulation of the neurotoxic proteins, mitochondria already present enzymatic failure and increased ROS

production, leading to the accumulation of cellular damage. Changes is size and shape as well as in fusion/fission regulations have also been reported. In the same way, Parkinson's disease (PD) is also associated with mitochondrial function and increased oxidative stress leading to the selective loss of dopaminergic neurons explaining the motor clinical manifestations of the disease. More precisely, PD's mitochondrial dysfunction is associated with Complex I deficiency which increases ROS production, leading subsequently to cytochrome c release and caspase 3 activation as well as ubiquitin proteasome system (UPS) dysfunction (Moon 2015).

As discussed previously, ETC dysfunction is also found in various type of cancers accumulating defective mitochondria, stimulating tumor growth and metastasis through increased ROS generation (Petros 2005, Ishikawa 2008).

Nowadays, mitochondrial ETC dysfunction is also associated with many other disorders such as cardiovascular diseases (hypertension, atherosclerosis, endothelial dysfunction) (Kanaan 2017), diabetes (Rocha 2016) and asthma (Reddy 2011), presenting all pathological levels of ROS.

II. Modulation of oxygen consumption

1. Modulators of oxygen consumption (OCR) on ETC complexes

With the years, several modulators of mitochondrial function were discovered and largely used to define the structure of the mitochondrial respiratory complexes as well as the electron flow across the MIM. In this paragraph, we will address several of these complexes' modulators, which are all depicted on **Fig.6.**

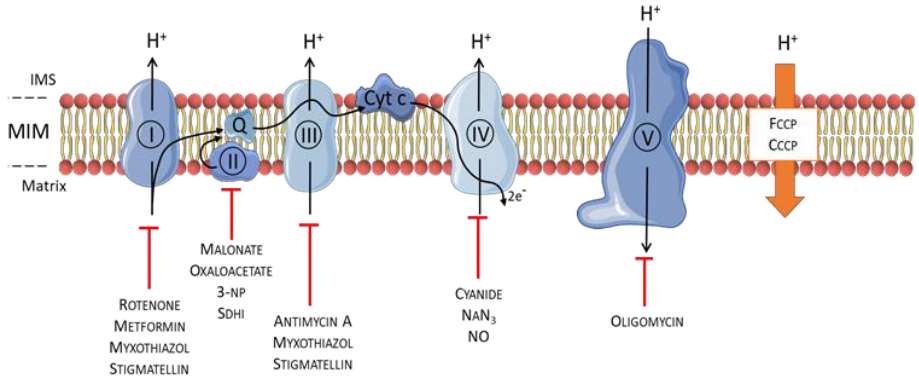

Figure 6: Schematic representation of the mitochondrial electron transport chain and OCR modulators with their site of action.

1.5. NADH-oxidase inhibitors

NADH:ubiquinone oxidoreductase (complex I or CI), the first and largest respiratory complex, initiates the electron transfer by oxidizing NADH and using ubiquinone as final electron acceptor. This two-electron transfer is also accompanied by translocation of 4 protons across the MIM to the intermembrane space. A wide variety of CI inhibitors act closely to the ubiquinone reducing site. Complex I is inhibited by more than 60 different families of compounds, detailed in a review (Esposti 1998). It is also commonly accepted that those inhibitors share the same binding site in the enzyme (Okun 1999) as their structure resembles ubiquinone with a cyclic `head' corresponding to the ubiquinone ring and a hydrophobic `tail'.

Among them, rotenone, a natural plant extract widely used as pesticide and most potent agent of the retinoid class, comprises the inhibition of electron transfer from the iron-sulfur centers to ubiquinone, hence blocking OCR and ATP synthesis. In addition, ROS production is increased due to incomplete electron transfer to molecular oxygen. Because of its high lipophilicity, rotenone crosses the blood brain barrier easily (Caboni 2004) and enters cells without needing specific transporters (Tieu, 2011), inducing rapid neurodegeneration (Hirsch 2003). Rotenone infusion is nowadays still used as Parkinson's disease model in rodents.

It is also established that metformin, a widely prescribed antidiabetic drug, inhibits CI enzymatic activity and thereby impairs both mitochondrial function and cell respiration (Owen 2000, Brunmair 2004).

Other classes of CI inhibitors such as piericidins, capsaicins and N-Methyl-4-phenylpyridinium (MPP^+) and its alkyl derivatives are potent CI-inhibitors used as probes to explore CI function (Miyoshi 1998). Short chain quinone analogues (Q-2, Q-3 and octyl-Q) act as enzyme substrate and become inhibitory once reduced, simultaneously increasing ROS production. Finally, myxobacteria are capable of producing antibiotics inhibiting CI, such as myxothiazol and stigmatellin. Among synthetic agents, we can also find pesticides now commercialized as acaricides (Dekeyser 2005).

1.6. Succinate-ubiquinone -oxidoreductase inhibitors

Succinate-ubiquinone-oxidoreductase (SDH/SQR, Complex II or CII) is a key transmembrane protein linking two energy converting pathways; the Krebs cycle and the mitochondrial ETC. Complex II oxidizes succinate into fumarate and transfers the electrons onto ubiquinone, hence fueling the downstream complexes III and IV.

Malonate and oxaloacetate (OAA) (**Fig.7B-C**) are well established competitive inhibitors of CII (Gutman 1977), occurring naturally in biological systems, like leguminous plants but also brain tissues. Along with CII inhibition, malonate also induces ROS production, participating to the characteristic striatal degeneration similar to that seen in Huntington's disease (HD).

Mycotoxin 3-Nitropropionic acid (3-NP) irreversibly binds to SDH and prevents its activity, as it structure is similar to SDH substrate; succinate **(Fig.7A**). In this way, 3N-P blocks cellular metabolic machinery, leading to systemic energy depletion (Alexi 1998). Basal ganglia seem however to be the most severely affected after 3-NP peripheral exposure, producing selective neurotoxicity in the striatum. 3-NP is nowadays still used to create animal models of HD (Brouillet 2014).

In agriculture, fungicides specifically inhibit fungal respiration by blocking the ubiquinone binding sites on CII. Nowadays, newer synthetic compound of the former carboxin agents are used for crop protection and play an important role in managing plant diseases. Some of these more recent fungicides are also capable of inhibiting Complex III (CIII) as well. Succinate dehydrogenase inhibitors (SDHIs) fungicides will be discussed more extensively in this work.

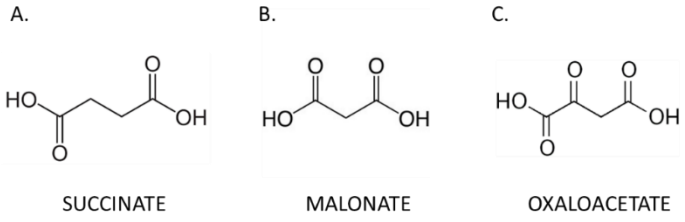

Figure 7: Chemical structure of SDH native substrate (**A**) succinate and natural inhibitors (**B**) malonate and (**C**) oxaloacetate.

1.7. Cytochrome c reductase inhibitors

Cytochrome c reductase (Complex III), a membrane bound complex forming the middle segment of the ETC, transfers the electrons from ubiquinol to ferro-cytochrome c located on the outer side of the MIM. This redox reaction is linked to a proton transfer across the membrane, by a mechanism called "protonmotive Q-cycle". Ubiquinol is oxidized at the Qo site of the enzyme by a "bifurcated" reaction that redirects the 2 electrons down divergent paths, reaching different acceptors; the Rieske Fe-S center (high potential chain) and cytochrome b (low potential chain).

Antimycin A, known since the 1950s, is considered the first and most potent inhibitor of CIII (Potter 1952). Nowadays it is well established that Antimycin A binds specifically to the quinone reduction site (Qi site) of the complex, blocking the oxidation of the cytochrome b hemes in the low potential chain (Quinlan 2011). This inhibition of electron transfer causes loss of mitochondrial membrane potential, leading to decreased OCR and increased ROS production.

Like SDH, complex III can be inhibited by fungicides such as Oomycete-specific Ametoctradin (Zhu 2015) and strobilurins fungicides (Wood 2003). Moreover, several inhibitors of CI and CII are also capable of inhibiting III at the same time. Previously discussed antibiotics, myxothiazol and stigmatellin, block CI and CIII (Esposti 1993) and new generation SDHIs such as Bixafen have inhibitory effects on CIII (Bénit 2019).

1.8. Cytochrome c oxidase inhibitors

Cytochrome c oxidase (COX, Complex IV) is the terminal respiratory complex of the ETC, transferring electrons from reduced cytochrome c to molecular oxygen and translocating protons to the IMS. COX activity is tightly regulated by multiple molecules, like hormones and second messengers, to meet the energy demands of the cell. In this way, COX can be regulated by thyroid hormone, cardiolipin and nitric oxide (NO). Its activity can also be modulated by allosteric (in)activation by phosphorylation.

Cyanide was one of the first potent inhibitors of COX, inhibiting cellular respiration and ATP production by binding to COX heme and subsequently inducing strong oxidative stress by increasing ROS production (Jones 2000). Sodium azide (NaN3) was also reported to induce

strong decrease in brain COX activity after infusion in rats (Bennett 1996), becoming since then a powerful tool to investigate OXPHOS mechanism in vitro and mitochondrial dysfunctions *in vivo*.

NO is a reversible and endogenous modulator of mitochondrial respiration, competing with oxygen at the oxygen binding site of COX (Sarti 2003). This NO-mediated inhibition of respiration was demonstrated in different cell types such as hepatocytes, neuronal cells and tumor cells (Brown 1999, Jordan 2004). Also, low endogenous levels of NO potentiate cyanide inhibition of COX (Leavesley 2008).

1.9. Mitochondrial uncouplers

Oxidation of substrates by the ETC is not entirely coupled to ATP synthesis. A fraction of this liberated energy from OXPHOS is dissipated as heat due to proton leakage reentering into the matrix independently of ATP synthase. This proton leak can be basal (around 30% of resting cellular metabolic rate) where H^+ diffuse across the MIM or be induced by specific proteins called uncoupling proteins (UCP) (Demine 2019). Synthetic and biological compounds are also capable of inducing mitochondrial uncoupling either by disrupting mitochondrial membrane potential or by modulating UCP activity. By increasing proton conductance across the membrane, these compounds are able to dissipate mitochondrial membrane potential and therefore increase oxygen consumption. Along with the decrease in local oxygen concentration, ROS production is subsequently decreased after uncoupling. Among endogenous modulators we find thyroid hormone T2 which abolishes allosteric ATP inhibition of COX, resulting in partial OXPHOS uncoupling. By translocating through anion carriers, fatty acids also demonstrated uncoupling effects (Wojtczak 1993). Components inducing extrinsic uncoupling (=reducing proton motive force) include commonly applied uncouplers carbonyl-cyanide-m-chlorophenyl-hydrazone (CCCP) and carbonyl-cyanide-p-tri-fluoro-methoxy-phenyl-hydrazone (FCCP), and molecules translocating protons (ionophores) such as valinomycin and nigericin (Kadenbach 2003).

2. *In vitro* methods to measure OCR

2.1. Clark electrode

The Clark oxygen electrode (and its varieties) was long considered as gold standard in research to measure pO_2 and oxygen consumption and is nowadays still widely used. This device consists of a chamber with 2 electrodes; a platinum cathode and a silver/silver chloride anode, filled with an electrolyte solution of potassium chloride (KCl). This chamber is surrounded with a teflon membrane permeable to gases, enabling its slow diffusion into the Clark electrode. This amperometric oxygen measurement technique is based on the production of a current between both electrodes when a voltage source of 0.6V is applied (**Fig.8**). When oxygen diffuses through the membrane, it is reduced at the cathode into hydroxide ions (OH^-) that are then migrating to the anode and cause the oxidation of silver. The silver then ultimately reacts with chloride ions (Cl^-) of the electrolyte solution to give electrons. This current flow is directly proportional to the oxygen tension in the solution (Von Heimburg 2005).

Despite its extensive use over the years, it comes with its limitations. For *in vitro* experiments, these include the consumption of oxygen by the electrode, the need of large assay volumes compared to other techniques and the stirring requirements that are capable of damaging the cells. However, a key advantage of the use of this technique is providing the opportunity to add additional agents during the experiments. Today, this sensor also enables *in vivo* and transcutaneous pO_2 measurements when attached to the skin.

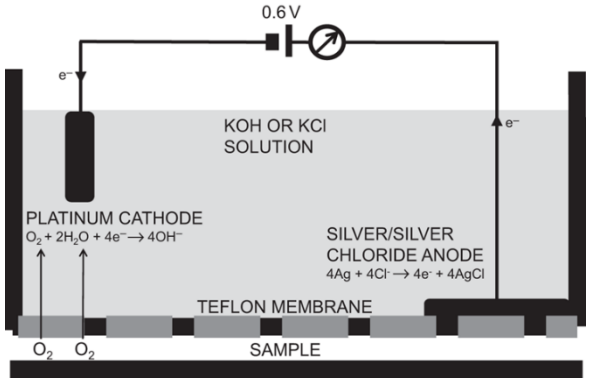

Figure 8*:* Schematic representation of the Clark electrode functioning. The electric current occurring from the chemical reactions at the cathode and anode is directly proportional to the pO_2 in the sample. Original figure from *Anesthesia Key* (Aneskey.com).

2.2. Seahorse XF

The Seahorse XF analyzer is used to measure the oxygen consumption rate (OCR) and extracellular acidification rate (ECAR) on adherent monolayered cells (Ferrick 2008). Using the specific Cell Mito Stress Test on live cells, Seahorse enables the measurement of key parameters of mitochondrial function in real-time by injecting specific modulators of respiration during the assay (**Fig.9**). The first modulator, oligomycin, inhibits ATP synthase and decreases OCR, enabling the measurement of basal mitochondrial respiration. The addition of FCCP then decouples the ETC by dissipating proton gradient and enhances electron flow, stimulating the ETC at maximal capacity (Maximal respiration). The subsequent addition of Rotenone/Antimycin A inhibits respiratory complexes I and III respectively, leads to the complete shutdown of mitochondrial respiration. This last step allows to measure spare respiratory capacity and non-mitochondrial respiration (due to cellular enzymes). This wide panel of features to measure mitochondrial function is one of this assay's major advantage. Compared to the Clark electrode, it does not require a large number of cells, and different cell lines and experimental conditions can be measured at the same time on a same plate. Automated drug injections and data recordings make it a very easy and powerful tool. This kit can also be used on isolated mitochondria (Long 2016) and organoids. Next to these clear advantages, this stress test kit also presents some limitations. Mito stress test kit's protocol is strict with cell operations, and cell density and count should be optimal to avoid clusters and ensure accurate OCR measurements (Luz 2015, Gu 2021). At last, it cannot be performed *in vivo* (Divakaruni 2014).

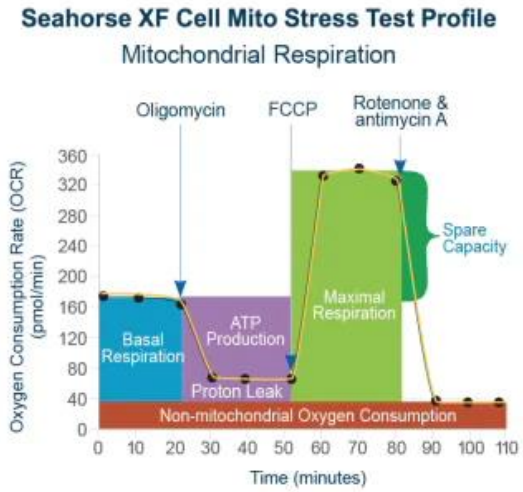

Figure 9: Mitochondrial respiration parameters measured by the Seahorse XF on plated cells using the Cell Mito Stress Test Kit (Agilent). Oxygen consumption rate (OCR) of cells is measured during time after successive addition of mitochondrial modulators; Oligomycin, FCCP, Rotenone and Antimycin A.

Original figure from *Agilent* products – (agilent.com/en/product/cell-analysis/real-time-cell-metabolic-analysis/xf-assay-kits-reagents-cell-assay-media/seahorse-xf-cell-mito-stress-test-kit-740885

2.3. X-band EPR-oximetry

Electron paramagnetic resonance (EPR) - oximetry with X-band is a magnetic resonance method that can be used to measure pO_2 and oxygen concentration in biological samples or tissues. Its principle relies on the detection of "paramagnetic" molecules (containing unpaired electrons) such as free radicals, metal ions and therefore molecular oxygen which possesses two unpaired electrons. However, oxygen cannot be detected directly by EPR when dissolved in fluids near room temperature because of its fast spin relaxation to the excited state, leading to broadening until becoming undetectable. Therefore, paramagnetic probes are used to monitor the presence and concentration of other paramagnetic species in a system. In this way, for *in vitro* measurements, OCR is measured with the use of a soluble nitroxide spin probe, ^{15}N-PDT (perdeuterated tempone), mixed into the cell suspension (**Fig.10A-B**). This probe is oxygen sensitive, meaning the interaction between molecular oxygen in the environment and the probe due to Heisenberg spin-spin exchange induces reversible changes in its EPR spectrum linewidth. When bimolecular collisions occurring between molecular oxygen and the probe increase, EPR spectrum's linewidth increases linearly (**Fig.10C**). Using a calibration curve linking this broadening with exact % of O_2, we can quantify oxygen levels in a sample (James 1995, Diepart 2010, Jordan 2002)(**Fig.10D**). To increase the sensitivity of nitroxides to oxygen, perdeuterated nitroxides are more convenient to use, making ^{15}N-PDT a great stable and non-toxic tool to measure oxygen with high sensitivity. These oxygen measurements can also be performed *in vivo* using L-band EPR operating at lower frequency (1.1GHz compared to 9.4GHz for X-band (EPR) and using charcoals as oxygen sensitive probes, like conducted previously in our lab (Jordan 2002; Gallez, 2004).

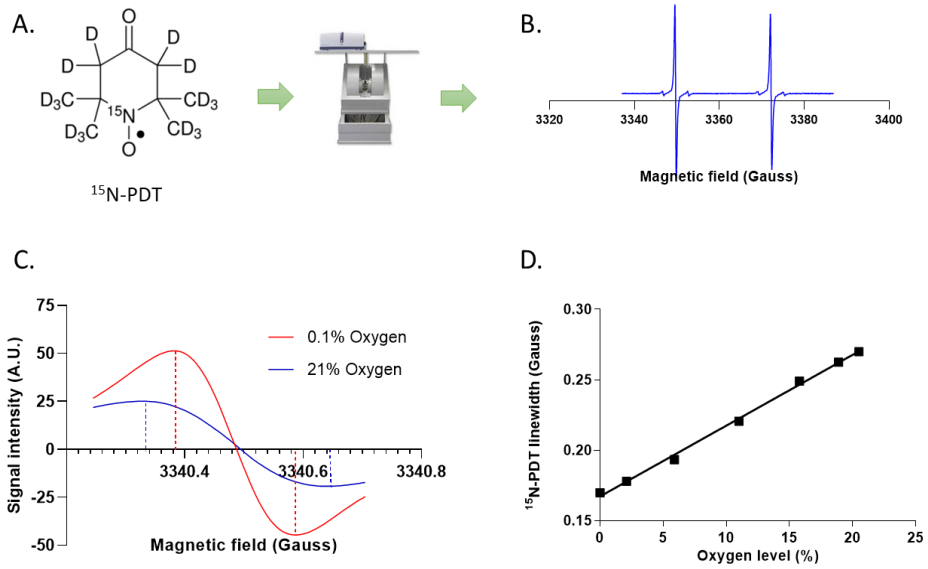

Figure 10: Experimental methodology of EPR-oximetry, from D. d'Hose 2021.
(**A**): Chemical structure of paramagnetic nitroxide ^{15}N-PDT.
(**B**): Representative global EPR spectrum of ^{15}N-PDT.
(**C**): Representative EPR spectra of ^{15}N-PDT in 0.1% and 21% of O_2 conditions.
(**D**): Calibration curve depicting the evolution of ^{15}N-PDT in function of O_2 levels.

III. Modulation of superoxide production

1. Modulators increasing mitochondrial superoxide production

As previously discussed in "modulation of the oxygen consumption", agents blocking the OCR by acting on ETC complexes can also induce superoxide production. The most known and used mitochondrial modulators to induce such increase in levels of superoxide are Rotenone (inhibitor of CI) and Antimycin A (inhibitor of CIII). At the cytoplasmic level, Phorbol 12-myristate 13-acetate (PMA) is also a well described and used agent to induce superoxide production via nicotinamide adenine dinucleotide phosphate (NADPH) oxidase (NOX) activation in phagocytic leucocytes (Forman 2002).

1.1. Rotenone

Rotenone (**Fig.11A**) is a phytotoxin extracted from the roots and stems of tropical plants *Derris elliptica*, *Lonchocarpus* and *Tephrosia* . It was extensively used as insecticide back in the 20ies and as component of many pesticides but is nowadays forbidden in the EU since 2009 because of its adverse toxic effects on humans and mammals in addition to being highly toxic to fish and insects. Rotenone mechanism of action is to inhibit CI near the ubiquinone binding site with high affinity, subsequently leading to an increased superoxide generation at the matrix side (Turrens 2003). Rotenone has therefore been extensively used to study the role of mitochondrial ETC in apoptosis and autophagy regulation (Porporato 2014, Chen 2008, Yang 2008). Because of its high lipophilicity, rotenone easily crosses biological membranes including the blood brain barrier (BBB), explaining its specific dopaminergic cell death induction *in vivo* due to increased oxidative damage (Sherer 2002, Radad 2006). Rotenone is nowadays still used to study Parkinson's disease when infused to rodents (Sherer 2003, Ravenstijn 2008, Zahra 2020).

1.2. Antimycin A

Antimycin A (AA, **Fig.11B**) is a natural metabolite produced by streptomyces bacteria. Like Rotenone, AA was used in the first place as pesticide to manage invasive fish population. In 1975, Boversis et al were the first to characterize ROS production using AA treatment on submitochondrial particles (SMPs) from rat and beef hearts (Boveris 1975). At that time, it was also detected solely at the matrix side of the SMPs (Boveris 1975, Turrens 1997). Later on, Turrens et al demonstrated that AA induced superoxide production at the ubisemiquinone site of CIII and that this production could be blocked by using stigmatellin and myxothiazol (Turrens 1985). Others reported afterwards that AA-induced superoxide production was actually bidirectional across the MIM and could also be detected at the cytosolic side of the membrane (Han 2001, Muller 2004). Nowadays, AA is also known to induce apoptosis in cells by collapsing the membrane potential, increasing ROS production and opening the permeability transition pore (PTP) to release proapoptotic proteins (Wolvetang 1994, Petronilli 2001). This was also observed in several human cancer cell lines such as human leukemia cells (HL-60), human cervical adenocarcinoma (HeLa) cells and human pulmonary adenocarcinoma (Calu-6) cells (King 2002, Park 2007, Han 2009).

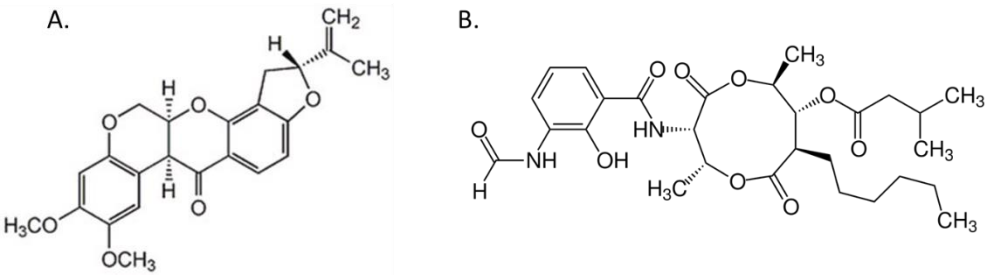

Figure 11: Chemical structure of NADH-oxidase (complex I) inhibitor, Rotenone (**A**) and cytochrome c reductase inhibitor, Antimycin A (**B**).

1.3. Paraquat

1,1'-dimethyl-4,4'-bipyridinium dichloride, also called Paraquat, is an organic heterocyclic herbicide used extensively in the United States for weed and grass control. It is however non-selective and therefore highly toxic for other living organisms, affecting many tissues such as brain, kidneys, liver and lungs. These toxicities are essentially mediated through its redox cycling process resulting in mitochondrial oxidative stress (**Fig.12**). Indeed, Paraquat enters mitochondrial matrix by a membrane potential -mediated carrier and is reduced by Complex I to a monocation free radical (PQ°+). In presence of oxygen, it is then rapidly oxidized to form superoxide, subsequently leading to the generation of other ROS and their associated deleterious effects (Dinis-Oliveira 2006). This Paraquat redox cycle was discovered to induce the death of dopaminergic neurons and therefore lead to the onset of Parkinsonian Syndrome (Greenamyre 2001). Paraquat is now commonly used as a model of superoxide production in research.

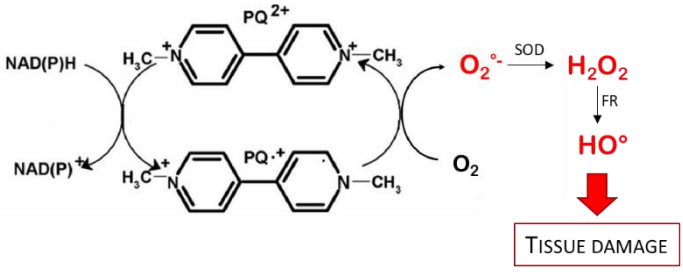

Figure 12: Schematic representation of Paraquat redox cycle and mediated toxicity.
PQ^{2+} : paraquat, $PQ^{\circ-}$: paraquat cation radical, SOD : superoxide dismutase, FR : Fenton reaction. Figure adapted from Dinis-Oliveira 2006.

1.4. Phorbol-12-myristate-13-acetate (PMA)

PMA is a tumor promotor capable of activating neutrophil function. It acts on protein kinase C (PKC), a diacylglycerol (DAG) and calcium-dependent kinase playing a major role in cellular signaling. Upon activation, PKC phosphorylates several proteins including NOX2 component p47phox (Deleo 1996, Rastogi 2016), enabling the assembly of the enzyme at the plasma membrane. When activated, NOX can produce superoxide using molecular oxygen and NADPH in order to break down phagocytosed organisms (**Fig.13**). In this way, NOX constitutes an important mechanism of host defense against invading microorganisms (Bedard 2007). PMA is nowadays still used to induce and detect a respiratory burst of superoxide production in leucocytes and macrophages (Dikalov 2011, Abbas 2014, Abbas 2016).

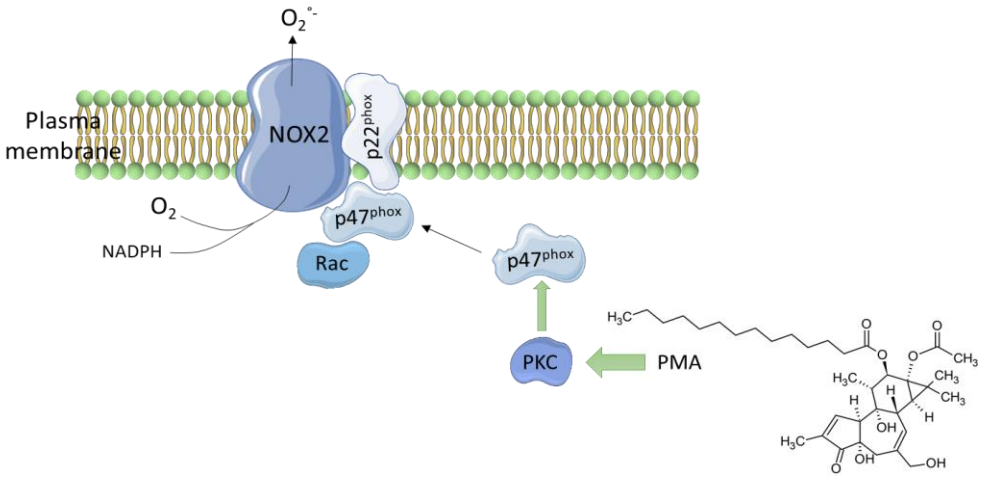

Figure 13: Schematic representation of PMA mechanism of action in activation of NADPH oxidase.
NOX2: NADPH oxidase 2, PKC: Protein Kinase C, p47phox: Neutrophil cytosol factor 1 and p22phox: Human neutrophil cytochrome b light chain.

2. Modulators decreasing mitochondrial superoxide production

2.1. Polyethylene Glycol-Superoxide dismutase (PEG-SOD)

SODs are key enzymes in the natural defense against ROS. As discussed earlier, SOD dismutates and inactivates the superoxide anion into hydrogen peroxide, decreasing in this way the superoxide cellular concentration to limit oxidative damage. When used in research experiments, SODs only target extracellular superoxide as they cannot cross cell membranes. To address this problem, Beckman *et al* synthetized cell permeable SOD by covalently conjugating polyethylene glycol (PEG) to the enzyme (Beckman 1988). They concomitantly demonstrated that PEG enhanced SOD cell penetration in endothelial cells and that preincubation was more efficient than with native enzymes. The authors also suggested binding to the membrane and endocytosis are the main mechanisms explaining the intracellular accumulation of these compounds. More than 30 years later, PEG-SOD is still used as specific control to measure the contribution of intracellular superoxide anion during EPR experiments (Dikalov 2011, Abbas 2014, Scheinok 2020).

2.2. Mitochondria targeting

Because of the implication of excessive levels of mtROS in mitochondrial dysfunction and contribution to many diseases (discussed earlier p.23-24), the development of mitochondrial-targeted probes and antioxidants to decrease damage became a major experimental and therapeutic tool. To enter the mitochondrial matrix, agents have to pass 3 membranes; the plasma membrane, the MOM and the MIM. Plasmic membrane and the MOM are both crossed more easily because they enable diffusion of large molecules (5-10kDa) though pores, whereas MIM passage is restricted to small molecules (Zielonka 2017). There are two ways to acquire matrix targeting: by potential driven force or mediated by the use of mitochondrial carriers. Whereas relying on carriers to selectively target mitochondrial matrix is limited, conjugating agents to lipophilic cations moieties such as triphenyl phosphonium (TPP^+) seems to be more promising (Murphy 2007)(**Fig.14**).

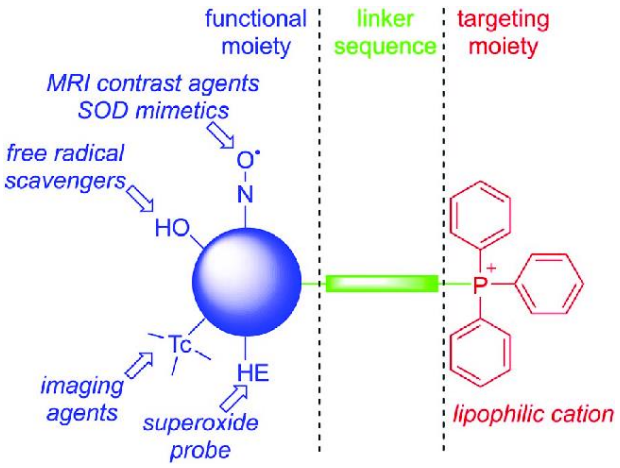

Figure 14: Typical structure of mitochondrially-targeted agents linked with triphenyl phosphonium moiety (TPP^+). Original figure from Zielonka 2017.

Mitochondrial membrane potential typically ranges around 100-150mV and is larger than other cellular membranes, resulting in the preferential accumulation of the cations into the mitochondria (100-1000 times higher than in the cytoplasm) (Smith 2003). Cellular uptake of the cations is also driven by plasma membrane potential (around 30-60mV). Also, mitochondrial-targeted compounds are accumulated preferentially in tumor mitochondria because of their higher (more negative) mitochondrial membrane potential (around 170-220mV)(Beckham 2013). Several TPP^+ linked probes and antioxidants such as MitoQ, MitoTEMPO and MitoMetformin derivates and their clinical relevance were recently reviewed (Zielonka 2017).

Metformin (dimethyl biguanide, MET) is a widely prescribed drug to lower blood glucose concentrations and improve insulin sensitivity in patients with type II diabetes mellitus (T2D). Next to its glucose lowering effect, MET also led to weight loss and reduces cardiovascular risk (Bailey 2008, Johnson 2005). Due to its positive charge, it accumulates into the mitochondrial matrix where it is known to inhibit CI subsequently decreasing ATP production as well as changing NAD^+/NADH ratios contributing to its effects on gluconeogenesis (Owen 2000, Bridges 2014). MET has also been demonstrated to have beneficial preventive (Currie 2009) and curing anti-cancer effects on diabetic patients with pancreatic cancer (Sadeghi 2012). It is also being currently repurposed as anti-cancer treatment based on its chemo-preventive properties. To improve its mitochondrial targeting and its anti-tumoral effects, several MET analogues were

synthetized and characterized. Thanks to the TPP^+ moiety, $MitoMET_{10}$ was proven to be 1000 more effective than MET in inhibiting pancreatic ductal adenoma cell (PDAC) proliferation *in vitro* and *in vivo* when used alone and in combination to radiation therapy (Cheng 2016). This effect could likely be attributed to the ROS-dependent AMPK pathway activation (Hwang 2014). Improved radiosensitivity could however also be explained by the increased tumor oxygenation due to $MitoMET_{10}$-induced OCR inhibition (Song 2012, Cheng 2016).

3. *In vitro* methods to measure superoxide production

Because of their low concentration and instability in biological media, radical species are complicated to measure in a sensitive and specific way. With increasing research interest linking production to many disorders, different techniques to detect those ROS (and more specifically superoxide) emerged and are still used at this day.

3.1. Chemiluminescent probes

Chemiluminescence is based on the detection of light emission after a chemical reaction between the probe and a ROS. The emitted photons are then detected by a luminometer or scintillation counter.

Lucigenin (bis-N-methylacridinium nitrate) and luminol (5 amino-2,3-dihydro-1,4-phthalazinedione) are the most common chemiluminescent probes used for the detection of ROS and superoxide in biological samples. Those probes react with ROS to transform into an electronically excited intermediate and emit a photon after returning to the ground state. In this way, luminol free radical reacts with superoxide and transforms into an unstable endoperoxide which produces a photon after returning to the ground state. However, luminol is not a specific indicator of superoxide as it reacts with various ROS (Kobayashi 2001) such as hydrogen peroxide, hydroxyl radical and peroxinitrite (ONOO-). Lucigenin reacts with superoxide to produce dioxane, emitting a photon after breaking down.

Despite their extensive use in research to monitor real time cellular superoxide with reasonable sensitivity, these probes are prone to auto-oxidation, overestimating the superoxide production due to redox cycling (Kalyanaraman 2012).

3.2. Fluorescent probes

Hydroethidine (HE, or dihydroethidium) and its mitochondrial-targeted derivative MitoSOX Red are also widely used probes to measure intracellular and mitochondrial superoxide, respectively. Those fluorogenic probes react with superoxide to form a red fluorescent product, 2-hydroxyethidium (2-OH-(mito-)E^+), initially believed to be the only product generated (**Fig.15**).

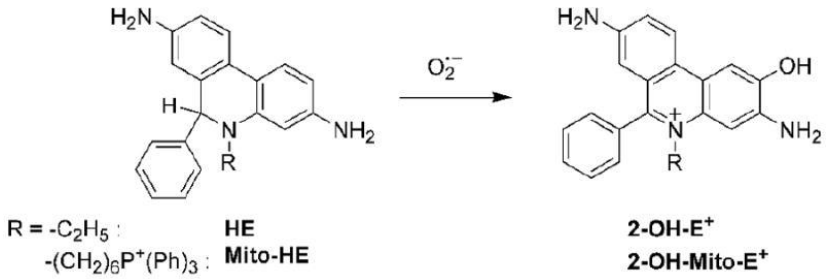

Figure 15: Structures of hydroethidine (HE) and its product hydroxyethidium (2-OH-E^+). Original figure from Zielonka 2010.

Many reports demonstrated the formation of nonspecific oxidation and dimerization products such as ethidium (E^+), diethidium (E^+-E^+) and HE-HE in the presence of other oxidants (Zielonka 2008, Zhao 2005, Kalyanaraman 2012) (**Fig.16**). Furthermore, those products have overlapping fluorescence spectra and E^+ tend also to be present at a higher concentration than 2-OH-E^+, making it impossible to measure relative concentration for 2-OH-E^+ (Zhao 2005) (**Fig.17**). However, high performance liquid chromatography (HPLC) profiles of 2-OH-E^+ and E^+ are well resolved and separated (Zielonka 2010, Kalyanaraman 2014). Fluorescence superoxide measurements should therefore be coupled to HPLC of Mass spectrometry (MS) to dissociate both products. Another limitation of this technique includes HE light sensitivity, generating E^+ due to photooxidation.

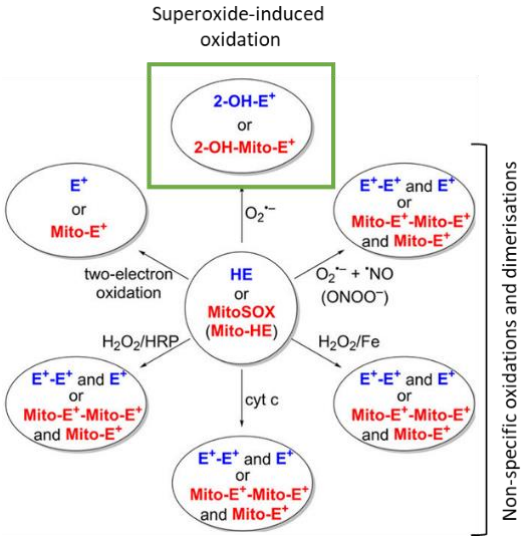

Figure 16: Oxidation products of HE (Blue) and Mito-HE (Red). Adapted from Kalyanaraman 2017.

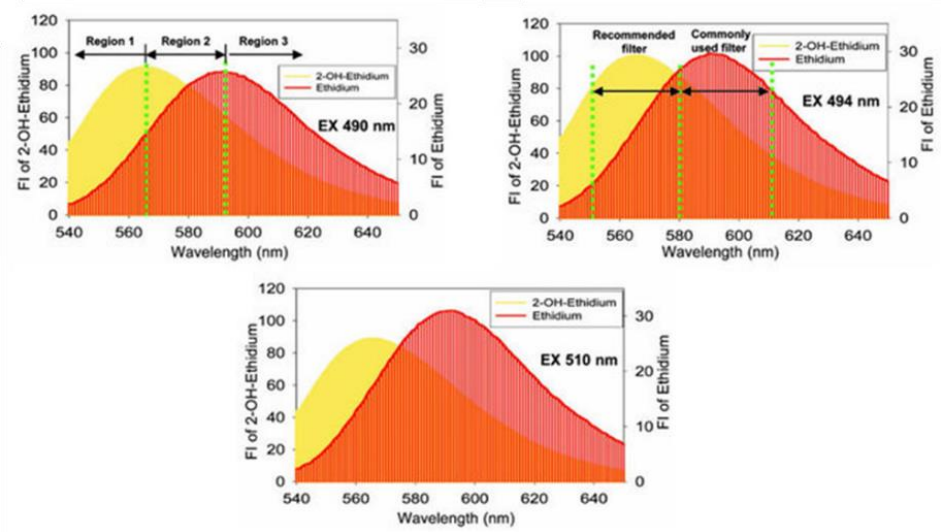

Figure 17: Fluorescence spectra of 2-hydroxyethidium (2-OH-E$^+$) and ethidium (E$^+$) according to different excitation wavelengths. Adapted from Kalyanaraman 2017.

3.3. X-band EPR – In vitro

Despite the high sensitivity of the EPR method to measure free radicals, it is possible to detect them directly only if they are stable enough and present in sufficiently high concentration in the biological media. Most biological radicals including superoxide have a too short half-life and exist around pico-nanomolar range (Hawkins 2014). Therefore, probes are used to react with those undetectable species to enhance their detection. Commonly used probes are spin traps, nitroxide and hydroxylamine spin probes (Scheinok 2018).

As discussed previously, EPR technology enables the detection of species with unpaired electrons, also referred to as "paramagnetic species". Spin traps (nitrones & nitroso compounds) are diamagnetic sensors, meaning they are not visible with EPR but can become paramagnetic when reacting with short-lived radicals. Those sensors react with the free radical by covalent bond formation, making a longer-lived detectable adduct with specific EPR signature depending on the trapped species. An example of a nitrone spin trap is 5-diisopropoxyphosphoryl-5-methyl-1-pyrroline N-oxide (DIPPMPO), enabling the detection of superoxide anion and hydroxyl radical. Spin traps' efficiency in trapping superoxide was measured on whole cells (Abbas 2014) as well as in intact mitochondria (Hardy 2007). Spin traps can also be linked with a TPP^+ moiety to target mitochondrial ROS. Despite their ability to trap superoxide, linear nitrone spin traps form a superoxide adduct that is still very unstable and remains undetectable with EPR (Bacic 2008). Nevertheless, cyclic nitrones are able to form more stable superoxide adducts and their use is therefore preferable. However, spin traps are facing some limitations in detecting ROS and superoxide in general compared to nitroxide and hydroxylamine spin probes. Spin traps react in multiple reactions with superoxide and at a low rate compared to cellular antioxidants, which can induce artefacts when detecting this species. The spin adduct's stability also depends on multiple factors such as temperature, pH and used solvent (Tordo 1998). Spin traps are also used at higher concentration to compete with cellular antioxidants and commonly added scavengers (EDTA, DTPA) and consequently are more toxic than hydroxylamines. In this way, hydroxylamine spin probes meet those needs by being less toxic, more stable and reliable to measure ROS and superoxide production.

Hydroxylamines are diamagnetic species turning into stable nitroxides (=paramagnetic species) when oxidized by cellular ROS. They do not bind to radicals unlike spin traps, making them

more stable. Rapid oxidation occurs with superoxide whereas it reacts slowly with H_2O_2 and organic peroxides (Dikalov 2011). They are not specific to certain ROS but with the use of specific scavengers, their contribution to the hydroxylamine oxidation can be monitored. In this way, the use of cell-permeable poly-ethylene glycol conjugated SOD inhibits the EPR signal of the probe by limiting its oxidation by superoxide (Dikalov 2018). Therefore, superoxide measurement is the major field of application using hydroxylamines. Cyclic hydroxylamines such as CMH and MitoTempo-H also emerged, giving highly stable nitroxides and a high reactivity due to its cell permeability. Recently, our lab demonstrated that those 2 cyclic hydrolylamines are the most sensitive probes to measure ROS and superoxide in biological samples when used with the appropriate control (Scheinok 2018). Different EPR ROS-sensors are represented on **Fig.18**.

While each EPR approach has its own merits and limitations, in the thesis, we have selected cyclic hydroxylamines as ROS sensor because they offer the highest sensitivity. While their oxidation into nitroxides is not specific to superoxide, the use of SOD (extracellular) or PEG-SOD (intra- and extracellular) as controls provide the contribution of superoxide to the nitroxide formation.

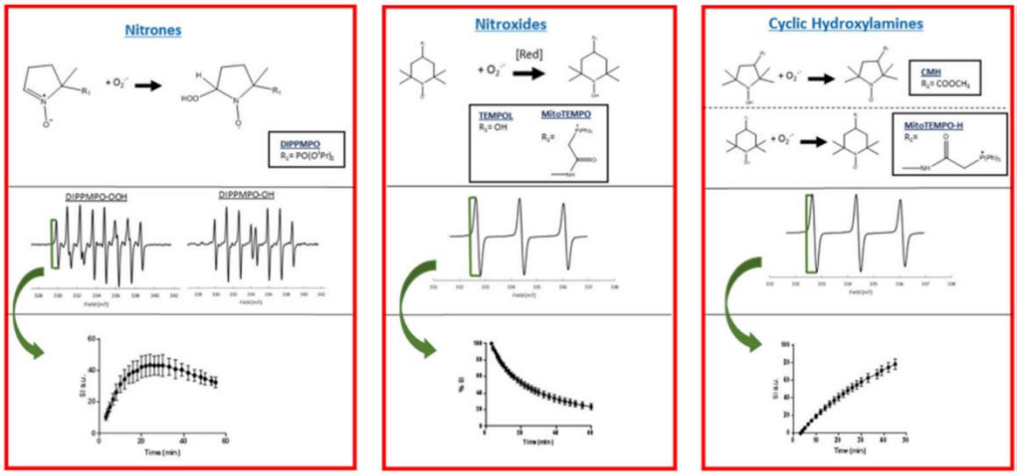

Figure 18: Structures, EPR spectra and evolution of EPR signal intensity of different types of EPR-ROS sensors. Adaped from Scheinok 2018.

IV. Inhibitors of the succinate dehydrogenase (SDHIs)

1. Succinate dehydrogenase (SDH)

1.1. Structure & functions

Succinate dehydrogenase, also referred to as succinate: ubiquinone oxidoreductase (SQR) is a crucial enzyme embedded in the MIM playing a role both in the Krebs cycle and the mitochondrial electron transport chain as complex II. By oxidizing succinate into fumarate within the Krebs cycle (SDH part of the enzyme), it drives electron transfer through its redox factors to reduce ubiquinone (SQR part of the enzyme). SDH is also the only respiratory complex which does not pump out protons to the IMS and therefore is not contributing to the generation of the electrochemical gradient which drives ATP synthesis.

Eukaryotic SDH is formed by 4 distinct subunits (sdhA, sdhB, sdhC and sdhD) encoded entirely by the nuclear genome, compared to other respiratory complexes composed of a mix of subunits encoded by nuclear DNA and mtDNA (Cecchini 2003)(**Fig.19**). Its structure consists of a hydrophobic tail rooted into the MIM (sdhC and sdhD = SDQ part) and a hydrophobic head protruding into the matrix (sdhA and sdhB = SDH part)(Yankovskaya 2003). SdhA (Flavoprotein) is the site where electron transport starts and contains the covalently-linked cofactor flavin adenine dinucleotide (FAD). After succinate dehydrogenation at the FAD-site, electrons are transferred through the 3 iron-sulfur clusters ([2Fe-2S], [4Fe-4S], and [3Fe-4S]) of SdhB to ubiquinone at the anchoring subunits sdhC and sdhD, also referred to as cytochrome bL and bS, linked by a heme b. This heme does not take part in this redox center chain because electron transfer is branched at [3Fe-4S] jumping either on ubiquinone or heme b. However, electron transfer to ubiquinone is favored because of its higher redox potential compared to heme b (+100mV and 36mV respectively). With electron density techniques, ubiquinone binding site was assigned in a pocket of residues derived from SdhB-C and D (Yankovskaya 1996). To this day, the structure of SDH from different species has been investigated and obtained, and showed similar architectural arrangements, electron transfer pathways and even the Q-binding sites among prokaryotes and eukaryotes (Zhou 2011).

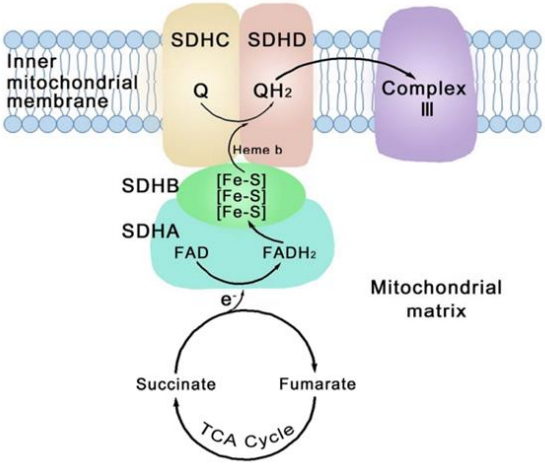

Figure 19: Structure of succinate dehydrogenase enzyme (SDH) constituted of 4 subunits; sdhA, sdhB, sdhC and sdhD. Original figures from Moosavi 2019.

1.2. SDH & apoptosis

The link between complex II dysfunction and induction of apoptosis was made several years ago by analyzing neurodegenerative diseases with sdhA mutations (Hwang 2014). Several studies on neuronal cells reported pro-apoptotic effects after CII inhibition with thenoyltrifluoroacetone (TTFA) and 3-NP. Indeed, SQR activity is reduced before apoptosis resulting in complex II inhibition and altered electron flow (Lemarie 2011, Albayrak 2003). Electrons then react with molecular oxygen, producing ROS, and more specifically superoxide, which eventually trigger cell death by increasing oxidative damage (Lemarie 2011, Ishii 2005).

Several studies demonstrated also that apoptosis induction could be mediated by sdhA and B dissociation from SQR through intracellular acidification (Lemarie 2011, Hwang 2010). When released into the mitochondrial matrix, SDH and SQR enzymatic activities are uncoupled, increasing electron leak and ROS generation and subsequently resulting in apoptosis due to excessive oxidative damage (Circu 2010).

1.3. Alterations of SDH & consequences

Complex II-related diseases are rare but are associated with a wide panel of clinical phenotypes usually associated with neurological impairments with or without muscular involvement (Rustin 1997). However, sdhA mutation show different clinical phenotypes than sdhB, C and D mutations. SdhA mutations present similarities with deficiencies in mitochondrial and Krebs cycle genes giving Leigh syndrome, leukodystrophy and optic atrophy, whereas other subunit mutations are more characterized by the induction of specific slow growing neuroectodermal tumors such as hereditary paraganglioma and pheochromocytoma (Baysal 2001, Gotlieb 2005, Rutter 2010) (**Fig.20**).

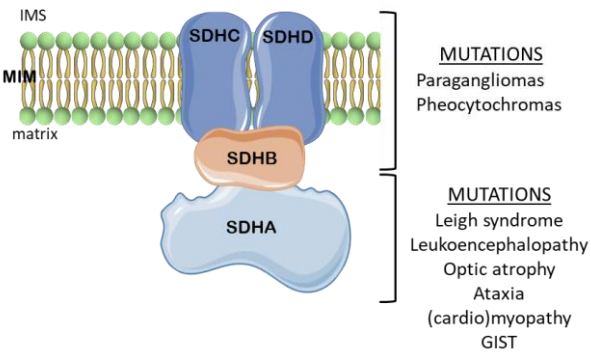

Figure 20: Schematic representation of succinate dehydrogenase subunits and their associated diseases when mutated.

The genes encoding for the sdhB,C,D subunits are therefore considered as mitochondrial tumor suppressors, showing loss of function mutations in tumors. Truncated proteins induce complex II assembly problems, hence preventing electron transport functions, impairing quinone binding and subsequently lead to TCA cycle dysfunction. This tumorigenesis can be explained by the overlapping of different mechanisms; the activation of pseudohypoxia by major ROS production and decreased programmed cell death (Gottlieb 2005).

Pseudohypoxia is characterized by the induction and stabilization of HIFα in normoxic conditions, stimulating genes that favor aerobic glycolysis, neovascularization and block

apoptosis. In this way, cells are able to survive stressful environments and get sufficient nutrients from increased blood supply. It is well established that blocking respiratory complexes including Complex II increases generation of ROS (Quinlan 2012). Those ROS participate in tumorigenesis by inducing nuclear DNA mutagenesis but also by stabilizing HIFα by prolyl hydroxylase (PHD) inhibition (Chandel 2000). It was also reported that succinate accumulation following SDH inhibition leads to PHD inhibition in the cytosol and HIF activation (Selak 2005, King 2006).

Enhanced glycolysis in tumors under aerobic conditions is nowadays a well-established feature of cancer. This phenomenon can be induced either by blocking mitochondrial metabolism or enhancing glycolysis. OXPHOS can be blocked by mtDNA mutations or Krebs cycle dysfunction and glycolysis can be promoted by oncogenes and HIF transcription factor. In some tumors presenting sdh subunits mutations, HIF pathway is activated, leading to angiogenic responses which explains the high vascularization in paragangliomas (Gimenez-Roqueplo 2001). Increased expression of "HIF signature" glycolytic genes was also reported when profiling phaeochromocytomas with sdhB and D mutations (Dahia 2005).

Selak et al was one of the first to demonstrate that succinate accumulation due to SDH dysfunction is used as a cellular messenger (Selak 2005) to modulate metabolism. When produced in large excess and leaked to the cytosol, succinate is able to stabilize HIF by inhibiting its prolyl hydroxylation, a specific tag for proteasomal degradation (Selak 2005, Pollard 2005). Prolyl hydroxylases actually use α-ketoglutarate and oxygen (with ferrous iron and ascorbate as cofactors) to convert prolyl residues on target proteins. Another product of this reaction is also succinate. Therefore, when succinate accumulates, PHD undergoes inhibition feedback, resulting in high HIF activity. By oxidizing its cofactors, ROS are also capable of inhibiting PHD activity. HIF activation is also known to enhance resistance to apoptotic signals (Lee 2005).

1.4. Succinate as oncometabolite

Due to its excessive accumulation following SDH mutation and TCA cycle dysfunction, succinate is known to drive cancer progression by remodeling tumor microenvironment. At this day, succinate is found in excessive levels in multiple types of cancers presenting SDH mutations such as renal carcinomas, thyroid cancers, pituitary tumors, paragangliomas and gastrointestinal tumors (Tretter 2016, Xekouki 2012, McWhinney 2007). Also, succinate is found at a concentration of 5 μM in blood samples of healthy patients, while it can exit cells and accumulate to 150 μM in plasma or urine in pathological conditions (Tretter 2016, Tannahil 2013). Increased plasma succinate is a common finding in patient presenting pathogenic mutations in PTEN, sdhB and sdhD (Hobert 2012). With ^{1}H-NMR spectroscopy-based metabolomic profiling, succinate was also found accumulated in feces of I/II stage (early stage) colorectal cancer patients compared to healthy patients (Lin 2016). In this way, succinate can be used as a useful biomarker for cancer screening and monitoring, while being less expensive than gene profiling.

1.5. Targeting SDH as part of anticancer therapy

Surgical removal, radiation therapy and chemotherapy are standard treatments used for cancers such as paragangliomas linked to SDH mutation. However, each have their own limitations and efficiencies. With the increasing understanding of SDH and succinate oncometabolite roles in metabolic pathways, new targeted molecular therapies were developed.

Because of succinate clear effects on angiogenesis via HIF activation and VEGF stimulation (Favier 2010), antiangiogenic therapies came on useful. Paragangliomas (PGL) and pheochromocytoma (PCC) cancers are indeed presenting high vascularization linked to VEGF overexpression (Salmenkivi 2003). These therapies target VEGF pathway by using anti-VEGF antibodies (Bevacizumab), tyrosine kinase inhibitors (Sunitinib or Sorafenib) or mTOR inhibitors such as Everolimus (RAD001). Sunitinib has already proven its efficiency for the treatment of advanced renal cell carcinomas and gastrointestinal stromal tumors (GIST). It is also currently assessed in patients with PGL and PCC cancers in a phase III clinical trial (FIRSTMAPPP) (https://clinicaltrials.gov/ct2/show/study/NCT01371201).

Others therapies target mtROS, increasing their production to induce cellular damage and apoptosis. Among them, α-Tocopheryl succinate (α -TOS), a vitamin E analogue lacking its

antioxidant activity, is capable of selectively killing malignant cells. Several studies demonstrated its pro-apoptotic properties in Jurkat T lymphoma, human colon cancer (Neuzil 1999, 2001) as well as hematopoietic, lung and breast cancer cells lines (Neuzil 2001b). The molecular mechanism underlying α-TOS-mediated apoptosis is explained by its hydrophobic nature, residing in cellular membranes where it activates PP2A phosphatase. In turn, PP2A inactivates PKC by dephosphorylation, leading to impaired cell cycle progression. Concomitantly, it dephosphorylates the anti-apoptotic proteins of Bcl-2 family (Bax & Bac), resulting in a pore formation in the MOM (Wei 2001). It is also believed to destabilize subcellular compartments such as mitochondria and lysosomes (Neuzil 2006), increasing ROS production (Ottino 1997), and releasing cytochrome c to form the apoptosome (Mignotte 1998). α-TOS can also act on complex II inducing ROS accumulation (Dong 2009), promoting apoptosis by MOM permeabilization (Prochazka 2010).

The addition of a triphenylphophonium (TPP^+) moiety to α -TOS is also used to target CII more efficiently. Indeed, TPP^+ enables the mitochondrial accumulation of the agent (MitoVES) at a concentration which is 1000 times more important than in the cytosol (Murphy 2007). In the same way as α -TOS, MitoVES interacts with the ubiquinone binding-site (Qp) at CII, leading to an increase in ROS generation which causes membrane permeabilization through BAX/BAK proteins pore formation (Kluckova 2012, Dong 2011). MitoVES is 20 to 50 times more efficient in inducing apoptosis than α -TOS thanks to its specific mitochondrial targeting (Dong 2011). However, due to its localization in mitochondria, MitoVES cannot destabilize other structures (lysosomes) like α -TOS, explaining why it did not induce apoptosis in Jurkat cells lacking Bax/Bak proteins (Dong 2011).

Other potential anticancer agents such as 3-bromopyruvate, troglitazone and lonidamine also demonstrated inhibitory effects on SDH activity, inducing apoptosis mediated by increased ROS generation (Dalla Pozza 2019). However, 3-bromopyruvate and troglitazone induce secondary neuronal and hepatic toxicities on normal cells and could therefore not be used as anticancer therapies despite their proapoptotic effect on malignant cells.

2. Inhibitors of SDH (SDHI) fungicides

Fungicides are specific types of pesticides used to prevent or limit the development of fungal diseases (i.e. rust, mildew and blights) damaging plants and crops. These diseases have a major economic impact on yield and quality of harvests, and could also generate natural mycotoxins in food, having adverse effects on humans and animals (Zain 2011). Fungicides also prevent blemishes on edible parts of the crops or their leaves, which are needed for photosynthesis. Storage life of fruits, vegetables and tubers after harvest is also increased when using fungicides. They are therefore important tools to manage plant diseases.

SDHI form a distinctive group among fungicides because of their specific mode of action inhibiting SDH. They are extensively used on grapes, cereals, colza and many fruit/vegetables cultures. Despite their great benefits in agriculture, SDHI's use is severely debated at this day as they were suggested to be non-specific for fungi and can also act on the SDH of other eukaryotes such as humans, lumbric and bees (Bénit 2019).

2.1. SDHI in agriculture and environment

SDHI fungicides are widely used for the prevention of plant diseases and molds on various seeds and crops such as cereals (wheat, barley), colza, fruit (strawberries, apples, melon) and vegetables (salads, carrots and leek). As listed in 2018 by the French Agency for Food, Environmental and Occupational Health & Safety (ANSES), 224 commercialized pesticide products containing one or several SDHI were identified from whom 156 are still accepted and used in France (Ref EPHY-ANSES). According to the results of 2017's investigation led by the Direction générale de la concurrence, de la consommation et de la répression des fraudes (DGCCRF) on EU vegetal food samples, more than 50% were detected with residual rates of pesticides from whom 2,3% were actually above the maximal accepted limit level. 7,3% of these residues were SDHI.

Among the known SDHI used today, the European Food Safety Authority (EFSA) reported in 2017 that Boscalid was the most found pesticide in food samples tested in Europe. Boscalid (2-chloro-N-(4'-chloro[1,1'-biphenyl]-2-yl)pyridine-3-carboxamide) has also been detected in multiple varieties of bee matrices and water samples: up to 9,8ng/g in bumblebees, 38ng/g in pollens and 2,3ng/g in honey samples (David 2016, jabot 2016) and up to 36 µg/L in main coastal estuaries in California (Reilly 2012). As a result of water pollution, Boscalid could be

capable of impacting health of aquatic non-target organisms and humans due to foodchain (Munze 2017). In the same list of compounds from ANSES discussed above, Boscalid is found in 43 commercialized products among which only 4 are forbidden whereas Boscalid was supposed to be drawn of the market in summer 2018 (ANSES). This deadline was elongated to July 2021 but nothing has moved since.

2.2. Mode of action

The first class of SDHI fungicides (Carboxamides) saw the light more than 50 years ago and was shown to only manage a narrow spectrum of plant pathogens; primarily controlling *basidiomycota* (Schmeling 1966). It wasn't until 2003, with the synthesis of Boscalid, that SDHI fungicides reached a broader foliar spectrum of activity, acting on *basidiomycota* as well as *adel oomycota* and *ascomycota* (Stammler 2007). Nowadays, SDHIs are the most fast-growing class of fungicides in term of new compound development and use on the market because of their high efficiency and the lack of proper and strong alternative options. Indeed, Fungicide Resistance Action Committee (FRAC) is currently listing 20 different SDHI fungicides including "new generation" SDHIs like Boscalid and Bixafen displaying more complex chemical structures (**Fig.21**).

SDHIs have their own specific mode of action compared to other fungicides used in crop protection. Like stated by their name "succinate dehydrogenase inhibitors", SDHI block fungi respiration and energy production by acting on the ubiquinone binding site (Qp) of the SDH, inhibiting in this way fungi development and sporulation. The Qp site is structurally defined by residues derived from SdhB-C and D (Yankovskaya 1996) proximal to the [3Fe–4S] cluster and heme b. These regions are also demonstrated to be highly conserved between bacteria and eukaryotes (Yankovskaya 2003, Sun 2005). Upon binding, SDHI block access to the substrate and its reduction, subsequently preventing further succinate oxidation.

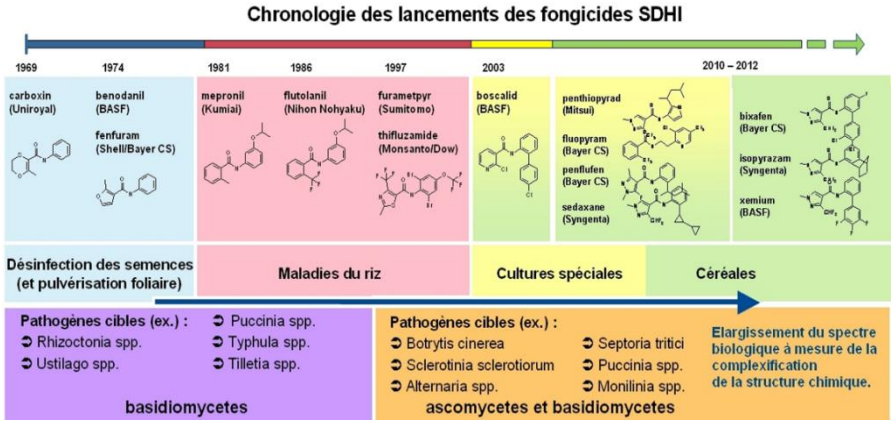

Figure 21: Chemical structures of SDHI compounds through the years. Figure originates from *Terre.net.*

2.3. Specificity

Although SDH is a central and universal component of the mitochondrial ETC in any living organisms, SDHI were long considered to be specific for fungi. As discussed earlier, SDHI binding regions are also strongly conserved in eukaryotes during evolution. Therefore, exposition to these fungicides could also be affecting non-targeted organisms.

Zebrafish share 70% of human protein-coding genes and 84% of genes are known to be associated with human diseases, making them perfect models to assess human health risk and predict developmental issues after exposure to an environmental agent (McGrath 2008). Recently, a study reported developmental deformities and histopathological changes as well as abnormal apoptosis induction in zebrafish embryos after Boscalid exposure (Qian 2018). Later on, the same team demonstrated Boscalid-induced gender specific alterations and adverse effects on reproduction (Qian 2020). In the same model, Boscalid was also demonstrated to induce neurodevelopment defects (measured with tail coiling frequency) and neurotoxicity *via* oxidative stress (Wang 2020). This increase in oxidative stress is also found in other eukaryotic organisms such as *chlorella vulgaris* algae (Qian 2018b). In the same way, Bixafen, another new generation and soil-persistent SDHI was also found to induce developmental delay and cardiac toxicity in zebrafish embryos (Li 2020, Yuan 2021).

In 2019, the team of Rustin demonstrated the adverse effects of 8 new generation SDHI on the SDH activity in honeybees, earthworms and human (embryonic kidney HEK293) cell lines (Bénit 2019). The IC50 of the SDHI (concentration necessary to inhibit 50% of SDH activity) was measured by spectrophotometry. They also reported that those different eukaryotic cell lines were more sensitive to the newer generation SDHI like Boscalid, Bixafen and Fluxapyroxad. In addition, Bixafen and Isopyrazam IC50 were less than 1µM in human cells, revolving importantly around the possible accumulated SDHI doses in humans. They also highlighted an increase of SOD activity after SDHI exposure, potentially revealing increased oxidative stress after SDHI exposure. At last, *in vitro* experiments performed on human peripheral blood lymphocytes with SIGNUM, a commercialized pesticide cocktail containing Boscalid and Pyraclostrobin, showed genotoxic and cytotoxic effects after exposure (Cayir 2014).

V. Statins as potential radiosensitizers

Inhibitors of 3-hydroxy-3-methylglutaryl-coenzyme A (HMG-CoA) reductase, also known as "statins" are widely prescribed drugs with lipid-lowering properties. By reducing endogenous cholesterol synthesis in dyslipidemia patients, statins became key players in the prevention of cardiovascular diseases (Chopra 2007, Young 2009, Ludman 2009).

1. Development & classification of statins

At the end of the 1970s, the first statin (now called Lovastatin) was isolated from as fungal metabolites from *Aspergillus terreus* (Alberts 1980). The drug was shown to dramatically decrease plasma low-density lipoprotein (LDL) in animals but also in patients with severe hypercholesterolemia without tumor induction nor severe side effects (Kuroda 1979, Tsujita 1979, Mabuchi 1981). Since then, 6 other analogs were put on the market, namely Simvastatin, Pravastatin, Rosuvastatin, Fluvastatin, Atorvastatin and Pitavastatin. At that time, Cerivastatin also saw the light but was withdrawn from the market in 2001 because of drug-induced rhabdomyolysis and kidney failure (Furberg 2001). All 7 statins are now classified according to their synthesis, liver metabolism, physico-chemical properties and specific activity (Lennernas 1997) (**Table 1**). Lovastatin, Simvastatin and Pravastatin are naturally obtained from fungal fermentation whereas the others have synthetic origins. Lovastatin, Simvastatin and Pravastatin share therefore a common naphthalene ring structure. Pravastatin is the most hydrophilic statin

of all and Fluvastatin has intermediate properties compared to the 4 others being lipophilic. All statins are administered orally in their active form except for Simvastatin and Lovastatin given in the lactone form (prodrug).

Table 1: Pharmacokinetics of HMG-CoA reductase inhibitors, from Saito 2009.

Statin	Pitavastatin	Atorvastatin	Fluvastatin	Lovastatin	Pravastatin	Rosuvastatin	Simvastatin
Molecular weight	881	1209	433.5	405	446.5	1001	418.15
Origin	Synthetic	Synthetic	Synthetic	Microbial	Semi-synthetic (microbial origin)	Synthetic	Semi-synthetic (microbial origin)
Racemic	No	No	Yes	No	No	No	No
Prodrug	No	No	No	Yes	No	No	Yes
Log *P*	1.49	1.11	1.27	1.70	−0.84	−0.33	1.60
Absorption (%)	80	30	98	31	37	50	65–85
Hepatic excretion (%)	NA	>70	68	>70	66	90	78–87
Bioavailability (%)	>60	12	10–35	<5	17	20	<5
Effect of food on bioavailability (%)	No	Yes (↓ 13)	Yes (↓ 15–25)	Yes (↑ 50)	Yes (↓ 30)	No	No
Protein binding (%)	96	>98	>98	96–98.5	43–54	88	>95
T_{max}	0.5–0.8	2.0–4.0	0.5–1.5	2.8	0.9–1.6	3	1.3–2.4
$T_{1/2}$	11	11–30	0.5–2.3	2.5–3.0	0.8–3.0	20	1.9–3.0
Renal excretion	<2	2	6	30	60	10	13
50% inhibitory concentration (nmol/L)	6.8	15.2	17.9	2.7–11.1	55.1	12	18.1
Lipid-lowering Metabolites	No	Yes, active	Yes, mainly inactive	Yes	Yes, mainly active	No	Yes
Range of dose (mg)	1–4	10–80	20–80	10–80	5–40	5–80	5–80
CYP isoforms primarily involved with metabolic pathway	CYP2C9 Minimally	CYP3A4	CYP2C9	CYP3A4	CYP3A4 Minimally	CYP2C9 Minimally	CYP3A4

2. Lipid-lowering effects

2.1. Cholesterol reduction

Cholesterol is a sterol constituting biological membranes, modulating its fluidity. It is also the precursor of vitamin D, bile acids and steroid hormones such as progesterone, testosterone, estradiol, and cortisol. Our body's cholesterol levels can come from dietary sources or by synthesis in the liver, contributing respectively for about 30 and 70% of daily cholesterol needs.

Cholesterol biosynthesis is a multienzymatic pathway taking place in the cytoplasm and endoplasmic reticulum (ER) of cells (**Fig.22)**. It begins with the conversion of Acetyl-CoA coming from the mitochondria, into HMG-CoA thanks to HMG-CoA synthase. HMG-CoA is then irreversibly reduced into Mevalonate by the HMG-CoA reductase. Afterwards, Mevalonate is transformed into isoprenoids such as isopentenyl pyrophosphate (IPP) after multiple phosphorylation and decarboxylation. The next reactions generate squalene and sterols, from which cholesterol is conversed.

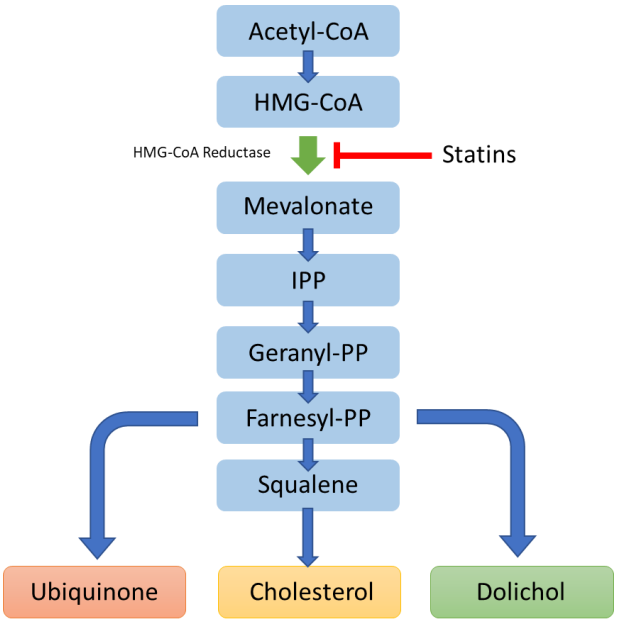

Figure 22: Schematic representation of cholesterol biosynthesis and related pathways. Inspired and adapted from Tobert 2003.

Statins inhibit the HMG-CoA reductase, the rate-limiting step in the synthesis of cholesterol. Statins' structure resembles the enzyme's natural substrate and, in this way, reversibly compete with it by changing the conformation of the binding site. Statins also have a higher affinity (nanomolar range) for the enzyme than Mevalonate (micromolar range) making them very efficient drugs (Istvan 2001). By binding specifically to HMG-CoA reductase, hepatic cholesterol levels decrease, leading to an increase in hepatic LDL receptors (LDL-R) promoting uptake of circulating LDL. This LDL reduction (up to 55%) due to statin treatment is strongly associated with decreased rates of cardiovascular events (Law 2003, Baigent 2010, Mihaylova 2012). The same efficacy is seen on triglycerides levels (Branchi 1999).

Next to the synthesis of cholesterol, the mevalonate pathway is also crucial for the production of other products such as ubiquinol (Coenzyme Q, CoQ_{10}), heme and isoprenoids. Although statins are very efficient drug to lower cholesterol, they do not work selectively. Indeed, several studies demonstrated the impact of statins on the CoQ_{10} levels in plasma and tissues of patients with up to a 50% decrease (Folkers 1990, Rundek 2004, Kawashiri 2008). The same trend (30% decrease) was also found in human muscle biopsies after simvastatin treatment (Paiva 2005). Because of CoQ_{10} central role in electron transport and energy production, this could explain the statin-induced muscle damage and myopathies identified in some cases (Tomlinson 2005, Mohaupt 2009)

2.2. Prenylation

Mevalonate is also the precursor of isoprenoids proteins such as farnesyl pyrophosphate (FPP) and geranylgeranyl pyrophosphate (GGPP) intermediates. They are crucial for posttranslational modification of signaling proteins such as the family of Rho-GTPases (small guanosine triphosphate-binding proteins) by isoprenylation (Hall 1998). This modification enables to activate the targeted proteins from their cytosolic state to membrane bound state. In this way, proper sub localization and intracellular trafficking is performed via covalent attachments to cell membranes. Small GTPases such as Ras, Rac and Rho are known to control actin cytoskeletal changes, microtubules and cell cycle progression (Takai 2001). FPP modifications are necessary for the localization of Ras proteins whereas GGPP is needed for Rho, Rab and Rap proteins (Van Aelst 1997).

3. Pleiotropic effects of statins

3.1. Statins & cardiovascular function

Next to its lipid lowering effects, statins also display numerous side effects, referred to as "pleiotropic effect". With their anti-inflammatory, anti-oxidant, anti-platelet and anti-fibrotic properties, statin treatment plays an important role in cardiovascular protection. Although mechanisms have not entirely been elucidated, several studies suggest the modulatory role of statins on endothelial nitric oxide synthase (eNOS) (Brouet 2001, Di Napoli 2001, Di Napoli 2005, Feron 2001, Ito 2010). In this case, vasodilatory actions, anti-inflammatory and anti-platelet properties linked to statin use could be directly mediated by nitric oxide (NO) generation.

NO, or also known as endothelium-derived relaxing factor (EDRF), is a molecule produced by the conversion of L-arginine in the endothelium of vessels by eNOS, regulating the vascular tonus and bloodflow. Before activation, eNOS are localized in caveolae due to caveoline-1 inhibition. In response to shear stress or vasodilators, released levels of Calcium (Ca^{2+}) displace Calmodulin (CaM) from calveolin-1, further activating eNOS. This activation process involves several co-factors such as NADPH and tetrahydrobiopterin (BH4). In turn, NO diffuses freely to vascular smooth muscle cells inducing relaxation via guanylate cyclase (GC) activation and cyclic guanosine monophosphate (cGMP) production. The eNOS signaling pathway and its activation is shown in more details on **Fig.23.** Vascular endothelial dysfunction is defined by an imbalance between vasodilatation and vasoconstriction. This occurs when the production and bioavailability of NO decreases, initiating processes promoting other cardiovascular events such as atherosclerosis, heart failure and myocardial infarction (Davignon 2004, Carnicer 2013, Erdmann 2013). This reduction in NO bioavailability can be explained by the inactivation or decreased expression of eNOS but also by the interaction of ROS with NO forming peroxynitrite ($ONOO^-$).

Endothelial function improvement is commonly associated with reduction in blood cholesterol levels. The beneficial effects of statins on CV events were therefore often attributed to their effect on cholesterol reduction. However, several studies demonstrated that the beneficial effects of statin treatments on endothelial function were already found before significant impact on cholesterol levels (O'Driscoll 1997). Furthermore, when comparing statin treatment with Ezetimibe, a cholesterol absorption inhibitor, only statin treatment improved endothelial

vasodilator function (Landmesser 2005, Fichtlscherrer 2006). This could be attributed to statins ability to stabilize and increase eNOS mRNA expression via inhibition of small GTPase RhoA pathway (Laufs 1998, Laufs 2003). By removing caveolin-1 inhibition on eNOS, statins also amplify eNOS activation. At last, statins were also proven to activate eNOS via phosphorylation through phosphatidylinositol-3 kinase (PI3K)/protein kinase Akt pathway (Kureishi 2000, Rikitake 2005).

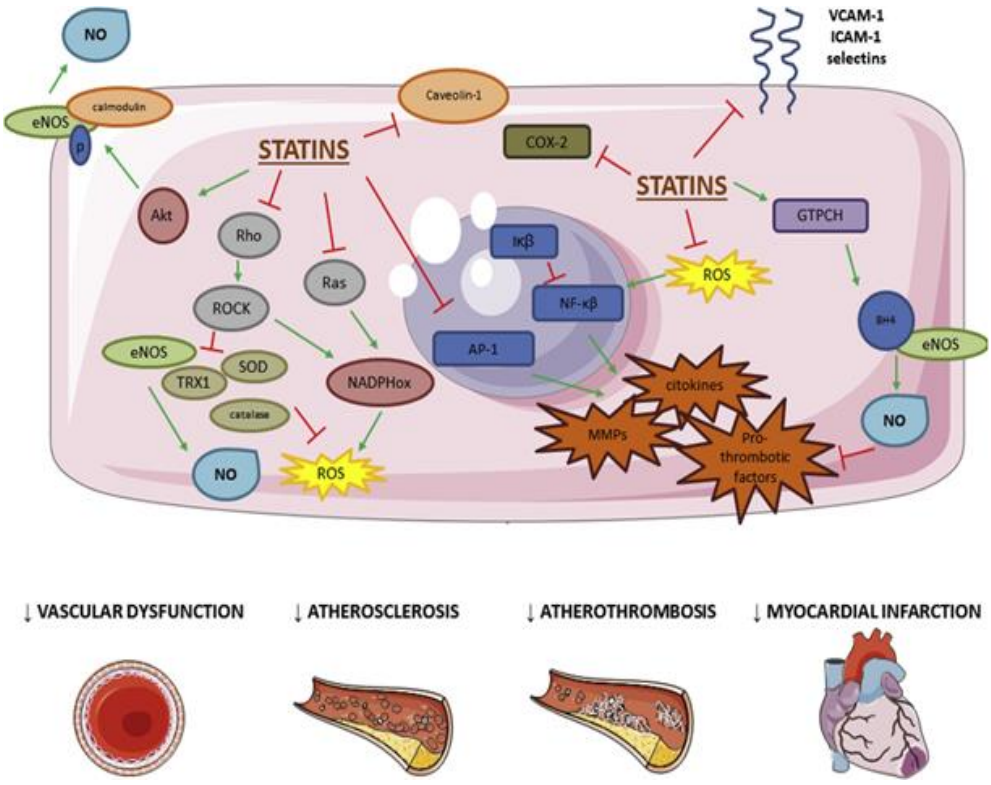

Figure 23: Schematic representation of statins' pleiotropic effects on endothelium and their role in cardiovascular events. Original figure from Liberale 2020.

3.2. Antioxidant activity

In a study led by Franzoni, antioxidant scavenger capacity of 4 statins (atorvastatin, simvastatin, pravastatin and Fluvastatin) were tested *in vitro* in neutralizing hydroxyl radicals ($HO^{\cdot}$) and peroxyl radicals ($ROO^{\cdot}$) and compared to uric acid and Trolox. All were proven to be efficient on the scavenging of both radicals. In addition, compared to uric acid, Simvastatin was 270% more efficient in scavenging $HO^{\cdot}$ (Franzoni 2003). The direct antioxidant effect of statins and metabolites was already demonstrated earlier in the late 90^{ies}, but their clinical relevance regarding the used doses were still to be established (Aviram 1998, Girona 1999).

Statins antioxidant effects were also linked to increased expression of antioxidant systems such as catalase (Wassmann 2002) and SOD activity levels (Chen 2013, Jiang 2014) while malondialdehyde (MDA) marker of lipid peroxidation were reduced (Jiang 2014). Wassmann also demonstrated that Atorvastatin antioxidant effects in vascular smooth muscle cells (VSMCs) reduced Nox1, an essential component of NOX, due to impaired action of Rac1. These effects were reversed by the addition of Mevalonate but not hydroxycholesterol, demonstrating the implication of isoprenylation processes independent of cholesterol contents.

3.3. Anti-Inflammatory activity

C-reactive protein (CRP) is a biomarker of chronic inflammation and its increase in inflammatory disorders such as chronic obstructive pulmonary disease (COPD) is associated with increased mortality (Man 2006). Pravastatin treatment was able to reduce CRP and interleukin 6 (IL6) levels compared to placebo treated COPD patients. Long-term statin treatment in COPD patients was also proven to reduce mortality up to 36% (Lahousse 2013). In subjects with and without CV diseases, Pravastatin was able to reduce CRP levels independently of LDL reduction (Albert 2001).

In the light of those results, it was suggested that statins could exert immunomodulating effects by inhibiting GTP binding proteins orchestrating immune responses. By inhibiting isoprenoids synthesis, statins are capable of downregulating the expression of adhesion molecules and chemokines (Barnes 2008, Carbone 2016). Simvastatin was also reported to reduce metallo-proteinases (MMPs) 9 and 12 remodeling the extracellular matrix (Emberson 2011).

3.4. Statins & diabetes

In many randomized trials and studies, the use of statins is associated with an increased risk in T2D development (Sattar 2010, Preiss 2011, Ridker 2012, Navarese 2013). However, statins cardiovascular related benefits still outweigh the T2D risk and the explanation behind the link between statins and T2D development could be related to confounding factors.

High doses of Atorvastatin treatment in mice showed decreased glucose transporter 4 (GLUT4) expression and accelerated glucose intolerance (Nakata 2006). Also, statin treatment as well as HMG-CoA reductase gene variants are associated with higher body weight and T2D risk (Swerdlow 2014). T2D could therefore be mediated through the HMG-CoA inhibition by statins and concomitantly by the high body weight which is a causal factor in T2D development (Holmes 2014). However, it still remains unclear whether statin treatment is the cause of T2D or if it accelerates its progression.

4. Statins as part of anti-cancer therapy

Because of statins' extensive use in humans, the antineoplastic effects related to their non-cholesterol dependent effects also rose with the years. Statins are now known to exert their antitumor effects by either acting on cell cycle inhibition, apoptosis induction and cell invasion/metastasis inhibition. These "off target" effects are currently being exploited in cancer therapy for the prevention and treatment of malignancies.

4.1. Anti-tumor activity of statins

Over the years, clinical and preclinical studies using statins demonstrated antitumor effects on various types of solid tumors, such as pancreatic adenocarcinoma, hepatocellular carcinoma, renal cell carcinoma and colorectal, lung and prostate cancer (Jian-Yu 2017, Simon 2019, Notarnicola 2004, Xia 2019 and other reviewed by Gobel 2020). By inhibiting isoprenoid intermediates synthesis, statins block the activation of small GTPase binding proteins which are key enzymes in cell signaling. In cancer, this results in decreased cell proliferation and in the induction of cell death (Gobel 2020). Indeed, Rho GTPases are capable of activating mTOR and MAPK to induce tumorigenesis (Konstantinopoulos 2007, Brendt 2011).

4.2. Apoptosis & cell cycle arrest

According to Cafforio, statins are capable of inhibiting apoptosis in many cancer cell types through the mitochondrial intrinsic pathway (Cafforio 2005). Indeed, it is suggested that statins could decrease anti-apoptotic protein Bcl-2 expression levels, leading to activation of caspases pathway and p53 (Wood 2013). Hoque et al demonstrated the same pathway activation in prostate cancer cell lines PC3, LNCaP and DU145 after simvastatin and lovastatin treatment (Hoque 2008). It was also reported that statins impair ERK1/2, Akt and mTOR signaling inducing apoptosis through decreased isoprenylation (Fujiwara 2017, Tsubaki 2017). Furthermore, the lactone structure of Lovastatin and Simvastatin can also inhibit proteasome activity and induce apoptosis (Efuet 2006). At last, statins could activate cytokine-induced cell death by upregulating Fas ligands and their receptors (Knapp 2000).

RhoA, one of the targets of posttranslational isoprenylation, is a crucial factor regulating downstream effectors of cell cycle progression. As demonstrated by Lee *et al*, Simvastatin treatment was able to inhibit RhoA activation by suppressing its geranylgeranylation (Lee 2007). In several cancer cells such as MCF-7 breast cancer and hepatocarcinoma, statins disrupted G1 and S phases of cell cycle, inducing apoptosis *in vitro* (Sutter 2005, Sanchez 2008). The statin-induced apoptosis was defined by inactivation of ERK1/2 and activation of p38MAPK (Sutter 2005).

4.3. Metastasis

Given the role of RhoA in cellular proliferation and metastasis, facilitating actin reorganization and cellular migration, it could be that statins treatment represses tumor initiation by blocking its activation (Lawson 2018). Rho proteins trigger cell signaling through activation of their effectors such as proteins kinases and adaptor molecules. In turn, Rho-associated protein kinases (ROCKs) activation regulates actomyosin and its increased activity was correlated with metastasis (Kale 2015). In addition, Rac1 and Rac3 were also found to be overexpressed in tumors indicating their potential implication in metastasis (Chan 2005).It was already demonstrated in different studies that Atorvastatin and Simvastatin suppress cancer cell invasion and metastatisation in ovarian cancer and in human cholangiocarcinoma cells (Jones 2017, Buranrat 2016), potentially through Akt/MAPK signaling. Survivin, A protein implicated in tumorigenesis, was also proven to be downregulated by Simvastatin in salivary adenoid cystic

carcinoma (SACC-83) therefore inhibiting its invasiveness (Cai 2018). In PC-3 prostate cancer cells, treatment with Simvastatin and Rosuvastatin reduced invasion (67%) through a matrigel barrier towards a chemoattractant (Brown 2012). Cells displayed reduced migration ability which was restored after GGPP addition. These anti-metastatic effects of statins could therefore be explained by the isoprenoid depletion induced by mevalonate pathway inhibition.

5. Oxygen effect and radiation therapy

5.1. Mechanism of radiosensibilization

It is nowadays well known that hypoxia renders solid tumors resistant to radiation therapy. Cells and tissues are indeed more sensitive to irradiation when in the presence of molecular oxygen (Fig.24A). To achieve the same biological effect, hypoxic regions require radiation doses that are three times higher than for well-oxygenated tissues. This ratio of doses under hypoxic and oxygenated conditions to achieve the same level of cell death is called the "oxygen enhancement ratio". Also, the radiosensitivity of tissues increases when oxygen tension varies from o to 30mm Hg and reaches a plateau at higher oxygen tensions (Fig.24B). Increasing well-oxygenated tissues is therefore not going to improve radiosensitivity.

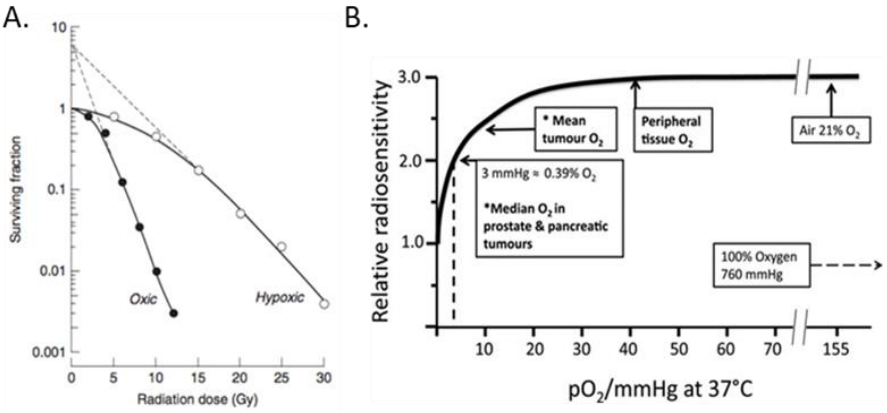

Figure 24: The Oxygen effect during radiation therapy.
(**A**) Survival curve of cells exposed to radiation therapy in the presence and absence of molecular oxygen. Original figure from "Basic Clinical Radiobiology" Fourth Edition by Joiner and Van der Kogel. **(B)** Representation of the relation between oxygen tension and radiosensitivity of tissues. The relative radiosensitivity is around 3 in well-oxygenated tissue and 2 or less in hypoxic tumors. Figure from Mc Keown 2014 already adapted from Hall 2012.

This oxygen enhancement effect potentiating radiation therapy can be explained by its impact on the free radical production and cascade fixing the damages at molecular level **(Fig.25**). In contrast, damage induced by ionized radiation may be repaired by the cell in absence of oxygen.

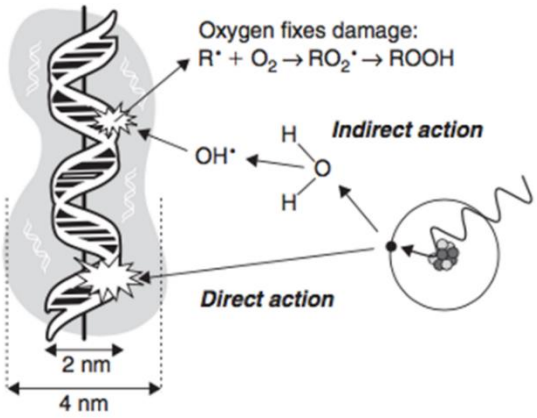

Figure 25: Schematic representation of the oxygen effect contributing to radiation therapy efficiency, called "oxygen fixation hypothesis". Figure from *Radiologykey.com.*

5.2. Statins and radiosensibilization

While the beneficial effect of statins is still debated, several large-scale cohort studies have indicated a better outcome of radiation therapy (RT) (external or brachytherapy) in prostate cancer patients under statin treatment (Kollmeier 2011, Moyad 2006, Oh 2015). In addition, a meta-analysis found a beneficial effect of statin use on recurrence free-survival in prostate cancer patients treated with RT, whereas this association could not be found among radical prostatectomy patients (Park 2013). Taken together, these clinical observations could suggest potential radiosensitizing property of statins.

Our hypothesis is that statins could improve response to RT in those patients receiving statins by inhibiting the OCR and thereby alleviate tumor hypoxia. Tumor hypoxia results from an imbalance between the limited oxygen delivery capacity of the abnormal vasculature and the high oxygen consumption of tumor cells (Vaupel 2001). It is also associated with in worsened clinical prognosis for cancer patient (Dhani 2015, Walsh 2014, Colliez 2017) as it renders solid tumors resistant to radiation therapy. Indeed, the radiation dose required to achieve the same biologic

effect is about three times higher in hypoxic tissues than in those with normal oxygen levels (Horsman 2009).

Theoretically, there are two ways to alleviate tumor hypoxia; by increasing the oxygen delivery to the tumor or by decreasing the oxygen consumption by tumor cells. However, it was suggested by a mathematical modelling described by Secomb et al. that decreasing tumor hypoxia by targeting the oxygen consumption of tumor cells would be more efficient that increasing the oxygen delivery (Secomb 1995). Nowadays, strategies designed to decrease the OCR in tumor cells already succeeded in enhancing the response to radiation therapy in tumor models (Crokart 2005b Crokart 2007, De Preter 2016, Diepart 2012, Gallez 2017, Jordan 2002, Jordan 2007, Zannella 2013).

The impact of statins on the oxygen consumption was already assessed in diverse types of normal cells, such as cardiomyocytes, skeletal muscle cells, and hepatocytes (Kwak 2012, Satoh 1994, Thews 1996). Its effect was also believed to be mediated mostly by the reduction of ubiquinol synthesis. However, Nadanaciva demonstrated a direct effect of statins on the activity of the mitochondrial respiratory complexes of isolated rat liver mitochondria (Nadanaciva 2007).

So far, only one study investigated the effect of statins on the OCR by tumor cells. This study evaluated the impact of lovastatin on DS sarcoma cells with the aim to evaluate the impact on DNA synthesis and OCR (Ferrick 2008). However, these authors did not investigate the consequences of the changes of OCR on the sensitivity to irradiation.

By inhibiting respiratory complexes of the ETC and decreasing subsequently the OCR in normal cells, statins could act in the same way on prostate cancer cells (and ideally on other cancer types) in order to alleviate tumor hypoxia and enhance radiosensitivity in cancer patients.

Aims of the thesis

Formerly considered to be only highly toxic and detrimental to cells, ROS and superoxide are now proven to have many roles in cellular health and physiology depending on their concentration. Because of its origin being principally mitochondrial, the ETC and its respiratory complexes have gained a lot of interest. With the years, different tools to measure OCR and superoxide production in cells and isolated mitochondria emerged in order to define mitochondrial function and dysfunction.

Nowadays, these same tools evolved. Several are still being used as gold-standard, like EPR-oximetry because of its high sensitivity and specificity using oxygen sensors (e.g. ^{15}N-PDT), while others are found to be less specific than thought. Indeed, although fluorescent probes are sensitive probes to measure global ROS production, DCFDA, hydroethidine (HE) and derivatives (Mito-HE, MitoSOX) are demonstrated not to be entirely specific for superoxide anion. By using the appropriate probes and controls, EPR technology could in this case be a technique of choice to measure both parameters sensitively and specifically.

The main goal of this thesis is, therefore, to develop a novel EPR tool enabling the dual measurement of the OCR and superoxide production in isolated mitochondria and whole cell models in the most sensitive and specific way possible in order to define mitochondrial function and dysfunction. Different projects also rose from the implementation of this EPR tool and became part of this thesis.

Potential toxic agents could induce deleterious effects on human cells by increasing superoxide generation. This EPR tool could therefore be used in toxicology to assess the impact of agents on mitochondrial function before outing them on the market. In this thesis, we tested SDHI fungicides Boscalid and Bixafen, which are still widely used on our crops and to which we are all daily exposed to. SDHI are thought to be specific for fungi, but recently the team of Rustin demonstrated otherwise. With this project, we explored the impact of those SDHI on the mitochondrial function of several human cell lines after a short-term exposure to SDHI fungicides.

Related to anticancer therapy, several drugs were shown to inhibit the OCR in tumors, subsequently enhancing the efficacy of radiation therapy by increasing tumor pO_2 and potentially leading to decreased tumor volume *via* superoxide-induced cell death. A meta-analysis demonstrated that statins, cholesterol-lowering drugs, had a beneficial effect on prostate cancer

patients treated with radiation therapy (RT). Our hypothesis was that statins could potentially act on mitochondrial respiration of tumor cells and enhance radiosensitivity. The aim of this new project was therefore to test the impact of different statins on mitochondrial function, *in vitro* and *in vivo* in prostate cancer tumor models.

Development of a novel method to characterize mitochondrial function

I. A versatile EPR toolbox for the simultaneous measurement of oxygen consumption and superoxide production

Article published in *Redox Biology*, 2021

D.d'Hose, Redox Biol, 2021, Apr;40:101852. doi: 10.1016/j.redox.2020.101852

Redox Biology 40 (2021) 101852

Contents lists available at ScienceDirect

Redox Biology

journal homepage: www.elsevier.com/locate/redox

Method

A versatile EPR toolbox for the simultaneous measurement of oxygen consumption and superoxide production

Donatienne d'Hose [a], Pierre Danhier [b], Heidi Northschield [a], Pauline Isenborghs [a], Bénédicte F. Jordan [a], Bernard Gallez [a,*]

[a] Biomedical Magnetic Resonance, Louvain Drug Research Institute (LDRI), Université Catholique de Louvain (UCLouvain), Brussels, Belgium
[b] Nuclear and Electron Spin Technologies (NEST) Platform, Université Catholique de Louvain (UCLouvain), Brussels, Belgium

ARTICLE INFO

Keywords:
EPR
ESR
Oxygen consumption rate (OCR)
Superoxide
Nitroxide
Hydroxylamine
Mitochondria
ETC

ABSTRACT

In this paper, we describe an assay to analyze simultaneously the oxygen consumption rate (OCR) and superoxide production in a biological system. The analytical set-up uses electron paramagnetic resonance (EPR) spectroscopy with two different isotopically-labelled sensors: ^{15}N-PDT (4-oxo-2,2,6,6-tetramethylpiperidine-d_{16}-^{15}N-1-oxyl) as oxygen-sensing probe and ^{14}N-CMH (1-hydroxy-3-methoxycarbonyl-2,2,5,5-tetramethylpyrrolidine, a cyclic hydroxylamine, as sensor of reactive oxygen species (ROS). The superoxide contribution to CMH oxidation is assessed using SOD or PEGSOD as controls. Because the EPR spectra are not superimposable, the variation of EPR linewidth of ^{15}N-PDT (linked to OCR) and the formation of the nitroxide from ^{14}N-CMH (linked to superoxide production) can be recorded simultaneously over time on a single preparation. The EPR toolbox was qualified in biological systems of increasing complexity. First, we used an enzymatic assay based on the hypoxanthine (HX)/xanthine oxidase (XO) which is a well described model of oxygen consumption and superoxide production. Second, we used a cellular model of superoxide production using macrophages exposed to phorbol 12-myristate 13-acetate (PMA) which stimulates the NADPH oxidase (NOX) to consume oxygen and produce superoxide. Finally, we exposed isolated mitochondria to established inhibitors of the electron transport chain (rotenone and metformin) in order to assess their impact on OCR and superoxide production. This EPR toolbox has the potential to screen the effect of intoxicants or drugs targeting the mitochondrial function.

1. Introduction

Over the past decades, research on mitochondria witnessed an important gain of interest, highlighting its implication in many physiological and pathological processes like diabetes [1], cardiovascular diseases [2] and neurodegenerative disorders. A growing body of evidence also indicates that mitochondria plays a key role in cancer progression and response to treatment due to its involvement at the crossroad of many cellular pathways. Mitochondrial implication in mediating programmed cell death has led to a great interest in exploiting radio- and chemo-therapeutic agents to trigger cancer cell death [3]. Also, altering the mitochondrial respiration has been associated with alleviation of tumor hypoxia and a consequent increase in radiosensitivity [4–6]. Mitochondria are the major producers of superoxide and other downstream ROS in the cell, the main sources of superoxide being complexes I and III of the electron transport chain (ETC). Cellular ROS are maintained in stable balance by antioxidant systems and enzymes such as superoxide dismutase (SOD), catalase, glutathione peroxidase and other accessory enzymes such as thioredoxins and peroxiredoxins [7]. When this balance is disrupted, increase in ROS concentration can cause DNA damage, lipid peroxidation and defects in cell signaling [8]. ROS induction is also a well-established cause of carcinogenesis [9,10]. Superoxide may trigger cell death when produced in large excess but, at moderate levels, it was suggested to be a key driver promoting cancer cell migration and metastasis [11].

Taken together, the dual dose-dependent effects on oxygen consumption rate (OCR) and superoxide production are crucial to consider when assessing mitochondrial function and/or dysfunction. So far, no technology is able to analyze simultaneously the oxygen consumption and superoxide production coming from the ETC. The ultimate goal of this paper was to provide an analytical set-up able to assess at the same time OCR and superoxide leakage on a single mitochondrial preparation.

* Corresponding author. Biomedical Magnetic Resonance Research Group Louvain Drug Research Institute, UCLouvain, Avenue Mounier 73 - B1.73.08, B-1200, Brussels, Belgium.
E-mail address: bernard.gallez@uclouvain.be (B. Gallez).

https://doi.org/10.1016/j.redox.2020.101852
Received 4 November 2020; Received in revised form 22 December 2020; Accepted 23 December 2020
Available online 28 December 2020

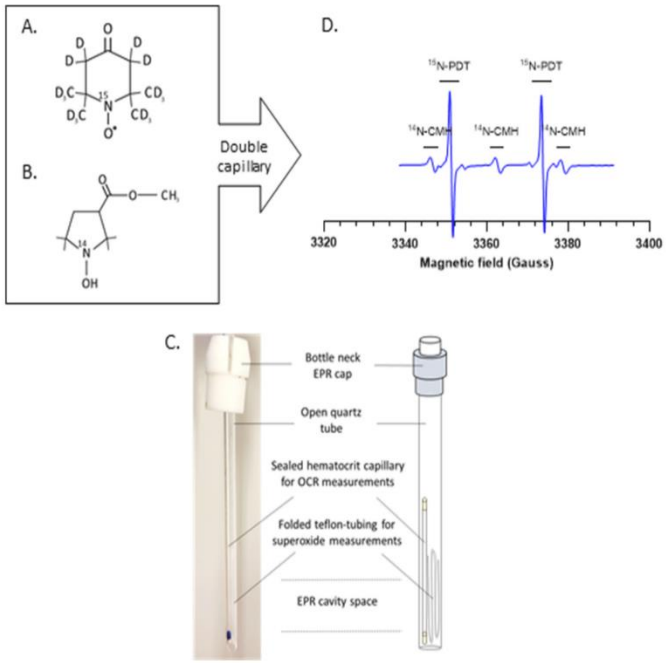

Fig. 1. Experimental set-up of the EPR-mitotoolbox.
(A) Chemical structure of ^{15}N-PDT, a paramagnetic nitroxide.
(B) Chemical structure of ^{14}N-CMH, a diamagnetic cyclic hydroxylamine.
(C) Schematic view of the double capillary device.
(D) Representative global EPR spectrum obtained by combining ^{15}N-PDT and ^{14}N-CMH in PBS buffer into a double capillary device, at a final concentration of 100 μM and 0.5 mM respectively.

For the purpose, we used electron paramagnetic resonance (EPR) spectrometry. OCR determination using EPR oximetry is based on the signal variation (change in EPR linewidth) of a paramagnetic oxygen sensing probe (for example, a nitroxide) in the presence of oxygen consuming cells in a closed system [4,12–14]. In addition, EPR is a suitable technology for the detection of superoxide. It has been shown that superoxide production can be monitored by the oxidation of cyclic hydroxylamines into nitroxides [15,16]. Because their oxidation into paramagnetic nitroxide can be due to several redox reactions, the contribution of superoxide to the nitroxide formation has to be deduced from experiments carried out in the presence and in the absence of SOD or PEGSOD (pegylated-superoxide dismutase) as appropriate controls [17]. In order to measure OCR and superoxide production simultaneously, we designed an assay with the ability to measure the variation of the EPR linewidth of one nitroxide, on the one hand, and the formation of another nitroxide, on the other hand. To separate the EPR signals coming from both nitroxides, we used different isotopically-labelled probes. For OCR measurements, we used ^{15}N-PDT (4-oxo-2,2,6,6-tetramethylpiperidine-d_{16}-^{15}N-1-oxyl) as oxygen-sensing probe (Fig. 1A). The EPR signal from this nitroxide is a doublet because of the coupling of the electron spin with ^{15}N which possess a nuclear spin $I = 1/2$. Because deuterium substitutes hydrogen in ^{15}N-PDT, the EPR linewidth is very narrow, providing a high sensitivity to measure the broadening induced by the oxygen content in the preparation [4,12].

For superoxide production, we used ^{14}N-CMH (1-hydroxy-3-methoxycarbonyl-2,2,5,5-tetramethylpyrrolidine, Fig. 1B), a cyclic hydroxylamine that detects superoxide in complex biological media with high sensitivity [17]. The superoxide-induced transformation of CMH into a nitroxide provides a three-lines EPR spectrum due to the coupling of the electron spin with ^{14}N which possess a nuclear spin $I = 1$. Because both EPR spectra are not superimposable, the variation of the linewidth of ^{15}N-PDT (linked to OCR) and the formation of ^{14}N-CMH (linked to superoxide production) can be recorded simultaneously over time on a single preparation (Fig. 1C).

The validation of this EPR assay was carried out in several steps. In a preliminary step, we optimized the experimental set-up in order to avoid cross-reaction between the nitroxide and the cyclic hydroxylamine. Then, we assessed the ability of the system to measure simultaneously OCR and superoxide production in biological systems of increasing complexity. First, we used an enzymatic assay based on the hypoxanthine (HX)/xanthine oxidase (XO) which is a well described model of oxygen consumption and superoxide production. Second, we used a cellular model of superoxide production using macrophages exposed to phorbol 12-myristate 13-acetate (PMA) which stimulates the NADPH oxidase (NOX) to consume oxygen and produce superoxide. Finally, we exposed isolated mitochondria to established inhibitors of the ETC in order to assess their impact on OCR and superoxide production.

2. Material & methods

2.1. Reagents

^{14}N-CMH (1-hydroxy-3-methoxycarbonyl-2,2,5,5-tetramethylpyrrolidine) and metformin were purchased from Enzo Lifescience (Antwerpen, Belgium). ^{15}N-PDT (4-oxo-2,2,6,6-tetramethylpiperidine-d_{16}-^{15}N-1-oxyl) originates from CDN Isotopes. Rotenone, superoxide dismutase (SOD), superoxide dismutase conjugated with polyethylene glycol (PEGSOD), xanthine oxidase (XO), hypoxanthine (HX), diethylenetriaminepentaacetic acid (DTPA), dextran from leuconostoc mesenteroides (average MW 60000–76000), adenosine triphosphate (ADP), pyruvate, succinate, malate and phorbol 12-myristate 13-acetate (PMA) were from Sigma-Aldrich (Overijse, Belgium). Mitochondrial assay buffer (MAS) concentrated 2 times (MAS 2x) was composed of sucrose (70 mM), mannitol (220 mM), KH_2PO_4 (10 mM), $MgCl_2$ (5 mM), HEPES (2 mM), EGTA (ethyleneglycol bis (α-aminoethylether)-N,N1-tetraacetic acid, 1 mM) and FA-free BSA (fatty acid free Bovine Serum Albumin, 0.2%). All MAS components were also purchased from Sigma-Aldrich.

2.2. Preliminary experiment showing the cross reaction between nitroxide and hydroxylamine

Perdeuterated nitroxides as ^{15}N-PDT (Fig. 1A) are very sensitive probes to measure oxygen levels in a medium using EPR-oximetry. Besides, cyclic hydroxylamines such as CMH (Fig. 1B) are capable of being oxidized into paramagnetic nitroxides (CM●) and therefore becoming EPR-visible. CMH, when used with appropriate controls, is a highly sensitive EPR tool to detect superoxide in complex biological media [17]. A preliminary experiment was performed using those two spin probes mixed together in PBS buffer into a single sealed hematocrit capillary to detect possible interferences. ^{15}N-PDT and ^{14}N-CMH were both mixed in PBS buffer at a final concentration of 100 μM and 0.5 mM respectively. ^{14}N-CMH was flushed with argon while pipetting to avoid oxidation by air. The final mixture was injected into a hematocrit capillary and inserted in a quartz tube into the EPR cavity. Acquisitions wer taken 1min after the probes were blended together. After 10 min, PDT spectrum was reduced to silence (supplementary data Fig. 1SA) while CM● signal intensity increased (supplementary data Fig. 1SB). These changes in spectra are due to electron transfer between both spin probes, oxidizing CMH without any superoxide source and transforming PDT into a diamagnetic hydroxylamine. To avoid this unspecific signaling in the experiments, both spin probes were each blended into a specific mix (respiration versus superoxide) and injected into two separate capillaries. In this way, both probes remain separated while being inserted into the same quartz tube and placed into the EPR cavity (Fig. 1D).

2.3. HX/XO superoxide production model

Hypoxanthine/xanthine oxidase couple forms a well described model of superoxide production. HX/XO were used at a final concentration of 1 mM and 5mU/mL, respectively in PBS, mixed with DTPA (1 mM). EPR probes (^{15}N-PDT and ^{14}N-CMH, 5 μL) were then each added to this final base mixture (95 μL) separately at final concentration of 100 μM and 0.5 mM, respectively and put into a sealed hematocrit capillary (Hirschmann Laborgeräte). Both capillaries were inserted into a quartz tube and placed into the EPR cavity. Superoxide production was determined by the addition of SOD at a final concentration of 200U/mL. Table 1A (Supplementary data) describes the stock solutions of all the used agents whereas Table 1B describes the exact base mixture formulation of the experiment (Supplementary data).

2.4. Whole cell superoxide production model

RAW 264.7 macrophages were purchased from ATCC (Manassas, USA) and cultured at 37 °C in a humidified atmosphere with 5% CO_2 maintained in Dulbecco's Modified Eagle Medium (DMEM, Thermo Fisher Scientific) supplemented with 10% heat-inactivated fetal bovine serum (FBS). At confluence, cells were exposed to 5 μM of PMA during 20 min at 37 °C, then washed with phosphate buffered saline (PBS), harvested and resuspended at two different concentrations ($10x10^6$ cells/mL for respiration and $20x10^6$ cells for superoxide production) in PBS to perform EPR experiments. At first, cells were mixed with a 20% dextran solution and DTPA (1 mM) at a final concentration of $5x10^6$ cells/mL and incubated with the oxygen sensor ^{15}N-PDT (100 μM) in order to measure oxygen levels in a sealed hematocrit capillary (Tab.2A supplementary data). At last, another mix was also prepared with macrophages ($20x10^6$ cells/mL) and DTPA (1 mM) incubated with ^{14}N-CMH (0.5 mM) injected in a gas-permeable polytetrafluoroethylene (PTFE) tubing (ZEUSS) to measure superoxide production (Tab.2B supplementary data). ^{14}N-CMH was flushed with argon while pipetting to avoid oxidation by air. Both capillaries were inserted into a quartz tube open at both ends and placed into the EPR cavity. Control experiments were carried out on PMA-unstimulated macrophages and specific superoxide production on PMA-stimulated cells was assessed using PEGSOD at a final concentration of 200 U/mL (10min preincubation). EPR acquisitions were started 3min after the probes were blended with the cells. Cell viability was verified after all experiments using trypan blue assay.

2.5. Fibroblast culture & mitochondrial isolation

3T3 fibroblasts were purchased from ATCC (Manassas, USA) and routinely cultured in Dulbecco's Modified Eagle Medium (DMEM containing High glucose (4.5 g/L), L-glutamine and HEPES) supplemented with 1% sodium pyruvate (Sigma) and 10% newborn calf serum (NCS) at 37 °C in a humidified atmosphere with 5% CO_2. Confluent cells were washed with PBS, then harvested and resuspended in PBS for mitochondrial isolation. 3T3 mitochondria were obtained by performing isolation based on Frezza's procedure [18] described on mouse embryonic fibroblasts (MEFs). At last, mitochondrial protein quantification was assessed by BCA protein assay for data normalization.

2.6. mitochondrial enrichment

Efficiency of mitochondrial isolation as well as mitochondrial enrichment was assessed by western blotting comparing whole cell lysate with mitochondrial lysate obtained after mitochondrial isolation (as previously described). Protein from whole cell lysates were extracted using RIPA lysis and extraction buffer (Thermo Scientific) supplemented with 1% phosphatase inhibitors and 1% protease inhibitors. Mitochondrial and whole cell lysate protein were then quantified by BCA assay. Fifteen micrograms of protein were resolved by SDS-polyacrylamide gel 4–15% (Bio-Rad) electrophoresis and transferred to PVDF membranes. Membranes were probed with the following primary antibodies: mitochondrial biomarker anti COX IV (1D6E1A8, Invitrogen) and cytosolic biomarker GAPDH (A21994, Invitrogen). Membranes were then incubated with a horseradish peroxidase-coupled secondary antibody (Cell Signaling Technology) and developed using SuperSignal™ West Pico Plus chemiluminescent substrate kit (Thermofisher). Films were scanned using ImageQuand LAS 500 and analyzed using the image processing software ImageJ.

2.7. Mitotoolbox procedure

Two different mixtures were made in order to measure oxygen consumption rate (OCR) and superoxide production simultaneously. Respiration mix contained respiratory substrates diluted in MAS buffer, DTPA (1 mM) and dextran to avoid sedimentation (Tab.3A supplementary data). The second mix contained the same components at identical concentration as the first one, except for dextran which is

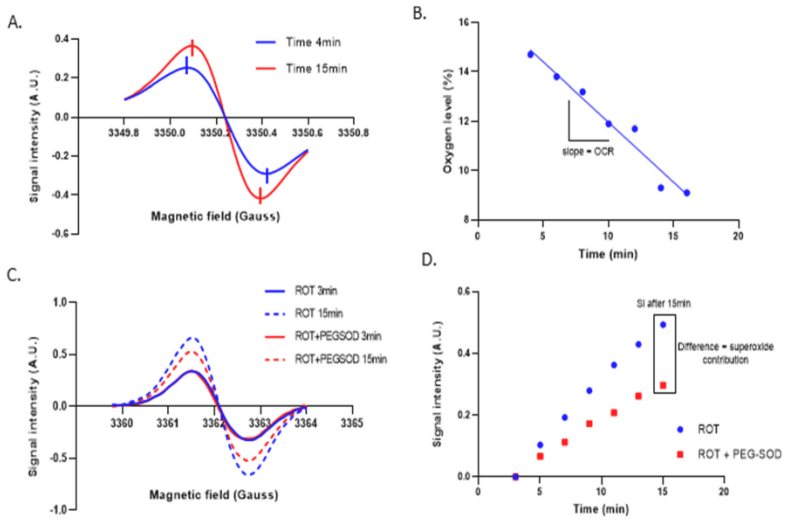

Fig. 2. Experimental methodology of the EPR-mitotoolbox.
(A) Representative zoomed spectra of ^{15}N-PDT linewidth decrease during time, assessing oxygen consumption by control 3T3 isolated mitochondria resuspended in MAS buffer and pyruvate/malate/succinate/ADP substrates. ^{15}N-PDT spectrum at time point 4min is represented in dark blue while time point 15min is represented in red. Vertical lines represent peak to peak linewidth of each spectrum.
(B) Evolution over time of the oxygen level in sealed tubes containing control 3T3 isolated mitochondria resuspended in MAS buffer and pyruvate/malate/succinate/ADP substrates. The exact oxygen consumption rate (OCR) of each experimental condition is determined by measuring the slope of oxygen level decrease in the medium after 15min.
(C) Representative spectra of CMH oxidation by 3T3 isolated mitochondria during time after rotenone treatment (1 μM) with and without PEG-SOD (200U/mL). CM● at time point 3min is represented with a continuous line while dotted line represent time point 15min (dark blue for rotenone and red for rotenone + PEG-SOD).
(D) Evolution of CM● signal intensity over time. Previous CMH oxidation spectra shown in (C) were double integrated to calculate signal intensities linked to every condition. Signal intensity (SI) of the first measurement (3min) is subtracted to all other SI values in order to plot them according to time. SI values at time point 15min are used to determine superoxide contribution.

replaced by PBS (Tab.3B supplementary data). Substrates supply included NADH-linked substrates; pyruvate (5 mM), malate (2.5 mM) and $FADH_2$-linked substrate; succinate (5 mM), as well as ADP (1.5 mM) to support state 3 respiration. 3 μL of concentrated mitochondria were homogenized in each mix (90 μL), followed up by the EPR probes (^{15}N-PDT and ^{14}N-CMH at 100 μM and 0.5 mM respectively). Final respiratory mix with oxygen sensor PDT was transferred rapidly into a sealed hematocrit capillary whereas superoxide mix with CMH was carefully injected into a PTFE tubing of 12 cm and folded in 4. Both capillaries were inserted into a quartz tube open at both ends and placed into the EPR cavity. For better functional responses, freshly isolated mitochondria were kept concentrated and stored on ice during the whole experiment. According to the protocol, mitochondria should also be used within 1–3 h after isolation.

2.8. ETC modulation

Mitochondrial ETC was modulated using two known and well described mitochondrial complex I inhibitors, rotenone and metformin. Mitochondria were treated without preincubation with the drugs at 1 μM and 3 mM final concentration, respectively. Superoxide production was assessed using PEGSOD (200U/mL, 10min preincubation) in control mitochondria as well as in modulator-treated mitochondria.

2.9. EPR settings

EPR measurements of all experiments were performed using a Bruker EMX-Plus spectrometer (Bruker, Germany) operating in X-band (9.85 GHz) and equipped with a PremiumX ultra low noise microwave bridge and a SHQ high sensitivity resonator. Typical parameters were set as follow: microwave power: 2.518 mW, modulation frequency: 100 kHz; modulation amplitude: 0.005 mT (for PDT) or 0.1 mT (for CMH); time constant: 20.48 ms; conversion time: 10.24 ms; sweep width: 1.5 mT.

2.10. EPR measurements & data analysis

The EPR cavity was heated at 310 K with air during all experiments. CMH measurements were performed 3 min after the probe injection and then every 2min after that (odd numbers of minutes) whereas PDT measurements were performed 4 min after the probe injection and then every 2 min after that (even number of minutes). All experiments were done in triplicates. Acquisitions and data were acquired and collected using the Bruker Xenon Spin fit program. All acquisitions were saved at each timepoint to analyze separately. OCR was calculated by measuring PDT spectrum's linewidth which is proportional to oxygen level in the capillary. CMH probe oxidation were analyzed by calculating the double integration of the spectrum over time. Superoxide net production was calculated by subtracting the double integration value at timepoint 15min of the CMH spectrum with PEGSOD to the CTR value.

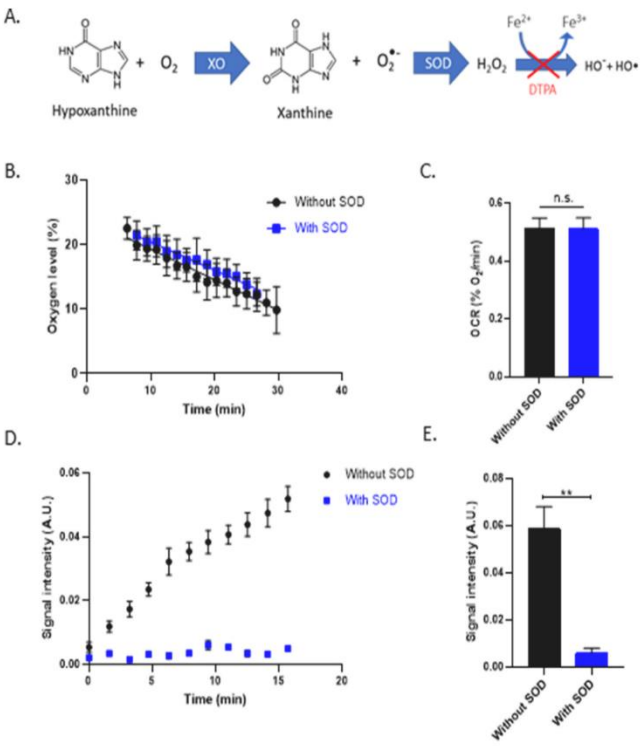

Fig. 3. OCR and superoxide production in the substrate/enzyme model HX/XO
(A) Chemical reaction of XO oxidizing HX into xanthine and superoxide. DTPA is used in the mixture to avoid Fenton reaction and therefore avoid the apparition of hydroxyl radical who is also capable of oxidizing the CMH.
(B) Evolution of the oxygen consumption of the substrate-enzyme couple HX/XO over time (at a final concentration in PBS of 1 mM and 0.005U/mL respectively), in the presence or in the absence of SOD (200U/mL). Points of the curve represent mean ± SEM ($\%O_2$) at each time point, N = 3.
(C) OCR of HX/XO system (at a final concentration in PBS of 1 mM and 0.005U/mL respectively) after 30min, in the presence or in the absence of SOD (200U/mL). Bars represent mean ± SEM ($\%O_2$/min). Mixture without SOD is represented in black and mixture with SOD in blue, N = 3.
(D) Evolution of the CMH oxidation during time within the HX/XO system (at a final concentration in PBS of 1 mM and 0.005U/mL respectively), in the presence or in the absence of SOD (200U/mL). Points of the curve represent mean ± SEM (arbitrary unities) after double integration of CMH spectra at each time point.
(E) Signal intensity after CMH spectrum double integration at time point 15 min in the presence or in the absence of SOD (200U/mL). Bars represent mean ± SEM (arbitrary unities). Mixture without SOD is represented in black and mixture with SOD in blue, N = 3, (**): $p < 0.01$.

2.11. Statistics

Data are represented as means ± SEM. All experiments were performed in triplicates except for mitochondrial ETC modulation who were repeated 6 times. Student T tests were applied for HX/XO experiments and mitochondrial enrichment experiments whereas One-way ANOVA were performed on all other experiments.

3. Results

3.1. EPR spectra analysis

When using the double capillary device, ^{15}N-PDT and ^{14}N-CMH spectra are recorded with their specific EPR settings and saved to analyze separately. Oxygen consumption is assessed by measuring the linewidth of ^{15}N-PDT spectra during time. The linewidth of ^{15}N -PDT spectra is narrowed during time as oxygen is consumed (Fig. 2A). The linewidth is then correlated to the oxygen level present in the media thanks to a calibration curve of the probe made with known % of oxygen. Oxygen consumption rate (OCR) is determined by calculating the slope of oxygen consumption during time (Fig. 2B). To assess superoxide production, initial recorded CM● spectra (Fig. 2C) are double integrated to obtain signal intensity (SI) values that can be plotted in function of time (Fig. 2D). PEGSOD is added as a control in order to determine the contribution of superoxide in the CMH oxidation by subtracting the PEGSOD SI value to the CTR SI value obtained after 15min of acquisition.

3.2. Substrate-enzyme couple: hypoxanthine/xanthine oxidase

We first tested the double capillary device with the duo of probes on a known system of superoxide production, notably the Hypoxanthine/Xanthine Oxidase (HX/XO) couple. XO uses oxygen to transform HX into xanthine and superoxide (Fig. 3A). The addition of SOD in the mix allows to consume the superoxide before it interacts with CMH, measuring in this way the specificity of the probe for superoxide. In addition, DTPA is incorporated each time to avoid Fenton reaction. Respiration was not altered in any of the conditions (Fig. 3B&C). HX/XO produces superoxide as proven by the addition of the SOD control (Fig. 3D&E).

3.3. Whole cell model: PMA stimulated RAW macrophages

Secondly, our device was also tested on a "whole cell" model of superoxide production using RAW 264.7 macrophages treated with PMA, stimulating the NADPH oxidase (NOX) to consume oxygen and produce superoxide [19] (Fig. 4A). Respiration was not altered in any of the conditions (Fig. 4B&C). PMA stimulated superoxide production in RAW cells proven by the addition of PEGSOD (Fig. 4D&E).

3.4. Mitochondrial enrichment

To assess mitochondrial enrichment, protein expression of COX IV

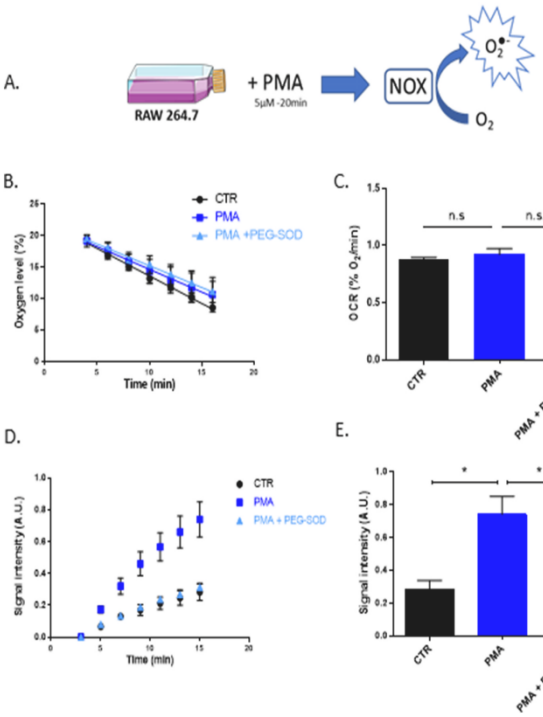

Fig. 4. OCR and superoxide production in the whole cell model using RAW macrophages.
(A) Experimental set-up of NOX-dependent superoxide production.
(B) Evolution of the oxygen consumption of RAW 264.7 macrophages over time when treated with PBS (CTR), 5 µM of phorbol-12-myristate-13-acetate (PMA) during 20 min, or PMA 5 µM during 20min then incubated with PEGSOD (200U/mL) for 10min before EPR measurement (PMA+PEGSOD). Points of the curve represent mean ± SEM (%O_2) at each time point, N = 3.
(C) Oxygen consumption rate of CTR, PMA-treated and PMA+PEGSOD-treated RAW 264.7 macrophages after 15min. Bars represent mean ± SEM (%O_2/min). CTR are represented in black, PMA condition in dark blue and PMA+PEGSOD condition in light blue, N = 3.
(D) Evolution of the CMH oxidation over time on RAW 264.7 macrophages, when treated with PBS (CTR), 5 µM of phorbol-12-myristate-13-acetate (PMA) during 20min, or PMA 5 µM during 20min then incubated with PEGSOD (200U/mL) for 10min before EPR measurement (PMA+PEGSOD). Points of the curve represent mean ± SEM (arbitrary unities) after double integration of CMH spectra at each time point. N = 3.
(E) Signal intensity after CMH spectrum double integration at time point 15 min of CTR, PMA-treated and PMA+PEGSOD-treated RAW 264.7 macrophages. Bars represent mean ± SEM (arbitrary unities). CTR are represented in black, PMA condition in dark blue and PMA+PEGSOD condition in light blue, N = 3, (*): $p < 0.05$.

and GAPDH were assessed on all cell lysates as well as on isolated mitochondria. After mitochondrial isolation using the protocol described by Frezza [18], COX IV bands were 28 times more intense, indicating a mitochondrial enrichment in the final fraction (Fig. 5B). GAPDH, a cytosolic protein, is present in whole cell lysate while it significantly decreases 5 times in isolated fraction, demonstrating minimal non-mitochondrial contamination.

3.5. Mitotoolbox - ETC modulation

At first, rotenone was tested on isolated 3T3-mitochondria to measure its effect on OCR and superoxide production. Rotenone at 1 µM final concentration was able to inhibit OCR in a significant way compared to control mitochondria (Fig. 5C). Secondly, when mitochondria were treated with 3 mM metformin, a well-described antidiabetic agent and ETC-complex I inhibitor, OCR was also significantly inhibited compared to control mitochondria (Fig. 5C). For both experiments, the addition of PEGSOD did not affect the OCR within a same condition (CTR or treated). At last, both drugs increased superoxide net production (after 15min of acquisition) in a significant way compared to CTR mitochondria (Fig. 5D).

4. Discussion

In this manuscript, we have described a new experimental set-up that allows the simultaneous determination of OCR and ROS production in a single preparation using EPR spectrometry. The nitroxide probes were selected in order to avoid overlapping EPR signal thanks to the use of different isotopically-labelled probes (Fig. 1D). On the one hand, ^{15}N-PDT was selected as oxygen sensor because of the sensitivity of its narrow EPR linewidth to variation of oxygen [14]. On the other hand, ^{14}N-CMH was chosen because it was previously demonstrated that this cyclic hydroxylamine CMH offers a high sensitivity of detection of superoxide compared to other EPR probes [17,20]. Experiments were also carried out using SOD or PEGSOD in order to assess the contribution of superoxide to CM● formation [17,21]. As we observed a cross-reaction between PDT and CMH (Fig. 1S A-B), it was crucial to keep both sensors in separate capillaries that were inserted together in the EPR cavity (Fig. 1C). For the proof of concept, the EPR toolbox was qualified using biological media of increasing complexity.

The experimental set-up was first tested on an enzymatic model using the couple HX/XO where oxygen is consumed by HX to produce XO and superoxide (Fig. 3A). In these experiments, we observed, as expected, that the pre-incubation in the presence of SOD did not alter the OCR (Fig. 3B and C) while SOD abolished the formation of CM● (Fig. 3D and E). It is known that nitroxides may also react with superoxide [17, 22,23] and may lead to an equilibrium between formation of a nitroxide induced by superoxide and its reverse reaction. In the present condition, we did not observe such an equilibrium in the short timeframe (15 min) used for monitoring the CM● formation as the EPR signal increased linearly over time (Fig. 2D). To avoid reaching this equilibrium, further EPR experiments were carried out within this short timeframe of 15 min.

The second model that we used relied on RAW 264.7 macrophages exposed to PMA which stimulates the NADH oxidase (NOX) to consume

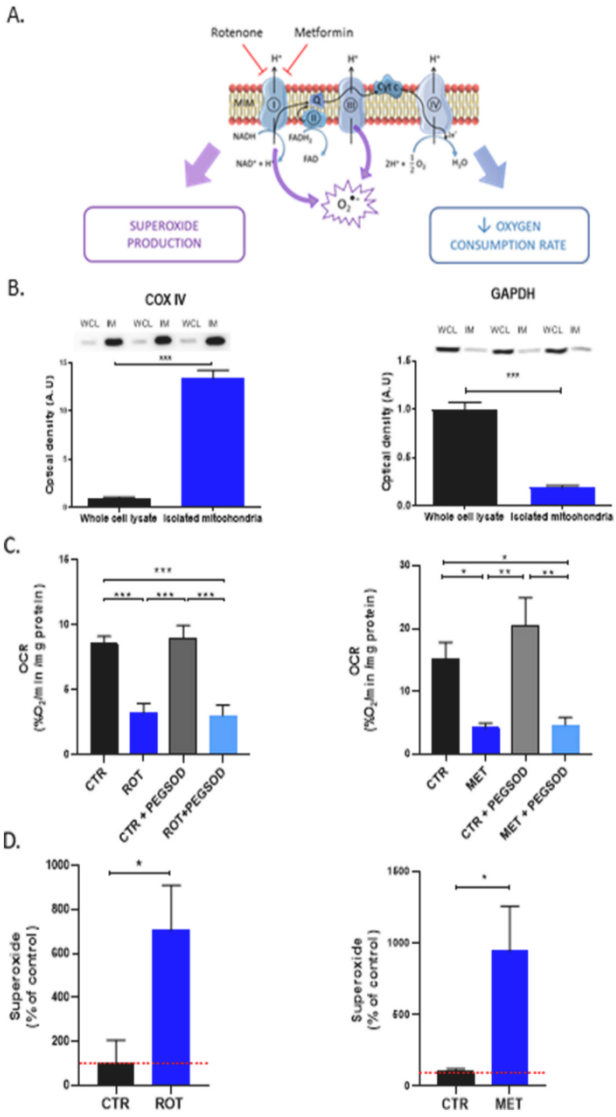

Fig. 5. Mitochondrial function and ETC modulation.
(A) Schematic representation of the mitochondrial ETC and sites of action of rotenone and metformin.
(B) Mitochondrial enrichment in final fraction after mitochondrial isolation using western blot analysis. Bars represent mean optical density ± SEM (arbitrary unities) for whole cell lysate (WSL) and isolated mitochondria fraction (IM). COX IV stands for mitochondrial marker whereas GAPDH is exclusively cytosolic. N = 3, (***): $p < 0.001$.
(C) Oxygen consumption rate of DMSO-treated (CTR), 1 μM Rotenone-treated (ROT) or 3 mM Metformin-treated (MET), PEGSOD-treated 200U/mL (PEGSOD) and ROT+PEGSOD or MET+PEGSOD 3T3 isolated mitochondria in a double capillary device containing a mix of MAS buffer and mitochondrial substrates (pyruvate/succinate/malate/ADP). Bars represent mean ± SEM ($\%O_2$/min and normalized by mg of mitochondrial protein). N = 6, (***): $p < 0.001$.
(D) Superoxide net production of CTR and 1 μM Rotenone- or 3 mM Metformin-treated 3T3 isolated mitochondria in a double capillary device containing a mix of MAS buffer and mitochondrial substrates (pyruvate/succinate/malate/ADP). Bars represent the mean of SI of CMH spectrum minus SI of the same condition with PEGSOD ± SEM, at time point 15 min. CTR were normalized to 100% (dotted red line) and all data were also normalized by mg of mitochondrial protein. N = 6, (*): $p < 0.05$.

oxygen and produce superoxide (Fig. 4A). In this system, superoxide is produced both extracellularly and intracellularly, as it is produced by membrane-bound NOX-2 [19]. Therefore, we used PEGSOD (instead of SOD) to induce the dismutation of superoxide in both compartments to assign the contribution of superoxide for CM● formation. Three interesting observations can be noticed from Fig. 4 D-E: 1) there was a spontaneous oxidation of CMH into CM● in this cellular system; 2) the PMA exposure led to an increased formation of CM●; 3) the pre-incubation with PEGSOD abolished the incremental oxidation of CMH induced by PMA exposure. The formation of nitroxides from cyclic hydroxylamines could involve other mechanisms than superoxide detection, including unspecific oxidation mechanisms or reaction with other ROS species. For example, it has been described that hydroxylamines can be oxidized by superoxide, but also H_2O_2, peroxynitrite and

derived nitrogen species ([17,24–26]. It is likely that some unspecific mechanisms or ROS are at the origin of the basal oxidation of CM● without PMA exposure, as this basal formation of CM● was not inhibited by the pre-incubation with PEGSOD (Fig. 3D and E). On the contrary, the contribution of unspecific mechanisms and ROS seems negligible when considering the effect of PMA, as the PMA-induced increase in EPR signal was abolished by PEGSOD, highlighting the main contribution of superoxide to CM● formation. Interestingly, we also observed that the exposure to PMA as well as the preincubation with PEGSOD did not affect the oxygen consumption by RAW 264.7 macrophages (Fig. 4B and C), highlighting that the oxygen consumption observed was mainly due to the cellular respiration and not due to the contribution of oxygen utilization by the NOX-2.

The third set of experiments was designed to qualify our approach of simultaneous measurement of OCR and superoxide production using isolated mitochondria exposed (or not) to inhibitors of the ETC. For the purpose, we used two compounds that are known inhibitors of NADH: ubiquinone oxidoreductase (complex I): rotenone [27,28] and metformin [29–31]. In this set-up, a significant decrease in OCR was induced by the exposure to rotenone or metformin (Fig. 5C), with no impact of PEGSOD. The superoxide net production was significantly increased for mitochondria exposed to rotenone (Fig. 5D), an observation consistent with those observed previously in the intracellular compartment [32] or in submitochondrial particles [27]. We also observed that metformin increased the superoxide net production in isolated mitochondria (Fig. 5D). While several reports described an increase in antioxidants systems on whole cells exposed to metformin [33,34], other reports highlighted an increase in ROS production including superoxide after metformin or mito-targeted metformin derivatives [32,35]. However, it should be noticed that the metformin-induced inhibition of respiration and superoxide production were observed for a relatively high concentration (3 mM). Further studies will be necessary to explore dose-effect relationships as plasma metformin levels reported are around 5 mg/L (30 μM) [36].

This integrative EPR toolbox for simultaneous measurement of OCR and superoxide production offers several advantages. First, this toolbox is less time consuming than sequential or separate experiments, allowing the characterization of more drugs or factors responsible for modulation in OCR or superoxide production. Second, measuring several parameters on the same cellular preparation or mitochondrial fraction dramatically improves the reproducibility of the experiments. The method described has the advantage to avoid variations in mitochondria preparations or recovery between separate experiments. Third, such approach is allowing more measurements since less cells or mitochondria are used to get a pattern of cellular or mitochondrial function. As shown by our experiments, the EPR toolbox described is rather versatile as it can be used to measure simultaneously OCR and ROS production on different types of preparations: substrate-enzyme solutions, whole cell suspensions or isolated organelles like mitochondria. The protocols described should be applicable on different cell lines and could potentially be used in other complex biological systems. However, this has yet to be proven knowing that there could be interferences with the hydroxylamine and the ferroxidase activity of ceruloplasmin found in blood samples, for example. Here, we used CMH as this compound is distributing in intra- and extracellular spaces. CMH could be swapped by mitochondria-targeted probes such as MitoTEMPO-H that accumulates into the mitochondrial compartment to measure mitochondrial ROS when using whole cell models. Regarding experiments on isolated mitochondria, the substrates used can be adapted depending on the type of state respiration studied. The method seems particularly suitable to screen the effect of compounds altering the mitochondrial function, for example toxic substances inducing mitochondrial dysfunction [37–39], new mitochondrial targeted anti-cancer agents [35,40,41] or modulators of metastatic progression through mitochondrial superoxide scavenging [11,42].

A potential limitation of the toolbox is the lack of selectivity of cyclic hydroxylamines towards superoxide scavenging. As already emphasized, control experiments using SOD or PEGSOD are necessary to assess the contribution of superoxide to CM● formation [17,21]. These specific superoxide scavengers are strong indicators that superoxide is involved in the nitroxide formation. Hence, the toolbox described should be considered as a first rapid screening tool for change in metabolic and/or ETC function in a biological preparation, and the unambiguous involvement of superoxide (compared to other ROS) should be confirmed in independent experiments. For example (mitochondrial) superoxide can be unequivocally detected using (mito-) hydroxyethidine and HPLC-based methods [43,44].

5. Conclusion

We have described an EPR toobox which is a rapid versatile platform to measure simultaneously superoxide production as well as oxygen consumption in biological systems. For the proof-of-concept, this toolbox has been applied in enzymatic systems, whole cells and mitochondrial fractions. This toolbox has the potential to screen the effect of modulators, intoxicants or drugs targeting the mitochondrial function.

Declaration of competing interest

The authors declare that they have no conflict of interest. The sponsors had no role in study design, in the collection, analysis and interpretation of data, in the writing of the report.

Acknowledgments

This research has been supported by the Foundation against Cancer (2016-087) and the Fonds National de la Recherche Scientifique FNRS (7652717F and J008220F). Bénédicte F. Jordan is Research Director of the FNRS. This study used equipments of the *Nuclear and Electron Spin Technologies* platform of the UCLouvain.

Appendix A. Supplementary data

Supplementary data to this article can be found online at https://doi.org/10.1016/j.redox.2020.101852.

References

[1] P. Newsholme, C. Gaudel, M. Krause, Mitochondria and diabetes. An intriguing pathogenetic role, Adv. Exp. Med. Biol. 942 (2012) 235–247, https://doi.org/10.1007/978-94-007-2869-1_10.
[2] S.W. Ballinger, Mitochondrial dysfunction in cardiovascular disease, Free Radic. Biol. Med. 38 (10) (2005) 1278–1295, https://doi.org/10.1016/j.freeradbiomed.2005.02.014.
[3] P. Costantini, Mitochondrion as a novel target of anticancer chemotherapy, J. Natl. Cancer Inst. 92 (13) (2000) 1042–1053, https://doi.org/10.1093/jnci/92.13.1042.
[4] B.F. Jordan, et al., Insulin increases the sensitivity of tumors to irradiation: involvement of an increase in tumor oxygenation mediated by a nitric oxide-dependent decrease of the tumor cells oxygen consumption, Canc. Res. 62 (12) (2002) 3555–3561.
[5] C. Diepart, et al., Arsenic trioxide treatment decreases the oxygen consumption rate of tumor cells and radiosensitizes solid tumors, Canc. Res. 72 (2) (2012) 482–490, https://doi.org/10.1158/0008-5472.CAN-11-1755.
[6] B. Gallez, M.A. Neveu, P. Danhier, B.F. Jordan, Manipulation of tumor oxygenation and radiosensitivity through modification of cell respiration. A critical review of approaches and imaging biomarkers for therapeutic guidance, Biochim. Biophys. Acta Bioenerg. 1858 (8) (2017) 700–711, https://doi.org/10.1016/j.bbabio.2017.01.002.
[7] I. Rahman, S.K. Biswas, "Oxidants and Antioxidants: Antioxidants, Enzymatic," in *Encyclopedia of Respiratory Medicine*, Four-Volume Set, 2006, pp. 258–266.
[8] V. Purohit, D.M. Simeone, C.A. Lyssiotis, Metabolic regulation of redox balance in cancer, Cancers 11 (7) (2019), https://doi.org/10.3390/cancers11070955.
[9] P. Amstad, D. Crawford, D. Muehlematter, I. Zbinden, R. Larsson, P. Cerutti, "Oxidants stress induces the proto-oncogenes, C-fos and C-myc in mouse epidermal cells," in, Bull. Canc. 77 (5) (1990) 501–502.
[10] J.E. Klaunig, Z. Wang, Oxidative stress in carcinogenesis, Curr. Opin. Toxicol. 7 (2018) 116–121, https://doi.org/10.1016/j.cotox.2017.11.014.
[11] P.E. Porporato, et al., A mitochondrial switch promotes tumor metastasis, Cell Rep. 8 (3) (2014) 754–766, https://doi.org/10.1016/j.celrep.2014.06.043.

SUPPLEMENTARY DATA

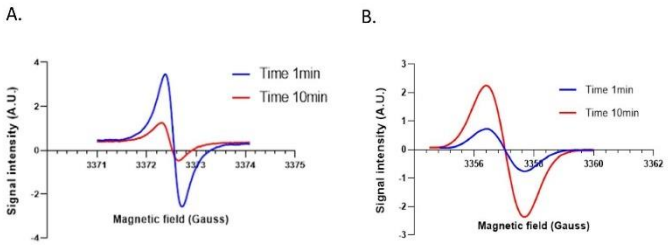

Figure 1S. Preliminary experiment showing nitroxide and hydroxylamine interference

(A) Representation of ^{15}N-PDT high-field line when combining ^{15}N-PDT and ^{14}N-CMH in PBS buffer into a same hematocrit capillary, at a final concentration of 100µM and 0.5mM respectively. Spectra were recorded at time 1min (blue line) and time 10min (red line) after probes being mixed together.

(B) Representation of ^{14}N-CM° center field line when combining ^{15}N-PDT and ^{14}N-CMH in PBS buffer into a same hematocrit capillary, at a final concentration of 100µM and 0.5mM respectively. Spectra were recorded at time 1min (blue line) and time 10min (red line) after probes being mixed together.

AGENT	STOCK	INTERMEDIATE DILUTION	FINAL CONCENTRATION
HX	5mM	/	1mM
XO	5U/mL	0.05U/mL	0.005U/mL
DTPA	100mM	/	1mM
^{14}N-CMH	10mM	/	1mM
^{15}N-PDT	2mM	/	100µM
SOD	1000U/mL	/	200U/mL

Table 1A. Agents and stock solutions used for HX/XO experiment

AGENT	VOLUME
PBS	138µL (or 98µL with SOD)
HX	40µL
XO	20µL
DTPA	2µL
SOD	40µL

Table 1B. Base mixture formulation used for HX/XO experiment

AGENT	STOCK	VOLUME
Cells	$10x10^6$/mL	55 µL
Dextran	20% in PBS	45 µL
DTPA	100mM	1µL
^{15}N-PDT	2mM	5µL
PBS or PEGSOD (for PMA+PEGSOD condition)	PEGSOD 4000U/mL	5µL

Table 2A. Respiration mix formulation used for RAW experiment

AGENT	VOLUME
Substrats	275µL
Dextran (20%)	132µL
MAS (2x)	137.5µL
DTPA	5.5µL

Table 3A. Respiration mix formulation used for experiments on isolated mitochondria

AGENT	VOLUME
Substrats	125µL
PBS	60µL
MAS (2x)	62.5µL
DTPA	2.5µL

Table 3B. Superoxide mix formulation used for experiments on isolated mitochondria

II. Measurement of mitochondrial (dys)function in cellular systems using EPR: oxygen consumption rate and superoxide production.

Article in press in *Methods of molecular biology* 2022

Measurement of mitochondrial (dys)function in cellular systems using Electron Paramagnetic Resonance (EPR): oxygen consumption rate and superoxide production.

Donatienne d'Hose and Bernard Gallez

Biomedical Magnetic Resonance, Louvain Drug Research Institute (LDRI),

Université catholique de Louvain (UCLouvain),

Avenue Mounier 73.08, 1200 Brussels, Belgium

donatienne.dhose@uclouvain.be

bernard.gallez@uclouvain.be

Running head:

EPR assays for oxygen consumption and superoxide production

Abstract

The oxygen consumption rate (OCR) and superoxide production are crucial when assessing mitochondrial function and/or dysfunction. EPR spectroscopy allows the measurement of both components either independently or simultaneously in a same cellular or mitochondrial preparation. OCR determination using EPR oximetry is based on the change in EPR linewidth of a paramagnetic oxygen sensing probe (a perdeuterated nitroxide) in the presence of oxygen consuming cells in a closed system. Superoxide production can be monitored by the oxidation of cyclic hydroxylamines into nitroxides. The contribution of superoxide to the nitroxide formation is deduced from experiments in the presence and in the absence of SOD and PEGSOD as appropriate controls.

Keywords: EPR, ETC, mitochondrial function, oximetry, oxygen consumption rate (OCR), superoxide, nitroxide, hydroxylamine

1. Introduction

Mitochondria have a pivotal role in cellular energetics including oxidative phosphorylation to produce cellular ATP, but they also have important roles in apoptosis and programmed cell death, and in ROS production. Mitochondrial dysfunction may lead to pathological processes like diabetes, cardiovascular diseases and neurodegenerative disorders. Over the years, several mitochondrial modulators have emerged, notably in the field of anticancer therapies targeting cellular oxygenation and mitochondrial metabolism. Their impact on the oxygen consumption rate (OCR) and bioenergetics of this organelle is nowadays well studied but little has been investigated on their potential underlying incidence on reactive oxygen species (ROS) production and oxidative damage occurring during those treatments. When the balance between antioxidant systems and cellular ROS is disrupted, oxidative stress overpowers and leads to the oxidation of macromolecules like DNA, proteins and lipids, consequently inducing cellular damage and defects in cell signaling . More specifically, superoxide may trigger cell death when produced in large excess but it was also suggested to be a key driver promoting cancer cell migration and metastasis when produced at more moderate levels . Therefore, the dual dose-dependent effects on oxygen consumption rate (OCR) and superoxide production are crucial to consider when assessing mitochondrial function and/or dysfunction.

Electron paramagnetic resonance (EPR) is a method of choice for assessing the oxygen consumption and the superoxide production. The OCR determination is based on the change in EPR linewidth of a paramagnetic oxygen sensing probe (here, a nitroxide) in the presence of oxygen consuming cells in a closed system . This method has been successfully applied to characterize the effect of inhibitors of the electron transport chain in cancer cells . In addition, EPR allows the detection of superoxide produced by the oxidation of cyclic hydroxylamines into nitroxides . Because their oxidation into paramagnetic nitroxide can be due to several redox reactions, the contribution of superoxide to the nitroxide formation has to be deduced from experiments carried out in the presence and in the absence of SOD or PEGSOD (pegylated-superoxide dismutase) as appropriate controls . As described in this paper, both parameters may be measured independently.

Recently, our lab also developed an integrated toolbox enabling the simultaneous analysis of the OCR and superoxide production on a single mitochondrial preparation . For the purpose, there is a need to measure the variation of the EPR linewidth of one nitroxide, on the one hand,

and the formation of another nitroxide, on the other hand. The separation of the EPR signals coming from both nitroxides can be done by using different isotopically-labelled probes: ^{15}N-PDT (4-oxo-2,2,6,6-tetramethylpiperidine-d_{16}-^{15}N-1-oxyl) is the nitroxide used for OCR measurement and ^{14}N-CMH (1-hydroxy-3-methoxycarbonyl-2,2,5,5-tetramethylpyrrolidine) is the cyclic hydroxylamine that will be transformed into a nitroxide after reaction with the superoxide. The EPR signal coming from both nitroxides are not superimposable as ^{15}N-PDT gives a doublet while ^{14}N-CMH gives a triplet (**Figure 1**). Therefore, the variation of the linewidth of ^{15}N-PDT (linked to OCR) and the formation of ^{14}N-CM$^{\bullet}$ (linked to superoxide production) can be recorded simultaneously on a single cellular or mitochondrial preparation .

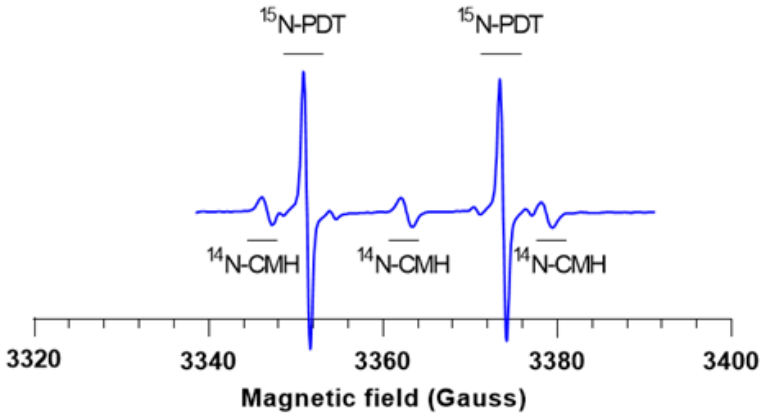

Figure 1: Representative global EPR spectrum of ^{15}N-PDT and ^{14}N-CMH in PBS buffer injected into two separate capillaries, and gathered into a same quartz tube. Final concentrations of the probes are 100µM and 0.5mM respectively.

2. Materials

2.1. EPR spectrometer

All EPR experiments were performed using a Bruker EMX-Plus spectrometer operating in X-band (9.85 GHz) and equipped with a PremiumX ultra low noise microwave bridge and a SHQ high sensitivity resonator (*see* **Note 1**). The EPR cavity was heated at 310 K with air during all experiments. OCR and superoxide measurements can be performed on whole cells as well as on isolated mitochondria without changing material nor method. Specific concentrations for both models are informed for each assay. Skip the mitochondrial isolation part if using a whole cell model.

2.2. EPR oximetry

1. Disposable microhematocrit capillaries in soda-lime glass (75mm/75µL).
2. Sealing gum for capillaries (*see* **Note 2**).
3. Phosphate buffered saline (PBS) from Gibco, pH 7.4, without calcium chloride nor magnesium chloride.
4. 20% Dextran from leuconostoc mesenteroides (average MW 60000–76000) solution diluted in PBS (*see* **Note 3**). Stock solution can be stored at 4°C during a month.
5. ^{15}N-PDT (4-oxo-2,2,6,6-tetramethylpiperidined$_{16}$-^{15}N-1-oxyl) used as oxygen sensor (*see* **Note 4**). The required stock solution is 2mM diluted into PBS. Store at 4°C for short term use. Other aliquots should be stored at -80°C until needed.
6. Biological system: depending on the type of experiment wanted: Stock solution of whole cells (around 5.10^{6}cells/mL culture media) (*see* **Note 5**) or suspension of isolated mitochondria.

2.3. Superoxide measurements

1. Gas-permeable polytetrafluoroethylene (PTFE) tubing (ZEUS) with inside diameter 0.025 in. and wall thickness 0.002 in., cut into 12cm sections.
2. 1ml syringes with 23G needles
3. PBS (Gibco), pH 7.4, without calcium chloride nor magnesium chloride.
4. Parafilm

5. Diethylenetriaminepentaacetic acid (DTPA): 100 mM stock solution in PBS. Store at room temperature.
6. Polyethylene glycol-superoxide dismutase (PEG-SOD): 4000U/mL stock solution in PBS. Store at -20°C.
7. Diamagnetic hydroxylamine for oxidation measurements: 1-Hydroxy-3-methoxycarbonyl-2,2,5,5-tetramethylpyrrolidine. HCl (CMH hydrochloride) used on mitochondria or (2-(2,2,6,6-Tetramethylpiperidin-1-oxyl-4-ylamino)-2-oxoethyl) triphenylphosphonium chloride (MitoTempo-H) for whole cell experiments. Stock solution are 10 mM and 1 mM, respectively, in PBS. Both probes are to be stored at -20°C and flushed with argon at every use to avoid probe oxidation.
8. Biological system: depending on the type of experiment wanted: Stock solution of whole cells (around 20.10^6cells/mL culture media) or suspension of isolated mitochondria.

2.4. Mitochondrial isolation

1. Cell line of interest, cultured in its recommended medium: about 40.10^6cells required resuspended in 1 mL of PBS (*see* **Note 6**).
2. Motor-driven Glass/Teflon potter homogenizer
3. 0.1 M Tris/MOPS: Dissolve 1.21 g Tris in 40ml distillated water, then adjust pH to 7.4 with MOPS powder. Bring to 50 mL and store at 4°C.
4. 1M EGTA/Tris: Dissolve 3.81 g EGTA in 40ml distillated water, then adjust pH to 7.4 with Tris powder. Bring to 50 mL and store at 4°C.
5. 1M sucrose: Dissolve 34.2 g Sucrose in 100 mL distilled water and separate in 5 aliquots. Store at -20°C.
6. Mitochondrial isolation buffer (100mL to aliquot): Mix 10 mL of Tris/MOPS (0.1 M) and 1 mL of EGTA/Tris (1 M) to 20mL of sucrose (1M). Bring the mixture to 100 mL with distilled water and adjust pH to 7.4. Store at -20°C.

2.5. Mitotoolbox

The Mitotoolbox combines OCR and superoxide measurements at the same time, meaning that all material listed for OCR and superoxide are also required for this experiment. Solutions and buffers are kept on ice during the mitochondrial isolation procedure. Listed substrate supply includes NADH- and $FADH_2$-linked substrates to support state 3 respiration.

1. Isolated mitochondria (*see* "mitochondrial isolation" in **Methods**)
2. 100 mM EGTA: Dissolve 76 mg in 20 mL of water.
3. Mitochondrial Assay buffer (MAS (x2): This buffer is two times concentrated: Combine 12 g Sucrose, 20 g Mannitol, 68 mg potassium phosphate monobasic (KH_2PO_4), 0.5 g $MgCl_2$ hexahydrate, 23.8 mg HEPES, 1 g FA-free BSA and 5 mL of EGTA stock solution (100 mM) in 250 mL of water. Adjust pH to 7.4 and aliquot. Store at -20°C.
4. 100 mM Pyruvate: dilute in PBS. Store at -80°C.
5. 500 mM Succinate: dilute in PBS. Store at -80°C.
6. 500 mM Malate: dilute in PBS. Store at -80°C.
7. 100 mM ADP: Mix 425 mg ADP with 1.2 mL of PBS (ADP does not dissolve at this point). Neutralize with 5 M KOH (approx. 450 µl). ADP will dissolve after addition of KOH. Adjust pH to 7.4 and bring to 10 mL with PBS. Store at -80°C.
8. Substrate Mix: Combine 300 µL of MAS (x2) with 216 µL PBS, 60µL pyruvate (100 mM), 6 µL succinate (500 mM), 6 µL Malate (500 mM) and 12 µL ADP (100 mM). This final volume is enough for 6 combined measurements of OCR and Superoxide.

3. Methods

3.1. EPR oximetry on whole cell model

Keep the cell stock solution (lid open) in a 37°C water bath during the experiments.

1. Turn on the X band EPR, heat the cavity at 310K using continuous nitrogen flow (400 L/h) (*see* **Note 7**) and open Bruker Xenon Spin fit program.
2. Tune the EPR cavity at 19 dB attenuation (2.518 mW) with a sealed hematocrit capillary filled with PBS transferred in a quartz tube (*see* **Note 8**)
3. Set experimental parameters for acquisition: microwave power: 2.518 mW; modulation frequency: 100 kHz; modulation amplitude: 0.005 mT; Center field: 335mT; Sweep width: 1.5 mT; Sweep time:15 s.
4. Combine 60 µL of cell suspension to 40 µL of Dextran 20% solution.
5. Add 4 µL of ^{15}N-PDT stock solution to the previous mixture and mix well.
6. Transfer mix into hematocrit capillary and seal with gum. Slip capillary carefully into a quartz tube and transfer it to the EPR cavity.
7. Tune the EPR cavity and wait 3min after the probe was mixed before launching an automated "2D-field-Delay" measurement counting 15 points with a time delay of 60000ms.
8. Save file and proceed to data analysis after all experiments are done: switch to processing mode and load your file. Select "Peak picking" and define the region containing the peak on all slices with "region qualifier". Select pick > Peak and through > Dist Algorithm > All slices > Pick > Report distances. The final file can be saved as ASCII file to extract linewidth data at each point.
9. Correlate ^{15}N-PDT linewidth with the % of oxygen with a calibration curve (*see* **Note 9** and **Figure 2**).
10. OCR corresponds to the slope of oxygen level during time.

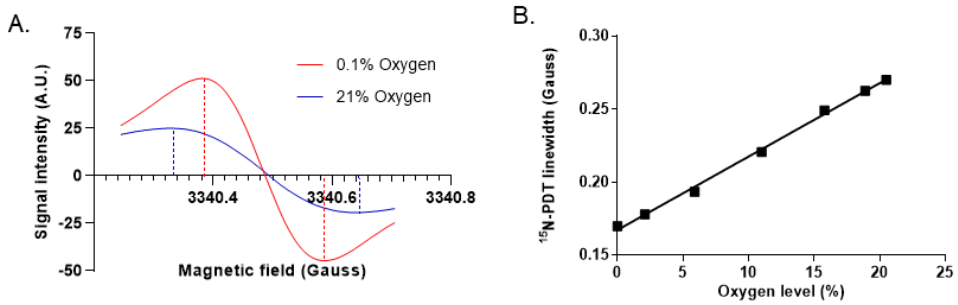

Figure 2: (**A**): ^{15}N-PDT spectra at 0.1% (red) and 21% (blue) of oxygen mixed with nitrogen. (**B**): ^{15}N-PDT calibration curve linking the probe's linewidth (Gauss) to oxygen level (%) present into the sealed hematocrit capillary. Both spectra correspond to the high-field line.

3.2. Superoxide measurement on whole cell model

Keep the cell stock solution (lid open) in a 37°C water bath during the experiments.

1. Turn on the X band EPR, heat the cavity at 310K using continuous air flow (400 L/h) and open Bruker Xenon Spin fit program.
2. Tune the EPR cavity at 10 dB attenuation (20 mW) with a 12 cm long PTFE tube folded in 4 filled with PBS, transferred in an open quartz tube (*see* **Note 10**). Seal the end of the quartz tube with a patch of parafilm to avoid a potential leak into the EPR cavity. Set experimental parameters for acquisition: microwave power: 20 mW; modulation frequency: 100 kHz; modulation amplitude: 0.1 mT; Center field: 336.5mT; Sweep width: 1.5 mT; Sweep time: 30.48s.
3. For control condition, combine 37 µL of cell suspension to 0.5 µL od DTPA (100mM), 5 µL of PBS and end by mixing 7.5 µL of MitoTempoH (1mM). To measure superoxide contribution, make another measurement using the same conditions but replacing 2.5 µL PBS by adding 2.5 µL of PEG-SOD (4000 U/mL). Let incubate 10 min before adding the MitoTempoH. It is mandatory to flush MitoTempoH stock solution with argon before and during pipetting to avoid probe oxidation.

4. Transfer mix into PTFA tube cutting using the needle. Fold in 4 and insert into the open quartz tube. Seal quartz tube with a patch of parafilm and transfer it to the EPR cavity.
5. Tune the EPR cavity and wait 3min after the probe was mixed before launching an automated "2D-field-Delay" measurement counting 11 points with a time delay of 40000 ms.
6. Save file and proceed to data analysis after all experiments are done: switch to processing mode and load your file (**Figure 3**). Select "Integration & derivative" and define the region containing the peak in all slices. Select "Double Integration" and copy results to primary. Then, switch to time domain > Store & return > Structure > Projection > Roof. The final file can be saved as ASCII file to extract double integration (DI) values for each timepoint (**Figure 4**).
7. Subtract point 1 DI from point 11 DI for each condition. Superoxide contribution is measured by subtracting mean PEGSOD DI to mean control DI.

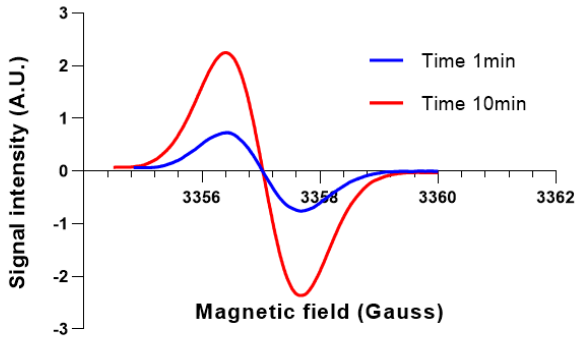

Figure 3: Representative example of ^{14}N-CMH oxidation spectra after 1min and 10min on whole cell model. These spectra are similar to those obtained with MitoTempoH probe. Both spectra correspond to the mid-field line.

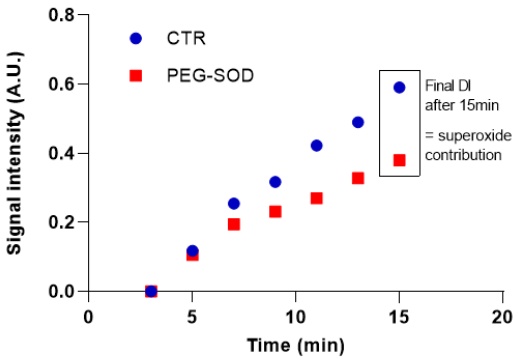

Figure 4: Representative example of MitoTempoH DI spectra during time on isolated mitochondria. Same kind of spectra are obtained when using a whole cell model as well. Blue dots represent control condition and red dots represent PEG-SOD condition. Superoxide contribution is measured by subtracting the PEGSOD DI to the CTR DI after 15min.

3.3. Mitochondrial isolation

Mitochondrial isolation buffer (MIB) should be toughed in advance and stored on ice. All steps of mitochondrial isolation are performed on ice or at 4°C to avoid damage by proteases and phospholipases. The potter homogenizer is precooled on ice before use. This protocol has been adapted from.

1. Harvest cultured cell line of interest to get around 40.10^6 cells (or more if needed, *see* **Notes 6 and 11**).
2. Resuspend cells in 1 mL PBS and centrifuge cells at 600 g at 4°C during 10 min.
3. Remove the supernatant and resuspend the cells in 3 mL of ice-cold MIB.
4. Transfer the cell mixture into the precooled potter and blend with the motor-driven pestle at 1600 rpm making 35 strokes. To maintain cooling temperature during homogenization, the entire device is placed in a box or beaker filled with ice. (*see* **Note 12**).
5. Transfer the homogenate to a 15 mL falcon tube and centrifuge at 600 g at 4°C during 10 min.
6. Collect the supernatant and centrifuge at 7000 g at 4°C during 10 min.

7. Remove the supernatant and wash the pellet with 200 µL of MIB before transferring the homogenate to a 1.5 mL Eppendorf.
8. Centrifuge the suspension at 7000 g at 4°C during 10 min.
9. Discard the supernatant and gently homogenize the mitochondria pellet with the little remaining supernatant left, avoiding bubble formation.
10. Store on ice. (*see* **Note 13**).

3.4. Mitotoolbox: OCR & superoxide simultaneous measurement

The Mitotoolbox combines oximetry and superoxide measurements at the same time on the same mitochondrial isolate, meaning that all material listed for EPR oximetry and superoxide measurements are also required to perform the experiment. Of note, this simultaneous measurement of mitochondrial function can also be measured on a whole cell model using the same EPR device as well as EPR parameters with the cell stock solutions given in the **Material** section "EPR oximetry" and "superoxide measurements".

1. Store mitochondrial isolate and substrate mix on ice.
2. Respiration mix (for 6 independent measurements): combine 275 µL substrates, 137.5 µL of MAS (x2), 132 µL dextran 20% and 5.5 µL DTPA. Mix well.
3. Superoxide mix (for 6 independent measurements): combine 125 µL substrates, 62.5 µL MAS (x2), 60 µL PBS and 2.5 µL DTPA. Mix well.
4. Turn on the X band EPR, heat the cavity at 310K using continuous air flow (400 L/h) and open Bruker Xenon Spin fit program.
5. Tune the EPR cavity at 19 dB attenuation (2.518 mW) with a 12 cm long PTFE tube folded in 4 filled with PBS and a sealed hematocrit capillary filled with PBS (*see* **Note 14** and **Figure 5**).
6. Create and save a separate OCR parameters file on Xenon: microwave power: 2.518 mW; modulation frequency: 100 kHz; modulation amplitude: 0.005 mT; Receiver gain: 45 dB; Center field:334 mT; Sweep width: 1.5 mT; Sweep time: 25 s.
7. Create and save a separate superoxide parameters file on Xenon: microwave power: 2.518 mW; modulation frequency: 100 kHz; modulation amplitude: 0.1 mT; Receiver gain: 60 dB; Center field: 334.4 mT; Sweep width: 1.5 mT; Sweep time: 25 s.

8. Final OCR solution for EPR: combine 85 µL of respiration mix with 7 µL PBS, 3 µL of isolated mitochondria and add 5 µL of ^{15}N-PDT (2 mM) at the last minute.
9. Final superoxide solution for EPR: combine 32 µL superoxide mix with 3 µL PBS, 3 µL isolated mitochondria and add 2 µL of ^{14}N-CMH (10 mM) at the last minute.
10. ^{15}N-PDT and ^{14}N-CMH should be inserted to their mix at the same time. Hematocrit capillary and PTFA tubing are filled with their corresponding final solution, and put together into the open quartz tube. Transfer the device into the EPR cavity.
11. 3 min after probes were added to their final mix, launch first superoxide acquisition with the corresponding parameters and save file. Launch OCR acquisition every even number of minutes and superoxide on odd number of minutes after probe addition. Save files on Xenon for data analysis.
12. To measure superoxide contribution, add 5 µL of PEG-SOD to final OCR solution and 2 µL PEG-SOD to the final superoxide solution (adding less PBS in consequence).
13. Data analysis are performed the same way as stated in section "EPR oximetry" and section "superoxide measurement" on whole cell model.
14. Normalization by mitochondrial protein quantification is recommended (*see* **Note 15**).

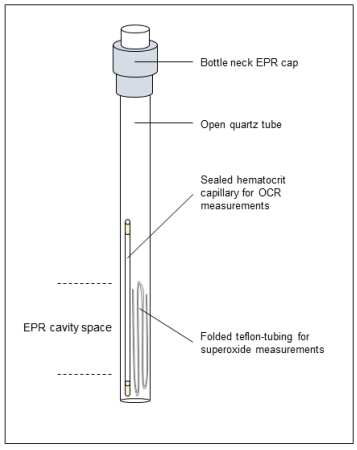

Figure 5: Schematic representation of the double capillary device used to measure OCR and superoxide simultaneously**.**

4. Notes

1. Any EPR spectrometer can be used as long as it is capable of being equilibrated at 310K with continuous gas flow.
2. Gum can contain paramagnetic manganese visible with EPR when inserted into the cavity's resonator. To avoid nonspecific spectra appearing during analysis, make sure the sealed part of the hematocrit capillary remains outside the resonator.
3. Dextran solution is used to keep cells or isolated mitochondria in suspension in the capillary during the whole measurement. Do not use dextran with a lower MW than stated, otherwise cells tend to sedimentate and EPR measurements will not be accurate.
4. ^{15}N-PDT (perdeuterated nitroxide) is a very sensitive probe to measure oxygen levels in a medium using EPR technology. Its linewidth is proportional to the oxygen level present into the capillary. A calibration linking the probe linewidth broadening to oxygen level should therefore first be performed in order to measure OCR during an experiment with cells or mitochondrial suspension.
5. For whole cells experiments, a stock solution of 5.10^6 cells/mL should be sufficient to measure a suitable oxygen consumption. However, depending on the cell type, this cell concentration can be fine-tuned beforehand by performing dose-response tests to get the best oxygen consumption curve (some cells are more rapidly consuming oxygen than others). This new stock concentration should therefore be used for all other oximetry experiments using this cell line.
6. Depending on the cell line, this initial cell number could be increased to have a better yield and perform more measurements from the same isolated batch of mitochondria. Typically, at the end of the process, enough mitochondria are collected (40µL with a mean of 25mg of protein/mL) to make 4 conditions with simultaneous measurements of OCR and superoxide, using 3T3 fibroblasts
7. In this case, EPR cavity can also be heated with air but nitrogen is less expensive. The capillary being sealed off, the type of gas used to heat the cavity does not matter because it will not affect the sample.
8. The tuning of the EPR cavity is performed at 19 dB attenuation (2.518 mW) with the same device used for the actual oximetry experiments, namely a sealed hematocrit capillary filled with PBS and ^{15}N-PDT (oxygen sensor), inserted into a quartz tube that is

then transferred to the EPR cavity. Mixing the oxygen sensor at this stage is not mandatory but recommended in order to find the exact magnetic field value where the ^{15}N-PDT spectrum is appearing.

9. The calibration to link ^{15}N-PDT linewidth with the level of oxygen in a capillary is performed using an EPR spectrometer connected to an Aalborg gas mixer and an oxygen analyzer (Servomex OA540). Calibration mixture contains PBS and Dextran (20%) at a final ratio 1:1 mixed with 4 µL of ^{15}N-PDT (2 mM). ^{15}N-PDT linewidth is measured at different % of oxygen (7pts between 0 and 21%) mixed with nitrogen. Wait 40sec before each measurement for the oximeter to equilibrate. The obtained curve equation is then used to measure % of oxygen during experiments on biological systems.
10. To fill the PTFA tubing, insert needle into a tube segment and suck up the PBS or final cell solution until the segment is entirely filled. Fold in 4 and insert the tube at the open end of the quartz tube.
11. Do not treat cells with any agents before harvesting. Mitochondrial isolation is performed on control/non-treated cells and treatment of any kind should be added in final OCR or final superoxide solutions as a new condition to analyze its impact on mitochondrial function.
12. Homogenization by a motor-driven Glass/Teflon potter tends to heat up the cell mixture. To avoid damaging activation of proteases and phosphatases and maintain mitochondrial integrity, keeping the potter on ice is essential.
13. Isolated mitochondria should be used within 1-3 hours for better responses.
14. The 2 tubes are inserted next to each other in the open quartz tube.
15. Protein quantification can be performed using BCA protein Assay. Mitochondrial isolates are diluted 1:20 and protein determination can be assessed following manufacturer's instructions.

Acknowledgments:

This research has been supported by the Foundation against Cancer (2016-087) and the Fonds National de la Recherche Scientifique FNRS (7652717F and J008220F).

References:

Ansiaux, R., C. Baudelet, B. F. Jordan, N. Crokart, P. Martinive, J. DeWever, V. Gregoire, O. Feron, and B. Gallez. 2006. 'Mechanism of reoxygenation after antiangiogenic therapy using SU5416 and its importance for guiding combined antitumor therapy', Cancer Res, 66: 9698-704.

Crokart, N., B. F. Jordan, C. Baudelet, R. Ansiaux, P. Sonveaux, V. Gregoire, N. Beghein, J. DeWever, C. Bouzin, O. Feron, and B. Gallez. 2005. 'Early reoxygenation in tumors after irradiation: determining factors and consequences for radiotherapy regimens using daily multiple fractions', Int J Radiat Oncol Biol Phys, 63: 901-10.

Crokart, N., B. F. Jordan, C. Baudelet, G. O. Cron, J. Hotton, K. Radermacher, V. Gregoire, N. Beghein, P. Martinive, C. Bouzin, O. Feron, and B. Gallez. 2007. 'Glucocorticoids modulate tumor radiation response through a decrease in tumor oxygen consumption', Clin Cancer Res, 13: 630-5.

d'Hose, D., P. Danhier, H. Northshield, P. Isenborghs, B. F. Jordan, and B. Gallez. 2021. 'A versatile EPR toolbox for the simultaneous measurement of oxygen consumption and superoxide production', Redox Biol, 40: 101852.

Danhier, P., T. Copetti, G. De Preter, P. Leveque, O. Feron, B. F. Jordan, P. Sonveaux, and B. Gallez. 2013. 'Influence of cell detachment on the respiration rate of tumor and endothelial cells', PLoS One, 8: e53324.

De Preter, G., C. Deriemaeker, P. Danhier, L. Brisson, T. T. Cao Pham, V. Gregoire, B. F. Jordan, P. Sonveaux, and B. Gallez. 2016. 'A Fast Hydrogen Sulfide-Releasing Donor Increases the Tumor Response to Radiotherapy', Mol Cancer Ther, 15: 154-61.

Diepart, C., O. Karroum, J. Magat, O. Feron, J. Verrax, P. B. Calderon, V. Gregoire, P. Leveque, J. Stockis, N. Dauguet, B. F. Jordan, and B. Gallez. 2012. 'Arsenic trioxide treatment decreases the oxygen consumption rate of tumor cells and radiosensitizes solid tumors', Cancer Res, 72: 482-90.

Diepart, C., J. Verrax, P. B. Calderon, O. Feron, B. F. Jordan, and B. Gallez. 2010. 'Comparison of methods for measuring oxygen consumption in tumor cells in vitro', Anal Biochem, 396: 250-6.

Dikalov, S. I., and D. G. Harrison. 2014. 'Methods for detection of mitochondrial and cellular reactive oxygen species', Antioxid Redox Signal, 20: 372-82.

Dikalov, S. I., I. A. Kirilyuk, M. Voinov, and I. A. Grigor'ev. 2011. 'EPR detection of cellular and mitochondrial superoxide using cyclic hydroxylamines', Free Radic Res, 45: 417-30.

Frezza, C., S. Cipolat, and L. Scorrano. 2007. 'Organelle isolation: functional mitochondria from mouse liver, muscle and cultured fibroblasts', Nat Protoc, 2: 287-95.

Jordan, B. F., V. Gregoire, R. J. Demeure, P. Sonveaux, O. Feron, J. O'Hara, V. P. Vanhulle, N. Delzenne, and B. Gallez. 2002. 'Insulin increases the sensitivity of tumors to irradiation: involvement of an increase in tumor oxygenation mediated by a nitric oxide-dependent decrease of the tumor cells oxygen consumption', Cancer Res, 62: 3555-61.

Jordan, B. F., P. Sonveaux, O. Feron, V. Gregoire, N. Beghein, C. Dessy, and B. Gallez. 2004. 'Nitric oxide as a radiosensitizer: evidence for an intrinsic role in addition to its effect on oxygen delivery and consumption', Int J Cancer, 109: 768-73.

Porporato, P. E., V. L. Payen, J. Perez-Escuredo, C. J. De Saedeleer, P. Danhier, T. Copetti, S. Dhup, M. Tardy, T. Vazeille, C. Bouzin, O. Feron, C. Michiels, B. Gallez, and P. Sonveaux. 2014. 'A mitochondrial switch promotes tumor metastasis', Cell Rep, 8: 754-66.

Purohit, V., D. M. Simeone, and C. A. Lyssiotis. 2019. 'Metabolic Regulation of Redox Balance in Cancer', Cancers (Basel), 11.

Scheinok, S., T. Capeloa, P. E. Porporato, P. Sonveaux, and B. Gallez. 2020. 'An EPR Study Using Cyclic Hydroxylamines To Assess The Level of Mitochondrial ROS in Superinvasive Cancer Cells', Cell Biochem Biophys, 78: 249-54.

Scheinok, S., P. Leveque, P. Sonveaux, B. Driesschaert, and B. Gallez. 2018. 'Comparison of different methods for measuring the superoxide radical by EPR spectroscopy in buffer, cell lysates and cells', Free Radic Res, 52: 1182-96.

Applications for mitochondrial function measurements

I. The short-term exposure to SDHI fungicides Boscalid and Bixafen induces a mitochondrial dysfunction in Selective human cell lines

Article published in *Molecules* 2021

D.d'Hose, Molecules 2021, 26(19), 5842; doi.org/10.3390/molecules26195842

molecules

MDPI

Article

The Short-Term Exposure to SDHI Fungicides Boscalid and Bixafen Induces a Mitochondrial Dysfunction in Selective Human Cell Lines

Donatienne d'Hose [1], Pauline Isenborghs [1], Davide Brusa [2], Bénédicte F. Jordan [1] and Bernard Gallez [1,*]

[1] Biomedical Magnetic Resonance, Louvain Drug Research Institute (LDRI), Université catholique de Louvain (UCLouvain), 1200 Brussels, Belgium; donatienne.dhose@uclouvain.be (D.d.); pauline.isenborghs@gmail.com (P.I.); benedicte.jordan@uclouvain.be (B.F.J.)

[2] CytoFlux-Flow Cytometry Platform, Institut de Recherche Expérimentale et Clinique, Université catholique de Louvain (UCLouvain), 1200 Brussels, Belgium; davide.brusa@uclouvain.be

* Correspondence: bernard.gallez@uclouvain.be

Abstract: Fungicides are used to suppress the growth of fungi for crop protection. The most widely used fungicides are succinate dehydrogenase inhibitors (SDHIs) that act by blocking succinate dehydrogenase, the complex II of the mitochondrial electron transport chain. As recent reports suggested that SDHI-fungicides could not be selective for their fungi targets, we tested the mitochondrial function of human cells (Peripheral Blood Mononuclear Cells or PBMCs, HepG2 liver cells, and BJ-fibroblasts) after exposure for a short time to Boscalid and Bixafen, the two most used SDHIs. Electron Paramagnetic Resonance (EPR) spectroscopy was used to assess the oxygen consumption rate (OCR) and the level of mitochondrial superoxide radical. The OCR was significantly decreased in the three cell lines after exposure to both SDHIs. The level of mitochondrial superoxide increased in HepG2 after Boscalid and Bixafen exposure. In BJ-fibroblasts, mitochondrial superoxide was increased after Bixafen exposure, but not after Boscalid. No significant increase in mitochondrial superoxide was observed in PBMCs. Flow cytometry revealed an increase in the number of early apoptotic cells in HepG2 exposed to both SDHIs, but not in PBMCs and BJ-fibroblasts, results consistent with the high level of mitochondrial superoxide found in HepG2 cells after exposure. In conclusion, short-term exposure to Boscalid and Bixafen induces a mitochondrial dysfunction in human cells.

Keywords: EPR; oxygen consumption rate (OCR); superoxide; mitochondria; SDHI; Boscalid; Bixafen

Citation: d'Hose, D.; Isenborghs, P.; Brusa, D.; Jordan, B.F.; Gallez, B. The Short-Term Exposure to SDHI Fungicides Boscalid and Bixafen Induces a Mitochondrial Dysfunction in Selective Human Cell Lines. *Molecules* **2021**, *26*, 5842. https://doi.org/10.3390/molecules26195842

Academic Editor: Alejandro Samhan-Arias

Received: 7 September 2021
Accepted: 24 September 2021
Published: 26 September 2021

1. Introduction

Fungicides are intensively used in agriculture to prevent or inhibit the growth of fungi causing plant damage. The most widely used fungicides are succinate dehydrogenase inhibitors (SDHIs) [1] that act by blocking succinate dehydrogenase (SDH), the complex II of the mitochondrial electron transport chain (ETC) (Figure 1). Of commercialized SDHIs, Bixafen and Boscalid account together for about 50% of the sales [2]. SDHIs are generally considered as safe by pesticide-manufacturing companies and safety agencies [1–3]. However, recent alarming reports have demonstrated that SDHIs used as fungicides were not selective for their fungi targets but also block the honeybee, earthworm and human SDH with IC50 values in the μM range [4]. This is likely due to the high degree of conservation of a large portion of the SDH sequences throughout different species [4]. The same authors also showed that pre-existing mitochondrial defects, such as partial SDH dysfunction, increased the susceptibility to SDHIs after several days of exposure [4].

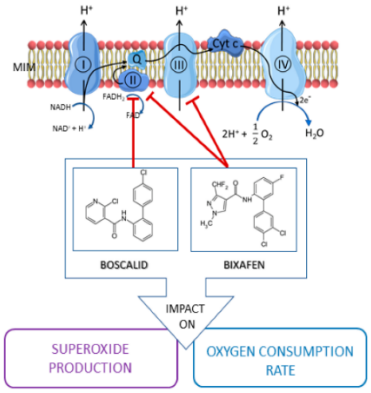

Figure 1. Effect of SDHI-fungicides on mitochondrial ETC. Boscalid and Bixafen block the complex II of the ETC, Bixafen also inhibiting complex III. By disrupting mitochondrial function, SDHIs may impact the production of mitochondrial superoxide radical and the oxygen consumption rate.

Other recent reports revealed neurodevelopmental defects in zebrafish models after exposure of embryos to Bixafen or Boscalid a few hours post-fertilization [5,6] as well as severe cardiac toxicity [7]. Chronic exposures (28 days) of adult zebrafish led to alterations in carbohydrate and lipid metabolism, and induced damage in the kidneys and the liver [8]. A genotoxic effect was also shown in human cells after chronic exposure. The frequencies of micronuclei and binucleated cells with micronuclei were increased in cultured human lymphocytes treated with Boscalid for 72 h [9]. Using an assay based on histone γH2AX phosphorylation, genotoxicity was also observed after 24 h of Bixafen treatment in SH-SY5Y kidney cell line and in human lymphocyte Jurkat Tcells [10].

All the effects described earlier were obtained after chronic exposure to SDHIs. Benit et al. considered it was relevant to use µM range concentrations as the Acceptable Daily Intake (ADI) values, which should lead to comparable concentrations in blood after exposure [4]. They calculated that an ADI of 0.04 and 0.02 mg/kg/day, for Boscalid and Bixafen, respectively, should lead to a blood concentration of approximately 1 µM [4]. This was criticized by the European Crop Protection Association (ECPA, representing companies marketing pesticides) in a comment on Benit's paper, considering that "*it does not account for the fact that SDHIs do not remain in the blood vessel compartment indefinitely but are rapidly distributed within the body*" [11]. We still believe that studying the effect in the µM range is appropriate. Indeed, it should be emphasized that the potential exposure limits for agricultural workers manipulating pesticides are much larger, as AOELs (Acceptable Operator Exposure Levels) for Boscalid and Bixafen are 0.1 mg/kg/day and 0.13 mg/kg/day, respectively. With the oversimplification of 100% of dose reaching the blood after absorption, for an operator with a body weight of 70 kg with 5 L of blood, it would lead to a peak concentration of 4.1 and 4.3 µM for Boscalid and Bixafen, respectively. Knowing that both compounds are readily absorbed after oral administration (83% and 56% for Bixafen and Boscalid, respectively) [12–14], and despite extensive metabolism and biliary excretion (elimination of radioactivity from radiolabeled Bixafen is characterized by a half-life in plasma of 8–9 h and a mean residence time of 13–19 h [12]), it is still reasonable to assume a theoretical short-term exposure of cells to µM concentration of SDHIs if exposed at levels close to the AOELs. The remaining issue to be resolved is to address the effect of short-term exposure to SDHIs of human cells exposed during their normal physiological functions.

To fill this gap, we tested the mitochondrial function of human cells exposed for a short time to Boscalid and Bixafen, the two most used SDHIs. For this purpose, we selected PBMCs (Peripheral Blood Mononuclear Cells), HepG2, and BJ human cell lines. Those cells are the most likely to be in contact with SDHIs after exposure: blood circulating cells and liver cells after oral intake (Bixafen and Boscalid accumulate in liver [12–14]), and fibroblasts after skin exposure. We focused on the mitochondrial ETC function of these cells. Interestingly, some SDH blockers (such as α-tocopheryl succinate, vitamin E-derived compounds linked to triphenylphosphonium group, malonate, 3-nitropropionate, lonidamine) have been evaluated in cancer therapy because the leakage of electrons to molecular oxygen leads to excessive production of superoxide ions and cancer cell apoptosis [15–20]. Hypothesizing that SDHIs-fungicides may present a similar mode of action, we used Electron Paramagnetic Resonance (EPR) spectroscopy which is particularly suitable to assess the oxygen consumption rate (OCR) [21–23] as well as the production of mitochondrial superoxide [23–29]. In addition, we evaluated the impact of short-term exposure to SDHIs on cell apoptosis and necrosis.

2. Results

2.1. Boscalid and Bixafen Decreased OCR in the Three Human Cell Lines

The OCR was significantly decreased in cells that were exposed for 2 h to 1µM Boscalid and Bixafen (Figure 2). For HepG2, both Boscalid and Bixafen decreased the OCR in a significant manner with 46% and 76% inhibition, respectively, compared with the controls. The same results were observed in PBMCs where Boscalid and Bixafen inhibited OCR by 75% and 83%, respectively, and in BJ-fibroblasts with an inhibition of OCR by 33% and 36%, respectively.

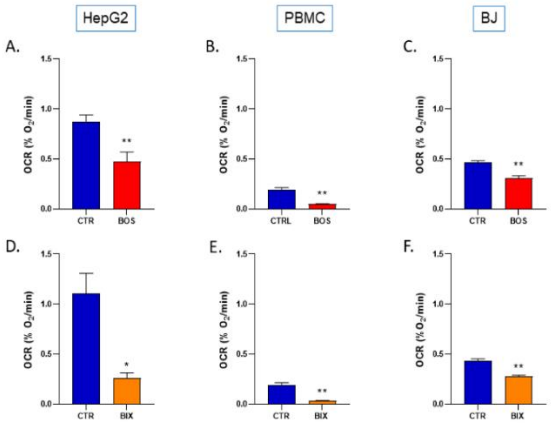

Figure 2. Oxygen consumption rate of control (DMSO 0.1%) and SDHIs-exposed human cells (1µM for 2 h). Top row: Boscalid-treated cells. (**A**): HepG2 liver cells, (**B**): PBMCs, (**C**): BJ-fibroblasts. Bottom row: Bixafen-treated cells. (**D**): HepG2 liver cells, (**E**): PBMCs, (**F**): BJ-fibroblasts. Bars represent mean ± SEM (%O_2/min). N = 3, (*): $p < 0.05$, (**): $p < 0.01$.

We further explored the metabolic consequences of the decrease in OCR in HepG2 cells. The change in the OCR observed did not lead to a change in the ATP level measured after 2 h or 24 h exposure to Boscalid and Bixafen (Figure 3).

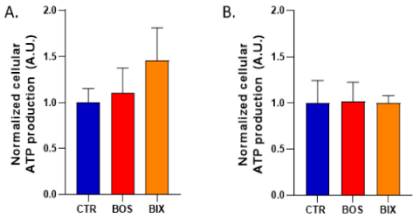

Figure 3. Cellular ATP production of HepG2 cells after treatment with DMSO 0.1% (CTR), Boscalid 1 µM (BOS) and Bixafen 1 µM (BIX) for 2 h (**A**) and 24 h (**B**). Data were normalized to controls. Bars represent mean ATP production ± SEM (A.U.), N = 3.

2.2. *Impact of SDHIs on Mitochondrial Superoxide Generation in Human Cell Lines*

Mitochondrial superoxide levels were determined using EPR with Mito-TEMPO-H as a specific mitochondrial superoxide probe ± PEG-SOD2 to specifically assign signals to mitochondrial superoxide [28] (Figure 4).

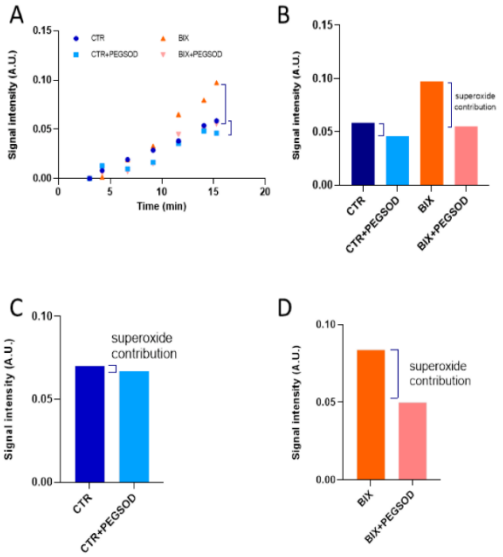

Figure 4. Illustration of the evaluation of mitochondrial superoxide assessment using EPR. Top row: typical experiment with exposure of HepG2 cells to Bixafen. (**A**): Time course evolution of EPR signal intensity of Mito-TEMPO• produced from Mito-TEMPO-H. (**B**): EPR signal intensity recorded for control cells and exposed cells 15 min after the start of the EPR experiment. The incubation with PEG-SOD2 allowed the evaluation of the superoxide contribution to the oxidation of the mitochondrial sensor. Bottom row: Mean values of EPR signal intensity at time t = 15 min recorded for 3 independent experiments. (**C**): Control HepG2 cells. (**D**): HepG2 cells exposed for 2 h to Bixafen.

After 2 hours' exposure, Boscalid and Bixafen (1 µM) induced a significant increase in mitochondrial superoxide production, multiplying its level by 8-fold and 12-fold, respectively, in HepG2 cells compared with untreated cells (Figure 5). Of note, the level of global ROS was unchanged in HepG2 cells as revealed by the H_2DCFDA assay (Figure 6). In PBMCs, the level of mitochondrial superoxide was not significantly changed after 2 hours' SDHI exposure. In BJ-fibroblasts, Bixafen treatment increased the superoxide production, while Boscalid did not. Of note, the level observed after Bixafen treatment in BJ was much lower than that achieved in HepG2 cells.

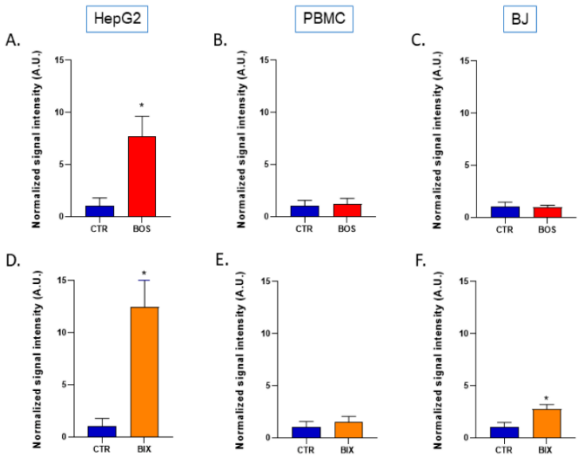

Figure 5. Level of mitochondrial superoxide in control (DMSO 0.1%) and SDHIs-exposed human cells (1 µM for 2 h). Signal intensity of Mito-TEMPO• at time point 15 min (normalized to control). Top row: Boscalid-treated cells. (**A**): HepG2 liver cells, (**B**): PBMCs, (**C**): BJ-fibroblasts. Bottom row: Bixafen-treated cells. (**D**): HepG2 liver cells, (**E**): PBMCs, (**F**): BJ-fibroblasts. Bars represent mean ± SEM. N = 3, (*): $p < 0.05$.

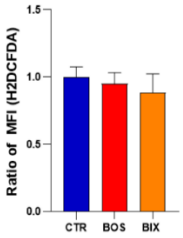

Figure 6. Total ROS production in HepG2 cells after treatment with DMSO 0.1% (CTR), 1 µM Boscalid (BOS) and 1 µM Bixafen (BIX) for 2 h, measured using H_2DFCDA probe. Data were normalized to controls. Bars represent mean ratio of MFI (mean fluorescence intensity) ± SEM (A.U.), N = 3.

2.3. Bixafen and Boscalid Induced Apoptosis in HepG2 Cells, but Not in PBMC and BJ Cells

By altering mitochondrial function, we hypothesized that SDHIs could induce apoptosis. Flow cytometry was used to assess early apoptotic and late apoptotic/necrotic cells

after SDHI exposure. A significant increase in early apoptotic cells, but not in late apoptotic/necrotic cells, was observed in HepG2 cells after 2 hours' exposure to Boscalid and Bixafen (Figure 7). In PBMC and BJ cells, no significant increase in cell mortality was found after short-term exposure to Boscalid and Bixafen (Figure 7).

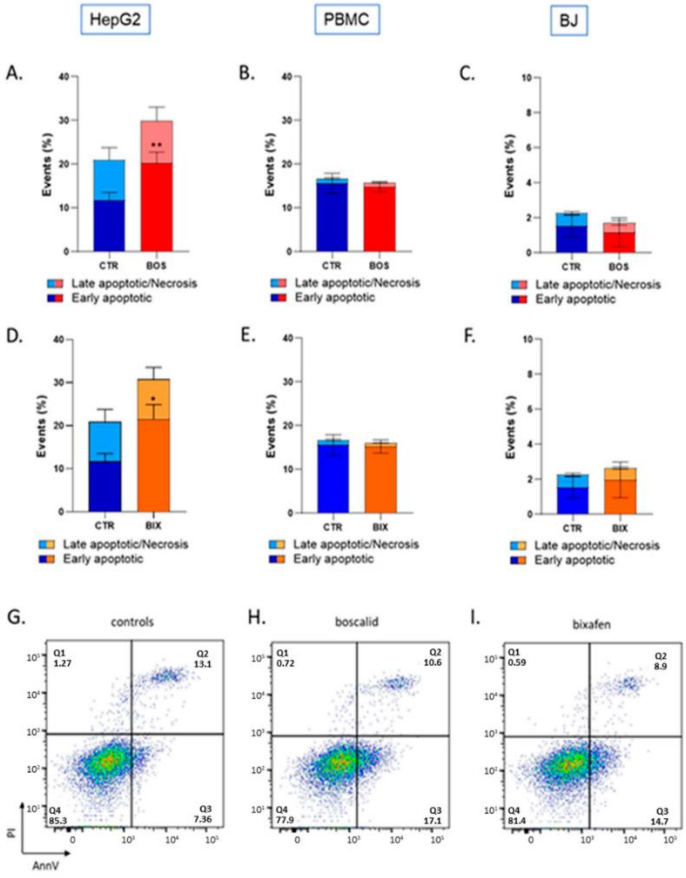

Figure 7. Effect of SDHI exposure on cytotoxicity. Top and middle rows: histograms of percentage of early apoptotic cells/late apoptotic or necrotic cells in control (DMSO 0.1%) and SDHIs-exposed human cells (1 µM for 2 h). Top row: Boscalid-treated cells. (**A**): HepG2 liver cells, (**): $p < 0.01$. (**B**): PBMCs, (**C**): BJ-fibroblasts. Middle row: Bixafen-treated cells. (**D**): HepG2 liver cells, (**E**): PBMCs, (**F**): BJ-fibroblasts. Bars represent mean ± SEM (% events). N = 3, (*): $p < 0.05$. Bottom row: Representative Annexin V/PI flow cytometry plots of HepG2 cells. (**G**): control cells, (**H**): Boscalid-treated cells, (**I**): Bixafen-treated cells.

3. Discussion

In this study, we found that short-term exposure (2 h) of three human cell lines to SDHI-fungicides Boscalid and Bixafen (1 µM) led to a mitochondrial dysfunction as the oxygen consumption was significantly reduced (Figure 2). Our results on the mitochondrial function are consistent with a previous study where enzymatic assays showed that SDHI-fungicides inhibited the human SDH with IC50 in the µM range [4]. We confirm here that SDHI-fungicides (Boscalid and Bixafen) are not selectively poisoning fungi, but are also active on non-target human cells. Despite this alteration in cell respiration, we did not observe a significant change in ATP level (Figure 3) after 2 hours' and 24 hours' exposure, suggesting that compensatory mechanisms may exist to keep cellular bioenergetics.

An important consequence of the inhibition of the ETC in human cells was the increase in mitochondrial superoxide level in HepG2 cells. In BJ-fibroblasts, only Bixafen induced an increase in mitochondrial superoxide production (Figure 5). The fact that BJ-fibroblasts display high antioxidant capacity [30] may likely explain the discrepancy between the effect on OCR and the absence of effect on mitochondrial superoxide production in this cell line. HepG2 cells were the most responsive to both SDHIs, with an 8-fold and 12-fold increase in superoxide after Boscalid and Bixafen treatment, respectively. These results agree with the important decrease in OCR observed in those cells after SDHI exposure and could be explained by the intrinsic feature of hepatocytes that contain more mitochondria compared with other cell types. Of note, as shown in Figure 2, basal OCR measured in HepG2 cells was much higher than in other cells analyzed in the present study. Regarding mitoROS production, Bixafen displayed more marked results than Boscalid (Figure 5). This could be explained by the fact that new generation SDHIs such as Bixafen possess a methyl-pyrazol fragment capable of inhibiting the ubiquinol cytochrome c reductase (complex III) of ETC, in addition to the inhibition of SDH (complex II) (Figure 1) [4]. Interestingly, the global level of ROS (as measured by the H_2DCFDA assay) after exposure of HepG2 cells was not significantly modified (Figure 5) while the level of mitochondrial superoxide was dramatically increased, suggesting that the higher ROS production seems confined to the mitochondrial compartment. A similar observation of selective mitochondrial superoxide production was previously reported in superinvasive cancer cells [27]. Of note, global ROS production was observed in other studies, but after longer exposure and higher concentrations of Boscalid in zebrafish (14.5 µM, 6 to 18 h post-fertilization) [6] and in *Chlorella vulgaris* (4.5 µM, 96 h) [31]. An increase in SOD activity was also reported in human fibroblasts (from a patient with familial Alzheimer disease) exposed during 13 days to 1 µM Bixafen [4]. In the future, it would be interesting to investigate the nature of ROS produced using other methods, for example, those using fluorescent probes coupled to HPLC [32–34].

We further explored if the increase in mitochondrial ROS could lead to the induction of apoptosis. By altering mitochondrial function, SDHIs could be capable of releasing cytochrome c and initiating the apoptotic cascade. Here also, HepG2 cells demonstrated a high susceptibility to SDHI exposure, as we observed an increase in early apoptotic cells after both Boscalid and Bixafen (1 µM) short-term exposure (Figure 7). No significant induction of apoptosis was observed in PBMCs and in BJ-fibroblasts (Figure 7). The latter results are the likely consequence of the smaller increase in mitochondrial ROS production (Figure 5) in those cells lines compared with HepG2 cells.

Overall, our results demonstrated that a short-term exposure to Boscalid and Bixafen leads to mitochondrial dysfunction in human cells. While bioenergetics was not affected, the SDHI exposure led to an increase in mitochondrial ROS in cells with insufficient antioxidant capacity and to an induction of apoptosis in cells with the highest production of mitochondrial superoxide.

As mentioned earlier, the cell lines used in the present study are representative of cells that are most likely to be in contact with SDHIs after exposure (blood, liver and skin). Of note, the HepG2 cell is not a normal hepatocyte but derives from a liver biopsy of a differentiated hepatocellular carcinoma. However, the HepG2 human cell line is a model

classically used by researchers and pharmaceutical companies to assess the hepatoxicity of chemicals or drugs [35–38]. In the future, it would be interesting to enlarge the effect of SDI-fungicides to other cell lines as SDH deficiency has been shown to be associated with encephalopathy and cardiomyopathy [39]. In addition, it would be interesting to assess the effect of repeated short-term exposure to SDHI-fungicides on human cells.

At this stage, it is premature to extrapolate these results to human health after SDHI exposure. As mentioned above, the concentration of 1 µM is likely close to concentrations achieved after exposure to levels close to the AOELs for operators. There is a large uncertainty regarding the real concentrations achieved in the blood of people potentially exposed to SDHI-fungicides. Many parameters such as frequency of spreading, exposure periods, amounts of SDHIs manipulated, protection means, and contaminated food diets may strongly influence the level of SDHIs that will be achieved in tissues. As far as we know, there are no epidemiologic data existing about blood concentration levels after exposure in humans. The exposure to pesticides in farmers and the general population living close to a treated area is mostly evaluated through quantification of pesticides in hair [40,41]. Our results call for such biomonitoring to evaluate the real level of exposure and to drive future research with a range of concentrations established experimentally rather than theoretically. Moreover, a reevaluation of AOELs/ADIs for SDHI-fungicides could be debated. AOELs/ADIs are established by extrapolation of toxicology data obtained in animals and by defining a theoretical security factor. Accounting for experimental dose/toxicity relationships in human cells could be desirable.

4. Materials and Methods

4.1. Reagents

^{15}N-PDT (4-oxo-2,2,6,6-tetramethylpiperidine-d_{16}-^{15}N-1-oxyl) (Figure 8) originated from CDN Isotopes (Pointe-Claire, Canada). Mito-TEMPO-H (2-(2,2,6,6-Tetramethylpiperidin-1-oxyl-4-ylamino)-2-oxoethyl triphenylphosphonium chloride) (Figure 7) was purchased from Enzo Lifescience (Antwerpen, Belgium). Boscalid (2-chloro-N-(4-chlorobiphenyl-2-yl)nicotinamide), Bixafen (N-[2-(3,4-dichlorophenyl)-4-fluorophenyl]-3-(difluoromethyl)-1-methylpyrazole-4-carboxamide), superoxide dismutase 2 conjugated with polyethylene glycol (PEGSOD2), ATP disodium, diethylenetriaminepentaacetic acid (DTPA), dextran from *Leuconostoc Mesenteroides* (average MW 60000–76000) and dimethyl sulfoxide (DMSO) were from Sigma-Aldrich (Overijse, Belgium). The cell-permeant 2′,7′-dichlorodihydrofluorescein diacetate (H_2DCFDA) came from Invitrogen™ (Waltham, MA, USA).

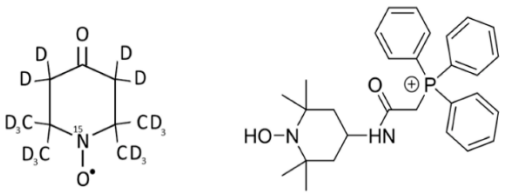

Figure 8. Chemical structures of ^{15}N-PDT used as a sensor for oximetry (**left**) and Mito-TEMPO-H used as a sensor for mitochondrial superoxide production (**right**).

4.2. Cell Lines and Culture

All cell lines were purchased from The American Type Culture Collection (Manassas, VA, USA) and maintained in a humidified atmosphere with 5% CO_2 at 37 °C. HepG2 (human hepatocarcinoma) and BJ (human skin fibroblasts) cells were routinely cultured in Eagle Minimum Essential Medium supplemented with 10% heat-inactivated fetal bovine serum (FBS) (Thermo Fisher Scientific). Hs27 (human skin fibroblasts) and PBMC (peripheral blood mononuclear cells) were cultured in Dulbecco's Modified Eagle's Medium (DMEM) and RPMI-1640 respectively, both supplemented with 10% of FBS.

4.3. EPR Oximetry

EPR oximetry is based on the use of an oxygen-sensing probe, ^{15}N-PDT (4-oxo-2,2,6,6-tetramethylpiperidine-d_{16}-^{15}N-1-oxyl), to measure variations in oxygen levels in samples, and subsequently cells' oxygen consumption rate (OCR) in a sealed capillary. ^{15}N-PDT EPR linewidth is very narrow due to deuterium substituting hydrogen, providing a high sensitivity to measure the broadening induced by the oxygen content in the preparation. Oxygen consumption rate (OCR) of cell lines was measured using a Bruker EMX-Plus spectrometer operating in X-band (9.85 GHz) and equipped with a PremiumX ultra low noise microwave bridge and a SHQ high sensitivity resonator. The EPR cavity was heated at 310 K with continuous nitrogen flow during all experiments. Respiration mixture was composed of 60 µL of previously harvested cells (stock solution 5.10^6 cells/mL of culture medium), 40 µL of Dextran solution (20%) and 4 µL of ^{15}N-PDT (2 mM), transferred into a hematocrit capillary sealed with gum. The final device was inserted into a quartz tube and put into the EPR cavity. Experimental parameters for acquisition set in the Bruker Xenon Spin fit program were: microwave power, 2.518 mW; modulation frequency, 100 kHz; modulation amplitude, 0.005 mT; center field, 335 mT; sweep width, 1.5 mT; sweep time, 15 s. An automated "2D-field-Delay" measurement was launched 3 min after probe mixing, counting 15 points with a time delay of 60,000 ms. Data analysis was performed switching to processing mode and using "peak picking" on selected regions of the ^{15}N-PDT –peaks. The final file was saved as an ASCII file to extract linewidth data at each point. ^{15}N-PDT linewidth was correlated with the % of oxygen with a calibration curve. OCR corresponded to the slope of oxygen level during time.

4.4. EPR Superoxide Measurement

Mitochondrial superoxide measurements by EPR were based on the use of Mito-TEMPO-H, a cyclic hydroxylamine, able to detect superoxide in complex biological media with high sensitivity. Thanks to its tryphenylphosphonium moiety (TPP^+), this probe enters into and accumulates within mitochondria, enabling specific measurement of mitochondrial superoxide. Superoxide production was monitored using a Bruker EMX-Plus spectrometer operating in X-band (9.85 GHz) and equipped with a PremiumX ultra low noise microwave bridge and a SHQ high sensitivity resonator. The EPR cavity was heated at 310 K with continuous air flow during all experiments. The mixture combined 37 µL of cell suspension (stock solution: 20.10^6 cells/mL culture medium), 0.56 µL of DTPA (100 mM), 5 µL of PBS ($(1\times)$ − pH 7.4) and 7.5 µL of Mito-TEMPO-H (1mM). Superoxide production contribution was assessed by making another measurement using the same conditions but adding 2.5 µL of PEG-SOD2 (4000 U/mL) to replace 2.5 µL of PBS. PEG-SOD2 was incubated 15 min before adding the Mito-TEMPO-H probe. Previous studies have shown that the pre-incubation of cells in the presence of PEG-SOD allows the cellular uptake of the enzyme and intracellular scavenging of superoxide [42]. Mito-TEMPO-H stock solution was flushed with Argon prior and during pipetting to avoid probe oxidation. The final solution was transferred into a PTFA tube (inside diameter 0.025 in., wall thickness 0.002 in.) cutting of 12 cm using a needle and folded in 6 before being inserted into an open quartz tube. Experimental parameters for acquisition set in the Bruker Xenon Spin fit program were: microwave power, 20 mW; modulation frequency, 100 kHz; modulation amplitude, 0.1 mT; center field, 336.5 mT; sweep width, 1.5 mT; sweep time, 30.48 s. An automated "2D-field-Delay" measurement was launched 3 min after probe mixing, counting 11 points with a time delay of 40,000 ms. Data analysis was performed switching to processing mode and using "Integration & derivative" and "double integration" on selected regions of the peaks. The final file was saved as an ASCII file to extract double integration (DI) data at each timepoint. Point 1 DI was subtracted from point 11 DI for each condition. Superoxide contribution was measured by subtracting mean PEGSOD2 DI to mean control DI.

4.5. Cell death Detection by Flow Cytometry

Apoptotic changes in cells were assessed using the eBioscience™ Annexin V Apoptosis Detection Kit APC (Thermofisher, Waltham, MA, USA). A total of 50,000 cells per condition were plated 2 days before treatment in T25 flasks. On the day of the experiment, cells were treated for 2 h with 1 µM of Boscalid, Bixafen or control solution (DMSO 0.1%) mixed into their respective culture media. Cells were then detached with trypsin (0.25% trypsin-EDTA was used for HepG2 cells), harvested into their respective old media, centrifuged and transferred into a FACS tube with fresh media. The staining protocol briefly included washing the cells with PBS, then adding 80 µL of binding buffer along with 5 µL Annexin V (AnnV) and 5 µL Propidium Iodide (PI) per tube. Cells were kept in the dark for 15 min until FACS assessment, with an additional 100 µL of binding buffer. Data were acquired using a BD FACSCantoII flow cytometer equipped with Diva Software and processed with FlowJo software. At least 10,000 events were analyzed for each condition. Cells' subpopulations were identified according to unstained control cells and distinguished between alive (AnV− PI−), early apoptotic (AnV+ PI−) and late apoptotic/necrotic (AnV+ PI+).

4.6. Global ROS Production Using H_2DCFDA

Intracellular ROS were detected by flow cytometry using a cell-permanent 2′,7′-dichlorofluorescein diacetate (H_2DCFDA) fluorescent probe. Once inside the cell, the probe was cleaved by endogenous esterases and became fluorescent after oxidation by ROS. HepG2 cells were treated for 2 h with 1 µM of Boscalid (BOS) and Bixafen (BIX), or control solution (DMSO 0.1%) then incubated with H_2DFCDA (10 µM final concentration) for 30 min at 37 °C. Cells were then harvested with 0.25% trypsin-EDTA solution, suspended into fresh medium, and immediately analyzed by flow cytometry. Data were acquired using a FACSCanto II cytofluorimeter equipped with Diva Software and processed with FlowJo software.

4.7. Cellular ATP Production

HepG2 ATP production was measured using the CellTiter-Glo® Luminescent Cell Viability Assay (Promega, Madison, WI, USA). HepG2 were cultured on a 96-well plate then treated the day after with 1 µM of Boscalid (BOS) and Bixafen (BIX), or control solution (DMSO 0.1%) for 2 and 24 h (100 µL media/well). ATP quantification was performed with a standard curve using ATP disodium (10 nM to 1 µM) in cell-free media. The entire plate was then mixed for 2 min on an orbital plate after 100 µL of reagent was added to each well. Luminescence was measured with the SpectraMax at 560 nm after 10 min incubation at RT to stabilize signal.

4.8. Statistics

Data were represented as means ± SEM. All experiments were performed in triplicates or more. Student T tests were applied for OCR and superoxide measurements experiments, whereas One-way ANOVA were performed on all other experiments.

5. Conclusions

A short-term exposure of the HepG2 human cell line to SDHI-fungicides Boscalid and Bixafen induces a mitochondrial dysfunction, altering the oxygen consumption, the mitochondrial ROS production, and eventually leading to apoptosis. Further research is warranted to assess the effect of repeated exposures and relevance of these observations for human health.

Author Contributions: Conceptualization, B.G; methodology, D.d., P.I., D.B., B.F.J. and B.G.; validation, D.d., D.B. and B.G.; formal analysis, D.d., P.I., D.B., B.F.J. and B.G.; investigation, D.d. and P.I.; resources, D.d., B.F.J. and B.G.; data curation, D.d.; writing—original draft preparation, D.d. and B.G.; writing—review and editing, D.d., P.I., D.B., B.F.J. and B.G.; visualization, D.d.; supervision, B.F.J. and B.G.; project administration, B.G.; funding acquisition, B.G. All authors have read and agreed to the published version of the manuscript.

Funding: "This research was funded by FNRS, grant number J008220F". Bénédicte F. Jordan is a Research Director of the FNRS. This study used the equipment of the Nuclear and Electron Spin Technologies platform and of the CytoFlux-Flow Cytometry platform of the UCLouvain.

Institutional Review Board Statement: Not applicable.

Informed Consent Statement: Not applicable.

Data Availability Statement: Available on request.

Conflicts of Interest: The authors declare no conflict of interest.

Sample Availability: Not applicable.

References

1. Umetsu, N.; Shirai, Y. Development of novel pesticides in the 21th century. *J. Pestic. Sci.* **2020**, *45*, 54–74. [CrossRef]
2. ANSES Report 2018-SA-0113. Available online: https://www.anses.fr/fr/system/files/PHYTO2018SA0113Ra.pdf (accessed on 26 July 2021).
3. Kamp, H.; Wahrheit, J.; Stinchcombe, S.; Walk, T.; Stauber, F.; Ravenzwaay, B. Succinate dehydrogenase inhibitors: In silico flux analysis and in vivo metabolomics investigations show no severe metabolic consequences for rats and humans. *Food Chem. Toxicol.* **2021**, *150*, 112085. [CrossRef]
4. Bénit, P.; Kahn, A.; Chretien, D.; Bortoli, S.; Huc, L.; Schiff, M.; Gimenez-Roqueplo, A.-P.; Favier, J.; Gressens, P.; Rak, M.; et al. Evolutionarily conserved susceptibility of the mitochondrial respiratory chain to SDHI pesticides and its consequence on the impact of SDHIs on human cultured cells. *PLoS ONE* **2019**, *14*, e0224132. [CrossRef]
5. Brenet, A.; Hassan-Abdi, R.; Soussi-Yanicostas, N. Bixafen, a succinate dehydrogenase inhibitor fungicide, causes microcephaly and motor neuron axon defects during development. *Chemosphere* **2020**, *265*, 128781. [CrossRef]
6. Wang, H.; Meng, Z.; Liu, F.; Zhou, L.; Su, M.; Meng, Y.; Zhang, S.; Liao, X.; Cao, Z.; Lu, H. Characterization of boscalid-induced oxidative stress and neurodevelopmental toxicity in zebrafish embryos. *Chemosphere* **2019**, *238*, 124753. [CrossRef] [PubMed]
7. Yuan, M.; Li, W.; Xiao, P. Bixafen causes cardiac toxicity in zebrafish (Danio rerio) embryos. *Environ. Sci. Pollut. Res.* **2021**, *28*, 1–11. [CrossRef]
8. Qian, L.; Zhang, J.; Chen, X.; Qi, S.; Wu, P.; Wang, C.; Wang, C. Toxic effects of boscalid in adult zebrafish (Danio rerio) on carbohydrate and lipid metabolism. *Environ. Pollut.* **2019**, *247*, 775–782. [CrossRef] [PubMed]
9. Cayyir, A.; Coskun, M.; Coskun, M. Micronuclei, nucleoplasmic bridges, and nuclear buds induced in human lymphocytes by the fungicide signum and its active ingredients (boscalid and pyraclostrobin). *Environ. Toxicol.* **2014**, *29*, 723–732. [CrossRef] [PubMed]
10. Graillot, V.; Tomasetig, F.; Cravedi, J.-P.; Audebert, M. Evidence of the in vitro genotoxicity of methyl-pyrazole pesticides in human cells. *Mutat. Res. Toxicol. Environ. Mutagen.* **2012**, *748*, 8–16. [CrossRef] [PubMed]
11. Evolutionarily Conserved Susceptibility of the Mitochondrial Respiratory Chain to SDHI Pesticides and Its Consequence on the Impact of SDHIs on Human Cultured Cells. Available online: https://journals.plos.org/plosone/article/comment?id=10.1371/annotation/400d52f8-f61f-4132-a94c-bee53565f35c (accessed on 26 July 2021).
12. Pesticide Fact Sheet. Available online: https://www3.epa.gov/pesticides/chem_search/reg_actions/registration/fs_PC-128008_01-Jul-03.pdf (accessed on 26 July 2021).
13. BIXAFEN (262). Available online: http://www.fao.org/fileadmin/templates/agphome/documents/Pests_Pesticides/JMPR/Evaluation13/Bixafen.pdf (accessed on 26 July 2021).
14. European Food Safety Authority (EFSA). Conclusion on Pesticide Peer Review. *EFSA J.* **2012**, *10*, 2917.
15. Pozza, E.D.; Dando, I.; Pacchiana, R.; Liboi, E.; Scupoli, M.T.; Donadelli, M.; Palmieri, M. Regulation of succinate dehydrogenase and role of succinate in cancer. *Semin. Cell Dev. Biol.* **2019**, *98*, 4–14. [CrossRef] [PubMed]
16. Weber, T.; Lu, M.; Andera, L.; Lahm, H.; Gellert, N.; Fariss, M.W.; Korinek, V.; Sattler, W.; Ucker, D.S.; Terman, A.; et al. Vitamin E succinate is a potent novel antineoplastic agent with high selectivity and cooperativity with tumor necrosis factor-related apoptosis-inducing ligand (Apo2 ligand) in vivo. *Clin. Cancer Res.* **2002**, *8*, 863–869. [PubMed]
17. Dong, L.-F.; Jameson, V.J.; Tilly, D.; Prochazka, L.; Rohlena, J.; Valis, K.; Truksa, J.; Zobalova, R.; Mahdavian, E.; Kluckova, K.; et al. Mitochondrial targeting of α-tocopheryl succinate enhances its pro-apoptotic efficacy: A new paradigm for effective cancer therapy. *Free. Radic. Biol. Med.* **2011**, *50*, 1546–1555. [CrossRef] [PubMed]
18. Lazaro, M.G.; Galindo, M.F.; De Mera, R.M.M.-F.; Fernandez-Gomez, F.J.; Concannon, C.G.; Segura, M.F.; Comella, J.X.; Prehn, J.H.M.; Jordan, J.; De Mera, R.M.M.F. Reactive Oxygen Species and p38 Mitogen-Activated Protein Kinase Activate Bax to Induce Mitochondrial Cytochrome c Release and Apoptosis in Response to Malonate. *Mol. Pharmacol.* **2006**, *71*, 736–743. [CrossRef] [PubMed]
19. Huang, L.-S.; Sun, G.; Cobessi, D.; Wang, A.C.; Shen, J.T.; Tung, E.Y.; Anderson, V.E.; Berry, E.A. 3-Nitropropionic Acid Is a Suicide Inhibitor of Mitochondrial Respiration That, upon Oxidation by Complex II, Forms a Covalent Adduct with a Catalytic Base Arginine in the Active Site of the Enzyme. *J. Biol. Chem.* **2006**, *281*, 5965–5972. [CrossRef] [PubMed]

20. Cheng, G.; Zhang, Q.; Pan, J.; Lee, Y.; Ouari, O.; Hardy, M.; Zielonka, M.; Myers, C.R.; Zielonka, J.; Weh, K.; et al. Targeting lonidamine to mitochondria mitigates lung tumorigenesis and brain metastasis. *Nat. Commun.* **2019**, *10*, 1–14. [CrossRef] [PubMed]
21. Jordan, B.F.; Grégoire, V.; Demeure, R.J.; Sonveaux, P.; Feron, O.; O'Hara, J.; VanHulle, V.P.; Delzenne, N.; Gallez, B. Insulin increases the sensitivity of tumors to irradiation: Involvement of an increase in tumor oxygenation mediated by a nitric oxide-dependent decrease of the tumor cells oxygen consumption. *Cancer Res.* **2002**, *62*, 3555–3561.
22. Diepart, C.; Verrax, J.; Calderon, P.B.; Feron, O.; Jordan, B.F.; Gallez, B. Comparison of methods for measuring oxygen consumption in tumor cells in vitro. *Anal. Biochem.* **2009**, *396*, 250–256. [CrossRef]
23. D'Hose, D.; Danhier, P.; Northshield, H.; Isenborghs, P.; Jordan, B.F.; Gallez, B. A versatile EPR toolbox for the simultaneous measurement of oxygen consumption and superoxide production. *Redox Biol.* **2020**, *40*, 101852. [CrossRef]
24. Dikalov, S.I.; Kirilyuk, I.; Voynov, M.; Grigor'Ev, I. EPR detection of cellular and mitochondrial superoxide using cyclic hydroxylamines. *Free. Radic. Res.* **2010**, *45*, 417–430. [CrossRef]
25. Dikalov, S.I.; Harrison, D.G. Methods for Detection of Mitochondrial and Cellular Reactive Oxygen Species. *Antioxid. Redox Signal.* **2014**, *20*, 372–382. [CrossRef]
26. Scheinok, S.; Leveque, P.; Sonveaux, P.; Driesschaert, B.; Gallez, B. Comparison of different methods for measuring the superoxide radical by EPR spectroscopy in buffer, cell lysates and cells. *Free Radic. Res.* **2018**, *52*, 1182–1196. [CrossRef]
27. Scheinok, S.; Driesschaert, B.; D'Hose, D.; Sonveaux, P.; Robiette, R.; Gallez, B. Synthesis and characterization of a 5-membered ring cyclic hydroxylamine coupled to triphenylphosphonium to detect mitochondrial superoxide by EPR spectrometry. *Free Radic. Res.* **2019**, *53*, 1135–1143. [CrossRef]
28. Scheinok, S.; Capeloa, T.; Porporato, P.E.; Sonveaux, P.; Gallez, B. An EPR Study Using Cyclic Hydroxylamines to Assess the Level of Mitochondrial ROS in Superinvasive Cancer Cells. *Cell Biophys.* **2020**, *78*, 249–254. [CrossRef]
29. d'Hose, D.; Gallez, B. Measurement of mitochondrial (dys)function in cellular systems using Electron Paramagnetic Resonance (EPR): Oxygen consumption rate and superoxide production. *Methods Mol. Biol.* **2021**, in press.
30. Lorenz, M.; Saretzki, G.; Sitte, N.; Metzkow, S.; von Zglinicki, T. BJ fibroblasts display high antioxidant capacity and slow telomere shortening independent of hTERT transfection. *Free. Radic. Biol. Med.* **2001**, *31*, 824–831. [CrossRef]
31. Qian, L.; Qi, S.; Cao, F.; Zhang, J.; Zhao, F.; Li, C.; Wang, C. Toxic effects of boscalid on the growth, photosynthesis, antioxidant system and metabolism of *Chlorella vulgaris*. *Environ. Pollut.* **2018**, *242*, 171–181. [CrossRef]
32. Hardy, M.; Zielonka, J.; Karoui, H.; Sikora, A.; Michalski, R.; Podsiadły, R.; Lopez, M.; Vasquez-Vivar, J.; Kalyanaraman, B.; Ouari, O. Detection and Characterization of Reactive Oxygen and Nitrogen Species in Biological Systems by Monitoring Species-Specific Products. *Antioxid Redox Signal.* **2018**, *28*, 1416–1432. [CrossRef]
33. Kalyanaraman, B.; Hardy, M.; Podsiadly, R.; Cheng, G.; Zielonka, J. Recent developments in detection of superoxide radical anion and hydrogen peroxide: Opportunities, challenges, and implications in redox signaling. *Arch. Biochem. Biophys.* **2016**, *617*, 38–47. [CrossRef] [PubMed]
34. Kalyanaraman, B.; Dranka, B.; Hardy, M.; Michalski, R.; Zielonka, J. HPLC-based monitoring of products formed from hydroethidine-based fluorogenic probes—The ultimate approach for intra- and extracellular superoxide detection. *Biochim. Biophys. Acta (BBA) Gen. Subj.* **2013**, *1840*, 739–744. [CrossRef] [PubMed]
35. Knasmüller, S.; Schwab, C.E.; Land, S.J.; Wang, C.Y.; Sanyal, R.; Kundi, M.; Parzefall, W.; Darroudi, F. Genotoxic effects of heterocyclic aromatic amines in human derived hepatoma (HepG2) cells. *Mutagenesis* **1999**, *14*, 533–540. [CrossRef]
36. Schoonen, W.G.; de Roos, J.A.; Westerink, W.M.; Débiton, E. Cytotoxic effects of 110 reference compounds on HepG2 cells and for 60 compounds on HeLa, ECC-1 and CHO cells: II Mechanistic assays on NAD(P)H, ATP and DNA contents. *Toxicol. Vitr.* **2005**, *19*, 491–503. [CrossRef] [PubMed]
37. O'Brien, P.J.; Irwin, W.; Diaz, D.; Howard-Cofield, E.; Krejsa, C.M.; Slaughter, M.R.; Gao, B.; Kaludercic, N.; Angeline, A.; Bernardi, P.; et al. High concordance of drug-induced human hepatotoxicity with in vitro cytotoxicity measured in a novel cell-based model using high content screening. *Arch. Toxicol.* **2006**, *80*, 580–604. [CrossRef]
38. Gerets, H.; Hanon, E.; Cornet, M.; Dhalluin, S.; Depelchin, O.; Canning, M.; Atienzar, F. Selection of cytotoxicity markers for the screening of new chemical entities in a pharmaceutical context: A preliminary study using a multiplexing approach. *Toxicol. Vitr.* **2009**, *23*, 319–332. [CrossRef] [PubMed]
39. Briere, J.-J.; Favier, J.; El Ghouzzi, V.; Djouadi, F.; Bénit, P.; Gimenez, A.-P.; Rustin, P. Succinate dehydrogenase deficiency in human. *Experientia* **2005**, *62*, 2317–2324. [CrossRef] [PubMed]
40. Polledri, E.; Mercadante, R.; Nijssen, R.; Consonni, D.; Mol, H.; Fustinoni, S. Hair as a matrix to evaluate cumulative and aggregate exposure to pesticides in winegrowers. *Sci. Total. Environ.* **2019**, *687*, 808–816. [CrossRef] [PubMed]
41. Polledri, E.; Mercadante, R.; Consonni, D.; Fustinoni, S. Cumulative pesticides exposure of children and their parents living near vineyards by hair analysis. *Int. J. Environ. Res. Public Health* **2021**, *18*, 3723. [CrossRef] [PubMed]
42. Beckman, J.S.; Minor, R.L., Jr.; White, C.W.; Repine, J.E.; Rosen, G.M.; Freeman, B.A. Superoxide dismutase and catalase conjugated to polyethylene glycol increases endothelial enzyme activity and oxidant resistance. *J. Biol. Chem.* **1988**, *263*, 6884–6892. [CrossRef]

II. Statins alleviate tumor hypoxia in prostate cancer models by decreasing oxygen consumption: an opportunity for radiosensitization?

Manuscript in preparation

Statins alleviate tumor hypoxia in prostate cancer models by decreasing oxygen consumption: an opportunity for radiosensitization?

Donatienne d'Hose[1], Lionel Mignion[1,2], Loïc Hamelin[3], Pierre Sonveaux[3], Bénédicte F. Jordan[1,2], and Bernard Gallez[1,2]

1 : Biomedical Magnetic Resonance, Louvain Drug Research Institute (LDRI),
Université catholique de Louvain (UCLouvain), Brussels, Belgium
2 : Nuclear and Electron Spin Technologies (NEST) platform,
Université catholique de Louvain (UCLouvain), Brussels, Belgium
3 : Pole of Pharmacotherapy, Institut de Recherches expérimentales et cliniques (IREC),
Université catholique de Louvain (UCLouvain), Brussels, Belgium

Work in progress - Manuscript in preparation

Corresponding author:
Prof. Bernard Gallez
Biomedical Magnetic Resonance Research Group
Louvain Drug Research Institute
UCLouvain
Avenue Mounier 73 - B1.73.08
B-1200 Brussels - Belgium
Phone: +32 2 7647391
Fax: +32 2 7647390
Email: bernard.gallez@uclouvain.be

Abstract

As a meta-analysis described a beneficial effect of statins on prostate cancer patients treated with radiation therapy (RT), it is crucial to investigate the mechanisms underlying the potential radiosensitizing properties of statins. Our hypothesis was that the alleviation of tumor hypoxia induced by an inhibition of oxygen consumption rate (OCR) could play a role in the improved response to RT in those patients receiving statins. The effect of statins on OCR has been indeed demonstrated in a variety of normal cells, such as cardiomyocytes, skeletal muscle cells, and hepatocytes but has never been described in cancer cells. A screening of five statins (simvastatin, fluvastatin, rosuvastatin, pravastatin, atorvastatin) using Seahorse XF revealed that a 24-hours exposure to simvastatin and fluvastatin significantly decreased the OCR in PC-3 prostate cancer cells. This effect was confirmed for both compounds using EPR respirometry in PC-3 and DU145 prostate cancer cells. To evaluate the relevance of these observations *in vivo*, we performed quantitative measurements of tumor oxygenation in the PC-3 prostate cancer model in mice. This model was found highly hypoxic at the basal level. When mice were treated by simvastatin or fluvastatin (daily injection of 20 mg/kg), the tumor oxygenation significantly increased 48 and 72 hours after initiation of the treatment. Irradiation experiments are in progress to assess the value of statins as potential radiosensitizers.

Introduction

Statins are cholesterol-lowering drugs widely used in the prevention of cardiovascular diseases. Statins inhibit HMG-CoA reductase and thus decrease biosynthesis of low-density lipoprotein cholesterol. Evidence from experimental and preclinical studies [1,2] has indicated that statins can inhibit tumor growth and induce apoptosis in several tumor types, including pancreatic carcinoma [3], breast cancer [4], small-cell lung cancer [5] and brain tumors [6]. Mechanistically, it has been suggested that, because statins reduce mevalonate synthesis, farnesylation and geranylgeranylation are decreased. As a result, there is a decrease in Ras, Rho, and c-Myc proteins expression which reduces tumor cell proliferation and migration, there is a reduction in matrix metalloproteinase-9 involved in metastasis, an inhibition of angiogenesis by increasing the inhibitory effect of TNF alpha, and the activation of caspase-9 and caspase-3 which leads to apoptosis [2]. The potential benefit of statins in cancer prevention and treatment has recently received significant interest with the aim to evaluate the impact of statins on the outcome of cancer treatments. In an analysis of about one thousand patients with a diagnosis of colon cancer, authors associated statin with reduced risk of death from any cause or from cancer [7]. Another meta-analysis suggested that the use of statin was associated with a reduced mortality and recurrence of hepatocellular carcinomas [8], improved survival in rectal cancer [9], in head and neck cancer [10], and in lung cancer [11]. However, other studies failed to demonstrate any clinical benefit from the use of statins in esophageal cancer [12], colorectal cancer [13], or small-cell lung cancer [14].

Interestingly, several large-scale cohort studies have recently indicated a better outcome of radiation therapy (RT) (external or brachytherapy) in prostate cancer patients under statin treatment [15-17]. A meta-analysis evaluated associations between statins and recurrence-free survival following treatment of localized prostate cancer and found a beneficial effect of statins on prostate cancer patients treated with RT but not among radical prostatectomy patients [18]. These clinical observations warrant further research on the potential mechanisms underlying a potential radiosensitizing property of statins.

Our hypothesis is that the alleviation of tumor hypoxia induced by an inhibition of oxygen consumption rate (OCR) could play a role in the improved response to RT in those patients receiving statins. It is important to remember that most malignant solid tumors contain

areas with hypoxia resulting in worsened clinical prognosis for cancer patient [19-21]. Tumor hypoxia results from an imbalance between the limited oxygen delivery capacity of the abnormal vasculature and the high oxygen consumption of tumor cells [22]. Tumor hypoxia is considered to be a crucial therapeutic issue, as it renders solid tumors resistant to radiation therapy. Because of the so-called "oxygen enhancement effect", the radiation dose required to achieve the same biologic effect is about three times higher in hypoxic tissues than in those with normal oxygen levels [23]. Tumor hypoxia may theoretically be alleviated by increasing the oxygen delivery or by decreasing the oxygen consumption by tumor cells. Mathematical modelling described by Secomb et al. suggested that tumor hypoxia can be abolished by a reduction in consumption rate of 30% [24]. Experimentally, several strategies designed to decrease the OCR in tumor cells succeeded in increasing the response to radiation therapy in tumor models [25-34]. The effect of statins on OCR has been demonstrated in a variety of normal cells, such as cardiomyocytes, skeletal muscle cells, and hepatocytes [35-37]. It is generally admitted that is effect is mediated by the reduction in synthesis of ubiquinol (Coenzyme Q10). So far, only one study investigated the effect of statins on the OCR by tumor cells. This study evaluated the impact of lovastatin (in comparison with fludarabin) on DS sarcoma cells with the aim to evaluate the impact on DNA synthesis and OCR [38]. However, these authors did not investigate the consequences of the changes of OCR on the sensitivity to irradiation.

The overall aim of the present study was to evaluate the impact of statins on tumor cell oxygen consumption, tumor hypoxia and response to irradiation. For the purpose, we first screened the effect of five statins (simvastatin, fluvastatin, rosuvastatin, pravastatin, atorvastatin; **Fig.1**) on the oxygen consumption by prostate cancer cells. Using Seahorse XF technology, we observed that 24-hours exposure of prostate cancer cells to simvastatin and fluvastatin significantly decreased the basal respiration while the other statins did not decrease the OCR. These results were confirmed using Electron Paramagnetic Resonance (EPR)-based OCR measurements. Because the alteration in electron transport chain function may lead to an increase in superoxide production, we investigated the impact of statins on the production of mitochondrial superoxide using EPR spectrometry. In addition, we performed quantitative measurements of tumor oxygenation in the PC-3 prostate cancer model in mice. When treated by simvastatin or fluvastatin (daily injection of 20 mg/kg), the

tumor oxygenation significantly increased 48 and 72 hours after starting the treatment. Irradiation experiments are in progress to assess the value of statins as potential radiosensitizers.

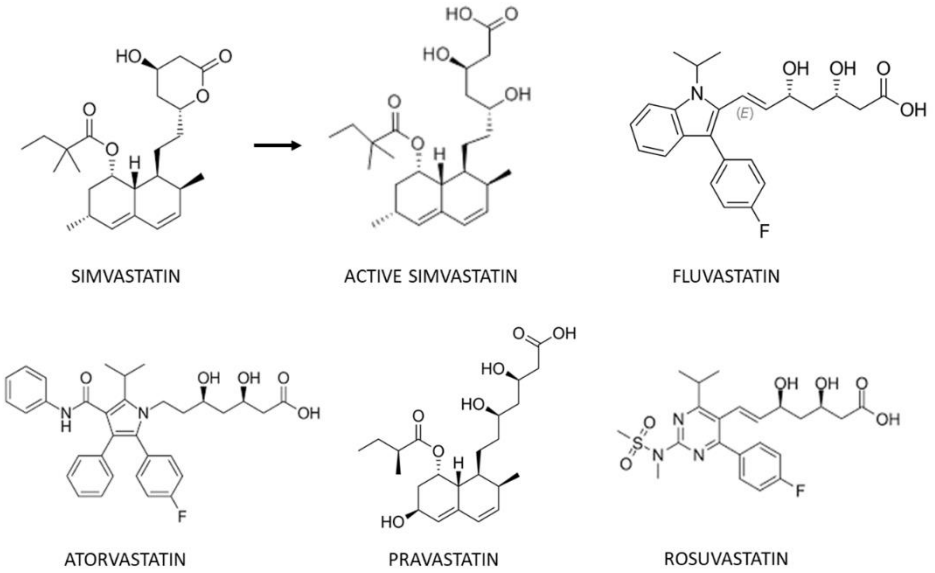

Fig.1. Structure of statins used in the present study: simvastatin, the active metabolite of simvastatin, fluvastatin, atorvastatin, rosuvastatin, pravastatin.

Material and Methods

Reagents

Simvastatin came from Enzo Lifescience (Antwerpen, Belgium) whereas all other statins (Atorvastatin, Pravastatin, Rosuvastatin and Fluvastatin) were purchased from Sigma Aldrich (Overijse). EPR probes ^{15}N-PDT (4-oxo-2,2,6,6-tetramethylpiperidine-d_{16}-^{15}N-1-oxyl) and MitoTEMPO-H (1-hydroxy-4-[2-triphenylphosphonio)-acetamido]-2,2,6,6-tetramethylpiperidine) originate from CDN Isotopes and Enzo Lifescience, respectively. Dimethyl sulfoxide (DMSO), superoxide dismutase conjugated with polyethylene glycol (PEGSOD2), diethylenetriaminepentaacetic acid (DTPA) and dextran from leuconostoc mesenteroides (average MW 60000–76000) were from Sigma-Aldrich (Overijse, Belgium).

Cell lines and culture

PC-3 cell line were purchased from The American Type Culture Collection (Manassas,VA, USA) and maintained in a humidified atmosphere with 5% CO_2 at 37 ◦C. They were routinely cultured in Ham's F-12K (Kaighn's) Medium with 10% heat-inactivated fetal bovine serum (FBS)(Thermo Fisher Scientific).

OCR measurements by Seahorse XF technology

OCR measurements were performed using a XF Cell Mitostress test kit (Agilent, cat.103015-100) with a Seahorse XF96 bioenergetic analyzer (Seahorse Bioscience; Massachusetts, USA) [39] according to the manufacturer's instructions. Cells were first seeded at 10000 cell/well onto a Seahorse XF96 V3 PS plate 24 h before treatment. Cells were then treated for 2 or 24h with statins or control solution (DMSO) 0.1%). Before the assay, cell medium was replaced by the conditional medium without sodium bicarbonate (Dilution of Dulbecco's modified Eagle's medium (Cat. D5030, Sigma-Aldrich) supplemented with 1.85g/L NaCl, phenol red, 10mM D-glucose, 2mM L-glutamine, 2mM Pyruvate and 0.5% FBS) with or without statin and incubated at 37°C without CO_2 for 1 h before completion of probe cartridge calibration. Following drugs were injected successively: oligomycin (1M), FCCP (2M) and Rotenone/Antimycin A (0.5M). Data were visualized and analyzed using Agilent Wave Software. Results were normalized to the total number of cells determined using a SpectraMax i3 plate imager (Molecular Devices, Sunnyvale, CA) and SoftMax Pro software (Molecular Devices). Basal mitochondrial OCR was determined by subtracting the OCR measured after injection of rotenone/antimycin A (=non-mitochondrial respiration) to OCR measured before any drug injection

OCR measurements by EPR respirometry

Oxygen measurements in vitro using EPR respirometry are based on the use of an oxygen-sensing probe, ^{15}N-PDT (4-oxo-2,2,6,6-tetramethylpiperidine-d_{16}-^{15}N-1-oxyl), to measure variations in oxygen levels in samples, and subsequently cells' OCR in a sealed capillary [27,40-41]. OCR was measured using a Bruker EMX-Plus spectrometer operating in X-band (9.85 GHz) and equipped with a PremiumX ultra low noise microwave bridge and a SHQ high sensitivity resonator. The EPR cavity was heated at 310 K with continuous nitrogen flow during all experiments. Respiration mixture was composed of 60 µL of previously harvested cells (stock

solution 5.10^6 cells/mL of culture medium), 40 µL of Dextran solution (20%) and 4 µL of ^{15}N-PDT (2 mM), transferred into a hematocrit capillary sealed with gum. The final device was inserted into a quartz tube and put into the EPR cavity. Experimental parameters for acquisition set in the Bruker Xenon Spin fit program were: microwave power, 2.518 mW; modulation frequency, 100 kHz; modulation amplitude, 0.005 mT; center field, 335 mT; sweep width, 1.5 mT; sweep time, 15 s. An automated "2D-field-Delay" measurement was launched 3 min after probe mixing, counting 15 points with a time delay of 60,000 ms. Data analysis was performed switching to processing mode and using "peak picking" on selected regions of the ^{15}N-PDT – peaks. The final file was saved as an ASCII file to extract linewidth data at each point. ^{15}N-PDT linewidth was correlated with the % of oxygen with a calibration curve. OCR corresponded to the slope of oxygen level during time.

Mitochondrial superoxide assessment by EPR spectrometry

Mitochondrial superoxide measurements by EPR were based on the use of Mito-TEMPO-H, a cyclic hydroxylamine, able to detect superoxide in complex biological media with high sensitivity [41-46]. Thanks to its tryphenylphosphonium moiety (TPP^+), this probe accumulates within mitochondria, enabling specific measurement of mitochondrial superoxide. Superoxide production was monitored using a Bruker EMX-Plus spectrometer operating in X-band (9.85 GHz) and equipped with a PremiumX ultra low noise microwave bridge and a SHQ high sensitivity resonator. The EPR cavity was heated at 310 K with continuous air flow during all experiments. The mixture combined 37 µL of cell suspension (stock solution: 20.10^6 cells/mL culture medium), 0.5 µL of DTPA (100 mM), 5 µL of PBS ((1×) − pH 7.4) and 7.5 µL of Mito-TEMPO-H (1mM). Superoxide production contribution was assessed by making another measurement using the same conditions but adding 2.5 µL of PEG-SOD2 (4000 U/mL) to replace 2.5 µL of PBS. PEG-SOD2 was incubated 15 min before adding the Mito-TEMPO-H probe. Previous studies have shown that the pre-incubation of cells in the presence of PEG-SOD allows the cellular uptake of the enzyme and intracellular scavenging of superoxide [47]. Mito-TEMPO-H stock solution was flushed with Argon prior and during pipetting to avoid probe oxidation. The final solution was transferred into a PTFA tube (inside diameter 0.025 in., wall thickness 0.002 in.) cutting of 12 cm using a needle and folded in 6 before being inserted into an open quartz tube. Experimental parameters for acquisition set in the Bruker Xenon Spin fit program were: microwave power, 20 mW; modulation frequency, 100 kHz; modulation

amplitude, 0.1 mT; center field, 336.5 mT; sweep width, 1.5 mT; sweep time, 30.48 s. The measurements were started 3 min after probe mixing with the cells, and repeated each 40 s. An automated "2D-field-Delay" measurement was launched 3 min after probe mixing, counting 11 points with a time delay of 40,000 ms. Data analysis was performed switching to processing mode and using "Integration & derivative" and "double integration" on selected regions of the peaks. The final file was saved as an ASCII file to extract double integration (DI) data at each timepoint. Point 1 DI was subtracted from point 11 DI for each condition. Superoxide contribution was measured by subtracting mean PEGSOD2 DI to mean control DI.

Tumor models in vivo and treatments

Six to eight-week old male NMRI nude mice (Charles Rivers Laboratories) were housed under standardized conditions of light and temperature (12-hour daylight cycle, 22 ± 2°C) before and during the experiments and all had ad libitum access to chow pellets and water. After 1 week of acclimatization, mice were each inoculated intramuscularly (IM) in their right leg with 5.10^6 PC-3 cells (100µL cell suspension in HBSS + 100µL Matrigel (Corning™ 356237)). Experiments were performed 3-4 weeks following tumor inoculation when xenograft diameter exceeded 8mm. Mice were then put into groups to have same starting mean tumor volume before experiment.

In vivo EPR oximetry

Animals were anesthetized by inhalation of isoflurane mixed with air (21 % oxygen) in a continuous flow (2 L/h), delivered by a nose cone. Induction of anesthesia was performed using 3 % isoflurane. It was then stabilized at 1.5 % for a minimum of 15 minutes before any measurement. It was previously demonstrated that this anesthesia regimen did not disturb the hemodynamics in rodents [48]. A warming blanket was used for animal-body temperature regulation at 37°C. To assess the tumor oxygenation *in vivo*, we used EPR oximetry that allows repeated and quantitative measurements of tissue oxygenation from the same site over long periods of time [49-52]. We used the charcoal (CX 0670-1; EM Sciences, Gibbstown, NJ) as oxygen sensor [53] to dynamically evaluate changes in tumor oxygenation during statin treatment. EPR spectra were recorded using an EPR spectrometer (electromagnet from Magnettech, Berlin, Germany; electronic console from Clin-EPR, Lyme, NH, USA) with a low frequency microwave bridge operating at 1.1 GHz and an extended loop resonator (Clin-EPR,

Lyme, NH, USA). A suspension of charcoal was injected into the center of the tumor 1 day before measurement (100 mg/mL; 50 μL injected, particle size of 1-25 μm). The localized EPR measurements correspond to an average of the pO_2 values in a volume of ~10 mm^3 (49). For the experiments, baseline values were performed after mice were anesthetized to determine the oxygen status of tumors before the first IP injection of the treatment. Then, the effect of simvastatin and fluvastatin (20 mg/kg) was measured by following tumor pO_2 daily 5min after statin IP injection.

Irradiation

The Male NMRI PC-3 tumor baring mice were put into 5 groups of same mean tumor volume (>270mm^3) and irradiated once at doses of 0-3-6-9-12Gy. After irradiation, tumor growth was measured 3 times a week to assess tumor growth-delay.

Statistics

Data are represented as means ± SEM. All experiments were performed in triplicates or more. Student T tests were applied for EPR OCR and superoxide measurements experiments, whereas One-way ANOVA were performed on all other experiments.

Results

OCR in prostate cancer cells is decreased by simvastatin and fluvastatin, but remained unchanged after pravastatin, rosuvastatin and atorvastatin exposure.

A first screening using Seahorse XF technology was performed on PC-3 cells that revealed that a 24 hours-exposure of prostate cancer cells to a concentration of 10 µM simvastatin and fluvastatin significantly decreased the basal respiration (< 0.005, Fig.2a). In contrast, pravastatin, rosuvastatin and atorvastatin did not alter significantly the OCR (**Fig.2A**). Fluvastatin and simvastatin were further considered for additional experiments. We found that a significant reduction was also observed using Seahorse XF after 2 hours-exposure (**Fig.2B**). We also found that lower concentration (2.5 µM) significantly decreased the basal respiration by 24 % and 25.8 %, for simvastatin and fluvastatin, respectively (Data not shown). In addition, we used *in vitro* EPR respirometry to assess the OCR by cancer cells. While the results obtained after 24-hours exposure were consistent between Seahorse XF and EPR assessments, we did not observe a significant effect of both statins after 2 hours-exposure using EPR respirometry (**Fig.3**).

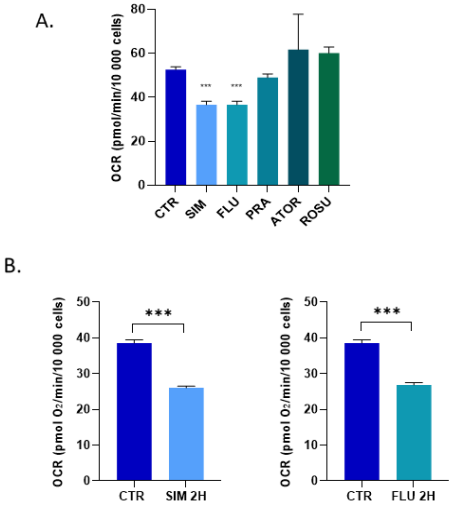

Fig.2 Impact of statins on the oxygen consumption rate (OCR) by prostate cancer cells as measured by Seahorse XF. **A.** Effect of 24 hours exposure of PC-3 cells to 5 different statins (10 µM) on the OCR. **B.** Effect of 2 hours exposure of PC-3 cells to simvastatin and fluvastatin (10 µM) on the OCR. Bars represent means ± SEM (pmol O_2/min/10000cells), (*) $p<0.05$, (**) $p<0.01$, One-way ANOVA & Student T-test, N=5.

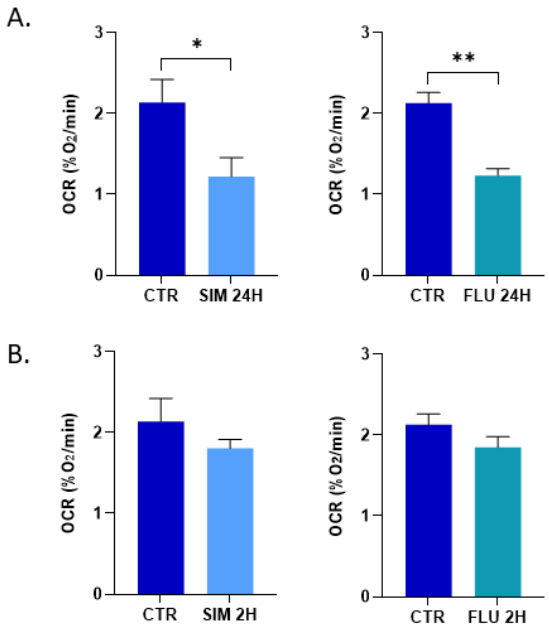

Fig.3 Impact of statins on the oxygen consumption rate (OCR) by prostate cancer cells as measured by EPR respirometry. **A.** Effect of 24 hours exposure of PC-3 cells to simvastatin and fluvastatin (10 µM) on the OCR. **B.** Effect of 2 hours exposure of PC-3 cells to simvastatin and fluvastatin (10 µM) on the OCR. Bars represent means ± SEM (%O_2/min), (*) $p<0.05$, (**) $p<0.01$, Student T-test, N=3.

Modulation of mitochondrial superoxide production by simvastatin and fluvastatin

Because a dysfunction in mitochondrial electron transport chain function may lead to an increase in superoxide production [54-55], we evaluated the potential change in mitochondrial superoxide level using EPR in cells exposed for 24 hours to 10 µM simvastatin or fluvastatin. The level of superoxide was significantly increased after exposure of prostate cancer cells to fluvastatin (Fig.4). While there was a trend for an increase in superoxide after simvastatin exposure, the level was not significantly different from the control (**Fig.4**).

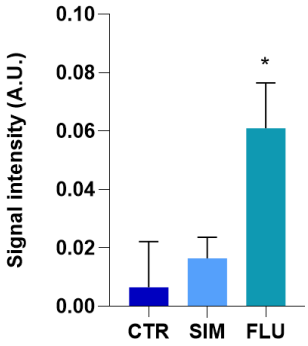

Fig.4 Impact of statins on the mitochondrial superoxide level in PC-3 cells exposed 24 hours to simvastatin and fluvastatin (10 µM). Mitochondrial superoxide was measured using mitoTEMPO-H as EPR sensor. The superoxide contribution was measured by making the difference between the signal intensities recorded in the absence and in the presence of PEGSOD2. Bars represent means ± SEM (A.U), (*) $p<0.05$, One-way ANOVA, N=3.

Simvastatin and fluvastatin alleviate tumor hypoxia in prostate cancer models

Because prostate cancer cells are sparing oxygen when exposed to simvastatin and fluvastatin, we anticipated that statin-based treatments could lead to a reoxygenation of tumors. The PC3 prostate tumor model was found highly hypoxic as the initial pO_2 before treatment was lower than 2 mmHg (Fig.5). Daily treatment with simvastatin and fluvastatin led to a dramatic increase in tumor oxygenation 48 hours and 72 hours after having started the treatment (**Fig.5**).

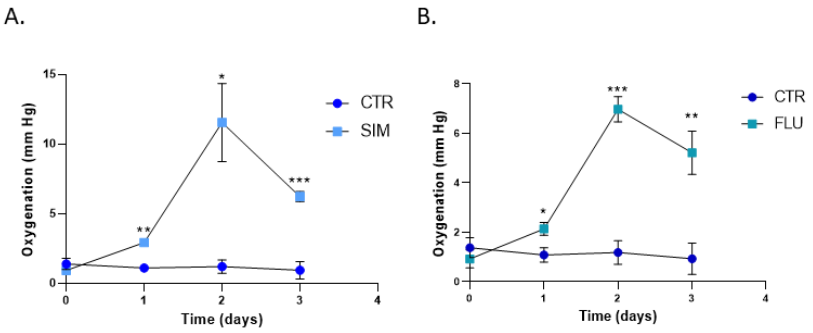

Fig.5 Effect of daily treatment with statins (20 mg/kg) on tumor oxygenation as measured by EPR oximetry: **A.** simvastatin (44 µmol/kg); **B.** fluvastatin (46 µmol/kg). Dots represent mean (mm Hg), (*) $p< 0.05$, (**) $p< 0.01$, (***) $p< 0.001$, Two-way ANOVA, N=4.

Does the combination statin/irradiation lead to an improved response to radiotherapy?

As the PC3 model was used for the first time in our laboratory, a pre-screening of irradiation dose was performed to establish a dose with a significant tumor growth delay without curative effect. At the time of the writing this thesis, the results of these experiments are not yet completed. Once established, our plans are to irradiate the tumors at the time of maximal reoxygenation and to follow daily the tumor growth. Several groups of mice will be used: control group (without irradiation), statin alone (without irradiation), RX alone, RX+statin. An additional group will include RX+statin+transient interruption of the blood flow at the time of irradiation. This last experiment will ascribe the contribution of the oxygen effect to the radiatiosensitizing property of the statin.

Discussion

The negative effect of tumor hypoxia on radiation therapy response has been demonstrated in a vast body of experimental works and clinical studies [21]. Several strategies have been designed to overcome this source of radioresistance including the decrease in tumor hypoxia, the chemical radiosensitization of hypoxic cells, or preferential killing of this resistant cell population by using a redistribution of the radiation dose. The most straightforward approach to decrease hypoxia is to combine radiation protocol together with the administration of an approved drug acting either on oxygen consumption and/or oxygen delivery. Illustrative successful examples in tumor models include the use of steroidal and non-steroidal anti-inflammatory agents [28,29] or metformin [32]. In this respect, if statins could be found as potential radiosensitizers, they would be particularly attractive regarding their massive use in the population to prevent cardiovascular diseases.

As a meta-analysis described a beneficial effect of statins on prostate cancer patients treated with RT [18], it seems crucial to investigate the mechanisms underlying the radiosensitizing properties of statins. A recent study suggested that simvastatin (μM range) combined with irradiation slightly affects cell growth, clonogenic survival, and DNA repair capacity in the breast cancer cell line MCF-7 in 2D-culture, but, surprisingly, not in 3D-culture [55]. Another study described that simvastatin (10 to 500 μM) compromises DNA double-strand

breaks repair by activating the expressions of histone 2A family member X (γ-H2AX) and phospho-checkpoint kinase 1 (p-CHK1), suggesting an underlying mechanism for this radiosensitization of prostate cancer cells (PC3 model) [56]. It was also found that simvastatin (1 to 5 μM) enhanced radiation sensitivity in vitro in different colorectal cancer cell lines [57]. In the present study, we explored another potential mechanism of radiosensitization, namely a potential change in tumor cell metabolism that should impact the tumor microenvironment. Our initial hypothesis of a change in oxygen consumption was verified in prostate cancer cells when exposed to simvastatin and fluvastatin (Fig.2). However, contrarily to our expectation, we did not observe a "class effect" as the OCR was not significantly changed when exposing the prostate cancer cells to pravastatin, rosuvastatin and atorvastatin (Fig.2). Moreover, as rosuvastatin and atorvastatin are more potent inhibitors of HMG-CoA reductase than simvastatin [58], this suggests that the effect observed on prostate cancer cells is not primarily mediated by the reduction in synthesis of Coenzyme Q10 (complex III of the mitochondrial electron transport chain). In the research on mechanisms associated with muscle toxicity, it has been described that statins inhibit the activity of enzyme complexes I and III on the electron transport chain, an inhibition that is dependent on individual statin [59]. Identifying the exact mechanism responsible for the change in OCR in cancer cells will require further investigation. Of note, we observed consistent results in OCR decrease using Seahorse XF and EPR respirometry after 24 hours exposure, but not after 2 hours exposure (Fig.2 and 3). While Seahorse XF is applied on adherent cells, EPR respirometry requires the cell detachment. A previous study revealed that cell detachment with trypsin may lead to slight change in cell respiration [60]. Interestingly, the consequence of the induced mitochondrial dysfunction in terms of superoxide production was different between statins. While simvastatin and fluvastatin had a comparable impact on OCR (Fig.2), the level of mitochondrial superoxide produced was higher after fluvastatin treatment than after simvastatin exposure (Fig.3). For the future, we plan to repeat those experiments in a second prostate cancer cell line (i.e. DU145).

An important consequence from the change in oxygen metabolism by prostate cancer cells is the alleviation of tumor hypoxia. To evaluate the impact of statin treatment in PC-3 cancer model *in vivo*, we selected EPR oximetry as this technique has the unique capabilities to make repeated measurements from the same site over long periods of time and to detect subtle variations in tissue oxygenation [51,61]. Consistently with our observations done *in vitro*, the increase in tumor oxygenation did not occur acutely after administration of the statins. The

maximal reoxygenation was observed 48 hours after the first injection (Fig.4). Of note, the pO_2 values increased from about 2 mmHg before treatment to 7 mmHg or 12 mmHg, after 2 days of treatment with fluvastatin and simvastatin, respectively. It is well established that the oxygen enhancement ratio (ratio in radiation dose to observe the same biological effect) dramatically varies between 1 and 10 mmHg [23,62,63]. We anticipate that this increase in tumor oxygenation can be beneficial in terms of radiosensitization if the irradiation is applied during the time window identified by EPR oximetry. Irradiation experiments have started to identify an optimal dose with a significant tumor growth delay without curative effect. Once identified, our irradiation protocol should inform us on the effectiveness of the statin treatment on the response to irradiation and the potential contribution of the oxygen effect to the sensitization by statins.

A limitation of our study relies on the statin dosage that has been used *in vitro* to study the effect of oxygen utilization. While our present study was performed using concentrations consistent with those used in other studies evaluating the impact of statins on tumor cell response [3-6,55-57], their relevance for immediate translation in humans is debatable. A publication performed a systematic literature search identifying *in vitro* experiments where mechanistic insights behind pleiotropic effects of statins were claimed [64]. In this paper, the authors concluded that the choice of statin concentration was frequently based on previous experiments from papers in high-impact journals. In these articles, pleiotropic effects of statins were only detected at statin concentrations of 1–50 μmol/L. This contrasts with the maximal concentration (Cmax) of statin found in the human serum (30 nmol/L for simvastatin after a dose of 40 mg or 40 nmol/L for atorvastatin after a dose of 20 mg) [63]. Here, taking the example of simvastatin, *in vitro*, we used a concentration of 10 μM in most experiments and have also observed an effect on oxygen consumption at a concentration of 2.5 μM. This represents about eighty times the Cmax observed in humans. Regarding the dose used *in vivo*, we administered a dose of 20 mg/kg of simvastatin while the maximal dose in humans is 80 mg per day for an adult, representing 1 mg/kg for an adult of 80 kg body weight. This represents approximately 20 times the dose used in humans. In other words, our study should be considered as a proof-of-concept and the immediate translation for human studies should be taken with caution.

References

1. Di Bello E, Zwergel C, Mai A, Valente S. The Innovative Potential of Statins in Cancer: New Targets for New Therapies. Front Chem. 2020;8:516.
2. Duarte JA, de Barros ALB, Leite EA. The potential use of simvastatin for cancer treatment: A review. Biomed Pharmacother. 2021;141:111858.
3. Muller C, Bockhorn AG, Klusmeier S, Kiehl M, Roeder C, Kalthoff H, Koch OM. Lovastatin inhibits proliferation of pancreatic cancer cell lines with mutant as well as with wild-type K-ras oncogene but has different effects on protein phosphorylation and induction of apoptosis. Int J Oncol 1998;12:717-723.
4. Kozar K, Kaminski R, Legat M, Kopec M, Nowis D, Skierski JS, Koronkiewicz M, Jakóbisiak M, Golab J. Cerivastatin demonstrates enhanced antitumor activity against human breast cancer cell lines when used in combination with doxorubicin or cisplatin. Int J Oncol. 2004;24:1149-57.
5. Khanzada UK, Pardo OE, Meier C, Downward J, Seckl MJ, Arcaro A. Potent inhibition of small-cell lung cancer cell growth by simvastatin reveals selective functions of Ras isoforms in growth factor signalling. Oncogene. 2006;25:877-87.
6. Afshari AR, Mollazadeh H, Henney NC, Jamialahmad T, Sahebkar A. Effects of statins on brain tumors: a review. Semin Cancer Biol. 2021;73:116-133.
7. Voorneveld PW, Reimers MS, Bastiaannet E, Jacobs RJ, van Eijk R, Zanders MMJ, Herings RMC, van Herk-Sukel MPP, Kodach LL, van Wezel T, Kuppen PJK, Morreau H, van de Velde CJH, Hardwick JCH, Liefers GJ. Statin Use After Diagnosis of Colon Cancer and Patient Survival. Gastroenterology. 2017;153:470-479.
8. Li X, Liu L, Hu Y. Statin use and the prognosis of patients with hepatocellular carcinoma: a meta-analysis. Biosci Rep. 2020;40:BSR20200232
9. Kotti A, Holmqvist A, Albertsson M, Sun XF. Survival benefit of statins in older patients with rectal cancer: A Swedish population-based cohort study. J Geriatr Oncol. 2019;10:690-697.
10. Gupta A, Stokes W, Eguchi M, Hararah M, Amini A, Mueller A, Morgan R, Bradley C, Raben D, McDermott J, Karam SD. Statin use associated with improved overall and cancer specific survival in patients with head and neck cancer. Oral Oncol. 2019;90:54-66.

11. Xia DK, Hu ZG, Tian YF, Zeng FJ. Statin use and prognosis of lung cancer: a systematic review and meta-analysis of observational studies and randomized controlled trials. Drug Des Devel Ther. 2019;13:405-422.
12. Cardwell CR, Spence AD, Hughes CM, Murray LJ. Statin use after esophageal cancer diagnosis and survival: A population based cohort study. Cancer Epidemiol 2017;48:124-130.
13. Gray RT, Loughrey MB, Bankhead P, Cardwell CR, McQuaid S, O'Neill RF, Arthur K, Bingham V, McGready C, Gavin AT, James JA, Hamilton PW, Salto-Tellez M, Murray LJ, Coleman HG. Statin use, candidate mevalonate pathway biomarkers, and colon cancer survival in a population-based cohort study. Br J Cancer 2017;116:1652-1659.
14. Seckl MJ, Ottensmeier CH, Cullen M, Schmid P, Ngai Y, Muthukumar D, Thompson J, Harden S, Middleton G, Fife KM, Crosse B, Taylor P, Nash S, Hackshaw A. Multicenter, Phase III, Randomized, Double-Blind, Placebo-Controlled Trial of Pravastatin Added to First-Line Standard Chemotherapy in Small-Cell Lung Cancer (LUNGSTAR). J Clin Oncol 2017;35: 1506-1514.
15. Kollmeier MA, Katz MS, Mak K, Yamada Y, Feder DJ, Zhang Z, Jia X, Shi W, Zelefsky MJ. Improved biochemical outcomes with statin use in patients with high-risk localized prostate cancer treated with radiotherapy. Int J Radiat Oncol Biol Phys 2011;79: 713-718.
16. Moyad MA, Merrick GS, Butler WM, Wallner KE, Galbreath RW, Butler EG, Allen ZA, Adamovich E. Statins, especially atorvastatin, may improve survival following brachytherapy for clinically localized prostate cancer. Urol Nurs 2006;26: 298-303.
17. Oh DS, Koontz B, Freedland SJ, Gerber L, Patel P, Lewis S, Yoo DS, Oleson J, Salama JK. Statin use is associated with decreased prostate cancer recurrence in men treated with brachytherapy. World J Urol 2015;33: 93-97.
18. Park HS, Schoenfeld JD, Mailhot RB, Shive M, Hartman RI, Ogembo R, Mucci LA. Statins and prostate cancer recurrence following radical prostatectomy or radiotherapy: a systematic review and meta-analysis. Ann Oncol 2013;24: 1427-1434.
19. Dhani N, Fyles A, Hedley D, Milosevic M. The clinical significance of hypoxia in human cancers. Semin Nucl Med 2015;45: 110-121.
20. Walsh JC, Lebedev A, Aten E, Madsen K, Marciano L, Kolb HC. The clinical importance of assessing tumor hypoxia: relationship of tumor hypoxia to prognosis and therapeutic opportunities. Antioxid Redox Signal 2014;21: 1516-1554.

21. Colliez F, Gallez B, Jordan BF. Assessing Tumor Oxygenation for Predicting Outcome in Radiation Oncology: A Review of Studies Correlating Tumor Hypoxic Status and Outcome in the Preclinical and Clinical Settings. Front Oncol. 2017;7:10.
22. Vaupel P, Kelleher DK, Hockel M. Oxygen status of malignant tumors: pathogenesis of hypoxia and significance for tumor therapy. Semin Oncol 2001;28: 29-35.
23. M.R. Horsman, B.G.Wouters, M.C. Joiner, J. Overgaard, The oxygen effect and fractionated radiotherapy, in: M. Joiner, A. van der Kogel (Eds.), Basic Clinical Radiobiology, fourth ed.H. Arnold, London 2009, pp. 207–216.
24. Secomb TW, Hsu R, Ong ET, Gross JF, Dewhirst MW. Analysis of the effects of oxygen supply and demand on hypoxic fraction in tumors. Acta Oncol 1995;34: 313-316.
25. Diepart C, Karroum O, Magat J, Feron O, Verrax J, Calderon PB, Grégoire V, Leveque P, Stockis J, Dauguet N, Jordan BF, Gallez B. Arsenic trioxide treatment decreases the oxygen consumption rate of tumor cells and radiosensitizes solid tumors. Cancer Res. 2012;72:482-90.
26. Jordan BF, Grégoire V, Demeure RJ, Sonveaux P, Feron O, O'Hara J, Vanhulle VP, Delzenne N, Gallez B. Insulin increases the sensitivity of tumors to irradiation: involvement of an increase in tumor oxygenation mediated by a nitric oxide-dependent decrease of the tumor cells oxygen consumption. Cancer Res. 2002;62:3555-61.
27. Crokart N, Radermacher K, Jordan BF, Baudelet C, Cron GO, Grégoire V, Beghein N, Bouzin C, Feron O, Gallez B. Tumor radiosensitization by antiinflammatory drugs: evidence for a new mechanism involving the oxygen effect. Cancer Res. 2005;65:7911-6.
28. Crokart N, Jordan BF, Baudelet C, Cron GO, Hotton J, Radermacher K, Grégoire V, Beghein N, Martinive P, Bouzin C, Feron O, Gallez B. Glucocorticoids modulate tumor radiation response through a decrease in tumor oxygen consumption. Clin Cancer Res. 2007;13:630-5.
29. Jordan BF, Christian N, Crokart N, Grégoire V, Feron O, Gallez B. Thyroid status is a key modulator of tumor oxygenation: implication for radiation therapy. Radiat Res. 2007;168:428-32.
30. Ashton TM, Fokas E, Kunz-Schughart LA, Folkes LK, Anbalagan S, Huether M, Kelly CJ, Pirovano G, Buffa FM, Hammond EM, Stratford M, Muschel RJ, Higgins GS, McKenna WG. The anti-malarial atovaquone increases radiosensitivity by alleviating tumour hypoxia. Nat Commun. 2016;7:12308.

31. Zannella VE, Dal Pra A, Muaddi H, McKee TD, Stapleton S, Sykes J, Glicksman R, Chaib S, Zamiara P, Milosevic M, Wouters BG, Bristow RG, Koritzinsky M. Reprogramming metabolism with metformin improves tumor oxygenation and radiotherapy response. Clin Cancer Res. 2013;19:6741-50.
32. De Preter G, Deriemaeker C, Danhier P, Brisson L, Cao Pham TT, Grégoire V, Jordan BF, Sonveaux P, Gallez B. A Fast Hydrogen Sulfide-Releasing Donor Increases the Tumor Response to Radiotherapy. Mol Cancer Ther. 2016;15:154-61.
33. Gallez B, Neveu MA, Danhier P, Jordan BF. Manipulation of tumor oxygenation and radiosensitivity through modification of cell respiration. A critical review of approaches and imaging biomarkers for therapeutic guidance. Biochim Biophys Acta Bioenerg. 2017;1858:700-711.
34. Bonifacio A, Mullen PJ, Mityko IS, Navegantes LC, Bouitbir J, Krähenbühl S. Simvastatin induces mitochondrial dysfunction and increased atrogin-1 expression in H9c2 cardiomyocytes and mice in vivo. Arch Toxicol 2016;90: 203-215.
35. Kwak HB, Thalacker-Mercer A, Anderson EJ, Lin CT, Kane DA, Lee NS, Cortright RN, Bamman MM, Neufer PD. Simvastatin impairs ADP-stimulated respiration and increases mitochondrial oxidative stress in primary human skeletal myotubes. Free Radic Biol Med 2012;52: 198-207.
36. Satoh K, Nakai T, Ichihara K. Influence of 3-hydroxy-3-methylglutaryl coenzyme A reductase inhibitors on mitochondrial respiration in rat liver during ischemia. Eur J Pharmacol 1994;270: 365-369.
37. Thews O, Kelleher DK, Vaupel P. In vivo oxygen consumption rate of DS sarcoma cells on inhibition of DNA synthesis. Cancer Res 1996;56: 2009-2012.
38. Ferrick DA, Neilson A, Beeson C. Advances in measuring cellular bioenergetics using extracellular flux. Drug Discov Today. 2008;13:268-74.
39. Diepart C, Verrax J, Calderon PB, Feron O, Jordan BF, Gallez B. Comparison of methods for measuring oxygen consumption in tumor cells in vitro. Anal Biochem. 2010;396:250-6.
40. d'Hose D, Danhier P, Northshield H, Isenborghs P, Jordan BF, Gallez B. A versatile EPR toolbox for the simultaneous measurement of oxygen consumption and superoxide production. Redox Biol. 2021;40:101852.
41. Dikalov SI, Harrison DG. Methods for Detection of Mitochondrial and Cellular Reactive Oxygen Species. Antioxid Redox Signal. 2014;20:372–382.

42. Dikalov SI, Kirilyuk I, Voynov M, Grigor'Ev I. EPR detection of cellular and mitochondrial superoxide using cyclic hydroxylamines. Free Radic Res. 2010; 45: 417–430.
43. Scheinok S, Leveque P, Sonveaux P, Driesschaert B, Gallez B. Comparison of different methods for measuring the superoxide radical by EPR spectroscopy in buffer, cell lysates and cells. Free Radic Res. 2018; 52: 1182–1196.
44. Scheinok S, Driesschaert B, d'Hose D, Sonveaux P, Robiette R, Gallez B. Synthesis and characterization of a 5-membered ring cyclic hydroxylamine coupled to triphenylphosphonium to detect mitochondrial superoxide by EPR spectrometry. Free Radic Res. 2019; 53: 1135–1143.
45. Scheinok S, Capeloa T, Porporato PE, Sonveaux P, Gallez B. An EPR Study Using Cyclic Hydroxylamines to Assess the Level of Mitochondrial ROS in Superinvasive Cancer Cells. Cell Biochem Biophys. 2020; 78: 249–254.
46. Beckman JS, Minor RL Jr, White CW, Repine JE, Rosen GM, Freeman BA. Superoxide dismutase and catalase conjugated to polyethylene glycol increases endothelial enzyme activity and oxidant resistance. J. Biol. Chem. 1988; 263: 6884–6892.
47. Baudelet C, Gallez B. Effect of anesthesia on the signal intensity in tumors using BOLD-MRI: comparison with flow measurements by Laser Doppler flowmetry and oxygen measurements by luminescence-based probes. Magn Reson Imaging. 2004;22:905-12.
48. Gallez B, Jordan BF, Baudelet C, Misson PD. Pharmacological modifications of the partial pressure of oxygen in murine tumors: evaluation using in vivo EPR oximetry. Magn Reson Med. 1999;42:627-30.
49. Gallez B, Baudelet C, Jordan BF. Assessment of tumor oxygenation by electron paramagnetic resonance: principles and applications. NMR Biomed. 2004;17:240-62.
50. Swartz HM, Flood AB, Schaner PE, Halpern H, Williams BB, Pogue BW, Gallez B, Vaupel P. How best to interpret measures of levels of oxygen in tissues to make them effective clinical tools for care of patients with cancer and other oxygen-dependent pathologies. Physiol Rep. 2020;8:e14541.
51. Gallez B. Oxygenation Status in Normal Tissues, Pathological Tissues and Malignant Tumors: A pO_2 Database Based on Electron Paramagnetic Resonance (EPR) Oximetry Measurements. Appl Magn Reson 2021; doi.org/10.1007/s00723-021-01358-7.

52. Jordan BF, Baudelet C, Gallez B. Carbon-centered radicals as oxygen sensors for in vivo electron paramagnetic resonance: screening for an optimal probe among commercially available charcoals. MAGMA. 1998;7:121-9.
53. Jezek J, Cooper KF, Strich R. Reactive Oxygen Species and Mitochondrial Dynamics: The Yin and Yang of Mitochondrial Dysfunction and Cancer Progression. Antioxidants 2018;7:13.
54. Kalyanaraman B, Cheng G, Hardy M, Ouari O, Bennett B, Zielonka J. Teaching the basics of reactive oxygen species and their relevance to cancer biology: Mitochondrial reactive oxygen species detection, redox signaling, and targeted therapies. Redox Biol. 2018;15:347-362.
55. Manda K, Juerß D, Fischer P, Schroder A, Koenen A, Hildebrandt G. Simvastatin treatment varies the radiation response of human breast cells in 2D or 3D culture. Invest New Drugs. 2021;39:658-669.
56. Chen YA, Shih HW, Lin YC, Hsu HY, Wu TF, Tsai CH, Wu CL, Wu HY, Hsieh JT, Tang CH, Lai CH. Simvastatin Sensitizes Radioresistant Prostate Cancer Cells by Compromising DNA Double-Strand Break Repair. Front Pharmacol. 2018;9:600.
57. Karagkounis G, DeVecchio J, Ferrandon S, Kalady MF. Simvastatin enhances radiation sensitivity of colorectal cancer cells. Surg Endosc. 2018;32:1533-1539.
58. McKenney JM. Pharmacologic characteristics of statins. Clin Cardiol. 2003;26(Suppl 3):III32-8.
59. Bouitbir J, Sanvee GM, Panajatovic MV, Singh F, Krahenbuhl S. Mechanisms of statin-associated skeletal muscle-associated symptoms. Pharmacol Res 2020; 154: 104201.
60. Danhier P, Copetti T, De Preter G, Leveque P, Feron O, Jordan BF, Sonveaux P, Gallez B. Influence of cell detachment on the respiration rate of tumor and endothelial cells. PLoS One. 2013;8:e53324.
61. Swartz HM, Flood AB, Schaner PE, Halpern H, Williams BB, Pogue BW, Gallez B, Vaupel P. How best to interpret measures of levels of oxygen in tissues to make them effective clinical tools for care of patients with cancer and other oxygen-dependent pathologies. Physiol Rep. 2020;8:e14541.
62. Whillans DW, Hunt JW. A rapid-mixing comparison of the mechanisms of radiosensitization by oxygen and misonidazole in CHO cells. Radiat Res. 1982;90:126-41.

63. Koch CJ, Stobbe CC, Bump EA. The effect on the Km for radiosensitization at 0 degree C of thiol depletion by diethylmaleate pretreatment: quantitative differences found using the radiation sensitizing agent misonidazole or oxygen. Radiat Res. 1984;98:141-53.
64. Björkhem-Bergman L, Lindh JD, Bergman P. What is a relevant statin concentration in cell experiments claiming pleiotropic effects? Br J Clin Pharmacol. 2011;72:164-5.

Discussion & perspectives

I. Main achievements of the thesis

With the implication of oxidative stress in the onset and progression of multiple diseases such as neurodegeneration, diabetes and cancer, the development of new analytical approaches to measure ROS drastically evolved. Although fluorescent probes dominated oxidative stress and cancer research by providing highly sensitive measurements of ROS in biological samples, they were however proven to lack specificity in measuring superoxide anion radicals except when used in combination with HPLC methods (Zielonka 2010, Kalyanaraman 2012). By using the appropriate probes and controls, EPR technology seemed to be a promising technique to measure both parameters sensitively and specifically (Dikalov 2014).

1. Dual EPR measurement to define mitochondrial (dys)function

The first goal of this thesis was to develop and validate a novel EPR tool enabling simultaneous measurement of OCR and superoxide production in biological samples. In the first place, we validated the probes (^{15}N-PDT and ^{14}N-CMH) in two known models of superoxide production as a proof of concept. The combination of these probes allowed us to develop a first design on isolated mitochondria, enabling the simultaneous measurement of OCR and superoxide. This tool was also validated with the use of well described modulators of the ETC. Later on, the project rapidly evolved into a versatile EPR tool which could be modulated according to the desired cellular model and parameter. ^{14}N-CMH distributes in intra- and extracellular spaces measuring global ROS production, whereas MitoTEMPO-H accumulates in the mitochondrial matrix to measure mtROS. According to a recent comparative study performed in our lab, these two hydroxylamine probes were demonstrated to be the most sensitive EPR probes to measure superoxide in biological samples (Scheinok 2018). To measure the generation of specific radicals such as superoxide and hydroxyl radical, samples are preincubated with appropriate pegylated controls; PEG-SOD and PEG-CAT respectively.

Another important aim of this thesis was to exploit this new experimental set-up in diverse projects. At this day, it is already contributing to toxicology and anticancer therapy projects.

2. Short-term exposure of SDHI induces mitochondrial function in human cell lines

Regarding toxicological assessments, this EPR tool can be used to determine the impact of agents (drugs, additives, polluants, …) on mitochondrial function. In our case, a recent paper depicting the deleterious impact of SDHI fungicides on worm, bees and humans was broadcasted worldwide into the news (Bénit 2019). From this, we took the opportunity to determine whether Boscalid and Bixafen could alter OCR and superoxide production after short-term exposure (2H) in diverse human cell lines; HepG2 hepatocarcinoma, BJ fibroblasts and peripheral blood mononuclear cells (PBMC). These cell lines are the most likely to be exposed to SDHI (liver, skin and blood). Boscalid and Bixafen were both demonstrated to alter OCR in all cell lines and HepG2 were most sensitive to both SDHI in term of superoxide production. By altering mitochondrial function, the SDHI were also able to induce apoptosis in HepG2 cells. Overall, using this new EPR tool, we expanded the results obtained by Bénit et al. showing the impact of short-term exposure to SDHI on human cells.

3. Simvastatin and Fluvastatin are potential candidates to enhance radiosensitivity in prostate cancer

Related to anticancer therapy, we aimed to demonstrate whether statins could potentially act on mitochondrial respiration of tumor cells and enhance radiosensitivity. In this project, we tested the impact of 5 different statins on mitochondrial function *in vitro* and *in vivo* in prostate cancer tumor models using EPR. Among the statin screening, Simvastatin and Fluvastatin decreased OCR in PC-3 cells *in vitro* as well as pO_2 of PC-3 tumors *in vivo*. They both remain potential good candidates to enhance radiosensitivity in prostate cancer patient treated with RT. However, their impact on tumor-growth when irradiated at maximal window of reoxygenation, superoxide production and potential metastasis induction *in vivo* are still to be assessed.

II. Discussion of limitations

1. Limitations of the newly developed EPR tool to define mitochondrial function

1.1. Isolated mitochondria versus whole cell models

During our first attempt in developing a novel EPR tool, we succeeded in measuring OCR and superoxide simultaneously from a same mitochondrial preparation when exposed to control and treated (ETC modulators) conditions. With this method, we were able to titrate mitochondrial function in a specific way. However, with the increasing interest in measuring superoxide in more complex environments, the EPR superoxide measurement part gained more importance and the tool was fine-tuned separately on whole cell models. Thus, in our efforts to improve the concept a step further, we did not manage to keep the measurements of OCR and superoxide simultaneously. However, it should be stressed that real time measurements of both parameters using whole cells instead of isolated mitochondria would be totally feasible. To achieve simultaneous measurement of OCR and superoxide, EPR parameters were modulated to have enough definition for both EPR probes' spectra and avoid distortion. However, to achieve a better and more precise data analysis for the superoxide assessment, performing the assay separately with appropriate EPR parameters seemed more promising.

1.2. The specificity of cyclic hydroxylamine probes for superoxide

The major limitation faced in the development of this new EPR tool is the specificity of the probes to measure superoxide anion radical. Indeed, cyclic hydroxylamines undergo a non-specific oxidation in presence of other free radicals or oxidants to form a paramagnetic species. When CMH or MitoTEMPO-H are put into our final cell suspension mix, they interact with all free radicals/oxidants that are generated by the cells in the experimental sample. The obtained EPR spectra during the experiment reflect therefore the global oxidation of the probe after 15min. The used probes in our experiments are in any case not specifically measuring superoxide production. At this day, many studies have been performed using these probes to detect superoxide while using an appropriate control; SOD or PEG-SOD (Dikalov 2002, 2007, Wyche 2004). Extracellular $O_2^{\bullet -}$ can be quantified with the use of SOD2 while PEGSOD2 measures both extra- and intracellular $O_2^{\bullet -}$. Although using SOD and PEGSOD is the best way so far to

measure superoxide with EPR, it can still add a measurement bias. In our experiments, PEGSOD was preincubated during 20min for the enzyme to cross membranes and penetrate into the cell and organelles. However, because PEGSOD is not specific for mitochondria, we do not know for sure if it reaches the mitochondria in sufficient concentration during that lapse of time. Thus, it could be that PEGSOD is still accumulated in the extracellular matrix more than in the cell and mitochondria, and that recorded $mtO_2^{\circ-}$ measurements are not reflecting the real situation. According to Beckman *et al.,* polyethylene glycol has surface active properties and can induce cell fusion to enhance transport of normally membrane-impermeable enzymes into the cells. They also suggested that PEGylated enzymes and other cargos are more likely to enter the cell by altering membrane fluidity via endocytosis rather than by direct membrane penetration. Also, rates of endocytosis are highly dependent on multiple factors such as incubation, temperature, size of cargo and cell type, making it complex to standardize a protocol for each research topic.

2. Limitations regarding the SDHI project

2.1. Choice of cell lines

In this project, we used the EPR tool to assess mitochondrial dysfunction in diverse human cell lines in order to demonstrate the potential off-target effects of SDHI. We tested Boscalid and Bixafen on cell types that were most likely to be in contact with fungicides such as liver, skin and blood. Among these cell lines, HepG2 cells are not normal hepatocytes but derive from a liver biopsy of a differentiated hepatocellular carcinoma. Cancer cells are known to adapt their metabolism in order to enhance tumor progression, and more certainly modulate mitochondrial function which is a central player in many pathophysiological processes. HepG2 have therefore the ability to switch to glycolysis to sustain proliferation in aerobic conditions, which could reduce sensitivity to mitochondrial toxicants (Kamalian 205). Testing the effects of SDHI on tumor-derived cells to prove mitochondrial dysfunction could therefore be questionable. However, these cells constitute an important model classically used by researchers and pharmaceutical companies to assess the hepatoxicity of chemicals or drugs (Knasmuller 1999, Schoonen 2005, Gerets 2009, O'Brien 2006). Moreover, HepG2 cells actually possess lots of genetic and phenotypic similarities with normal hepatocytes (Thabrew 1997, Guo 2011). Their main advantage next to easy culturing and lifespan resides in their stable phenotype which is not

dependent on donor characteristics (Donato 2015). Despite their lower expression in certain drug metabolizing enzymes and transporters compared to primary human hepatocytes, HepG2 still remain a valuable model in toxicological risk assessment (Guo 2011).

2.2. Treatment concentration

The treatment concentrations of Boscalid and Bixafen used in our experiments were based on the findings of Benit et al., on the impact of SDHI on the activity of SDH enzyme (IC50 Boscalid ~5µM and Bixafen <1µM)(Benit 2019). Furthermore, 1µM concentration is likely close to concentrations achieved for operators (farmers or people living nearby fields) after exposure to levels close to the operators' AOEL (maximal dose the operator may be exposed to without adverse effects). With the lack of epidemiologic data about fungicide blood concentration levels after exposure in humans, the relevance of SDHI treatment concentration in research is however often discussed. Indeed, exposure to SDHI fungicides depends on many parameters such as amounts of SDHI manipulated, exposure time, frequency of field spreading, protection means, contaminated diet or air/soil pollution, which all induce variability in term of achieved SDHI concentrations in tissues. Pesticide exposure in farmers and people living nearby treated areas is mostly evaluated through quantification in hair (Polledri 2019,2021). Also, genetic predisposition could make some people more susceptible to SDHI-induced mitochondrial dysfunction. At this day, there is still a lot of work to perform concerning pesticide measurements in tissues as well as their accumulation in the environment, in order to define more clearly the exposition of any living organism to these agents.

3. Limitations regarding the statin project

A limitation encountered in this project is the relevance of the used *in vitro* statin concentration (10µM) to study the effect of oxygen consumption. While our chosen experimental treatments were consistent with those from other studies evaluating the impact of statins on tumor cell responses (Muller 1998, Kozar 2004, Karagkanis 2018), they still remain debatable when considering potential translation in human studies. Indeed, the maximal concentration of statin found in the human serum (30 nM for simvastatin after a dose of 40 mg or 40 nM for atorvastatin after a dose of 20 mg) contrasts with the in vitro concentrations (around 1 to 50µM) used to detect pleiotropic effects of statins (Koch 1984). Regarding the dose used *in vivo*, we administered a dose of 20 mg/kg of simvastatin while the maximal dose in humans is 80 mg per day for an

adult, representing 1 mg/kg for an adult of 80 kg body weight. This represents approximately 20 times the dose used in humans. In a phase I clinical trial with Lovastatin treated patients per os with ranging doses from 2-45mg/kg of bodyweight daily during 7days courses monthly, the reached statin's serum levels ranged from 0.10 to 3.92 μM. Side effects of statin treatment were mild when administered doses were <25mg/kg/day, and the severity of myopathies decreased significantly when patients were supplemented with ubiquinone (~240mg/day) (Thibault 1996). In another clinical trial (Phase I-II) in patients with high-grade glioma, daily 30mg/kg doses of Lovastatin were well tolerated with concurrent radiation (Larner 1998). This could suggest that high doses of statin therapy could be used with short term treatment to enhance tumor reoxygenation at time of radiation. However, at this time our study should be considered as a proof-of-concept and the immediate translation for human studies should still be taken with cautious.

III. Perspectives

1. Perspectives originating from the EPR tool development

1.1. MitoSOD

As discussed in this thesis, many potential anticancer agents and ROS probes are being developed to target mitochondria by linking a TPP+ moiety to the desired molecule. To enhance superoxide scavenging and subsequently improve mitochondrial superoxide detection, it would be interesting to develop mitochondrial targeted SOD2. Of note, over the years, SOD mimetics were also developed and already extensively used in animal studies showing beneficial effects in diabetes, inflammation and neuronal oxidative stress (Bonetta 2018). In 2012, Kelso et al., synthetized MitoSOD, reacting selectively with superoxide compared to other SOD analogs and mimetics which also react with other radicals such as ONOO- (Kelso, 2012, Salvemini 2002). However, his work was rapidly criticized regarding its efficiency compared to native SOD and the used model to demonstrate the efficiency of the tool (Liochev 2013). So far, nobody found a proper alternative to improve the selectivity of existing SOD analogs and their mitochondrial targeting. The development of SOD2 surexpressing cell lines like recently performed by Scheinok could however also be interesting to use in order to investigate the nature of mitochondrial ROS (Scheinok 2020).

1.2. mtROS measurements in vivo

One of the main perspectives related to this EPR tool development is its translation into *in vivo* models. While EPR-oximetry and ^{17}O-MRS are already extensively used in research projects as advanced technique to measure tissue and tumor pO_2 (Diepart 2009, Desmet 2018, Neveu 2017), the characterization of *in vivo* mtROS to optimize anti-cancer treatments yet remains a challenge. As part of a new PhD thesis at our lab, the goal would be to implement an in vivo EPR/MRI toolbox to study cancer models where mtROS are hypothesized to play a crucial role. When a nitroxide probe is administered in vivo, it is rapidly metabolized into its hydroxylamine form. This intrinsic reduction of the probe can be modified by tissue redox conditions such as hypoxia and oxidative stress related to excessive ROS production (Matsumoto 2011). In this way, *in vivo* redox status could be assessed by using EPR to monitor the decay of the EPR signal of the nitroxide probe over time. In addition, the paramagnetism of nitroxides enables to use the same probe as MRI contrast agent by decreasing the T1 relaxation time (Gallez 1993, Gallez 1996). The kinetics analysis of contrast loss can ultimately be related to the tissue redox status and be used to provide high resolution redox maps (Matsumoto 2011, 2018, Uchida 2020). Today, MitoTEMPO° has already been used *in vitro* using EPR and MRI (Zhelev 2019, Bakalova 2015) as well as *in vivo* in magnetic resonance redox imaging providing redox mapping in mice models such as Parkinson's disease and kidney dysfunction (Zhelev 2013, Lazarova 2019) and is now considered a useful redox sensor in the detection and visualization of ROS production. So far, mitochondrial targeted sensors have not yet been used *in vivo* in cancer models for mitoROS detection.

1.3. Extension to other applications

The versatility of our toolbox offers multiple options in term of choice of model (isolated mitochondria or whole cell model), cell line and probe for accumulation in specific cellular compartments. OCR and superoxide production measurements were also relevant in our two projects for the assessment of SDHI toxicity and statins' radiosensitizing properties. However, other EPR probes such as pH sensitive probes can also be used for other applications using this toolbox (Driesschaert 2012). Indeed, many cellular functions, enzymes and organelles are dependent on the pH and its deregulation is often associated with diseases as chronic heart failure and cancer.

In addition, it would be interesting to compare results with Oroboros experiments which is also able to measure many cellular parameters such as oxygen consumption, redox state, pH and membrane potential using only small amounts of biological samples. This could be done in the future in collaboration with Prof. Mouithys of the Université de Liège.

Also, measuring the impact of our treatments on the redox state of GSH et the oxidation of cysteines in our cell lines through proteomics in order to complete our global view on the cellular redox balance.

2. Perspectives to continue defining the impact of SDHI on mitochondrial function

2.1. Cell lines

Regarding recent warnings about the potential impact of SDHI on human health, it would be interesting to take our project a step further and continue our evaluation on other cell lines. First, it would be more adequate to assess SDHI impact on human primary cell lines. In addition, SDH deficiency is usually associated with neurological impairments with or without muscular involvement (Rustin 1997). It has also been reported to induce encephalopathy and cardiomyopathy in childhood (Brière 2005). This might suggest muscle and central nervous cells could be more susceptible to SDHI exposure. Therefore, we could enlarge our experiments to human muscle cells, cardiomyocytes and neurons.

Finally, because of pesticides' agricultural spreading, SDHI could reach our respiratory system. Analyzing the impact of SDHI on lung cells would therefore make a great addition to this project. It should also be reminded that SDH is a universal component of the mitochondria in any living organisms and that SDHI might impact mitochondrial function of all mammals. Our options regarding cell lines are thereby numerous.

2.2. Cell death assays and ATP production

During our experiments, we investigated whether 1µM SDHI treatment could induce apoptosis on different human cell lines. Although superoxide production was increased in some cases, SDHI treatment was not able to induce apoptosis in all cell lines. It could therefore also be interesting to assess other types of cell death that don't require energy, such as autophagy *via*

Western blotting of LC3 (autophagosome marker) or by monitoring autophagic flux with a fluorescent dye labeling autophagic vacuoles using flow cytometry. Also, cellular ATP production assays were only preformed on HepG2 cells whereas it could be interesting to measure this parameter on the other cell lines. Furthermore, to complete our panel of experiments, the activity of energy sensor AMPK could also be measured after SDHI treatment.

2.3. SDHI choice & cocktail effects

Today, the SDHI family counts more than 20 compounds, binding to the same ubiquinone binding site at the SDH. As discussed earlier, our choice of SDHI was based on previous work made by the team of Rustin (Bénit 2019) which tested 8 SDHI on SDH activity. Among those 8, Bixafen was one of the most potent fungicides to inhibit SDH activity. Although Boscalid did not present the lowest IC_{50} concentrations in humans, it remained still highly relevant to test its impact on human cells given it was supposed to be withdrawn from the market (as well as our crops) in July 2018. Because of fast developing SDHI resistance, operators use different SDHI in cycle, explaining the large panel of existing SDHI and the great need in developing new and more effective SDHI. New generation SDHI (comprising Bixafen, Isopyrazam, Fluopyram and Fluxapyroxad) are also believed to act on CIII of the ETC, which could explain their higher efficiency compared to older generation SDHI. Demonstrating the impact of these SDHI on mitochondrial function would therefore be interesting to support or moderate the mediatic fight against SDHI fungicides and make people more aware of the potential treats linked to their exposure. Along with their significant effect measured on human SDH activity, Isopyrazam and Fluxapyroxad would be excellent candidates to test on human cells after short-term exposure.

Furthermore, fungicidal sprays do not contain just one molecule but are actually made of 2 or more active ingredients together, often strobilurins (e.g. *Pristine* and *Signum* both made with Boscalid + Pyraclostrobin). Like SDHI, strobilurins induce fungi death by inhibiting mitochondrial respiration (Bartlett 2002). This means that we are daily exposed to a multitude of pesticides. In addition, Strobilurins such as Pyraclostrobin are reported to be highly toxic for zebra fish by inducing hepatic oxidative stress (Zhang 2017). They are also able to impact reproduction and growth of *D.Magma* crustacea at environmentally relevant concentrations (Cui 2017). It would therefore also be interesting to treat our different cell lines with a combination

of SDHI and Strobilurin to assess potential "fungicide cocktail" effects on mitochondrial function.

2.4. Repeated SDHI short-term exposures

Another valuable experiment would be to assess SDHI treatment at repeated short-term exposure. Although our current exposure levels of SDHI are still to be quantified, we are however in contact with diverse fungicides daily through contaminated diet or particles in the air. In addition, all these perspectives regarding the assessment of SDHI impact on the mitochondrial function of human cells will continue to be evaluated as part of a master thesis project.

3. Perspectives to confirm statins' potential radiosensitizing effects on cancer

3.1. Effects of statins on different cancer cell lines

To demonstrate statins' potential effect on tumor reoxygenation in prostate cancer, it would be of great interest to repeat our experiments on other prostatic cell lines such as DU145 and LnCaP cells. Also, in the light of studies reporting statins' effect on OCR on other (but normal) cell lines, it still might be possible that statins act on other types of cancer cell types *in vitro* and *in vivo*. These results would clearly raise statins' importance as potential anti-cancer therapy if it could act on diverse cancer types (and regardless of its metabolism). To determine if the impact of statins is metabolic-phenotype dependent, we can evaluate the effect of statins on glycolytic phenotype cells (breast cancer MDA-MB-231 and NT2) and oxidative phenotype cells (cervix cancer SiHa and fibrosarcoma FSaII).

3.2. Effects of statins on tumor growth-delay in vivo

After *in vitro* statin screening, this thesis enabled the identification of 2 statins decreasing significantly the OCR in PC- 3 prostate cancer cells. Both statins were also shown to increase PC-3 tumor reoxygenation around 48-72h treatment at 20mg/kg *in vivo*, with Simvastatin being the most potent to increase tumor pO_2. Based on these findings and ongoing experiment to find the ideal irradiation dose, an irradiation plan has been defined for future experiments. To assess the impact of Simvastatin on tumor response to irradiation, 5 groups of mice will be used: control

group, statin alone, RX alone, RX+statin and an additional group RX+statin with transient interruption of the blood flow at the time of irradiation. The last group will ascribe the contribution of the oxygen effect to the radio sensitizing property of the statin. This experiment's protocol could also be used to assess the effect of other potential oxygen-modulators on tumor growth and response to irradiation. Indeed, with the development of the EPR toolbox, we had the opportunity to test Mito-metformin$_{10}$, a mitochondria-targeted metformin analogue, which was recently demonstrated to decrease OCR, cell proliferation and tumor growth of PDAC cells *in vitro* and *in vivo* (Cheng 2016) at lower concentrations than Metformin. MitoMetformin$_{10}$ was also proven to have radiosensitizing effects on the same cell line *in vitro*. So far, no one assessed this new analogue's effect on tumor response to irradiation *in vivo* after treatment. At our lab, preliminary experiments using MitoMet$_{10}$ have shown to decrease OCR significantly after 24H at 1µM treatment on PC-3 cells (**Fig.26A**). Also, we demonstrated similar effects than statins on tumor reoxygenation in PC-3 tumor bearing mice (**Fig.26B**). Its effect on superoxide production at the same conditions has yet still to be assessed. Using the same mice model and *in vivo* set-up than for the statin project, MitoMet$_{10}$'s efficiency in increasing tumor response to irradiation will also be analyzed. This rising project will soon be taken over by a Master thesis to address MitoMet$_{10}$'s potential use as radiosensitizer in tumor cells.

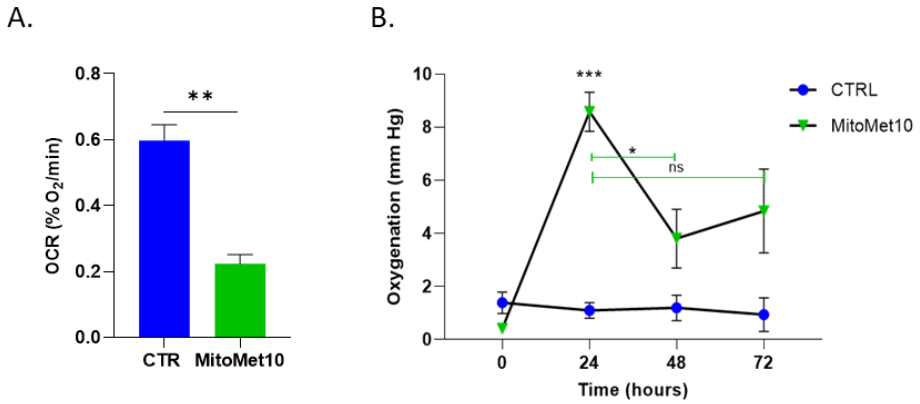

Figure 26: Impact of Mito-metformin$_{10}$ *in vitro* and *in vivo*.

(**A**): Impact of 1µM treatment of Mito-metformin$_{10}$ during 24H on the oxygen consumption rate (OCR) of PC-3 prostate cancer cells using EPR-oximetry. Bars represent means ± SEM (%O_2/min), (**) p<0.01, Student T-test, N=3.

(**B**) Effect of daily treatment with Mito-metformin$_{10}$ (2 mg/kg) on PC-3 prostate tumor oxygenation as measured by EPR oximetry: Dots represent mean (mm Hg), (*) p< 0.05, (***) p< 0.001, Two-way ANOVA, N=4.

3.3. Mechanism of action behind statins' impact on OCR in vitro

Our findings that different statins have a differential impact on the OCR of PC-3 cells could suggest that their mechanism of action is not mediated by inhibition of cholesterol synthesis. However, those differences can be due to the presence or absence of the statins' transporters at the cell membrane. To address this question, western blots can be performed to measure the presence of these transporters in our cell lines. Also, working on permeabilized cells could bypass this potential entry limitation to assess the statins' impact on OCR. In addition, it would be interesting to carry out reversibility experiments like performed by Feron (Feron 2001). Indeed, the addition of ubiquinone or cholesterol in the media of control and statin-treated cells could inform us whether statins act on OCR by decreasing ubiquinol synthesis or by inhibiting respiratory complexes directly. Statins' inhibitory effects on mitochondrial respiratory chain enzymatic activities can also be investigated later on using spectrophotometry.

3.4. Mechanism of action behind statins' impact on tumor oxygenation

One of our hypotheses is that statin may increase the oxygenation and radiosensitivity through the activation of eNOS. Indeed, by decreasing caveoline-1 expression in endothelial cells, statins are able to promote NO production (Feron 2001). Insulin infusions activating eNOS were also demonstrated to be responsible for an increase in tumor oxygenation and an increase in response to irradiation (Jordan 2002). In addition, nitric oxide has intrinsic radiosensitizing properties that may add to the oxygen effect (Jordan 2004). Changes of tumor oxygenation during our *in vivo* experiments may therefore be due to the statins' pleiotropic effect on NO-dependent impact on the mitochondrial respiration (NO inhibits complex IV). To address this question, statin-treated or control tumors can be homogenized and processed for eNOS phosphorylation quantification with immunoblotting. Using EPR oximetry, injecting a NOS inhibitor (L-NAME) before statin treatment could also evaluate NO-dependent reoxygenation. If these results suggest a role of NOS, tumors bearing eNOS knock-out (KO, -/-) and wild type (WT, +/+) mice could be used to validate or invalidate the role of eNOS in the effect of statins on tumor oxygenation and response to irradiation. Finally, due to NO vasorelaxant properties, tumor perfusion can also be investigated using Dynamic contrast-enhanced MRI (Fruytier 2014).

Bibliography

Abbas, K., N. Babic, and F. Peyrot. "Use of Spin Traps to Detect Superoxide Production in Living Cells by Electron Paramagnetic Resonance (Epr) Spectroscopy." *Methods* 109 (Oct 15 2016): 31-43. https://doi.org/10.1016/j.ymeth.2016.05.001. https://www.ncbi.nlm.nih.gov/pubmed/27163864.

Abbas, K., M. Hardy, F. Poulhes, H. Karoui, P. Tordo, O. Ouari, and F. Peyrot. "Detection of Superoxide Production in Stimulated and Unstimulated Living Cells Using New Cyclic Nitrone Spin Traps." *Free Radic Biol Med* 71 (Jun 2014): 281-90. https://doi.org/10.1016/j.freeradbiomed.2014.03.019. https://www.ncbi.nlm.nih.gov/pubmed/24662195.

Albayrak, T., V. Scherhammer, N. Schoenfeld, E. Braziulis, T. Mund, M. K. Bauer, I. E. Scheffler, and S. Grimm. "The Tumor Suppressor Cybl, a Component of the Respiratory Chain, Mediates Apoptosis Induction." *Mol Biol Cell* 14, no. 8 (Aug 2003): 3082-96. https://doi.org/10.1091/mbc.e02-10-0631. https://www.ncbi.nlm.nih.gov/pubmed/12925748.

Albert, M. A., E. Danielson, N. Rifai, P. M. Ridker, and Prince Investigators. "Effect of Statin Therapy on C-Reactive Protein Levels: The Pravastatin Inflammation/Crp Evaluation (Prince): A Randomized Trial and Cohort Study." *JAMA* 286, no. 1 (Jul 4 2001): 64-70. https://doi.org/10.1001/jama.286.1.64. https://www.ncbi.nlm.nih.gov/pubmed/11434828.

Alberts, A. W., J. Chen, G. Kuron, V. Hunt, J. Huff, C. Hoffman, J. Rothrock*, et al.* "Mevinolin: A Highly Potent Competitive Inhibitor of Hydroxymethylglutaryl-Coenzyme a Reductase and a Cholesterol-Lowering Agent." *Proc Natl Acad Sci U S A* 77, no. 7 (Jul 1980): 3957-61. https://doi.org/10.1073/pnas.77.7.3957. https://www.ncbi.nlm.nih.gov/pubmed/6933445.

Alexi, T., P. E. Hughes, R. L. Faull, and C. E. Williams. "3-Nitropropionic Acid's Lethal Triplet: Cooperative Pathways of Neurodegeneration." *Neuroreport* 9, no. 11 (Aug 3 1998): R57-64. https://doi.org/10.1097/00001756-199808030-00001. https://www.ncbi.nlm.nih.gov/pubmed/9721909.

Ansiaux, R., C. Baudelet, B. F. Jordan, N. Crokart, P. Martinive, J. DeWever, V. Gregoire, O. Feron, and B. Gallez. "Mechanism of Reoxygenation after Antiangiogenic Therapy Using Su5416 and Its Importance for Guiding Combined Antitumor Therapy." *Cancer Res* 66, no. 19 (Oct 1 2006): 9698-704. https://doi.org/10.1158/0008-5472.CAN-06-1854. https://www.ncbi.nlm.nih.gov/pubmed/17018628.

Aviram, M., M. Rosenblat, C. L. Bisgaier, and R. S. Newton. "Atorvastatin and Gemfibrozil Metabolites, but Not the Parent Drugs, Are Potent Antioxidants against Lipoprotein Oxidation." *Atherosclerosis* 138, no. 2 (Jun 1998): 271-80. https://doi.org/10.1016/s0021-9150(98)00032-x. https://www.ncbi.nlm.nih.gov/pubmed/9690910.

Bacic, G., I. Spasojevic, B. Secerov, and M. Mojovic. "Spin-Trapping of Oxygen Free Radicals in Chemical and Biological Systems: New Traps, Radicals and Possibilities." *Spectrochim Acta A Mol Biomol Spectrosc* 69, no. 5 (May 2008): 1354-66. https://doi.org/10.1016/j.saa.2007.09.047. https://www.ncbi.nlm.nih.gov/pubmed/18255335.

Bailey, C. J. "Metformin: Effects on Micro and Macrovascular Complications in Type 2 Diabetes." *Cardiovasc Drugs Ther* 22, no. 3 (Jun 2008): 215-24. https://doi.org/10.1007/s10557-008-6092-0. https://www.ncbi.nlm.nih.gov/pubmed/18288595.

Bakalova, R., E. Georgieva, D. Ivanova, Z. Zhelev, I. Aoki, and T. Saga. "Magnetic Resonance Imaging of Mitochondrial Dysfunction and Metabolic Activity, Accompanied by Overproduction of Superoxide." *ACS Chem Neurosci* 6, no. 12 (Dec 16 2015): 1922-9. https://doi.org/10.1021/acschemneuro.5b00220. https://www.ncbi.nlm.nih.gov/pubmed/26367059.

Barnes, P. J. "Future Treatments for Chronic Obstructive Pulmonary Disease and Its Comorbidities." *Proc Am Thorac Soc* 5, no. 8 (Dec 1 2008): 857-64. https://doi.org/10.1513/pats.200807-069TH. https://www.ncbi.nlm.nih.gov/pubmed/19017741.

Baysal, B. E., W. S. Rubinstein, and P. E. Taschner. "Phenotypic Dichotomy in Mitochondrial Complex Ii Genetic Disorders." *J Mol Med (Berl)* 79, no. 9 (Sep 2001): 495-503. https://doi.org/10.1007/s001090100267. https://www.ncbi.nlm.nih.gov/pubmed/11692162.

Beckman, J. S., R. L. Minor, Jr., C. W. White, J. E. Repine, G. M. Rosen, and B. A. Freeman. "Superoxide Dismutase and Catalase Conjugated to Polyethylene Glycol Increases Endothelial Enzyme Activity and Oxidant Resistance." *J Biol Chem* 263, no. 14 (May 15 1988): 6884-92. https://www.ncbi.nlm.nih.gov/pubmed/3129432.

Bedard, K., and K. H. Krause. "The Nox Family of Ros-Generating Nadph Oxidases: Physiology and Pathophysiology." *Physiol Rev* 87, no. 1 (Jan 2007): 245-313. https://doi.org/10.1152/physrev.00044.2005. https://www.ncbi.nlm.nih.gov/pubmed/17237347.

Benit, P., A. Kahn, D. Chretien, S. Bortoli, L. Huc, M. Schiff, A. P. Gimenez-Roqueplo*, et al.* "Evolutionarily Conserved Susceptibility of the Mitochondrial Respiratory Chain to Sdhi Pesticides and Its Consequence on the Impact of Sdhis on Human Cultured Cells." *PLoS One* 14, no. 11 (2019): e0224132. https://doi.org/10.1371/journal.pone.0224132. https://www.ncbi.nlm.nih.gov/pubmed/31697708.

Bennett, M. C., G. W. Mlady, Y. H. Kwon, and G. M. Rose. "Chronic in Vivo Sodium Azide Infusion Induces Selective and Stable Inhibition of Cytochrome C Oxidase." *J Neurochem* 66, no. 6 (Jun 1996): 2606-11. https://doi.org/10.1046/j.1471-4159.1996.66062606.x. https://www.ncbi.nlm.nih.gov/pubmed/8632188.

Berndt, N., A. D. Hamilton, and S. M. Sebti. "Targeting Protein Prenylation for Cancer Therapy." *Nat Rev Cancer* 11, no. 11 (Oct 24 2011): 775-91. https://doi.org/10.1038/nrc3151. https://www.ncbi.nlm.nih.gov/pubmed/22020205.

Birben, E., U. M. Sahiner, C. Sackesen, S. Erzurum, and O. Kalayci. "Oxidative Stress and Antioxidant Defense." *World Allergy Organ J* 5, no. 1 (Jan 2012): 9-19. https://doi.org/10.1097/WOX.0b013e3182439613. https://www.ncbi.nlm.nih.gov/pubmed/23268465.

Bonetta, R. "Potential Therapeutic Applications of Mnsods and Sod-Mimetics." *Chemistry* 24, no. 20 (Apr 6 2018): 5032-41. https://doi.org/10.1002/chem.201704561. https://www.ncbi.nlm.nih.gov/pubmed/29131419.

Boveris, A., and E. Cadenas. "Mitochondrial Production of Superoxide Anions and Its Relationship to the Antimycin Insensitive Respiration." *FEBS Lett* 54, no. 3 (Jul 1 1975): 311-4. https://doi.org/10.1016/0014-5793(75)80928-8. https://www.ncbi.nlm.nih.gov/pubmed/236930.

Branchi, A., A. M. Fiorenza, A. Rovellini, A. Torri, F. Muzio, S. Macor, and D. Sommariva. "Lowering Effects of Four Different Statins on Serum Triglyceride Level." *Eur J Clin*

Pharmacol 55, no. 7 (Sep 1999): 499-502. https://doi.org/10.1007/s002280050663. https://www.ncbi.nlm.nih.gov/pubmed/10501818.

Brand, M. D. "Mitochondrial Generation of Superoxide and Hydrogen Peroxide as the Source of Mitochondrial Redox Signaling." *Free Radic Biol Med* 100 (Nov 2016): 14-31. https://doi.org/10.1016/j.freeradbiomed.2016.04.001. https://www.ncbi.nlm.nih.gov/pubmed/27085844.

———. "The Sites and Topology of Mitochondrial Superoxide Production." *Exp Gerontol* 45, no. 7-8 (Aug 2010): 466-72. https://doi.org/10.1016/j.exger.2010.01.003. https://www.ncbi.nlm.nih.gov/pubmed/20064600.

Bridges, H. R., A. J. Jones, M. N. Pollak, and J. Hirst. "Effects of Metformin and Other Biguanides on Oxidative Phosphorylation in Mitochondria." *Biochem J* 462, no. 3 (Sep 15 2014): 475-87. https://doi.org/10.1042/BJ20140620. https://www.ncbi.nlm.nih.gov/pubmed/25017630.

Brieger, K., S. Schiavone, F. J. Miller, Jr., and K. H. Krause. "Reactive Oxygen Species: From Health to Disease." *Swiss Med Wkly* 142 (2012): w13659. https://doi.org/10.4414/smw.2012.13659. https://www.ncbi.nlm.nih.gov/pubmed/22903797.

Briere, J. J., J. Favier, V. El Ghouzzi, F. Djouadi, P. Benit, A. P. Gimenez, and P. Rustin. "Succinate Dehydrogenase Deficiency in Human." *Cell Mol Life Sci* 62, no. 19-20 (Oct 2005): 2317-24. https://doi.org/10.1007/s00018-005-5237-6. https://www.ncbi.nlm.nih.gov/pubmed/16143825.

Brouet, A., P. Sonveaux, C. Dessy, S. Moniotte, J. L. Balligand, and O. Feron. "Hsp90 and Caveolin Are Key Targets for the Proangiogenic Nitric Oxide-Mediated Effects of Statins." *Circ Res* 89, no. 10 (Nov 9 2001): 866-73. https://doi.org/10.1161/hh2201.100319. https://www.ncbi.nlm.nih.gov/pubmed/11701613.

Brouillet, E. "The 3-Np Model of Striatal Neurodegeneration." *Curr Protoc Neurosci* 67 (Apr 10 2014): 9 48 1-14. https://doi.org/10.1002/0471142301.ns0948s67. https://www.ncbi.nlm.nih.gov/pubmed/24723322.

Brown, G. C., and V. Borutaite. "Nitric Oxide, Cytochrome C and Mitochondria." *Biochem Soc Symp* 66 (1999): 17-25. https://doi.org/10.1042/bss0660017. https://www.ncbi.nlm.nih.gov/pubmed/10989653.

Brown, M., C. Hart, T. Tawadros, V. Ramani, V. Sangar, M. Lau, and N. Clarke. "The Differential Effects of Statins on the Metastatic Behaviour of Prostate Cancer." *Br J Cancer* 106, no. 10 (May 8 2012): 1689-96. https://doi.org/10.1038/bjc.2012.138. https://www.ncbi.nlm.nih.gov/pubmed/22531631.

Brunmair, B., K. Staniek, F. Gras, N. Scharf, A. Althaym, R. Clara, M. Roden, *et al.* "Thiazolidinediones, Like Metformin, Inhibit Respiratory Complex I: A Common Mechanism Contributing to Their Antidiabetic Actions?". *Diabetes* 53, no. 4 (Apr 2004): 1052-9. https://doi.org/10.2337/diabetes.53.4.1052. https://www.ncbi.nlm.nih.gov/pubmed/15047621.

Buranrat, B., L. Senggunprai, A. Prawan, and V. Kukongviriyapan. "Simvastatin and Atorvastatin as Inhibitors of Proliferation and Inducers of Apoptosis in Human Cholangiocarcinoma Cells." *Life Sci* 153 (May 15 2016): 41-9. https://doi.org/10.1016/j.lfs.2016.04.018. https://www.ncbi.nlm.nih.gov/pubmed/27098189.

Caboni, P., T. B. Sherer, N. Zhang, G. Taylor, H. M. Na, J. T. Greenamyre, and J. E. Casida. "Rotenone, Deguelin, Their Metabolites, and the Rat Model of Parkinson's Disease."

Chem Res Toxicol 17, no. 11 (Nov 2004): 1540-8. https://doi.org/10.1021/tx049867r. https://www.ncbi.nlm.nih.gov/pubmed/15540952.

Cafforio, P., F. Dammacco, A. Gernone, and F. Silvestris. "Statins Activate the Mitochondrial Pathway of Apoptosis in Human Lymphoblasts and Myeloma Cells." *Carcinogenesis* 26, no. 5 (May 2005): 883-91. https://doi.org/10.1093/carcin/bgi036. https://www.ncbi.nlm.nih.gov/pubmed/15705602.

Cai, W. Y., Y. Zhuang, F. Yan, T. Li, W. T. Song, and J. H. Sun. "Effect of Survivin Downregulation by Simvastatin on the Growth and Invasion of Salivary Adenoid Cystic Carcinoma." *Mol Med Rep* 18, no. 2 (Aug 2018): 1939-46. https://doi.org/10.3892/mmr.2018.9204. https://www.ncbi.nlm.nih.gov/pubmed/29956779.

Carbone, F., L. Liberale, A. Bonaventura, M. Cea, and F. Montecucco. "Targeting Inflammation in Primary Cardiovascular Prevention." *Curr Pharm Des* 22, no. 37 (2016): 5662-75. https://doi.org/10.2174/1381612822666160822124546. https://www.ncbi.nlm.nih.gov/pubmed/27549380.

Carnicer, R., M. J. Crabtree, V. Sivakumaran, B. Casadei, and D. A. Kass. "Nitric Oxide Synthases in Heart Failure." *Antioxid Redox Signal* 18, no. 9 (Mar 20 2013): 1078-99. https://doi.org/10.1089/ars.2012.4824. https://www.ncbi.nlm.nih.gov/pubmed/22871241.

Cayir, A., M. Coskun, and M. Coskun. "Micronuclei, Nucleoplasmic Bridges, and Nuclear Buds Induced in Human Lymphocytes by the Fungicide Signum and Its Active Ingredients (Boscalid and Pyraclostrobin)." *Environ Toxicol* 29, no. 7 (May 2014): 723-32. https://doi.org/10.1002/tox.21789. https://www.ncbi.nlm.nih.gov/pubmed/22730168.

Cecchini, G. "Function and Structure of Complex Ii of the Respiratory Chain." *Annu Rev Biochem* 72 (2003): 77-109. https://doi.org/10.1146/annurev.biochem.72.121801.161700. https://www.ncbi.nlm.nih.gov/pubmed/14527321.

Chai, Y. C., S. S. Ashraf, K. Rokutan, R. B. Johnston, Jr., and J. A. Thomas. "S-Thiolation of Individual Human Neutrophil Proteins Including Actin by Stimulation of the Respiratory Burst: Evidence against a Role for Glutathione Disulfide." *Arch Biochem Biophys* 310, no. 1 (Apr 1994): 273-81. https://doi.org/10.1006/abbi.1994.1167. https://www.ncbi.nlm.nih.gov/pubmed/8161216.

Chan, A. Y., S. J. Coniglio, Y. Y. Chuang, D. Michaelson, U. G. Knaus, M. R. Philips, and M. Symons. "Roles of the Rac1 and Rac3 Gtpases in Human Tumor Cell Invasion." *Oncogene* 24, no. 53 (Nov 24 2005): 7821-9. https://doi.org/10.1038/sj.onc.1208909. https://www.ncbi.nlm.nih.gov/pubmed/16027728.

Chandel, N. S., E. Maltepe, E. Goldwasser, C. E. Mathieu, M. C. Simon, and P. T. Schumacker. "Mitochondrial Reactive Oxygen Species Trigger Hypoxia-Induced Transcription." *Proc Natl Acad Sci U S A* 95, no. 20 (Sep 29 1998): 11715-20. https://doi.org/10.1073/pnas.95.20.11715. https://www.ncbi.nlm.nih.gov/pubmed/9751731.

Chandel, N. S., D. S. McClintock, C. E. Feliciano, T. M. Wood, J. A. Melendez, A. M. Rodriguez, and P. T. Schumacker. "Reactive Oxygen Species Generated at Mitochondrial Complex Iii Stabilize Hypoxia-Inducible Factor-1alpha During Hypoxia: A Mechanism of O2 Sensing." *J Biol Chem* 275, no. 33 (Aug 18 2000): 25130-8. https://doi.org/10.1074/jbc.M001914200. https://www.ncbi.nlm.nih.gov/pubmed/10833514.

Chen, M., H. Li, and Y. Wang. "Protection by Atorvastatin Pretreatment in Patients Undergoing Primary Percutaneous Coronary Intervention Is Associated with the Lower Levels of Oxygen Free Radicals." *J Cardiovasc Pharmacol* 62, no. 3 (Sep 2013): 320-4. https://doi.org/10.1097/FJC.0b013e31829be05b. https://www.ncbi.nlm.nih.gov/pubmed/23714773.

Chen, Y., E. McMillan-Ward, J. Kong, S. J. Israels, and S. B. Gibson. "Oxidative Stress Induces Autophagic Cell Death Independent of Apoptosis in Transformed and Cancer Cells." *Cell Death Differ* 15, no. 1 (Jan 2008): 171-82. https://doi.org/10.1038/sj.cdd.4402233. https://www.ncbi.nlm.nih.gov/pubmed/17917680.

Cheng, G., J. Zielonka, O. Ouari, M. Lopez, D. McAllister, K. Boyle, C. S. Barrios, *et al.* "Mitochondria-Targeted Analogues of Metformin Exhibit Enhanced Antiproliferative and Radiosensitizing Effects in Pancreatic Cancer Cells." *Cancer Res* 76, no. 13 (Jul 1 2016): 3904-15. https://doi.org/10.1158/0008-5472.CAN-15-2534. https://www.ncbi.nlm.nih.gov/pubmed/27216187.

Cholesterol Treatment Trialists, Collaboration, C. Baigent, L. Blackwell, J. Emberson, L. E. Holland, C. Reith, N. Bhala, *et al.* "Efficacy and Safety of More Intensive Lowering of Ldl Cholesterol: A Meta-Analysis of Data from 170,000 Participants in 26 Randomised Trials." *Lancet* 376, no. 9753 (Nov 13 2010): 1670-81. https://doi.org/10.1016/S0140-6736(10)61350-5. https://www.ncbi.nlm.nih.gov/pubmed/21067804.

Cholesterol Treatment Trialists, Collaborators, B. Mihaylova, J. Emberson, L. Blackwell, A. Keech, J. Simes, E. H. Barnes, *et al.* "The Effects of Lowering Ldl Cholesterol with Statin Therapy in People at Low Risk of Vascular Disease: Meta-Analysis of Individual Data from 27 Randomised Trials." *Lancet* 380, no. 9841 (Aug 11 2012): 581-90. https://doi.org/10.1016/S0140-6736(12)60367-5. https://www.ncbi.nlm.nih.gov/pubmed/22607822.

Chopra, V., P. U. Choksi, and E. Cavusoglu. "Beyond Lipid Lowering: The Anti-Hypertensive Role of Statins." *Cardiovasc Drugs Ther* 21, no. 3 (Jun 2007): 161-9. https://doi.org/10.1007/s10557-007-6025-3. https://www.ncbi.nlm.nih.gov/pubmed/17468937.

Circu, M. L., and T. Y. Aw. "Reactive Oxygen Species, Cellular Redox Systems, and Apoptosis." *Free Radic Biol Med* 48, no. 6 (Mar 15 2010): 749-62. https://doi.org/10.1016/j.freeradbiomed.2009.12.022. https://www.ncbi.nlm.nih.gov/pubmed/20045723.

Colliez, F., B. Gallez, and B. F. Jordan. "Assessing Tumor Oxygenation for Predicting Outcome in Radiation Oncology: A Review of Studies Correlating Tumor Hypoxic Status and Outcome in the Preclinical and Clinical Settings." *Front Oncol* 7 (2017): 10. https://doi.org/10.3389/fonc.2017.00010. https://www.ncbi.nlm.nih.gov/pubmed/28180110.

Conley, K. E., S. A. Jubrias, and P. C. Esselman. "Oxidative Capacity and Ageing in Human Muscle." *J Physiol* 526 Pt 1 (Jul 1 2000): 203-10. https://doi.org/10.1111/j.1469-7793.2000.t01-1-00203.x. https://www.ncbi.nlm.nih.gov/pubmed/10878112.

Crokart, N., B. F. Jordan, C. Baudelet, R. Ansiaux, P. Sonveaux, V. Gregoire, N. Beghein, *et al.* "Early Reoxygenation in Tumors after Irradiation: Determining Factors and Consequences for Radiotherapy Regimens Using Daily Multiple Fractions." *Int J Radiat Oncol Biol Phys* 63, no. 3 (Nov 1 2005): 901-10.

https://doi.org/10.1016/j.ijrobp.2005.02.038.
https://www.ncbi.nlm.nih.gov/pubmed/16199320.

Crokart, N., B. F. Jordan, C. Baudelet, G. O. Cron, J. Hotton, K. Radermacher, V. Gregoire, *et al.* "Glucocorticoids Modulate Tumor Radiation Response through a Decrease in Tumor Oxygen Consumption." *Clin Cancer Res* 13, no. 2 Pt 1 (Jan 15 2007): 630-5. https://doi.org/10.1158/1078-0432.CCR-06-0802.
https://www.ncbi.nlm.nih.gov/pubmed/17255286.

Crokart, N., K. Radermacher, B. F. Jordan, C. Baudelet, G. O. Cron, V. Gregoire, N. Beghein, *et al.* "Tumor Radiosensitization by Antiinflammatory Drugs: Evidence for a New Mechanism Involving the Oxygen Effect." *Cancer Res* 65, no. 17 (Sep 1 2005): 7911-6. https://doi.org/10.1158/0008-5472.CAN-05-1288.
https://www.ncbi.nlm.nih.gov/pubmed/16140962.

Cui, F., T. Chai, X. Liu, and C. Wang. "Toxicity of Three Strobilurins (Kresoxim-Methyl, Pyraclostrobin, and Trifloxystrobin) on Daphnia Magna." *Environ Toxicol Chem* 36, no. 1 (Jan 2017): 182-89. https://doi.org/10.1002/etc.3520.
https://www.ncbi.nlm.nih.gov/pubmed/27283376.

d'Hose, D., P. Danhier, H. Northshield, P. Isenborghs, B. F. Jordan, and B. Gallez. "A Versatile Epr Toolbox for the Simultaneous Measurement of Oxygen Consumption and Superoxide Production." *Redox Biol* 40 (Apr 2021): 101852. https://doi.org/10.1016/j.redox.2020.101852.
https://www.ncbi.nlm.nih.gov/pubmed/33418140.

Dahia, P. L., K. N. Ross, M. E. Wright, C. Y. Hayashida, S. Santagata, M. Barontini, A. L. Kung, *et al.* "A Hif1alpha Regulatory Loop Links Hypoxia and Mitochondrial Signals in Pheochromocytomas." *PLoS Genet* 1, no. 1 (Jul 2005): 72-80. https://doi.org/10.1371/journal.pgen.0010008.
https://www.ncbi.nlm.nih.gov/pubmed/16103922.

Dalla Pozza, E., I. Dando, R. Pacchiana, E. Liboi, M. T. Scupoli, M. Donadelli, and M. Palmieri. "Regulation of Succinate Dehydrogenase and Role of Succinate in Cancer." *Semin Cell Dev Biol* 98 (Feb 2020): 4-14. https://doi.org/10.1016/j.semcdb.2019.04.013.
https://www.ncbi.nlm.nih.gov/pubmed/31039394.

Danhier, P., T. Copetti, G. De Preter, P. Leveque, O. Feron, B. F. Jordan, P. Sonveaux, and B. Gallez. "Influence of Cell Detachment on the Respiration Rate of Tumor and Endothelial Cells." *PLoS One* 8, no. 1 (2013): e53324. https://doi.org/10.1371/journal.pone.0053324.
https://www.ncbi.nlm.nih.gov/pubmed/23382841.

Dastoor, Z., and J. L. Dreyer. "Potential Role of Nuclear Translocation of Glyceraldehyde-3-Phosphate Dehydrogenase in Apoptosis and Oxidative Stress." *J Cell Sci* 114, no. Pt 9 (May 2001): 1643-53. https://www.ncbi.nlm.nih.gov/pubmed/11309196.

David, A., C. Botias, A. Abdul-Sada, E. Nicholls, E. L. Rotheray, E. M. Hill, and D. Goulson. "Widespread Contamination of Wildflower and Bee-Collected Pollen with Complex Mixtures of Neonicotinoids and Fungicides Commonly Applied to Crops." *Environ Int* 88 (Mar 2016): 169-78. https://doi.org/10.1016/j.envint.2015.12.011.
https://www.ncbi.nlm.nih.gov/pubmed/26760714.

Davignon, J., and P. Ganz. "Role of Endothelial Dysfunction in Atherosclerosis." *Circulation* 109, no. 23 Suppl 1 (Jun 15 2004): III27-32. https://doi.org/10.1161/01.CIR.0000131515.03336.f8.
https://www.ncbi.nlm.nih.gov/pubmed/15198963.

De Preter, G., C. Deriemaeker, P. Danhier, L. Brisson, T. T. Cao Pham, V. Gregoire, B. F. Jordan, P. Sonveaux, and B. Gallez. "A Fast Hydrogen Sulfide-Releasing Donor Increases the Tumor Response to Radiotherapy." *Mol Cancer Ther* 15, no. 1 (Jan 2016): 154-61. https://doi.org/10.1158/1535-7163.MCT-15-0691-T. https://www.ncbi.nlm.nih.gov/pubmed/26682572.

de Vries, H. E., M. Witte, D. Hondius, A. J. Rozemuller, B. Drukarch, J. Hoozemans, and J. van Horssen. "Nrf2-Induced Antioxidant Protection: A Promising Target to Counteract Ros-Mediated Damage in Neurodegenerative Disease?". *Free Radic Biol Med* 45, no. 10 (Nov 15 2008): 1375-83. https://doi.org/10.1016/j.freeradbiomed.2008.09.001. https://www.ncbi.nlm.nih.gov/pubmed/18824091.

DeBerardinis, R. J., and N. S. Chandel. "Fundamentals of Cancer Metabolism." *Sci Adv* 2, no. 5 (May 2016): e1600200. https://doi.org/10.1126/sciadv.1600200. https://www.ncbi.nlm.nih.gov/pubmed/27386546.

Degli Esposti, M. "Inhibitors of Nadh-Ubiquinone Reductase: An Overview." *Biochim Biophys Acta* 1364, no. 2 (May 6 1998): 222-35. https://doi.org/10.1016/s0005-2728(98)00029-2. https://www.ncbi.nlm.nih.gov/pubmed/9593904.

Dekeyser, M. A. "Acaricide Mode of Action." *Pest Manag Sci* 61, no. 2 (Feb 2005): 103-10. https://doi.org/10.1002/ps.994. https://www.ncbi.nlm.nih.gov/pubmed/15625668.

DeLeo, F. R., and M. T. Quinn. "Assembly of the Phagocyte Nadph Oxidase: Molecular Interaction of Oxidase Proteins." *J Leukoc Biol* 60, no. 6 (Dec 1996): 677-91. https://doi.org/10.1002/jlb.60.6.677. https://www.ncbi.nlm.nih.gov/pubmed/8975869.

Demine, S., P. Renard, and T. Arnould. "Mitochondrial Uncoupling: A Key Controller of Biological Processes in Physiology and Diseases." *Cells* 8, no. 8 (Jul 30 2019). https://doi.org/10.3390/cells8080795. https://www.ncbi.nlm.nih.gov/pubmed/31366145.

Desmet, C. M., G. Vandermeulen, C. Bouzin, M. C. Lam, V. Preat, P. Leveque, and B. Gallez. "Epr Monitoring of Wound Oxygenation as a Biomarker of Response to Gene Therapy Encoding Hcap-18/Ll37 Peptide." *Magn Reson Med* 79, no. 6 (Jun 2018): 3267-73. https://doi.org/10.1002/mrm.26956. https://www.ncbi.nlm.nih.gov/pubmed/28983954.

Dhani, N., A. Fyles, D. Hedley, and M. Milosevic. "The Clinical Significance of Hypoxia in Human Cancers." *Semin Nucl Med* 45, no. 2 (Mar 2015): 110-21. https://doi.org/10.1053/j.semnuclmed.2014.11.002. https://www.ncbi.nlm.nih.gov/pubmed/25704384.

Di Napoli, P., A. Antonio Taccardi, A. Grilli, R. Spina, M. Felaco, A. Barsotti, and R. De Caterina. "Simvastatin Reduces Reperfusion Injury by Modulating Nitric Oxide Synthase Expression: An Ex Vivo Study in Isolated Working Rat Hearts." *Cardiovasc Res* 51, no. 2 (Aug 1 2001): 283-93. https://doi.org/10.1016/s0008-6363(01)00306-6. https://www.ncbi.nlm.nih.gov/pubmed/11470468.

Di Napoli, P., A. A. Taccardi, A. Grilli, M. A. De Lutiis, A. Barsotti, M. Felaco, and R. De Caterina. "Chronic Treatment with Rosuvastatin Modulates Nitric Oxide Synthase Expression and Reduces Ischemia-Reperfusion Injury in Rat Hearts." *Cardiovasc Res* 66, no. 3 (Jun 1 2005): 462-71. https://doi.org/10.1016/j.cardiores.2005.02.008. https://www.ncbi.nlm.nih.gov/pubmed/15914111.

Dickinson, B. C., and C. J. Chang. "Chemistry and Biology of Reactive Oxygen Species in Signaling or Stress Responses." *Nat Chem Biol* 7, no. 8 (Jul 18 2011): 504-11.

https://doi.org/10.1038/nchembio.607.
https://www.ncbi.nlm.nih.gov/pubmed/21769097.

Diepart, C., B. F. Jordan, and B. Gallez. "A New Epr Oximetry Protocol to Estimate the Tissue Oxygen Consumption in Vivo." *Radiat Res* 172, no. 2 (Aug 2009): 220-5. https://doi.org/10.1667/RR1448.1.
https://www.ncbi.nlm.nih.gov/pubmed/19630526.

Diepart, C., O. Karroum, J. Magat, O. Feron, J. Verrax, P. B. Calderon, V. Gregoire*, et al.* "Arsenic Trioxide Treatment Decreases the Oxygen Consumption Rate of Tumor Cells and Radiosensitizes Solid Tumors." *Cancer Res* 72, no. 2 (Jan 15 2012): 482-90. https://doi.org/10.1158/0008-5472.CAN-11-1755.
https://www.ncbi.nlm.nih.gov/pubmed/22139377.

Diepart, C., J. Verrax, P. B. Calderon, O. Feron, B. F. Jordan, and B. Gallez. "Comparison of Methods for Measuring Oxygen Consumption in Tumor Cells in Vitro." *Anal Biochem* 396, no. 2 (Jan 15 2010): 250-6. https://doi.org/10.1016/j.ab.2009.09.029.
https://www.ncbi.nlm.nih.gov/pubmed/19766582.

Dikalov, S. I., and D. G. Harrison. "Methods for Detection of Mitochondrial and Cellular Reactive Oxygen Species." *Antioxid Redox Signal* 20, no. 2 (Jan 10 2014): 372-82. https://doi.org/10.1089/ars.2012.4886.
https://www.ncbi.nlm.nih.gov/pubmed/22978713.

Dikalov, S. I., I. A. Kirilyuk, M. Voinov, and I. A. Grigor'ev. "Epr Detection of Cellular and Mitochondrial Superoxide Using Cyclic Hydroxylamines." *Free Radic Res* 45, no. 4 (Apr 2011): 417-30. https://doi.org/10.3109/10715762.2010.540242.
https://www.ncbi.nlm.nih.gov/pubmed/21128732.

Dikalov, S. I., W. Li, P. Mehranpour, S. S. Wang, and A. M. Zafari. "Production of Extracellular Superoxide by Human Lymphoblast Cell Lines: Comparison of Electron Spin Resonance Techniques and Cytochrome C Reduction Assay." *Biochem Pharmacol* 73, no. 7 (Apr 1 2007): 972-80. https://doi.org/10.1016/j.bcp.2006.12.012.
https://www.ncbi.nlm.nih.gov/pubmed/17222393.

Dikalov, S. I., Y. F. Polienko, and I. Kirilyuk. "Electron Paramagnetic Resonance Measurements of Reactive Oxygen Species by Cyclic Hydroxylamine Spin Probes." *Antioxid Redox Signal* 28, no. 15 (May 20 2018): 1433-43. https://doi.org/10.1089/ars.2017.7396.
https://www.ncbi.nlm.nih.gov/pubmed/29037084.

Dikalov, S., U. Landmesser, and D. G. Harrison. "Geldanamycin Leads to Superoxide Formation by Enzymatic and Non-Enzymatic Redox Cycling. Implications for Studies of Hsp90 and Endothelial Cell Nitric-Oxide Synthase." *J Biol Chem* 277, no. 28 (Jul 12 2002): 25480-5. https://doi.org/10.1074/jbc.M203271200.
https://www.ncbi.nlm.nih.gov/pubmed/11983711.

Distelmaier, F., H. J. Visch, J. A. Smeitink, E. Mayatepek, W. J. Koopman, and P. H. Willems. "The Antioxidant Trolox Restores Mitochondrial Membrane Potential and Ca2+ -Stimulated Atp Production in Human Complex I Deficiency." *J Mol Med (Berl)* 87, no. 5 (May 2009): 515-22. https://doi.org/10.1007/s00109-009-0452-5.
https://www.ncbi.nlm.nih.gov/pubmed/19255735.

Divakaruni, A. S., G. W. Rogers, and A. N. Murphy. "Measuring Mitochondrial Function in Permeabilized Cells Using the Seahorse Xf Analyzer or a Clark-Type Oxygen Electrode." *Curr Protoc Toxicol* 60 (May 27 2014): 25 2 1-16. https://doi.org/10.1002/0471140856.tx2502s60.
https://www.ncbi.nlm.nih.gov/pubmed/24865646.

Donato, M. T., L. Tolosa, and M. J. Gomez-Lechon. "Culture and Functional Characterization of Human Hepatoma Hepg2 Cells." *Methods Mol Biol* 1250 (2015): 77-93. https://doi.org/10.1007/978-1-4939-2074-7_5. https://www.ncbi.nlm.nih.gov/pubmed/26272135.

Dong, L. F., R. Freeman, J. Liu, R. Zobalova, A. Marin-Hernandez, M. Stantic, J. Rohlena, *et al.* "Suppression of Tumor Growth in Vivo by the Mitocan Alpha-Tocopheryl Succinate Requires Respiratory Complex Ii." *Clin Cancer Res* 15, no. 5 (Mar 1 2009): 1593-600. https://doi.org/10.1158/1078-0432.CCR-08-2439. https://www.ncbi.nlm.nih.gov/pubmed/19223492.

Dong, L. F., V. J. Jameson, D. Tilly, J. Cerny, E. Mahdavian, A. Marin-Hernandez, L. Hernandez-Esquivel, *et al.* "Mitochondrial Targeting of Vitamin E Succinate Enhances Its Pro-Apoptotic and Anti-Cancer Activity Via Mitochondrial Complex Ii." *J Biol Chem* 286, no. 5 (Feb 4 2011): 3717-28. https://doi.org/10.1074/jbc.M110.186643. https://www.ncbi.nlm.nih.gov/pubmed/21059645.

Driesschaert, B., V. Marchand, P. Leveque, B. Gallez, and J. Marchand-Brynaert. "A Phosphonated Triarylmethyl Radical as a Probe for Measurement of Ph by Epr." *Chem Commun (Camb)* 48, no. 34 (Apr 28 2012): 4049-51. https://doi.org/10.1039/c2cc00025c. https://www.ncbi.nlm.nih.gov/pubmed/22314917.

E, J. Y., S. E. Lu, Y. Lin, J. M. Graber, D. Rotter, L. Zhang, G. M. Petersen, *et al.* "Differential and Joint Effects of Metformin and Statins on Overall Survival of Elderly Patients with Pancreatic Adenocarcinoma: A Large Population-Based Study." *Cancer Epidemiol Biomarkers Prev* 26, no. 8 (Aug 2017): 1225-32. https://doi.org/10.1158/1055-9965.EPI-17-0227. https://www.ncbi.nlm.nih.gov/pubmed/28619830.

Efuet, E. T., and K. Keyomarsi. "Farnesyl and Geranylgeranyl Transferase Inhibitors Induce G1 Arrest by Targeting the Proteasome." *Cancer Res* 66, no. 2 (Jan 15 2006): 1040-51. https://doi.org/10.1158/0008-5472.CAN-05-3416. https://www.ncbi.nlm.nih.gov/pubmed/16424040.

Erdmann, J., K. Stark, U. B. Esslinger, P. M. Rumpf, D. Koesling, C. de Wit, F. J. Kaiser, *et al.* "Dysfunctional Nitric Oxide Signalling Increases Risk of Myocardial Infarction." *Nature* 504, no. 7480 (Dec 19 2013): 432-6. https://doi.org/10.1038/nature12722. https://www.ncbi.nlm.nih.gov/pubmed/24213632.

Favier, J., and A. P. Gimenez-Roqueplo. "Pheochromocytomas: The (Pseudo)-Hypoxia Hypothesis." *Best Pract Res Clin Endocrinol Metab* 24, no. 6 (Dec 2010): 957-68. https://doi.org/10.1016/j.beem.2010.10.004. https://www.ncbi.nlm.nih.gov/pubmed/21115164.

Feron, O., C. Dessy, J. P. Desager, and J. L. Balligand. "Hydroxy-Methylglutaryl-Coenzyme a Reductase Inhibition Promotes Endothelial Nitric Oxide Synthase Activation through a Decrease in Caveolin Abundance." *Circulation* 103, no. 1 (Jan 2 2001): 113-8. https://doi.org/10.1161/01.cir.103.1.113. https://www.ncbi.nlm.nih.gov/pubmed/11136695.

Ferrick, D. A., A. Neilson, and C. Beeson. "Advances in Measuring Cellular Bioenergetics Using Extracellular Flux." *Drug Discov Today* 13, no. 5-6 (Mar 2008): 268-74. https://doi.org/10.1016/j.drudis.2007.12.008. https://www.ncbi.nlm.nih.gov/pubmed/18342804.

Fichtlscherer, S., C. Schmidt-Lucke, S. Bojunga, L. Rossig, C. Heeschen, S. Dimmeler, and A. M. Zeiher. "Differential Effects of Short-Term Lipid Lowering with Ezetimibe and

Statins on Endothelial Function in Patients with Cad: Clinical Evidence for 'Pleiotropic' Functions of Statin Therapy." *Eur Heart J* 27, no. 10 (May 2006): 1182-90. https://doi.org/10.1093/eurheartj/ehi881. https://www.ncbi.nlm.nih.gov/pubmed/16621868.

Folkers, K., P. Langsjoen, R. Willis, P. Richardson, L. J. Xia, C. Q. Ye, and H. Tamagawa. "Lovastatin Decreases Coenzyme Q Levels in Humans." *Proc Natl Acad Sci U S A* 87, no. 22 (Nov 1990): 8931-4. https://doi.org/10.1073/pnas.87.22.8931. https://www.ncbi.nlm.nih.gov/pubmed/2247468.

Formosa, L. E., and M. T. Ryan. "Mitochondrial Oxphos Complex Assembly Lines." *Nat Cell Biol* 20, no. 5 (May 2018): 511-13. https://doi.org/10.1038/s41556-018-0098-z. https://www.ncbi.nlm.nih.gov/pubmed/29662174.

Franzoni, F., A. Quinones-Galvan, F. Regoli, E. Ferrannini, and F. Galetta. "A Comparative Study of the in Vitro Antioxidant Activity of Statins." *Int J Cardiol* 90, no. 2-3 (Aug 2003): 317-21. https://doi.org/10.1016/s0167-5273(02)00577-6. https://www.ncbi.nlm.nih.gov/pubmed/12957768.

Frezza, C., S. Cipolat, and L. Scorrano. "Organelle Isolation: Functional Mitochondria from Mouse Liver, Muscle and Cultured Fibroblasts." *Nat Protoc* 2, no. 2 (2007): 287-95. https://doi.org/10.1038/nprot.2006.478. https://www.ncbi.nlm.nih.gov/pubmed/17406588.

Fruytier, A. C., J. Magat, M. A. Neveu, O. Karroum, C. Bouzin, O. Feron, B. Jordan, G. O. Cron, and B. Gallez. "Dynamic Contrast-Enhanced Mri in Mouse Tumors at 11.7 T: Comparison of Three Contrast Agents with Different Molecular Weights to Assess the Early Effects of Combretastatin A4." *NMR Biomed* 27, no. 11 (Nov 2014): 1403-12. https://doi.org/10.1002/nbm.3220. https://www.ncbi.nlm.nih.gov/pubmed/25323069.

Fujiwara, D., M. Tsubaki, T. Takeda, Y. Tomonari, Y. I. Koumoto, K. Sakaguchi, and S. Nishida. "Statins Induce Apoptosis through Inhibition of Ras Signaling Pathways and Enhancement of Bim and P27 Expression in Human Hematopoietic Tumor Cells." *Tumour Biol* 39, no. 10 (Oct 2017): 1010428317734947. https://doi.org/10.1177/1010428317734947. https://www.ncbi.nlm.nih.gov/pubmed/28990465.

Furberg, C. D., and B. Pitt. "Withdrawal of Cerivastatin from the World Market." *Curr Control Trials Cardiovasc Med* 2, no. 5 (2001): 205-07. https://doi.org/10.1186/cvm-2-5-205. https://www.ncbi.nlm.nih.gov/pubmed/11806796.

Gallez, B., G. Bacic, F. Goda, J. Jiang, J. A. O'Hara, J. F. Dunn, and H. M. Swartz. "Use of Nitroxides for Assessing Perfusion, Oxygenation, and Viability of Tissues: In Vivo Epr and Mri Studies." *Magn Reson Med* 35, no. 1 (Jan 1996): 97-106. https://doi.org/10.1002/mrm.1910350113. https://www.ncbi.nlm.nih.gov/pubmed/8771027.

Gallez, B., C. Baudelet, and B. F. Jordan. "Assessment of Tumor Oxygenation by Electron Paramagnetic Resonance: Principles and Applications." *NMR Biomed* 17, no. 5 (Aug 2004): 240-62. https://doi.org/10.1002/nbm.900. https://www.ncbi.nlm.nih.gov/pubmed/15366026.

Gallez, B., R. Debuyst, R. Demeure, F. Dejehet, C. Grandin, B. Van Beers, H. Taper, J. Pringot, and P. Dumont. "Evaluation of a Nitroxyl Fatty Acid as Liver Contrast Agent for Magnetic Resonance Imaging." *Magn Reson Med* 30, no. 5 (Nov 1993): 592-9. https://doi.org/10.1002/mrm.1910300510. https://www.ncbi.nlm.nih.gov/pubmed/8259059.

Gallez, B., M. A. Neveu, P. Danhier, and B. F. Jordan. "Manipulation of Tumor Oxygenation and Radiosensitivity through Modification of Cell Respiration. A Critical Review of Approaches and Imaging Biomarkers for Therapeutic Guidance." *Biochim Biophys Acta Bioenerg* 1858, no. 8 (Aug 2017): 700-11. https://doi.org/10.1016/j.bbabio.2017.01.002. https://www.ncbi.nlm.nih.gov/pubmed/28088332.

Gella, A., and N. Durany. "Oxidative Stress in Alzheimer Disease." *Cell Adh Migr* 3, no. 1 (Jan-Mar 2009): 88-93. https://doi.org/10.4161/cam.3.1.7402. https://www.ncbi.nlm.nih.gov/pubmed/19372765.

Gerets, H. H., E. Hanon, M. Cornet, S. Dhalluin, O. Depelchin, M. Canning, and F. A. Atienzar. "Selection of Cytotoxicity Markers for the Screening of New Chemical Entities in a Pharmaceutical Context: A Preliminary Study Using a Multiplexing Approach." *Toxicol In Vitro* 23, no. 2 (Mar 2009): 319-32. https://doi.org/10.1016/j.tiv.2008.11.012. https://www.ncbi.nlm.nih.gov/pubmed/19110050.

Gimenez-Roqueplo, A. P., J. Favier, P. Rustin, J. J. Mourad, P. F. Plouin, P. Corvol, A. Rotig, and X. Jeunemaitre. "The R22x Mutation of the Sdhd Gene in Hereditary Paraganglioma Abolishes the Enzymatic Activity of Complex Ii in the Mitochondrial Respiratory Chain and Activates the Hypoxia Pathway." *Am J Hum Genet* 69, no. 6 (Dec 2001): 1186-97. https://doi.org/10.1086/324413. https://www.ncbi.nlm.nih.gov/pubmed/11605159.

Girona, J., A. E. La Ville, R. Sola, N. Plana, and L. Masana. "Simvastatin Decreases Aldehyde Production Derived from Lipoprotein Oxidation." *Am J Cardiol* 83, no. 6 (Mar 15 1999): 846-51. https://doi.org/10.1016/s0002-9149(98)01071-6. https://www.ncbi.nlm.nih.gov/pubmed/10190397.

Gobel, A., M. Rauner, L. C. Hofbauer, and T. D. Rachner. "Cholesterol and Beyond - the Role of the Mevalonate Pathway in Cancer Biology." *Biochim Biophys Acta Rev Cancer* 1873, no. 2 (Apr 2020): 188351. https://doi.org/10.1016/j.bbcan.2020.188351. https://www.ncbi.nlm.nih.gov/pubmed/32007596.

Gottlieb, E., and I. P. Tomlinson. "Mitochondrial Tumour Suppressors: A Genetic and Biochemical Update." *Nat Rev Cancer* 5, no. 11 (Nov 2005): 857-66. https://doi.org/10.1038/nrc1737. https://www.ncbi.nlm.nih.gov/pubmed/16327764.

Grune, T., T. Reinheckel, and K. J. Davies. "Degradation of Oxidized Proteins in Mammalian Cells." *FASEB J* 11, no. 7 (Jun 1997): 526-34. https://www.ncbi.nlm.nih.gov/pubmed/9212076.

Gu, X., Y. Ma, Y. Liu, and Q. Wan. "Measurement of Mitochondrial Respiration in Adherent Cells by Seahorse Xf96 Cell Mito Stress Test." *STAR Protoc* 2, no. 1 (Mar 19 2021): 100245. https://doi.org/10.1016/j.xpro.2020.100245. https://www.ncbi.nlm.nih.gov/pubmed/33458707.

Guo, L., S. Dial, L. Shi, W. Branham, J. Liu, J. L. Fang, B. Green, *et al.* "Similarities and Differences in the Expression of Drug-Metabolizing Enzymes between Human Hepatic Cell Lines and Primary Human Hepatocytes." *Drug Metab Dispos* 39, no. 3 (Mar 2011): 528-38. https://doi.org/10.1124/dmd.110.035873. https://www.ncbi.nlm.nih.gov/pubmed/21149542.

Gutman, M. "Regulation of Mitochondrial Succinate Dehydrogenase by Substrate Type Activators." *Biochemistry* 16, no. 14 (Jul 12 1977): 3067-72.

https://doi.org/10.1021/bi00633a004.
https://www.ncbi.nlm.nih.gov/pubmed/889791.

Guzy, R. D., B. Sharma, E. Bell, N. S. Chandel, and P. T. Schumacker. "Loss of the Sdhb, but Not the Sdha, Subunit of Complex Ii Triggers Reactive Oxygen Species-Dependent Hypoxia-Inducible Factor Activation and Tumorigenesis." *Mol Cell Biol* 28, no. 2 (Jan 2008): 718-31. https://doi.org/10.1128/MCB.01338-07.
https://www.ncbi.nlm.nih.gov/pubmed/17967865.

Hall, A. "Rho Gtpases and the Actin Cytoskeleton." *Science* 279, no. 5350 (Jan 23 1998): 509-14. https://doi.org/10.1126/science.279.5350.509.
https://www.ncbi.nlm.nih.gov/pubmed/9438836.

Han, Y. H., and W. H. Park. "Growth Inhibition in Antimycin a Treated-Lung Cancer Calu-6 Cells Via Inducing a G1 Phase Arrest and Apoptosis." *Lung Cancer* 65, no. 2 (Aug 2009): 150-60. https://doi.org/10.1016/j.lungcan.2008.11.005.
https://www.ncbi.nlm.nih.gov/pubmed/19111365.

Hardy, M., A. Rockenbauer, J. Vasquez-Vivar, C. Felix, M. Lopez, S. Srinivasan, N. Avadhani, P. Tordo, and B. Kalyanaraman. "Detection, Characterization, and Decay Kinetics of Ros and Thiyl Adducts of Mito-Depmpo Spin Trap." *Chem Res Toxicol* 20, no. 7 (Jul 2007): 1053-60. https://doi.org/10.1021/tx700101d.
https://www.ncbi.nlm.nih.gov/pubmed/17559235.

Hashimoto, M., E. Rockenstein, L. Crews, and E. Masliah. "Role of Protein Aggregation in Mitochondrial Dysfunction and Neurodegeneration in Alzheimer's and Parkinson's Diseases." *Neuromolecular Med* 4, no. 1-2 (2003): 21-36.
https://doi.org/10.1385/NMM:4:1-2:21.
https://www.ncbi.nlm.nih.gov/pubmed/14528050.

Hauptmann, S., U. Keil, I. Scherping, A. Bonert, A. Eckert, and W. E. Muller. "Mitochondrial Dysfunction in Sporadic and Genetic Alzheimer's Disease." *Exp Gerontol* 41, no. 7 (Jul 2006): 668-73. https://doi.org/10.1016/j.exger.2006.03.012.
https://www.ncbi.nlm.nih.gov/pubmed/16677790.

Hawkins, C. L., and M. J. Davies. "Detection and Characterisation of Radicals in Biological Materials Using Epr Methodology." *Biochim Biophys Acta* 1840, no. 2 (Feb 2014): 708-21. https://doi.org/10.1016/j.bbagen.2013.03.034.
https://www.ncbi.nlm.nih.gov/pubmed/23567797.

Hirsch, E. C., G. Hoglinger, E. Rousselet, T. Breidert, K. Parain, J. Feger, M. Ruberg*, et al.* "Animal Models of Parkinson's Disease in Rodents Induced by Toxins: An Update." *J Neural Transm Suppl*, no. 65 (2003): 89-100. https://doi.org/10.1007/978-3-7091-0643-3_6. https://www.ncbi.nlm.nih.gov/pubmed/12946051.

Hobert, J. A., J. L. Mester, J. Moline, and C. Eng. "Elevated Plasma Succinate in Pten, Sdhb, and Sdhd Mutation-Positive Individuals." *Genet Med* 14, no. 6 (Jun 2012): 616-9.
https://doi.org/10.1038/gim.2011.63.
https://www.ncbi.nlm.nih.gov/pubmed/22261759.

Holmes, M. V., L. A. Lange, T. Palmer, M. B. Lanktree, K. E. North, B. Almoguera, S. Buxbaum*, et al.* "Causal Effects of Body Mass Index on Cardiometabolic Traits and Events: A Mendelian Randomization Analysis." *Am J Hum Genet* 94, no. 2 (Feb 6 2014): 198-208. https://doi.org/10.1016/j.ajhg.2013.12.014.
https://www.ncbi.nlm.nih.gov/pubmed/24462370.

Hoque, A., H. Chen, and X. C. Xu. "Statin Induces Apoptosis and Cell Growth Arrest in Prostate Cancer Cells." *Cancer Epidemiol Biomarkers Prev* 17, no. 1 (Jan 2008): 88-94.

https://doi.org/10.1158/1055-9965.EPI-07-0531.
https://www.ncbi.nlm.nih.gov/pubmed/18199714.

Hwang, A. B., E. A. Ryu, M. Artan, H. W. Chang, M. H. Kabir, H. J. Nam, D. Lee, *et al.* "Feedback Regulation Via Ampk and Hif-1 Mediates Ros-Dependent Longevity in Caenorhabditis Elegans." *Proc Natl Acad Sci U S A* 111, no. 42 (Oct 21 2014): E4458-67. https://doi.org/10.1073/pnas.1411199111.
https://www.ncbi.nlm.nih.gov/pubmed/25288734.

Ishii, T., K. Yasuda, A. Akatsuka, O. Hino, P. S. Hartman, and N. Ishii. "A Mutation in the Sdhc Gene of Complex Ii Increases Oxidative Stress, Resulting in Apoptosis and Tumorigenesis." *Cancer Res* 65, no. 1 (Jan 1 2005): 203-9.
https://www.ncbi.nlm.nih.gov/pubmed/15665296.

Ishikawa, K., K. Takenaga, M. Akimoto, N. Koshikawa, A. Yamaguchi, H. Imanishi, K. Nakada, Y. Honma, and J. Hayashi. "Ros-Generating Mitochondrial DNA Mutations Can Regulate Tumor Cell Metastasis." *Science* 320, no. 5876 (May 2 2008): 661-4.
https://doi.org/10.1126/science.1156906.
https://www.ncbi.nlm.nih.gov/pubmed/18388260.

Istvan, E. S., and J. Deisenhofer. "Structural Mechanism for Statin Inhibition of Hmg-Coa Reductase." *Science* 292, no. 5519 (May 11 2001): 1160-4.
https://doi.org/10.1126/science.1059344.
https://www.ncbi.nlm.nih.gov/pubmed/11349148.

Ito, D., O. Ito, N. Mori, Y. Muroya, P. Y. Cao, K. Takashima, M. Kanazawa, and M. Kohzuki. "Atorvastatin Upregulates Nitric Oxide Synthases with Rho-Kinase Inhibition and Akt Activation in the Kidney of Spontaneously Hypertensive Rats." *J Hypertens* 28, no. 11 (Nov 2010): 2278-88. https://doi.org/10.1097/HJH.0b013e32833e0924.
https://www.ncbi.nlm.nih.gov/pubmed/20724941.

Jabot, C., G. Daniele, B. Giroud, S. Tchamitchian, L. P. Belzunces, H. Casabianca, and E. Vulliet. "Detection and Quantification of Boscalid and Its Metabolites in Honeybees." *Chemosphere* 156 (Aug 2016): 245-51.
https://doi.org/10.1016/j.chemosphere.2016.04.135.
https://www.ncbi.nlm.nih.gov/pubmed/27179242.

James, P. E., S. K. Jackson, O. Y. Grinberg, and H. M. Swartz. "The Effects of Endotoxin on Oxygen Consumption of Various Cell Types in Vitro: An Epr Oximetry Study." *Free Radic Biol Med* 18, no. 4 (Apr 1995): 641-7. https://doi.org/10.1016/0891-5849(94)00179-n. https://www.ncbi.nlm.nih.gov/pubmed/7750788.

Jenner, P. "Oxidative Stress in Parkinson's Disease." *Ann Neurol* 53 Suppl 3 (2003): S26-36; discussion S36-8. https://doi.org/10.1002/ana.10483.
https://www.ncbi.nlm.nih.gov/pubmed/12666096.

Jiang, F., J. Yang, L. Zhang, R. Li, L. Zhuo, L. Sun, and Q. Zhao. "Rosuvastatin Reduces Ischemia-Reperfusion Injury in Patients with Acute Coronary Syndrome Treated with Percutaneous Coronary Intervention." *Clin Cardiol* 37, no. 9 (Sep 2014): 530-5.
https://doi.org/10.1002/clc.22292.
https://www.ncbi.nlm.nih.gov/pubmed/25156269.

Johnson, J. A., S. H. Simpson, E. L. Toth, and S. R. Majumdar. "Reduced Cardiovascular Morbidity and Mortality Associated with Metformin Use in Subjects with Type 2 Diabetes." *Diabet Med* 22, no. 4 (Apr 2005): 497-502. https://doi.org/10.1111/j.1464-5491.2005.01448.x. https://www.ncbi.nlm.nih.gov/pubmed/15787679.

Jones, D. C., P. G. Gunasekar, J. L. Borowitz, and G. E. Isom. "Dopamine-Induced Apoptosis Is Mediated by Oxidative Stress and Is Enhanced by Cyanide in Differentiated Pc12

Cells." *J Neurochem* 74, no. 6 (Jun 2000): 2296-304. https://doi.org/10.1046/j.1471-4159.2000.0742296.x. https://www.ncbi.nlm.nih.gov/pubmed/10820189.

Jones, H. M., Z. Fang, W. Sun, L. H. Clark, J. E. Stine, A. Q. Tran, S. A. Sullivan, *et al.* "Atorvastatin Exhibits Anti-Tumorigenic and Anti-Metastatic Effects in Ovarian Cancer in Vitro." *Am J Cancer Res* 7, no. 12 (2017): 2478-90. https://www.ncbi.nlm.nih.gov/pubmed/29312801.

Jordan, B. F., N. Christian, N. Crokart, V. Gregoire, O. Feron, and B. Gallez. "Thyroid Status Is a Key Modulator of Tumor Oxygenation: Implication for Radiation Therapy." *Radiat Res* 168, no. 4 (Oct 2007): 428-32. https://doi.org/10.1667/RR0931.1. https://www.ncbi.nlm.nih.gov/pubmed/17903037.

Jordan, B. F., V. Gregoire, R. J. Demeure, P. Sonveaux, O. Feron, J. O'Hara, V. P. Vanhulle, N. Delzenne, and B. Gallez. "Insulin Increases the Sensitivity of Tumors to Irradiation: Involvement of an Increase in Tumor Oxygenation Mediated by a Nitric Oxide-Dependent Decrease of the Tumor Cells Oxygen Consumption." *Cancer Res* 62, no. 12 (Jun 15 2002): 3555-61. https://www.ncbi.nlm.nih.gov/pubmed/12068004.

Jordan, B. F., P. Sonveaux, O. Feron, V. Gregoire, N. Beghein, C. Dessy, and B. Gallez. "Nitric Oxide as a Radiosensitizer: Evidence for an Intrinsic Role in Addition to Its Effect on Oxygen Delivery and Consumption." *Int J Cancer* 109, no. 5 (May 1 2004): 768-73. https://doi.org/10.1002/ijc.20046. https://www.ncbi.nlm.nih.gov/pubmed/14999787.

Kadenbach, B. "Intrinsic and Extrinsic Uncoupling of Oxidative Phosphorylation." *Biochim Biophys Acta* 1604, no. 2 (Jun 5 2003): 77-94. https://doi.org/10.1016/s0005-2728(03)00027-6. https://www.ncbi.nlm.nih.gov/pubmed/12765765.

Kadenbach, B., R. Ramzan, and S. Vogt. "Degenerative Diseases, Oxidative Stress and Cytochrome C Oxidase Function." *Trends Mol Med* 15, no. 4 (Apr 2009): 139-47. https://doi.org/10.1016/j.molmed.2009.02.004. https://www.ncbi.nlm.nih.gov/pubmed/19303362.

Kale, V. P., J. A. Hengst, D. H. Desai, S. G. Amin, and J. K. Yun. "The Regulatory Roles of Rock and Mrck Kinases in the Plasticity of Cancer Cell Migration." *Cancer Lett* 361, no. 2 (Jun 1 2015): 185-96. https://doi.org/10.1016/j.canlet.2015.03.017. https://www.ncbi.nlm.nih.gov/pubmed/25796438.

Kalyanaraman, B., V. Darley-Usmar, K. J. Davies, P. A. Dennery, H. J. Forman, M. B. Grisham, G. E. Mann, *et al.* "Measuring Reactive Oxygen and Nitrogen Species with Fluorescent Probes: Challenges and Limitations." *Free Radic Biol Med* 52, no. 1 (Jan 1 2012): 1-6. https://doi.org/10.1016/j.freeradbiomed.2011.09.030. https://www.ncbi.nlm.nih.gov/pubmed/22027063.

Kalyanaraman, B., B. P. Dranka, M. Hardy, R. Michalski, and J. Zielonka. "Hplc-Based Monitoring of Products Formed from Hydroethidine-Based Fluorogenic Probes--the Ultimate Approach for Intra- and Extracellular Superoxide Detection." *Biochim Biophys Acta* 1840, no. 2 (Feb 2014): 739-44. https://doi.org/10.1016/j.bbagen.2013.05.008. https://www.ncbi.nlm.nih.gov/pubmed/23668959.

Kalyanaraman, B., M. Hardy, R. Podsiadly, G. Cheng, and J. Zielonka. "Recent Developments in Detection of Superoxide Radical Anion and Hydrogen Peroxide: Opportunities, Challenges, and Implications in Redox Signaling." *Arch Biochem Biophys* 617 (Mar 1 2017): 38-47. https://doi.org/10.1016/j.abb.2016.08.021. https://www.ncbi.nlm.nih.gov/pubmed/27590268.

Kamalian, L., A. E. Chadwick, M. Bayliss, N. S. French, M. Monshouwer, J. Snoeys, and B. K. Park. "The Utility of Hepg2 Cells to Identify Direct Mitochondrial Dysfunction in the Absence of Cell Death." *Toxicol In Vitro* 29, no. 4 (Jun 2015): 732-40. https://doi.org/10.1016/j.tiv.2015.02.011. https://www.ncbi.nlm.nih.gov/pubmed/25746382.

Kanaan, G. N., and M. E. Harper. "Cellular Redox Dysfunction in the Development of Cardiovascular Diseases." *Biochim Biophys Acta Gen Subj* 1861, no. 11 Pt A (Nov 2017): 2822-29. https://doi.org/10.1016/j.bbagen.2017.07.027. https://www.ncbi.nlm.nih.gov/pubmed/28778485.

Karagkounis, G., J. DeVecchio, S. Ferrandon, and M. F. Kalady. "Simvastatin Enhances Radiation Sensitivity of Colorectal Cancer Cells." *Surg Endosc* 32, no. 3 (Mar 2018): 1533-39. https://doi.org/10.1007/s00464-017-5841-1. https://www.ncbi.nlm.nih.gov/pubmed/28916945.

Kawashiri, M. A., A. Nohara, H. Tada, M. Mori, M. Tsuchida, S. Katsuda, A. Inazu*, et al.* "Comparison of Effects of Pitavastatin and Atorvastatin on Plasma Coenzyme Q10 in Heterozygous Familial Hypercholesterolemia: Results from a Crossover Study." *Clin Pharmacol Ther* 83, no. 5 (May 2008): 731-9. https://doi.org/10.1038/sj.clpt.6100396. https://www.ncbi.nlm.nih.gov/pubmed/17957184.

Kehrer, J. P. "Free Radicals as Mediators of Tissue Injury and Disease." *Crit Rev Toxicol* 23, no. 1 (1993): 21-48. https://doi.org/10.3109/10408449309104073. https://www.ncbi.nlm.nih.gov/pubmed/8471159.

Kelso, G. F., A. Maroz, H. M. Cocheme, A. Logan, T. A. Prime, A. V. Peskin, C. C. Winterbourn*, et al.* "A Mitochondria-Targeted Macrocyclic Mn(Ii) Superoxide Dismutase Mimetic." *Chem Biol* 19, no. 10 (Oct 26 2012): 1237-46. https://doi.org/10.1016/j.chembiol.2012.08.005. https://www.ncbi.nlm.nih.gov/pubmed/23102218.

Khan, K. H., M. Blanco-Codesido, and L. R. Molife. "Cancer Therapeutics: Targeting the Apoptotic Pathway." *Crit Rev Oncol Hematol* 90, no. 3 (Jun 2014): 200-19. https://doi.org/10.1016/j.critrevonc.2013.12.012. https://www.ncbi.nlm.nih.gov/pubmed/24507955.

Kim, J. W., and C. V. Dang. "Multifaceted Roles of Glycolytic Enzymes." *Trends Biochem Sci* 30, no. 3 (Mar 2005): 142-50. https://doi.org/10.1016/j.tibs.2005.01.005. https://www.ncbi.nlm.nih.gov/pubmed/15752986.

King, A., M. A. Selak, and E. Gottlieb. "Succinate Dehydrogenase and Fumarate Hydratase: Linking Mitochondrial Dysfunction and Cancer." *Oncogene* 25, no. 34 (Aug 7 2006): 4675-82. https://doi.org/10.1038/sj.onc.1209594. https://www.ncbi.nlm.nih.gov/pubmed/16892081.

King, M. A., and M. A. Radicchi-Mastroianni. "Antimycin a-Induced Apoptosis of Hl-60 Cells." *Cytometry* 49, no. 3 (Nov 1 2002): 106-12. https://doi.org/10.1002/cyto.10156. https://www.ncbi.nlm.nih.gov/pubmed/12442310.

Kluckova, K., A. Bezawork-Geleta, J. Rohlena, L. Dong, and J. Neuzil. "Mitochondrial Complex Ii, a Novel Target for Anti-Cancer Agents." *Biochim Biophys Acta* 1827, no. 5 (May 2013): 552-64. https://doi.org/10.1016/j.bbabio.2012.10.015. https://www.ncbi.nlm.nih.gov/pubmed/23142170.

Knapp, A. C., J. Huang, G. Starling, and P. A. Kiener. "Inhibitors of Hmg-Coa Reductase Sensitize Human Smooth Muscle Cells to Fas-Ligand and Cytokine-Induced Cell

Death." *Atherosclerosis* 152, no. 1 (Sep 2000): 217-27. https://doi.org/10.1016/s0021-9150(99)00462-1. https://www.ncbi.nlm.nih.gov/pubmed/10996358.

Knasmuller, S., C. E. Schwab, S. J. Land, C. Y. Wang, R. Sanyal, M. Kundi, W. Parzefall, and F. Darroudi. "Genotoxic Effects of Heterocyclic Aromatic Amines in Human Derived Hepatoma (Hepg2) Cells." *Mutagenesis* 14, no. 6 (Nov 1999): 533-40. https://doi.org/10.1093/mutage/14.6.533. https://www.ncbi.nlm.nih.gov/pubmed/10567027.

Kobayashi, H., E. Gil-Guzman, A. M. Mahran, Rakesh, D. R. Nelson, A. J. Thomas, Jr., and A. Agarwa. "Quality Control of Reactive Oxygen Species Measurement by Luminol-Dependent Chemiluminescence Assay." *J Androl* 22, no. 4 (Jul-Aug 2001): 568-74. https://www.ncbi.nlm.nih.gov/pubmed/11451353.

Koch, C. J., C. C. Stobbe, and E. A. Bump. "The Effect on the Km for Radiosensitization at 0 Degree C of Thiol Depletion by Diethylmaleate Pretreatment: Quantitative Differences Found Using the Radiation Sensitizing Agent Misonidazole or Oxygen." *Radiat Res* 98, no. 1 (Apr 1984): 141-53. https://www.ncbi.nlm.nih.gov/pubmed/6718689.

Kollmeier, M. A., M. S. Katz, K. Mak, Y. Yamada, D. J. Feder, Z. Zhang, X. Jia, W. Shi, and M. J. Zelefsky. "Improved Biochemical Outcomes with Statin Use in Patients with High-Risk Localized Prostate Cancer Treated with Radiotherapy." *Int J Radiat Oncol Biol Phys* 79, no. 3 (Mar 1 2011): 713-8. https://doi.org/10.1016/j.ijrobp.2009.12.006. https://www.ncbi.nlm.nih.gov/pubmed/20452139.

Konstantinopoulos, P. A., M. V. Karamouzis, and A. G. Papavassiliou. "Post-Translational Modifications and Regulation of the Ras Superfamily of Gtpases as Anticancer Targets." *Nat Rev Drug Discov* 6, no. 7 (Jul 2007): 541-55. https://doi.org/10.1038/nrd2221. https://www.ncbi.nlm.nih.gov/pubmed/17585331.

Kozar, K., R. Kaminski, M. Legat, M. Kopec, D. Nowis, J. S. Skierski, M. Koronkiewicz, M. Jakobisiak, and J. Golab. "Cerivastatin Demonstrates Enhanced Antitumor Activity against Human Breast Cancer Cell Lines When Used in Combination with Doxorubicin or Cisplatin." *Int J Oncol* 24, no. 5 (May 2004): 1149-57. https://www.ncbi.nlm.nih.gov/pubmed/15067336.

Kureishi, Y., Z. Luo, I. Shiojima, A. Bialik, D. Fulton, D. J. Lefer, W. C. Sessa, and K. Walsh. "The Hmg-Coa Reductase Inhibitor Simvastatin Activates the Protein Kinase Akt and Promotes Angiogenesis in Normocholesterolemic Animals." *Nat Med* 6, no. 9 (Sep 2000): 1004-10. https://doi.org/10.1038/79510. https://www.ncbi.nlm.nih.gov/pubmed/10973320.

Kuroda, M., Y. Tsujita, K. Tanzawa, and A. Endo. "Hypolipidemic Effects in Monkeys of Ml-236b, a Competitive Inhibitor of 3-Hydroxy-3-Methylglutaryl Coenzyme a Reductase." *Lipids* 14, no. 6 (Jun 1979): 585-9. https://doi.org/10.1007/BF02533537. https://www.ncbi.nlm.nih.gov/pubmed/110993.

Kwak, H. B., A. Thalacker-Mercer, E. J. Anderson, C. T. Lin, D. A. Kane, N. S. Lee, R. N. Cortright, M. M. Bamman, and P. D. Neufer. "Simvastatin Impairs Adp-Stimulated Respiration and Increases Mitochondrial Oxidative Stress in Primary Human Skeletal Myotubes." *Free Radic Biol Med* 52, no. 1 (Jan 1 2012): 198-207. https://doi.org/10.1016/j.freeradbiomed.2011.10.449. https://www.ncbi.nlm.nih.gov/pubmed/22080086.

Lahousse, L., D. W. Loth, G. F. Joos, A. Hofman, H. G. Leufkens, G. G. Brusselle, and B. H. Stricker. "Statins, Systemic Inflammation and Risk of Death in Copd: The Rotterdam

Study." *Pulm Pharmacol Ther* 26, no. 2 (Apr 2013): 212-7. https://doi.org/10.1016/j.pupt.2012.10.008. https://www.ncbi.nlm.nih.gov/pubmed/23142156.

Landmesser, U., F. Bahlmann, M. Mueller, S. Spiekermann, N. Kirchhoff, S. Schulz, C. Manes, *et al.* "Simvastatin Versus Ezetimibe: Pleiotropic and Lipid-Lowering Effects on Endothelial Function in Humans." *Circulation* 111, no. 18 (May 10 2005): 2356-63. https://doi.org/10.1161/01.CIR.0000164260.82417.3F. https://www.ncbi.nlm.nih.gov/pubmed/15867181.

Larner, J., J. Jane, E. Laws, R. Packer, C. Myers, and M. Shaffrey. "A Phase I-Ii Trial of Lovastatin for Anaplastic Astrocytoma and Glioblastoma Multiforme." *Am J Clin Oncol* 21, no. 6 (Dec 1998): 579-83. https://doi.org/10.1097/00000421-199812000-00010. https://www.ncbi.nlm.nih.gov/pubmed/9856659.

Laufs, U., V. La Fata, J. Plutzky, and J. K. Liao. "Upregulation of Endothelial Nitric Oxide Synthase by Hmg Coa Reductase Inhibitors." *Circulation* 97, no. 12 (Mar 31 1998): 1129-35. https://doi.org/10.1161/01.cir.97.12.1129. https://www.ncbi.nlm.nih.gov/pubmed/9537338.

Laufs, U., and J. K. Liao. "Isoprenoid Metabolism and the Pleiotropic Effects of Statins." *Curr Atheroscler Rep* 5, no. 5 (Sep 2003): 372-8. https://doi.org/10.1007/s11883-003-0008-z. https://www.ncbi.nlm.nih.gov/pubmed/12911847.

Law, M. R., N. J. Wald, and A. R. Rudnicka. "Quantifying Effect of Statins on Low Density Lipoprotein Cholesterol, Ischaemic Heart Disease, and Stroke: Systematic Review and Meta-Analysis." *BMJ* 326, no. 7404 (Jun 28 2003): 1423. https://doi.org/10.1136/bmj.326.7404.1423. https://www.ncbi.nlm.nih.gov/pubmed/12829554.

Lawson, C. D., and A. J. Ridley. "Rho Gtpase Signaling Complexes in Cell Migration and Invasion." *J Cell Biol* 217, no. 2 (Feb 5 2018): 447-57. https://doi.org/10.1083/jcb.201612069. https://www.ncbi.nlm.nih.gov/pubmed/29233866.

Lazarova, D., S. Shibata, I. Ishii, G. Zlateva, Z. Zhelev, I. Aoki, T. Higashi, and R. Bakalova. "Nitroxide-Enhanced Magnetic Resonance Imaging of Kidney Dysfunction in Vivo Based on Redox-Imbalance and Oxidative Stress." *Gen Physiol Biophys* 38, no. 3 (May 2019): 191-204. https://doi.org/10.4149/gpb_2019001. https://www.ncbi.nlm.nih.gov/pubmed/31184306.

Lee, M. H., Y. S. Cho, and Y. M. Han. "Simvastatin Suppresses Self-Renewal of Mouse Embryonic Stem Cells by Inhibiting Rhoa Geranylgeranylation." *Stem Cells* 25, no. 7 (Jul 2007): 1654-63. https://doi.org/10.1634/stemcells.2006-0753. https://www.ncbi.nlm.nih.gov/pubmed/17464088.

Lee, S., E. Nakamura, H. Yang, W. Wei, M. S. Linggi, M. P. Sajan, R. V. Farese, *et al.* "Neuronal Apoptosis Linked to Egln3 Prolyl Hydroxylase and Familial Pheochromocytoma Genes: Developmental Culling and Cancer." *Cancer Cell* 8, no. 2 (Aug 2005): 155-67. https://doi.org/10.1016/j.ccr.2005.06.015. https://www.ncbi.nlm.nih.gov/pubmed/16098468.

Lee, S. R., K. S. Yang, J. Kwon, C. Lee, W. Jeong, and S. G. Rhee. "Reversible Inactivation of the Tumor Suppressor Pten by H2o2." *J Biol Chem* 277, no. 23 (Jun 7 2002): 20336-42. https://doi.org/10.1074/jbc.M111899200. https://www.ncbi.nlm.nih.gov/pubmed/11916965.

Lemarie, A., L. Huc, E. Pazarentzos, A. L. Mahul-Mellier, and S. Grimm. "Specific Disintegration of Complex Ii Succinate:Ubiquinone Oxidoreductase Links Ph

Changes to Oxidative Stress for Apoptosis Induction." *Cell Death Differ* 18, no. 2 (Feb 2011): 338-49. https://doi.org/10.1038/cdd.2010.93. https://www.ncbi.nlm.nih.gov/pubmed/20706275.

Lennernas, H., and G. Fager. "Pharmacodynamics and Pharmacokinetics of the Hmg-Coa Reductase Inhibitors. Similarities and Differences." *Clin Pharmacokinet* 32, no. 5 (May 1997): 403-25. https://doi.org/10.2165/00003088-199732050-00005. https://www.ncbi.nlm.nih.gov/pubmed/9160173.

Li, W., M. Yuan, Y. Wu, and X. Liu. "Bixafen Exposure Induces Developmental Toxicity in Zebrafish (Danio Rerio) Embryos." *Environ Res* 189 (Oct 2020): 109923. https://doi.org/10.1016/j.envres.2020.109923. https://www.ncbi.nlm.nih.gov/pubmed/32980012.

Liiv, I., U. Haljasorg, K. Kisand, J. Maslovskaja, M. Laan, and P. Peterson. "Aire-Induced Apoptosis Is Associated with Nuclear Translocation of Stress Sensor Protein Gapdh." *Biochem Biophys Res Commun* 423, no. 1 (Jun 22 2012): 32-7. https://doi.org/10.1016/j.bbrc.2012.05.057. https://www.ncbi.nlm.nih.gov/pubmed/22613203.

Lin, Y., C. Ma, C. Liu, Z. Wang, J. Yang, X. Liu, Z. Shen, and R. Wu. "Nmr-Based Fecal Metabolomics Fingerprinting as Predictors of Earlier Diagnosis in Patients with Colorectal Cancer." *Oncotarget* 7, no. 20 (May 17 2016): 29454-64. https://doi.org/10.18632/oncotarget.8762. https://www.ncbi.nlm.nih.gov/pubmed/27107423.

Liochev, S. I., and I. Fridovich. "Does Mitosod Protect against the Toxicity of Paraquat toward Mitochondria by Acting as a Superoxide Dismutase Mimic?". *Free Radic Biol Med* 65 (Dec 2013): 1534. https://doi.org/10.1016/j.freeradbiomed.2013.02.010. https://www.ncbi.nlm.nih.gov/pubmed/23434767.

Liu, S. T., G. Hui, C. Mathis, K. Chamie, A. J. Pantuck, and A. Drakaki. "The Current Status and Future Role of the Phosphoinositide 3 Kinase/Akt Signaling Pathway in Urothelial Cancer: An Old Pathway in the New Immunotherapy Era." *Clin Genitourin Cancer* 16, no. 2 (Apr 2018): e269-e76. https://doi.org/10.1016/j.clgc.2017.10.011. https://www.ncbi.nlm.nih.gov/pubmed/29199023.

Long, J. Z., K. J. Svensson, L. A. Bateman, H. Lin, T. Kamenecka, I. A. Lokurkar, J. Lou*, et al.* "The Secreted Enzyme Pm20d1 Regulates Lipidated Amino Acid Uncouplers of Mitochondria." *Cell* 166, no. 2 (Jul 14 2016): 424-35. https://doi.org/10.1016/j.cell.2016.05.071. https://www.ncbi.nlm.nih.gov/pubmed/27374330.

Ludman, A., V. Venugopal, D. M. Yellon, and D. J. Hausenloy. "Statins and Cardioprotection--More Than Just Lipid Lowering?". *Pharmacol Ther* 122, no. 1 (Apr 2009): 30-43. https://doi.org/10.1016/j.pharmthera.2009.01.002. https://www.ncbi.nlm.nih.gov/pubmed/19318042.

Luz, A. L., L. L. Smith, J. P. Rooney, and J. N. Meyer. "Seahorse Xfe 24 Extracellular Flux Analyzer-Based Analysis of Cellular Respiration in Caenorhabditis Elegans." *Curr Protoc Toxicol* 66 (Nov 2 2015): 25 7 1-15. https://doi.org/10.1002/0471140856.tx2507s66. https://www.ncbi.nlm.nih.gov/pubmed/26523474.

M.R. Horsman, B.G.Wouters, M.C. Joiner, J. Overgaard. "The Oxygen Effect and Fractionated Radiotherapy." In *Basic Clinical Radiobiology*, edited by A. van der Kogel M. Joiner, 207–16, 2009.

Mabuchi, H., T. Haba, R. Tatami, S. Miyamoto, Y. Sakai, T. Wakasugi, A. Watanabe, J. Koizumi, and R. Takeda. "Effect of an Inhibitor of 3-Hydroxy-3-Methyglutaryl Coenzyme a Reductase on Serum Lipoproteins and Ubiquinone-10-Levels in Patients with Familial Hypercholesterolemia." *N Engl J Med* 305, no. 9 (Aug 27 1981): 478-82. https://doi.org/10.1056/NEJM198108273050902. https://www.ncbi.nlm.nih.gov/pubmed/7254297.

Man, S. F., J. E. Connett, N. R. Anthonisen, R. A. Wise, D. P. Tashkin, and D. D. Sin. "C-Reactive Protein and Mortality in Mild to Moderate Chronic Obstructive Pulmonary Disease." *Thorax* 61, no. 10 (Oct 2006): 849-53. https://doi.org/10.1136/thx.2006.059808. https://www.ncbi.nlm.nih.gov/pubmed/16738034.

Matsumoto, K., F. Hyodo, K. Anzai, H. Utsumi, J. B. Mitchell, and M. C. Krishna. "Brain Redox Imaging." *Methods Mol Biol* 711 (2011): 397-419. https://doi.org/10.1007/978-1-61737-992-5_20. https://www.ncbi.nlm.nih.gov/pubmed/21279614.

Matsumoto, K. I., J. B. Mitchell, and M. C. Krishna. "Comparative Studies with Epr and Mri on the in Vivo Tissue Redox Status Estimation Using Redox-Sensitive Nitroxyl Probes: Influence of the Choice of the Region of Interest." *Free Radic Res* 52, no. 2 (Feb 2018): 248-55. https://doi.org/10.1080/10715762.2018.1427235. https://www.ncbi.nlm.nih.gov/pubmed/29320888.

McGrath, P., and C. Q. Li. "Zebrafish: A Predictive Model for Assessing Drug-Induced Toxicity." *Drug Discov Today* 13, no. 9-10 (May 2008): 394-401. https://doi.org/10.1016/j.drudis.2008.03.002. https://www.ncbi.nlm.nih.gov/pubmed/18468556.

McWhinney, S. R., B. Pasini, C. A. Stratakis, Triad International Carney, and Consortium Carney-Stratakis Syndrome. "Familial Gastrointestinal Stromal Tumors and Germ-Line Mutations." *N Engl J Med* 357, no. 10 (Sep 6 2007): 1054-6. https://doi.org/10.1056/NEJMc071191. https://www.ncbi.nlm.nih.gov/pubmed/17804857.

Mignotte, B., and J. L. Vayssiere. "Mitochondria and Apoptosis." *Eur J Biochem* 252, no. 1 (Feb 15 1998): 1-15. https://doi.org/10.1046/j.1432-1327.1998.2520001.x. https://www.ncbi.nlm.nih.gov/pubmed/9523706.

Miyoshi, H. "Structure-Activity Relationships of Some Complex I Inhibitors." *Biochim Biophys Acta* 1364, no. 2 (May 6 1998): 236-44. https://doi.org/10.1016/s0005-2728(98)00030-9. https://www.ncbi.nlm.nih.gov/pubmed/9593914.

Mohaupt, M. G., R. H. Karas, E. B. Babiychuk, V. Sanchez-Freire, K. Monastyrskaya, L. Iyer, H. Hoppeler, F. Breil, and A. Draeger. "Association between Statin-Associated Myopathy and Skeletal Muscle Damage." *CMAJ* 181, no. 1-2 (Jul 7 2009): E11-8. https://doi.org/10.1503/cmaj.081785. https://www.ncbi.nlm.nih.gov/pubmed/19581603.

Moon, H. E., and S. H. Paek. "Mitochondrial Dysfunction in Parkinson's Disease." *Exp Neurobiol* 24, no. 2 (Jun 2015): 103-16. https://doi.org/10.5607/en.2015.24.2.103. https://www.ncbi.nlm.nih.gov/pubmed/26113789.

Moran, M., H. Rivera, M. Sanchez-Arago, A. Blazquez, B. Merinero, C. Ugalde, J. Arenas, J. M. Cuezva, and M. A. Martin. "Mitochondrial Bioenergetics and Dynamics Interplay in Complex I-Deficient Fibroblasts." *Biochim Biophys Acta* 1802, no. 5 (May 2010): 443-53. https://doi.org/10.1016/j.bbadis.2010.02.001. https://www.ncbi.nlm.nih.gov/pubmed/20153825.

Moyad, M. A., G. S. Merrick, W. M. Butler, K. E. Wallner, R. W. Galbreath, E. G. Butler, Z. A. Allen, and E. Adamovich. "Statins, Especially Atorvastatin, May Improve Survival Following Brachytherapy for Clinically Localized Prostate Cancer." *Urol Nurs* 26, no. 4 (Aug 2006): 298-303. https://www.ncbi.nlm.nih.gov/pubmed/16939047.

Muller, C., A. G. Bockhorn, S. Klusmeier, M. Kiehl, C. Roeder, H. Kalthoff, and O. M. Koch. "Lovastatin Inhibits Proliferation of Pancreatic Cancer Cell Lines with Mutant as Well as with Wild-Type K-Ras Oncogene but Has Different Effects on Protein Phosphorylation and Induction of Apoptosis." *Int J Oncol* 12, no. 3 (Mar 1998): 717-23. https://doi.org/10.3892/ijo.12.3.717. https://www.ncbi.nlm.nih.gov/pubmed/9472115.

Muller, F. L., Y. Liu, and H. Van Remmen. "Complex Iii Releases Superoxide to Both Sides of the Inner Mitochondrial Membrane." *J Biol Chem* 279, no. 47 (Nov 19 2004): 49064-73. https://doi.org/10.1074/jbc.M407715200. https://www.ncbi.nlm.nih.gov/pubmed/15317809.

Munze, R., C. Hannemann, P. Orlinskiy, R. Gunold, A. Paschke, K. Foit, J. Becker*, et al.* "Pesticides from Wastewater Treatment Plant Effluents Affect Invertebrate Communities." *Sci Total Environ* 599-600 (Dec 1 2017): 387-99. https://doi.org/10.1016/j.scitotenv.2017.03.008. https://www.ncbi.nlm.nih.gov/pubmed/28478367.

Murphy, M. P. "How Mitochondria Produce Reactive Oxygen Species." *Biochem J* 417, no. 1 (Jan 1 2009): 1-13. https://doi.org/10.1042/BJ20081386. https://www.ncbi.nlm.nih.gov/pubmed/19061483.

Murphy, M. P., and R. A. Smith. "Targeting Antioxidants to Mitochondria by Conjugation to Lipophilic Cations." *Annu Rev Pharmacol Toxicol* 47 (2007): 629-56. https://doi.org/10.1146/annurev.pharmtox.47.120505.105110. https://www.ncbi.nlm.nih.gov/pubmed/17014364.

Nadanaciva, S., J. A. Dykens, A. Bernal, R. A. Capaldi, and Y. Will. "Mitochondrial Impairment by Ppar Agonists and Statins Identified Via Immunocaptured Oxphos Complex Activities and Respiration." *Toxicol Appl Pharmacol* 223, no. 3 (Sep 15 2007): 277-87. https://doi.org/10.1016/j.taap.2007.06.003. https://www.ncbi.nlm.nih.gov/pubmed/17658574.

Nakata, M., S. Nagasaka, I. Kusaka, H. Matsuoka, S. Ishibashi, and T. Yada. "Effects of Statins on the Adipocyte Maturation and Expression of Glucose Transporter 4 (Slc2a4): Implications in Glycaemic Control." *Diabetologia* 49, no. 8 (Aug 2006): 1881-92. https://doi.org/10.1007/s00125-006-0269-5. https://www.ncbi.nlm.nih.gov/pubmed/16685502.

Navarese, E. P., A. Buffon, F. Andreotti, M. Kozinski, N. Welton, T. Fabiszak, S. Caputo*, et al.* "Meta-Analysis of Impact of Different Types and Doses of Statins on New-Onset Diabetes Mellitus." *Am J Cardiol* 111, no. 8 (Apr 15 2013): 1123-30. https://doi.org/10.1016/j.amjcard.2012.12.037. https://www.ncbi.nlm.nih.gov/pubmed/23352266.

Neuzil, J., I. Svensson, T. Weber, C. Weber, and U. T. Brunk. "Alpha-Tocopheryl Succinate-Induced Apoptosis in Jurkat T Cells Involves Caspase-3 Activation, and Both Lysosomal and Mitochondrial Destabilisation." *FEBS Lett* 445, no. 2-3 (Feb 26 1999): 295-300. https://doi.org/10.1016/s0014-5793(99)00141-6. https://www.ncbi.nlm.nih.gov/pubmed/10094476.

Neuzil, J., X. F. Wang, L. F. Dong, P. Low, and S. J. Ralph. "Molecular Mechanism of 'Mitocan'-Induced Apoptosis in Cancer Cells Epitomizes the Multiple Roles of

Reactive Oxygen Species and Bcl-2 Family Proteins." *FEBS Lett* 580, no. 22 (Oct 2 2006): 5125-9. https://doi.org/10.1016/j.febslet.2006.05.072. https://www.ncbi.nlm.nih.gov/pubmed/16979626.

Neuzil, J., T. Weber, N. Gellert, and C. Weber. "Selective Cancer Cell Killing by Alpha-Tocopheryl Succinate." *Br J Cancer* 84, no. 1 (Jan 5 2001): 87-9. https://doi.org/10.1054/bjoc.2000.1559. https://www.ncbi.nlm.nih.gov/pubmed/11139318.

Neuzil, J., T. Weber, A. Terman, C. Weber, and U. T. Brunk. "Vitamin E Analogues as Inducers of Apoptosis: Implications for Their Potential Antineoplastic Role." *Redox Rep* 6, no. 3 (2001): 143-51. https://doi.org/10.1179/135100001101536247. https://www.ncbi.nlm.nih.gov/pubmed/11523588.

Neveu, M. A., N. Joudiou, G. De Preter, J. P. Dehoux, B. F. Jordan, and B. Gallez. "(17) O Mrs Assesses the Effect of Mild Hypothermia on Oxygen Consumption Rate in Tumors." *NMR Biomed* 30, no. 8 (Aug 2017). https://doi.org/10.1002/nbm.3726. https://www.ncbi.nlm.nih.gov/pubmed/28430379.

Notarnicola, M., C. Messa, M. Pricci, V. Guerra, D. F. Altomare, S. Montemurro, and M. G. Caruso. "Up-Regulation of 3-Hydroxy-3-Methylglutaryl Coenzyme a Reductase Activity in Left-Sided Human Colon Cancer." *Anticancer Res* 24, no. 6 (Nov-Dec 2004): 3837-42. https://www.ncbi.nlm.nih.gov/pubmed/15736419.

O'Brien, P. J., W. Irwin, D. Diaz, E. Howard-Cofield, C. M. Krejsa, M. R. Slaughter, B. Gao*, et al.* "High Concordance of Drug-Induced Human Hepatotoxicity with in Vitro Cytotoxicity Measured in a Novel Cell-Based Model Using High Content Screening." *Arch Toxicol* 80, no. 9 (Sep 2006): 580-604. https://doi.org/10.1007/s00204-006-0091-3. https://www.ncbi.nlm.nih.gov/pubmed/16598496.

O'Driscoll, G., D. Green, and R. R. Taylor. "Simvastatin, an Hmg-Coenzyme a Reductase Inhibitor, Improves Endothelial Function within 1 Month." *Circulation* 95, no. 5 (Mar 4 1997): 1126-31. https://doi.org/10.1161/01.cir.95.5.1126. https://www.ncbi.nlm.nih.gov/pubmed/9054840.

Oh, D. S., B. Koontz, S. J. Freedland, L. Gerber, P. Patel, S. Lewis, D. S. Yoo, J. Oleson, and J. K. Salama. "Statin Use Is Associated with Decreased Prostate Cancer Recurrence in Men Treated with Brachytherapy." *World J Urol* 33, no. 1 (Jan 2015): 93-7. https://doi.org/10.1007/s00345-014-1281-x. https://www.ncbi.nlm.nih.gov/pubmed/24671610.

Okun, J. G., P. Lummen, and U. Brandt. "Three Classes of Inhibitors Share a Common Binding Domain in Mitochondrial Complex I (Nadh:Ubiquinone Oxidoreductase)." *J Biol Chem* 274, no. 5 (Jan 29 1999): 2625-30. https://doi.org/10.1074/jbc.274.5.2625. https://www.ncbi.nlm.nih.gov/pubmed/9915790.

Ottino, P., and J. R. Duncan. "Effect of Alpha-Tocopherol Succinate on Free Radical and Lipid Peroxidation Levels in Bl6 Melanoma Cells." *Free Radic Biol Med* 22, no. 7 (1997): 1145-51. https://doi.org/10.1016/s0891-5849(96)00529-1. https://www.ncbi.nlm.nih.gov/pubmed/9098087.

Owen, M. R., E. Doran, and A. P. Halestrap. "Evidence That Metformin Exerts Its Anti-Diabetic Effects through Inhibition of Complex 1 of the Mitochondrial Respiratory Chain." *Biochem J* 348 Pt 3 (Jun 15 2000): 607-14. https://www.ncbi.nlm.nih.gov/pubmed/10839993.

Paiva, H., K. M. Thelen, R. Van Coster, J. Smet, B. De Paepe, K. M. Mattila, J. Laakso*, et al.* "High-Dose Statins and Skeletal Muscle Metabolism in Humans: A Randomized, Controlled Trial." *Clin Pharmacol Ther* 78, no. 1 (Jul 2005): 60-8.

https://doi.org/10.1016/j.clpt.2005.03.006.
https://www.ncbi.nlm.nih.gov/pubmed/16003294.

Palade, G. E. "A Study of Fixation for Electron Microscopy." *J Exp Med* 95, no. 3 (Mar 1952): 285-98. https://doi.org/10.1084/jem.95.3.285.
https://www.ncbi.nlm.nih.gov/pubmed/14927794.

Park, H. S., J. D. Schoenfeld, R. B. Mailhot, M. Shive, R. I. Hartman, R. Ogembo, and L. A. Mucci. "Statins and Prostate Cancer Recurrence Following Radical Prostatectomy or Radiotherapy: A Systematic Review and Meta-Analysis." *Ann Oncol* 24, no. 6 (Jun 2013): 1427-34. https://doi.org/10.1093/annonc/mdt077.
https://www.ncbi.nlm.nih.gov/pubmed/23508824.

Park, W. H., Y. W. Han, S. H. Kim, and S. Z. Kim. "An Ros Generator, Antimycin a, Inhibits the Growth of Hela Cells Via Apoptosis." *J Cell Biochem* 102, no. 1 (Sep 1 2007): 98-109. https://doi.org/10.1002/jcb.21280.
https://www.ncbi.nlm.nih.gov/pubmed/17372917.

Pastorino, J. G., N. Shulga, and J. B. Hoek. "Mitochondrial Binding of Hexokinase Ii Inhibits Bax-Induced Cytochrome C Release and Apoptosis." *J Biol Chem* 277, no. 9 (Mar 1 2002): 7610-8. https://doi.org/10.1074/jbc.M109950200.
https://www.ncbi.nlm.nih.gov/pubmed/11751859.

Pedersen, P. L., S. Mathupala, A. Rempel, J. F. Geschwind, and Y. H. Ko. "Mitochondrial Bound Type Ii Hexokinase: A Key Player in the Growth and Survival of Many Cancers and an Ideal Prospect for Therapeutic Intervention." *Biochim Biophys Acta* 1555, no. 1-3 (Sep 10 2002): 14-20. https://doi.org/10.1016/s0005-2728(02)00248-7.
https://www.ncbi.nlm.nih.gov/pubmed/12206885.

Perevoshchikova, I. V., C. L. Quinlan, A. L. Orr, A. A. Gerencser, and M. D. Brand. "Sites of Superoxide and Hydrogen Peroxide Production During Fatty Acid Oxidation in Rat Skeletal Muscle Mitochondria." *Free Radic Biol Med* 61 (Aug 2013): 298-309. https://doi.org/10.1016/j.freeradbiomed.2013.04.006.
https://www.ncbi.nlm.nih.gov/pubmed/23583329.

Petronilli, V., D. Penzo, L. Scorrano, P. Bernardi, and F. Di Lisa. "The Mitochondrial Permeability Transition, Release of Cytochrome C and Cell Death. Correlation with the Duration of Pore Openings in Situ." *J Biol Chem* 276, no. 15 (Apr 13 2001): 12030-4. https://doi.org/10.1074/jbc.M010604200.
https://www.ncbi.nlm.nih.gov/pubmed/11134038.

Petros, J. A., A. K. Baumann, E. Ruiz-Pesini, M. B. Amin, C. Q. Sun, J. Hall, S. Lim*, et al.* "Mtdna Mutations Increase Tumorigenicity in Prostate Cancer." *Proc Natl Acad Sci U S A* 102, no. 3 (Jan 18 2005): 719-24. https://doi.org/10.1073/pnas.0408894102.
https://www.ncbi.nlm.nih.gov/pubmed/15647368.

Pollard, P. J., J. J. Briere, N. A. Alam, J. Barwell, E. Barclay, N. C. Wortham, T. Hunt*, et al.* "Accumulation of Krebs Cycle Intermediates and over-Expression of Hif1alpha in Tumours Which Result from Germline Fh and Sdh Mutations." *Hum Mol Genet* 14, no. 15 (Aug 1 2005): 2231-9. https://doi.org/10.1093/hmg/ddi227.
https://www.ncbi.nlm.nih.gov/pubmed/15987702.

Polledri, E., R. Mercadante, D. Consonni, and S. Fustinoni. "Cumulative Pesticides Exposure of Children and Their Parents Living near Vineyards by Hair Analysis." *Int J Environ Res Public Health* 18, no. 7 (Apr 2 2021). https://doi.org/10.3390/ijerph18073723.
https://www.ncbi.nlm.nih.gov/pubmed/33918339.

Polledri, E., R. Mercadante, R. Nijssen, D. Consonni, H. Mol, and S. Fustinoni. "Hair as a Matrix to Evaluate Cumulative and Aggregate Exposure to Pesticides in

Winegrowers." *Sci Total Environ* 687 (Oct 15 2019): 808-16. https://doi.org/10.1016/j.scitotenv.2019.06.061. https://www.ncbi.nlm.nih.gov/pubmed/31412484.

Porporato, P. E., V. L. Payen, J. Perez-Escuredo, C. J. De Saedeleer, P. Danhier, T. Copetti, S. Dhup, *et al.* "A Mitochondrial Switch Promotes Tumor Metastasis." *Cell Rep* 8, no. 3 (Aug 7 2014): 754-66. https://doi.org/10.1016/j.celrep.2014.06.043. https://www.ncbi.nlm.nih.gov/pubmed/25066121.

Potter, V. R., and A. E. Reif. "Inhibition of an Electron Transport Component by Antimycin A." *J Biol Chem* 194, no. 1 (Jan 1952): 287-97. https://www.ncbi.nlm.nih.gov/pubmed/14927618.

Preiss, D., S. R. Seshasai, P. Welsh, S. A. Murphy, J. E. Ho, D. D. Waters, D. A. DeMicco, *et al.* "Risk of Incident Diabetes with Intensive-Dose Compared with Moderate-Dose Statin Therapy: A Meta-Analysis." *JAMA* 305, no. 24 (Jun 22 2011): 2556-64. https://doi.org/10.1001/jama.2011.860. https://www.ncbi.nlm.nih.gov/pubmed/21693744.

Prochazka, L., L. F. Dong, K. Valis, R. Freeman, S. J. Ralph, J. Turanek, and J. Neuzil. "Alpha-Tocopheryl Succinate Causes Mitochondrial Permeabilization by Preferential Formation of Bak Channels." *Apoptosis* 15, no. 7 (Jul 2010): 782-94. https://doi.org/10.1007/s10495-010-0482-z. https://www.ncbi.nlm.nih.gov/pubmed/20217235.

Purohit, V., D. M. Simeone, and C. A. Lyssiotis. "Metabolic Regulation of Redox Balance in Cancer." *Cancers (Basel)* 11, no. 7 (Jul 8 2019). https://doi.org/10.3390/cancers11070955. https://www.ncbi.nlm.nih.gov/pubmed/31288436.

Qian, L., F. Cui, Y. Yang, Y. Liu, S. Qi, and C. Wang. "Mechanisms of Developmental Toxicity in Zebrafish Embryos (Danio Rerio) Induced by Boscalid." *Sci Total Environ* 634 (Sep 1 2018): 478-87. https://doi.org/10.1016/j.scitotenv.2018.04.012. https://www.ncbi.nlm.nih.gov/pubmed/29631138.

Qian, L., S. Qi, F. Cao, J. Zhang, F. Zhao, C. Li, and C. Wang. "Toxic Effects of Boscalid on the Growth, Photosynthesis, Antioxidant System and Metabolism of Chlorella Vulgaris." *Environ Pollut* 242, no. Pt A (Nov 2018): 171-81. https://doi.org/10.1016/j.envpol.2018.06.055. https://www.ncbi.nlm.nih.gov/pubmed/29980035.

Qian, L., S. Qi, J. Zhang, M. Duan, D. Schlenk, J. Jiang, and C. Wang. "Exposure to Boscalid Induces Reproductive Toxicity of Zebrafish by Gender-Specific Alterations in Steroidogenesis." *Environ Sci Technol* 54, no. 22 (Nov 17 2020): 14275-87. https://doi.org/10.1021/acs.est.0c02871. https://www.ncbi.nlm.nih.gov/pubmed/33138376.

Quinlan, C. L., A. A. Gerencser, J. R. Treberg, and M. D. Brand. "The Mechanism of Superoxide Production by the Antimycin-Inhibited Mitochondrial Q-Cycle." *J Biol Chem* 286, no. 36 (Sep 9 2011): 31361-72. https://doi.org/10.1074/jbc.M111.267898. https://www.ncbi.nlm.nih.gov/pubmed/21708945.

Quinlan, C. L., A. L. Orr, I. V. Perevoshchikova, J. R. Treberg, B. A. Ackrell, and M. D. Brand. "Mitochondrial Complex Ii Can Generate Reactive Oxygen Species at High Rates in Both the Forward and Reverse Reactions." *J Biol Chem* 287, no. 32 (Aug 3 2012): 27255-64. https://doi.org/10.1074/jbc.M112.374629. https://www.ncbi.nlm.nih.gov/pubmed/22689576.

Radad, K., W. D. Rausch, and G. Gille. "Rotenone Induces Cell Death in Primary Dopaminergic Culture by Increasing Ros Production and Inhibiting Mitochondrial Respiration." *Neurochem Int* 49, no. 4 (Sep 2006): 379-86. https://doi.org/10.1016/j.neuint.2006.02.003. https://www.ncbi.nlm.nih.gov/pubmed/16580092.

Rastogi, R., X. Geng, F. Li, and Y. Ding. "Nox Activation by Subunit Interaction and Underlying Mechanisms in Disease." *Front Cell Neurosci* 10 (2016): 301. https://doi.org/10.3389/fncel.2016.00301. https://www.ncbi.nlm.nih.gov/pubmed/28119569.

Ravenstijn, P. G., M. Merlini, M. Hameetman, T. K. Murray, M. A. Ward, H. Lewis, G. Ball*, et al.* "The Exploration of Rotenone as a Toxin for Inducing Parkinson's Disease in Rats, for Application in Bbb Transport and Pk-Pd Experiments." *J Pharmacol Toxicol Methods* 57, no. 2 (Mar-Apr 2008): 114-30. https://doi.org/10.1016/j.vascn.2007.10.003. https://www.ncbi.nlm.nih.gov/pubmed/18155613.

Reddy, P. H. "Mitochondrial Dysfunction and Oxidative Stress in Asthma: Implications for Mitochondria-Targeted Antioxidant Therapeutics." *Pharmaceuticals (Basel)* 4, no. 3 (Feb 25 2011): 429-56. https://doi.org/10.3390/ph4030429. https://www.ncbi.nlm.nih.gov/pubmed/21461182.

Ren, D., H. C. Tu, H. Kim, G. X. Wang, G. R. Bean, O. Takeuchi, J. R. Jeffers*, et al.* "Bid, Bim, and Puma Are Essential for Activation of the Bax- and Bak-Dependent Cell Death Program." *Science* 330, no. 6009 (Dec 3 2010): 1390-3. https://doi.org/10.1126/science.1190217. https://www.ncbi.nlm.nih.gov/pubmed/21127253.

Rhee, S. G., Y. S. Bae, S. R. Lee, and J. Kwon. "Hydrogen Peroxide: A Key Messenger That Modulates Protein Phosphorylation through Cysteine Oxidation." *Sci STKE* 2000, no. 53 (Oct 10 2000): pe1. https://doi.org/10.1126/stke.2000.53.pe1. https://www.ncbi.nlm.nih.gov/pubmed/11752613.

Rich, P. R., and A. Marechal. "The Mitochondrial Respiratory Chain." *Essays Biochem* 47 (2010): 1-23. https://doi.org/10.1042/bse0470001. https://www.ncbi.nlm.nih.gov/pubmed/20533897.

Ridker, P. M., A. Pradhan, J. G. MacFadyen, P. Libby, and R. J. Glynn. "Cardiovascular Benefits and Diabetes Risks of Statin Therapy in Primary Prevention: An Analysis from the Jupiter Trial." *Lancet* 380, no. 9841 (Aug 11 2012): 565-71. https://doi.org/10.1016/S0140-6736(12)61190-8. https://www.ncbi.nlm.nih.gov/pubmed/22883507.

Rikitake, Y., and J. K. Liao. "Rho Gtpases, Statins, and Nitric Oxide." *Circ Res* 97, no. 12 (Dec 9 2005): 1232-5. https://doi.org/10.1161/01.RES.0000196564.18314.23. https://www.ncbi.nlm.nih.gov/pubmed/16339495.

Robin, E. D., and R. Wong. "Mitochondrial DNA Molecules and Virtual Number of Mitochondria Per Cell in Mammalian Cells." *J Cell Physiol* 136, no. 3 (Sep 1988): 507-13. https://doi.org/10.1002/jcp.1041360316. https://www.ncbi.nlm.nih.gov/pubmed/3170646.

Rocha, M., N. Diaz-Morales, S. Rovira-Llopis, I. Escribano-Lopez, C. Banuls, A. Hernandez-Mijares, E. Diamanti-Kandarakis, and V. M. Victor. "Mitochondrial Dysfunction and Endoplasmic Reticulum Stress in Diabetes." *Curr Pharm Des* 22, no. 18 (2016): 2640-9. https://doi.org/10.2174/1381612822666160209152033. https://www.ncbi.nlm.nih.gov/pubmed/26861650.

Rundek, T., A. Naini, R. Sacco, K. Coates, and S. DiMauro. "Atorvastatin Decreases the Coenzyme Q10 Level in the Blood of Patients at Risk for Cardiovascular Disease and Stroke." *Arch Neurol* 61, no. 6 (Jun 2004): 889-92. https://doi.org/10.1001/archneur.61.6.889. https://www.ncbi.nlm.nih.gov/pubmed/15210526.

Rustin, P., T. Bourgeron, B. Parfait, D. Chretien, A. Munnich, and A. Rotig. "Inborn Errors of the Krebs Cycle: A Group of Unusual Mitochondrial Diseases in Human." *Biochim Biophys Acta* 1361, no. 2 (Aug 22 1997): 185-97. https://doi.org/10.1016/s0925-4439(97)00035-5. https://www.ncbi.nlm.nih.gov/pubmed/9300800.

Rutter, J., D. R. Winge, and J. D. Schiffman. "Succinate Dehydrogenase - Assembly, Regulation and Role in Human Disease." *Mitochondrion* 10, no. 4 (Jun 2010): 393-401. https://doi.org/10.1016/j.mito.2010.03.001. https://www.ncbi.nlm.nih.gov/pubmed/20226277.

Sabharwal, S. S., and P. T. Schumacker. "Mitochondrial Ros in Cancer: Initiators, Amplifiers or an Achilles' Heel?". *Nat Rev Cancer* 14, no. 11 (Nov 2014): 709-21. https://doi.org/10.1038/nrc3803. https://www.ncbi.nlm.nih.gov/pubmed/25342630.

Sadeghi, N., J. L. Abbruzzese, S. C. Yeung, M. Hassan, and D. Li. "Metformin Use Is Associated with Better Survival of Diabetic Patients with Pancreatic Cancer." *Clin Cancer Res* 18, no. 10 (May 15 2012): 2905-12. https://doi.org/10.1158/1078-0432.CCR-11-2994. https://www.ncbi.nlm.nih.gov/pubmed/22465831.

Salmenkivi, K., P. Heikkila, J. Liu, C. Haglund, and J. Arola. "Vegf in 105 Pheochromocytomas: Enhanced Expression Correlates with Malignant Outcome." *APMIS* 111, no. 4 (Apr 2003): 458-64. https://doi.org/10.1034/j.1600-0463.2003.1110402.x. https://www.ncbi.nlm.nih.gov/pubmed/12780519.

Salvemini, D., D. P. Riley, and S. Cuzzocrea. "Sod Mimetics Are Coming of Age." *Nat Rev Drug Discov* 1, no. 5 (May 2002): 367-74. https://doi.org/10.1038/nrd796. https://www.ncbi.nlm.nih.gov/pubmed/12120412.

Sanchez, C. A., E. Rodriguez, E. Varela, E. Zapata, A. Paez, F. A. Masso, L. F. Montano, and R. Loopez-Marure. "Statin-Induced Inhibition of Mcf-7 Breast Cancer Cell Proliferation Is Related to Cell Cycle Arrest and Apoptotic and Necrotic Cell Death Mediated by an Enhanced Oxidative Stress." *Cancer Invest* 26, no. 7 (Aug 2008): 698-707. https://doi.org/10.1080/07357900701874658. https://www.ncbi.nlm.nih.gov/pubmed/18608208.

Sareila, O., T. Kelkka, A. Pizzolla, M. Hultqvist, and R. Holmdahl. "Nox2 Complex-Derived Ros as Immune Regulators." *Antioxid Redox Signal* 15, no. 8 (Oct 15 2011): 2197-208. https://doi.org/10.1089/ars.2010.3635. https://www.ncbi.nlm.nih.gov/pubmed/20919938.

Sarti, P., A. Giuffre, M. C. Barone, E. Forte, D. Mastronicola, and M. Brunori. "Nitric Oxide and Cytochrome Oxidase: Reaction Mechanisms from the Enzyme to the Cell." *Free Radic Biol Med* 34, no. 5 (Mar 1 2003): 509-20. https://doi.org/10.1016/s0891-5849(02)01326-6. https://www.ncbi.nlm.nih.gov/pubmed/12614840.

Satoh, K., T. Nakai, and K. Ichihara. "Influence of 3-Hydroxy-3-Methylglutaryl Coenzyme a Reductase Inhibitors on Mitochondrial Respiration in Rat Liver During Ischemia." *Eur J Pharmacol* 270, no. 4 (Aug 3 1994): 365-9. https://doi.org/10.1016/0926-6917(94)90014-0. https://www.ncbi.nlm.nih.gov/pubmed/7805787.

Sattar, N., D. Preiss, H. M. Murray, P. Welsh, B. M. Buckley, A. J. de Craen, S. R. Seshasai, *et al.* "Statins and Risk of Incident Diabetes: A Collaborative Meta-Analysis of

Randomised Statin Trials." *Lancet* 375, no. 9716 (Feb 27 2010): 735-42. https://doi.org/10.1016/S0140-6736(09)61965-6. https://www.ncbi.nlm.nih.gov/pubmed/20167359.

Scheinok, S., T. Capeloa, P. E. Porporato, P. Sonveaux, and B. Gallez. "An Epr Study Using Cyclic Hydroxylamines to Assess the Level of Mitochondrial Ros in Superinvasive Cancer Cells." *Cell Biochem Biophys* 78, no. 3 (Sep 2020): 249-54. https://doi.org/10.1007/s12013-020-00921-6. https://www.ncbi.nlm.nih.gov/pubmed/32488461.

Scheinok, S., P. Leveque, P. Sonveaux, B. Driesschaert, and B. Gallez. "Comparison of Different Methods for Measuring the Superoxide Radical by Epr Spectroscopy in Buffer, Cell Lysates and Cells." *Free Radic Res* 52, no. 10 (Oct 2018): 1182-96. https://doi.org/10.1080/10715762.2018.1541321. https://www.ncbi.nlm.nih.gov/pubmed/30362382.

Schieber, M., and N. S. Chandel. "Ros Function in Redox Signaling and Oxidative Stress." *Curr Biol* 24, no. 10 (May 19 2014): R453-62. https://doi.org/10.1016/j.cub.2014.03.034. https://www.ncbi.nlm.nih.gov/pubmed/24845678.

Schleich, K., and I. N. Lavrik. "Mathematical Modeling of Apoptosis." *Cell Commun Signal* 11, no. 1 (Jun 26 2013): 44. https://doi.org/10.1186/1478-811X-11-44. https://www.ncbi.nlm.nih.gov/pubmed/23803157.

Schmeling, B. V., and M. Kulka. "Systemic Fungicidal Activity of 1,4-Oxathiin Derivatives." *Science* 152, no. 3722 (Apr 29 1966): 659-60. https://doi.org/10.1126/science.152.3722.659. https://www.ncbi.nlm.nih.gov/pubmed/17779512.

Schoonen, W. G., J. A. de Roos, W. M. Westerink, and E. Debiton. "Cytotoxic Effects of 110 Reference Compounds on Hepg2 Cells and for 60 Compounds on Hela, Ecc-1 and Cho Cells. Ii Mechanistic Assays on Nad(P)H, Atp and DNA Contents." *Toxicol In Vitro* 19, no. 4 (Jun 2005): 491-503. https://doi.org/10.1016/j.tiv.2005.01.002. https://www.ncbi.nlm.nih.gov/pubmed/15826807.

Secomb, T. W., R. Hsu, E. T. Ong, J. F. Gross, and M. W. Dewhirst. "Analysis of the Effects of Oxygen Supply and Demand on Hypoxic Fraction in Tumors." *Acta Oncol* 34, no. 3 (1995): 313-6. https://doi.org/10.3109/02841869509093981. https://www.ncbi.nlm.nih.gov/pubmed/7779415.

Seelert, H., D. N. Dani, S. Dante, T. Hauss, F. Krause, E. Schafer, M. Frenzel*, et al.* "From Protons to Oxphos Supercomplexes and Alzheimer's Disease: Structure-Dynamics-Function Relationships of Energy-Transducing Membranes." *Biochim Biophys Acta* 1787, no. 6 (Jun 2009): 657-71. https://doi.org/10.1016/j.bbabio.2009.02.028. https://www.ncbi.nlm.nih.gov/pubmed/19281792.

Selak, M. A., S. M. Armour, E. D. MacKenzie, H. Boulahbel, D. G. Watson, K. D. Mansfield, Y. Pan*, et al.* "Succinate Links Tca Cycle Dysfunction to Oncogenesis by Inhibiting Hif-Alpha Prolyl Hydroxylase." *Cancer Cell* 7, no. 1 (Jan 2005): 77-85. https://doi.org/10.1016/j.ccr.2004.11.022. https://www.ncbi.nlm.nih.gov/pubmed/15652751.

Sen, N., M. R. Hara, M. D. Kornberg, M. B. Cascio, B. I. Bae, N. Shahani, B. Thomas*, et al.* "Nitric Oxide-Induced Nuclear Gapdh Activates P300/Cbp and Mediates Apoptosis." *Nat Cell Biol* 10, no. 7 (Jul 2008): 866-73. https://doi.org/10.1038/ncb1747. https://www.ncbi.nlm.nih.gov/pubmed/18552833.

Sena, L. A., and N. S. Chandel. "Physiological Roles of Mitochondrial Reactive Oxygen Species." *Mol Cell* 48, no. 2 (Oct 26 2012): 158-67. https://doi.org/10.1016/j.molcel.2012.09.025. https://www.ncbi.nlm.nih.gov/pubmed/23102266.

Shamas-Din, A., H. Brahmbhatt, B. Leber, and D. W. Andrews. "Bh3-Only Proteins: Orchestrators of Apoptosis." *Biochim Biophys Acta* 1813, no. 4 (Apr 2011): 508-20. https://doi.org/10.1016/j.bbamcr.2010.11.024. https://www.ncbi.nlm.nih.gov/pubmed/21146563.

Sherer, T. B., R. Betarbet, J. H. Kim, and J. T. Greenamyre. "Selective Microglial Activation in the Rat Rotenone Model of Parkinson's Disease." *Neurosci Lett* 341, no. 2 (May 1 2003): 87-90. https://doi.org/10.1016/s0304-3940(03)00172-1. https://www.ncbi.nlm.nih.gov/pubmed/12686372.

Sherer, T. B., R. Betarbet, A. K. Stout, S. Lund, M. Baptista, A. V. Panov, M. R. Cookson, and J. T. Greenamyre. "An in Vitro Model of Parkinson's Disease: Linking Mitochondrial Impairment to Altered Alpha-Synuclein Metabolism and Oxidative Damage." *J Neurosci* 22, no. 16 (Aug 15 2002): 7006-15. https://doi.org/20026721. https://www.ncbi.nlm.nih.gov/pubmed/12177198.

Short, K. R., M. L. Bigelow, J. Kahl, R. Singh, J. Coenen-Schimke, S. Raghavakaimal, and K. S. Nair. "Decline in Skeletal Muscle Mitochondrial Function with Aging in Humans." *Proc Natl Acad Sci U S A* 102, no. 15 (Apr 12 2005): 5618-23. https://doi.org/10.1073/pnas.0501559102. https://www.ncbi.nlm.nih.gov/pubmed/15800038.

Simon, T. G., A. S. Duberg, S. Aleman, H. Hagstrom, L. H. Nguyen, H. Khalili, R. T. Chung, and J. F. Ludvigsson. "Lipophilic Statins and Risk for Hepatocellular Carcinoma and Death in Patients with Chronic Viral Hepatitis: Results from a Nationwide Swedish Population." *Ann Intern Med* 171, no. 5 (Sep 3 2019): 318-27. https://doi.org/10.7326/M18-2753. https://www.ncbi.nlm.nih.gov/pubmed/31426090.

Smith, R. A., C. M. Porteous, A. M. Gane, and M. P. Murphy. "Delivery of Bioactive Molecules to Mitochondria in Vivo." *Proc Natl Acad Sci U S A* 100, no. 9 (Apr 29 2003): 5407-12. https://doi.org/10.1073/pnas.0931245100. https://www.ncbi.nlm.nih.gov/pubmed/12697897.

Song, C. W., H. Lee, R. P. Dings, B. Williams, J. Powers, T. D. Santos, B. H. Choi, and H. J. Park. "Metformin Kills and Radiosensitizes Cancer Cells and Preferentially Kills Cancer Stem Cells." *Sci Rep* 2 (2012): 362. https://doi.org/10.1038/srep00362. https://www.ncbi.nlm.nih.gov/pubmed/22500211.

Sosa, V., T. Moline, R. Somoza, R. Paciucci, H. Kondoh, and L. Leonart ME. "Oxidative Stress and Cancer: An Overview." *Ageing Res Rev* 12, no. 1 (Jan 2013): 376-90. https://doi.org/10.1016/j.arr.2012.10.004. https://www.ncbi.nlm.nih.gov/pubmed/23123177.

Stammler, G., Brix, H.D., Glättli, A., Semar, M., Schoefl, U. "Biological Properties of the Carboxamide Boscalid Including Recent Studies on Its Mode of Action." Paper presented at the Proceedings XVI International Plant Protection Congress Glasgow, 2007.

Sun, F., X. Huo, Y. Zhai, A. Wang, J. Xu, D. Su, M. Bartlam, and Z. Rao. "Crystal Structure of Mitochondrial Respiratory Membrane Protein Complex Ii." *Cell* 121, no. 7 (Jul 1 2005): 1043-57. https://doi.org/10.1016/j.cell.2005.05.025. https://www.ncbi.nlm.nih.gov/pubmed/15989954.

Sutter, A. P., K. Maaser, M. Hopfner, A. Huether, D. Schuppan, and H. Scherubl. "Cell Cycle Arrest and Apoptosis Induction in Hepatocellular Carcinoma Cells by Hmg-Coa Reductase Inhibitors. Synergistic Antiproliferative Action with Ligands of the Peripheral Benzodiazepine Receptor." *J Hepatol* 43, no. 5 (Nov 2005): 808-16. https://doi.org/10.1016/j.jhep.2005.04.010. https://www.ncbi.nlm.nih.gov/pubmed/16083991.

Swerdlow, D. I., D. Preiss, K. B. Kuchenbaecker, M. V. Holmes, J. E. Engmann, T. Shah, R. Sofat, *et al.* "Hmg-Coenzyme a Reductase Inhibition, Type 2 Diabetes, and Bodyweight: Evidence from Genetic Analysis and Randomised Trials." *Lancet* 385, no. 9965 (Jan 24 2015): 351-61. https://doi.org/10.1016/S0140-6736(14)61183-1. https://www.ncbi.nlm.nih.gov/pubmed/25262344.

Takai, Y., T. Sasaki, and T. Matozaki. "Small Gtp-Binding Proteins." *Physiol Rev* 81, no. 1 (Jan 2001): 153-208. https://doi.org/10.1152/physrev.2001.81.1.153. https://www.ncbi.nlm.nih.gov/pubmed/11152757.

Tannahill, G. M., A. M. Curtis, J. Adamik, E. M. Palsson-McDermott, A. F. McGettrick, G. Goel, C. Frezza, *et al.* "Succinate Is an Inflammatory Signal That Induces Il-1beta through Hif-1alpha." *Nature* 496, no. 7444 (Apr 11 2013): 238-42. https://doi.org/10.1038/nature11986. https://www.ncbi.nlm.nih.gov/pubmed/23535595.

Tarze, A., A. Deniaud, M. Le Bras, E. Maillier, D. Molle, N. Larochette, N. Zamzami, *et al.* "Gapdh, a Novel Regulator of the Pro-Apoptotic Mitochondrial Membrane Permeabilization." *Oncogene* 26, no. 18 (Apr 19 2007): 2606-20. https://doi.org/10.1038/sj.onc.1210074. https://www.ncbi.nlm.nih.gov/pubmed/17072346.

Thabrew, M. I., R. D. Hughes, and I. G. McFarlane. "Screening of Hepatoprotective Plant Components Using a Hepg2 Cell Cytotoxicity Assay." *J Pharm Pharmacol* 49, no. 11 (Nov 1997): 1132-5. https://doi.org/10.1111/j.2042-7158.1997.tb06055.x. https://www.ncbi.nlm.nih.gov/pubmed/9401951.

Thews, O., D. K. Kelleher, and P. Vaupel. "In Vivo Oxygen Consumption Rate of Ds Sarcoma Cells on Inhibition of DNA Synthesis." *Cancer Res* 56, no. 9 (May 1 1996): 2009-12. https://www.ncbi.nlm.nih.gov/pubmed/8616841.

Thibault, A., D. Samid, A. C. Tompkins, W. D. Figg, M. R. Cooper, R. J. Hohl, J. Trepel, *et al.* "Phase I Study of Lovastatin, an Inhibitor of the Mevalonate Pathway, in Patients with Cancer." *Clin Cancer Res* 2, no. 3 (Mar 1996): 483-91. https://www.ncbi.nlm.nih.gov/pubmed/9816194.

Tieu, K. "A Guide to Neurotoxic Animal Models of Parkinson's Disease." *Cold Spring Harb Perspect Med* 1, no. 1 (Sep 2011): a009316. https://doi.org/10.1101/cshperspect.a009316. https://www.ncbi.nlm.nih.gov/pubmed/22229125.

Tomlinson, S. S., and K. K. Mangione. "Potential Adverse Effects of Statins on Muscle." *Phys Ther* 85, no. 5 (May 2005): 459-65. https://www.ncbi.nlm.nih.gov/pubmed/15842193.

Tordo, P. "Spin-Trapping: Recent Developments and Applications." In *Electron Paramagnetic Resonance*, 1998.

Tretter, L., A. Patocs, and C. Chinopoulos. "Succinate, an Intermediate in Metabolism, Signal Transduction, Ros, Hypoxia, and Tumorigenesis." *Biochim Biophys Acta* 1857, no. 8 (Aug 2016): 1086-101. https://doi.org/10.1016/j.bbabio.2016.03.012. https://www.ncbi.nlm.nih.gov/pubmed/26971832.

Tristan, C., N. Shahani, T. W. Sedlak, and A. Sawa. "The Diverse Functions of Gapdh: Views from Different Subcellular Compartments." *Cell Signal* 23, no. 2 (Feb 2011): 317-23. https://doi.org/10.1016/j.cellsig.2010.08.003. https://www.ncbi.nlm.nih.gov/pubmed/20727968.

Tsubaki, M., D. Fujiwara, T. Takeda, T. Kino, Y. Tomonari, T. Itoh, M. Imano, *et al.* "The Sensitivity of Head and Neck Carcinoma Cells to Statins Is Related to the Expression of Their Ras Expression Status, and Statin-Induced Apoptosis Is Mediated Via Suppression of the Ras/Erk and Ras/Mtor Pathways." *Clin Exp Pharmacol Physiol* 44, no. 2 (Feb 2017): 222-34. https://doi.org/10.1111/1440-1681.12690. https://www.ncbi.nlm.nih.gov/pubmed/27805296.

Tsujita, Y., M. Kuroda, K. Tanzawa, N. Kitano, and A. Endo. "Hypolipidemic Effects in Dogs of Ml-236b, a Competitive Inhibitor of 3-Hydroxy-3-Methylglutaryl Coenzyme a Reductase." *Atherosclerosis* 32, no. 3 (Mar 1979): 307-13. https://doi.org/10.1016/0021-9150(79)90174-6. https://www.ncbi.nlm.nih.gov/pubmed/223590.

Turrens, J. F. "Mitochondrial Formation of Reactive Oxygen Species." *J Physiol* 552, no. Pt 2 (Oct 15 2003): 335-44. https://doi.org/10.1113/jphysiol.2003.049478. https://www.ncbi.nlm.nih.gov/pubmed/14561818.

———. "Superoxide Production by the Mitochondrial Respiratory Chain." *Biosci Rep* 17, no. 1 (Feb 1997): 3-8. https://doi.org/10.1023/a:1027374931887. https://www.ncbi.nlm.nih.gov/pubmed/9171915.

Turrens, J. F., A. Alexandre, and A. L. Lehninger. "Ubisemiquinone Is the Electron Donor for Superoxide Formation by Complex Iii of Heart Mitochondria." *Arch Biochem Biophys* 237, no. 2 (Mar 1985): 408-14. https://doi.org/10.1016/0003-9861(85)90293-0. https://www.ncbi.nlm.nih.gov/pubmed/2983613.

Uchida, T., H. Togashi, Y. Kuroda, A. Yamashita, N. Itoh, K. Haga, M. Sadahiro, and T. Kayama. "In Vivo Analysis of Redox Status in Organs - from Bench to Bedside." *Free Radic Res* 54, no. 11-12 (Dec 2020): 961-68. https://doi.org/10.1080/10715762.2020.1772470. https://www.ncbi.nlm.nih.gov/pubmed/32458704.

Van Aelst, L., and C. D'Souza-Schorey. "Rho Gtpases and Signaling Networks." *Genes Dev* 11, no. 18 (Sep 15 1997): 2295-322. https://doi.org/10.1101/gad.11.18.2295. https://www.ncbi.nlm.nih.gov/pubmed/9308960.

Vasquez-Vivar, J., B. Kalyanaraman, and M. C. Kennedy. "Mitochondrial Aconitase Is a Source of Hydroxyl Radical. An Electron Spin Resonance Investigation." *J Biol Chem* 275, no. 19 (May 12 2000): 14064-9. https://doi.org/10.1074/jbc.275.19.14064. https://www.ncbi.nlm.nih.gov/pubmed/10799480.

Vaupel, P., D. K. Kelleher, and M. Hockel. "Oxygen Status of Malignant Tumors: Pathogenesis of Hypoxia and Significance for Tumor Therapy." *Semin Oncol* 28, no. 2 Suppl 8 (Apr 2001): 29-35. https://doi.org/10.1016/s0093-7754(01)90210-6. https://www.ncbi.nlm.nih.gov/pubmed/11395850.

von Heimburg, D., K. Hemmrich, S. Zachariah, H. Staiger, and N. Pallua. "Oxygen Consumption in Undifferentiated Versus Differentiated Adipogenic Mesenchymal Precursor Cells." *Respir Physiol Neurobiol* 146, no. 2-3 (Apr 15 2005): 107-16. https://doi.org/10.1016/j.resp.2004.12.013. https://www.ncbi.nlm.nih.gov/pubmed/15766899.

Walsh, J. C., A. Lebedev, E. Aten, K. Madsen, L. Marciano, and H. C. Kolb. "The Clinical Importance of Assessing Tumor Hypoxia: Relationship of Tumor Hypoxia to

Prognosis and Therapeutic Opportunities." *Antioxid Redox Signal* 21, no. 10 (Oct 1 2014): 1516-54. https://doi.org/10.1089/ars.2013.5378. https://www.ncbi.nlm.nih.gov/pubmed/24512032.

Wang, H., Z. Meng, F. Liu, L. Zhou, M. Su, Y. Meng, S. Zhang, *et al.* "Characterization of Boscalid-Induced Oxidative Stress and Neurodevelopmental Toxicity in Zebrafish Embryos." *Chemosphere* 238 (Jan 2020): 124753. https://doi.org/10.1016/j.chemosphere.2019.124753. https://www.ncbi.nlm.nih.gov/pubmed/31545217.

Wassmann, S., U. Laufs, K. Muller, C. Konkol, K. Ahlbory, A. T. Baumer, W. Linz, M. Bohm, and G. Nickenig. "Cellular Antioxidant Effects of Atorvastatin in Vitro and in Vivo." *Arterioscler Thromb Vasc Biol* 22, no. 2 (Feb 1 2002): 300-5. https://doi.org/10.1161/hq0202.104081. https://www.ncbi.nlm.nih.gov/pubmed/11834532.

Wei, M. C., W. X. Zong, E. H. Cheng, T. Lindsten, V. Panoutsakopoulou, A. J. Ross, K. A. Roth, *et al.* "Proapoptotic Bax and Bak: A Requisite Gateway to Mitochondrial Dysfunction and Death." *Science* 292, no. 5517 (Apr 27 2001): 727-30. https://doi.org/10.1126/science.1059108. https://www.ncbi.nlm.nih.gov/pubmed/11326099.

Winge, D. R. "Sealing the Mitochondrial Respirasome." *Mol Cell Biol* 32, no. 14 (Jul 2012): 2647-52. https://doi.org/10.1128/MCB.00573-12. https://www.ncbi.nlm.nih.gov/pubmed/22586278.

Wojtczak, L., and P. Schonfeld. "Effect of Fatty Acids on Energy Coupling Processes in Mitochondria." *Biochim Biophys Acta* 1183, no. 1 (Nov 2 1993): 41-57. https://doi.org/10.1016/0005-2728(93)90004-y. https://www.ncbi.nlm.nih.gov/pubmed/8399375.

Wolvetang, E. J., K. L. Johnson, K. Krauer, S. J. Ralph, and A. W. Linnane. "Mitochondrial Respiratory Chain Inhibitors Induce Apoptosis." *FEBS Lett* 339, no. 1-2 (Feb 14 1994): 40-4. https://doi.org/10.1016/0014-5793(94)80380-3. https://www.ncbi.nlm.nih.gov/pubmed/8313978.

Wong, H. S., P. A. Dighe, V. Mezera, P. A. Monternier, and M. D. Brand. "Production of Superoxide and Hydrogen Peroxide from Specific Mitochondrial Sites under Different Bioenergetic Conditions." *J Biol Chem* 292, no. 41 (Oct 13 2017): 16804-09. https://doi.org/10.1074/jbc.R117.789271. https://www.ncbi.nlm.nih.gov/pubmed/28842493.

Wood, P. M., and D. W. Hollomon. "A Critical Evaluation of the Role of Alternative Oxidase in the Performance of Strobilurin and Related Fungicides Acting at the Qo Site of Complex Iii." *Pest Manag Sci* 59, no. 5 (May 2003): 499-511. https://doi.org/10.1002/ps.655. https://www.ncbi.nlm.nih.gov/pubmed/12741518.

Wood, W. G., U. Igbavboa, W. E. Muller, and G. P. Eckert. "Statins, Bcl-2, and Apoptosis: Cell Death or Cell Protection?". *Mol Neurobiol* 48, no. 2 (Oct 2013): 308-14. https://doi.org/10.1007/s12035-013-8496-5. https://www.ncbi.nlm.nih.gov/pubmed/23821030.

Wyche, K. E., S. S. Wang, K. K. Griendling, S. I. Dikalov, H. Austin, S. Rao, B. Fink, D. G. Harrison, and A. M. Zafari. "C242t Cyba Polymorphism of the Nadph Oxidase Is Associated with Reduced Respiratory Burst in Human Neutrophils." *Hypertension* 43, no. 6 (Jun 2004): 1246-51. https://doi.org/10.1161/01.HYP.0000126579.50711.62. https://www.ncbi.nlm.nih.gov/pubmed/15078863.

Xekouki, P., and C. A. Stratakis. "Succinate Dehydrogenase (Sdhx) Mutations in Pituitary Tumors: Could This Be a New Role for Mitochondrial Complex Ii and/or Krebs Cycle Defects?". *Endocr Relat Cancer* 19, no. 6 (Dec 2012): C33-40. https://doi.org/10.1530/ERC-12-0118. https://www.ncbi.nlm.nih.gov/pubmed/22889736.

Xia, D. K., Z. G. Hu, Y. F. Tian, and F. J. Zeng. "Statin Use and Prognosis of Lung Cancer: A Systematic Review and Meta-Analysis of Observational Studies and Randomized Controlled Trials." *Drug Des Devel Ther* 13 (2019): 405-22. https://doi.org/10.2147/DDDT.S187690. https://www.ncbi.nlm.nih.gov/pubmed/30774306.

Yang, J., L. J. Wu, S. Tashino, S. Onodera, and T. Ikejima. "Reactive Oxygen Species and Nitric Oxide Regulate Mitochondria-Dependent Apoptosis and Autophagy in Evodiamine-Treated Human Cervix Carcinoma Hela Cells." *Free Radic Res* 42, no. 5 (May 2008): 492-504. https://doi.org/10.1080/10715760802112791. https://www.ncbi.nlm.nih.gov/pubmed/18484413.

Yankovskaya, V., R. Horsefield, S. Tornroth, C. Luna-Chavez, H. Miyoshi, C. Leger, B. Byrne, G. Cecchini, and S. Iwata. "Architecture of Succinate Dehydrogenase and Reactive Oxygen Species Generation." *Science* 299, no. 5607 (Jan 31 2003): 700-4. https://doi.org/10.1126/science.1079605. https://www.ncbi.nlm.nih.gov/pubmed/12560550.

Yankovskaya, V., S. O. Sablin, R. R. Ramsay, T. P. Singer, B. A. Ackrell, G. Cecchini, and H. Miyoshi. "Inhibitor Probes of the Quinone Binding Sites of Mammalian Complex Ii and Escherichia Coli Fumarate Reductase." *J Biol Chem* 271, no. 35 (Aug 30 1996): 21020-4. https://doi.org/10.1074/jbc.271.35.21020. https://www.ncbi.nlm.nih.gov/pubmed/8702865.

Young, R. P., R. Hopkins, and T. E. Eaton. "Potential Benefits of Statins on Morbidity and Mortality in Chronic Obstructive Pulmonary Disease: A Review of the Evidence." *Postgrad Med J* 85, no. 1006 (Aug 2009): 414-21. https://doi.org/10.1136/pgmj.2008.078477. https://www.ncbi.nlm.nih.gov/pubmed/19633007.

Yuan, M., W. Li, and P. Xiao. "Bixafen Causes Cardiac Toxicity in Zebrafish (Danio Rerio) Embryos." *Environ Sci Pollut Res Int* 28, no. 27 (Jul 2021): 36303-13. https://doi.org/10.1007/s11356-021-13238-5. https://www.ncbi.nlm.nih.gov/pubmed/33694115.

Zahra, W., S. N. Rai, H. Birla, S. S. Singh, A. S. Rathore, H. Dilnashin, R. Singh, *et al.* "Neuroprotection of Rotenone-Induced Parkinsonism by Ursolic Acid in Pd Mouse Model." *CNS Neurol Disord Drug Targets* 19, no. 7 (2020): 527-40. https://doi.org/10.2174/1871527319666200812224457. https://www.ncbi.nlm.nih.gov/pubmed/32787765.

Zain, ME. "Impact of Mycotoxins on Humans and Animals." *Journal of Saudi chemical society* 15, no. 2 (2011): 129-44.

Zannella, V. E., A. Dal Pra, H. Muaddi, T. D. McKee, S. Stapleton, J. Sykes, R. Glicksman, *et al.* "Reprogramming Metabolism with Metformin Improves Tumor Oxygenation and Radiotherapy Response." *Clin Cancer Res* 19, no. 24 (Dec 15 2013): 6741-50. https://doi.org/10.1158/1078-0432.CCR-13-1787. https://www.ncbi.nlm.nih.gov/pubmed/24141625.

Zhang, C., J. Wang, S. Zhang, L. Zhu, Z. Du, and J. Wang. "Acute and Subchronic Toxicity of Pyraclostrobin in Zebrafish (Danio Rerio)." *Chemosphere* 188 (Dec 2017): 510-16.

https://doi.org/10.1016/j.chemosphere.2017.09.025.
https://www.ncbi.nlm.nih.gov/pubmed/28910725.

Zhang, Q., J. Pi, C. G. Woods, and M. E. Andersen. "A Systems Biology Perspective on Nrf2-Mediated Antioxidant Response." *Toxicol Appl Pharmacol* 244, no. 1 (Apr 1 2010): 84-97. https://doi.org/10.1016/j.taap.2009.08.018.
https://www.ncbi.nlm.nih.gov/pubmed/19716833.

Zhang, Z., S. Zhou, X. Jiang, Y. H. Wang, F. Li, Y. G. Wang, Y. Zheng, and L. Cai. "The Role of the Nrf2/Keap1 Pathway in Obesity and Metabolic Syndrome." *Rev Endocr Metab Disord* 16, no. 1 (Mar 2015): 35-45. https://doi.org/10.1007/s11154-014-9305-9.
https://www.ncbi.nlm.nih.gov/pubmed/25540093.

Zhao, H., J. Joseph, H. M. Fales, E. A. Sokoloski, R. L. Levine, J. Vasquez-Vivar, and B. Kalyanaraman. "Detection and Characterization of the Product of Hydroethidine and Intracellular Superoxide by Hplc and Limitations of Fluorescence." *Proc Natl Acad Sci U S A* 102, no. 16 (Apr 19 2005): 5727-32.
https://doi.org/10.1073/pnas.0501719102.
https://www.ncbi.nlm.nih.gov/pubmed/15824309.

Zhelev, Z., R. Bakalova, I. Aoki, D. Lazarova, and T. Saga. "Imaging of Superoxide Generation in the Dopaminergic Area of the Brain in Parkinson's Disease, Using Mito-Tempo." *ACS Chem Neurosci* 4, no. 11 (Nov 20 2013): 1439-45.
https://doi.org/10.1021/cn400159h.
https://www.ncbi.nlm.nih.gov/pubmed/24024751.

Zhelev, Z., E. Georgieva, D. Lazarova, S. Semkova, I. Aoki, M. Gulubova, T. Higashi, and R. Bakalova. ""Redox Imaging" to Distinguish Cells with Different Proliferative Indexes: Superoxide, Hydroperoxides, and Their Ratio as Potential Biomarkers." *Oxid Med Cell Longev* 2019 (2019): 6373685. https://doi.org/10.1155/2019/6373685.
https://www.ncbi.nlm.nih.gov/pubmed/31089411.

Zhou, Q., Y. Zhai, J. Lou, M. Liu, X. Pang, and F. Sun. "Thiabendazole Inhibits Ubiquinone Reduction Activity of Mitochondrial Respiratory Complex Ii Via a Water Molecule Mediated Binding Feature." *Protein Cell* 2, no. 7 (Jul 2011): 531-42.
https://doi.org/10.1007/s13238-011-1079-1.
https://www.ncbi.nlm.nih.gov/pubmed/21822798.

Zhu, X., M. Zhang, J. Liu, J. Ge, and G. Yang. "Ametoctradin Is a Potent Qo Site Inhibitor of the Mitochondrial Respiration Complex Iii." *J Agric Food Chem* 63, no. 13 (Apr 8 2015): 3377-86. https://doi.org/10.1021/acs.jafc.5b00228.
https://www.ncbi.nlm.nih.gov/pubmed/25784492.

Zielonka, J., J. Joseph, A. Sikora, M. Hardy, O. Ouari, J. Vasquez-Vivar, G. Cheng, M. Lopez, and B. Kalyanaraman. "Mitochondria-Targeted Triphenylphosphonium-Based Compounds: Syntheses, Mechanisms of Action, and Therapeutic and Diagnostic Applications." *Chem Rev* 117, no. 15 (Aug 9 2017): 10043-120.
https://doi.org/10.1021/acs.chemrev.7b00042.
https://www.ncbi.nlm.nih.gov/pubmed/28654243.

Zielonka, J., and B. Kalyanaraman. "Hydroethidine- and Mitosox-Derived Red Fluorescence Is Not a Reliable Indicator of Intracellular Superoxide Formation: Another Inconvenient Truth." *Free Radic Biol Med* 48, no. 8 (Apr 15 2010): 983-1001.
https://doi.org/10.1016/j.freeradbiomed.2010.01.028.
https://www.ncbi.nlm.nih.gov/pubmed/20116425.

Zielonka, J., S. Srinivasan, M. Hardy, O. Ouari, M. Lopez, J. Vasquez-Vivar, N. G. Avadhani, and B. Kalyanaraman. "Cytochrome C-Mediated Oxidation of Hydroethidine and

Mito-Hydroethidine in Mitochondria: Identification of Homo- and Heterodimers." *Free Radic Biol Med* 44, no. 5 (Mar 1 2008): 835-46. https://doi.org/10.1016/j.freeradbiomed.2007.11.013. https://www.ncbi.nlm.nih.gov/pubmed/18155177.

Zuo, L., N. P. Otenbaker, B. A. Rose, and K. S. Salisbury. "Molecular Mechanisms of Reactive Oxygen Species-Related Pulmonary Inflammation and Asthma." *Mol Immunol* 56, no. 1-2 (Nov 2013): 57-63. https://doi.org/10.1016/j.molimm.2013.04.002. https://www.ncbi.nlm.nih.gov/pubmed/23665383.